REPUBLIC OF CAMEROON
Peace-Work-Fatherland
****
UNIVERSITY OF YAOUNDE I
****
FACULTY OF SCIENCE
****
PO. BOX 812 Yaounde

REPUBLIQUE DU CAMEROUN
Paix-Travail-Patrie
****
UNIVERSITE DE YAOUNDE I
****
FACULTE DES SCIENCES
****
BP 812 Yaoundé

DEPARTMENT OF ORGANIC CHEMISTRY

DEPARTEMENT DE CHIMIE ORGANIQUE

Speciality: Natural Products

Specialité: Substances Naturelles

Chemical constituents and antiplasmodial activity of *Dacryodes edulis* (G.Don) H.J.Lam (Burseraceae) and *Celtis adolphi-friderici* Engl. (Cannabaceae)

Thesis

Submitted and defended publicly for the award of the Doctorate/PhD *degree* of the University of Yaounde I

By

DONGMO JUMETA Johane Kevin

Registration number: 16X5884
Master in Organic Chemistry

Under the supervision of

NGOUELA Silvère Augustin
Professor

Year 2021

REPUBLIQUE DU CAMEROUN
Paix-Travail-Patrie
****
UNIVERSITÉ DE YAOUNDÉ I
****
FACULTE DES SCIENCES
****

REPUBLIC OF CAMEROON
Peace-Work-Fatherland
****
THE UNIVERSITY OF YAOUNDE I
****
FACULTY OF SCIENCE
****

DEPARTEMENT DE CHIMIE ORGANIQUE
DEPARTMENT OF ORGANIC CHEMISTRY

ATTESTATION DE CORRECTION DE MEMOIRE DE THESE DE DOCTORAT/*Ph.D* DE MADAME DONGMO JUMETA Johane Kevine

Titre de thèse: CHEMICAL CONSTITUENTS AND ANTIPLASMODIAL ACTIVITY OF *DACRYODES EDULIS* (G.DON) H.J.LAM (BURSERACEAE) AND *CELTIS ADOLPHI-FRIDERICI* ENGL. (CANNABACEAE)

Nous soussignés, enseignants ci-dessous nommés, membres du jury de soutenance de thèse de Doctorat/*Ph.D* de Madame **DONGMO JUMETA Johane Kevine**, Matricule **16X5884**, attestons que cette candidate a bel et bien pris en compte dans la mouture finale de sa thèse, toutes corrections et recommandations qui lui ont été faites au cours de sa soutenance en date du 14 Décembre 2021.

En foi de quoi, la présente attestation de correction lui est délivrée pour servir et valoir ce que de droit.

Fait à Yaoundé, le 03 Janvier 2022

Le Jury :

Le Président :
NKENGFACK Augustin Ephrem, *Professeur*

Le rapporteur :
NGOUELA Silvère Augustin, *Professeur*

Les membres

WANDJI Jean, *Professeur*

LENTA NDJAKOU Bruno, *Professeur*

KAPCHE WABO FOTSO Gilbert Deccaux, *Professeur*

FEKAM BOYOM Fabrice, *Professeur*

OFFICIAL LIST OF THE LECTURERS OF THE FACULTY OF SCIENCE

LIST OF PERMANENT TEACHING STAFF

ACADEMIC YEAR 2021/2022
(By Department and by Grade)
UPDATE DATE: 22 September 2021

ADMINISTRATION

DEAN: TCHOUANKEU Jean-Claude, Associate Professor
VICE DEAN/DPSAA: ATCHADE Alex de Théodore, Associate Professor
VICE DEAN/DSSE: NYEGUE Maximilienne Ascension, Professor
VICE DEAN/DRC: ABOSSOLO Monique, Associate Professor
Head of Administrative and Financial Division: NDOYE FOE Florentine Marie Chantal, Associate Professor
Head of Academic Affairs, Education and Research Division DAASR: AJEAGAH Gideon AGHAINDUM, Professor

1- DEPARTMENT OF BIOCHEMISTRY (BC) (38)

N°	NAMES AND SURNAMES	Grade	Observations
1	BIGOGA DAIGA Jude	Professor	On duty
2	FEKAM BOYOM Fabrice	Professor	On duty
3	FOKOU Elie	Professor	On duty
4	KANSCI Germain	Professor	On duty
5	MBACHAM FON Wilfried	Professor	On duty
6	MOUNDIPA FEWOU Paul	Professor	*Head of Department*
7	NINTCHOM PENLAP V. spouse BENG	Professor	On duty
8	OBEN Julius ENYONG	Professor	On duty
9	ACHU Merci BIH	Associate Professor	On duty
10	ATOGHO Barbara Mma	Associate Professor	On duty
11	AZANTSA KINGUE GABIN BORIS	Associate Professor	On duty
12	BELINGA born NDOYE FOE F. M. C.	Associate Professor	*Head AFD/FS*
13	BOUDJEKO Thaddée	Associate Professor	On duty
14	DJUIDJE NGOUNOUE Marcelline	Associate Professor	On duty
15	EFFA ONOMO Pierre	Associate Professor	On duty
16	EWANE Cécile Anne	Associate Professor	On duty
17	MOFOR born TEUGWA Clotilde	Associate Professor	*Service Inspector MINESUP*
18	NANA Louise spouse WAKAM	Associate Professor	On duty
19	NGONDI Judith Laure	Associate Professor	On duty
20	NGUEFACK Julienne	Associate Professor	On duty
21	NJAYOU Frédéric Nico	Associate Professor	On duty
22	TCHANA KOUATCHOUA Angèle	Associate Professor	On duty
23	AKINDEH MBUH NJI	Lecturer	On duty
24	BEBEE Fadimatou	Lecturer	On duty
25	BEBOY EDJENGUELE Sara Nathalie	Lecturer	On duty
26	DAKOLE DABOY Charles	Lecturer	On duty
27	DJUIKWO NKONGA Ruth Viviane	Lecturer	On duty
28	DONGMO LEKAGNE Joseph Blaise	Lecturer	On duty
29	FONKOUA Martin	Lecturer	On duty
30	KOTUE KAPTUE Charles	Lecturer	On duty

31	LUNGA Paul KEILAH	Lecturer	On duty
32	MANANGA Marlyse Joséphine	Lecturer	On duty
33	MBONG ANGIE M. Mary Anne	Lecturer	On duty
34	Palmer MASUMBE NETONGO	Lecturer	On duty
35	PECHANGOU NSANGOU Sylvain	Lecturer	On duty
36	MBOUCHE FANMOE Marceline Joëlle	Assistant lecturer	On duty
37	OWONA AYISSI Vincent Brice	Assistant lecturer	On duty
38	WILFRIED ANGIE Abia	Assistant lecturer	On duty

2- DEPARTMENT OF BIOLOGY AND ANIMAL PHYSIOLOGY (BAP) (46)

1	AJEAGAH Gideon AGHAINDUM	Professor	*VICE-DEAN DSSE*
2	BILONG BILONG Charles-Félix	Professor	*Head of Department*
3	DIMO Théophile	Professor	On duty
4	DJIETO LORDON Champlain	Professor	On duty
5	DZEUFIET DJOMENI Paul Désiré	Professor	Vice Dean/FMBS/UYI
6	ESSOMBA born NTSAMA MBALA	Professor	On duty
7	FOMENA Abraham	Professor	On duty
8	KAMTCHOUING Pierre	Professor	On duty
9	KEKEUNOU Sévilor	Professor	On duty
10	NJAMEN Dieudonné	Professor	On duty
11	NJIOKOU Flobert	Professor	On duty
12	NOLA Moïse	Professor	*Service Inspector of Coord.Progr./MINSANTE*
13	TAN Paul VERNYUY	Professor	On duty
14	TCHUEM TCHUENTE Louis Albert	Professor	On duty
15	ZEBAZE TOGOUET Serge Hubert	Professor	On duty
16	BILANDA Danielle Claude	Associate Professor	On duty
17	DJIOGUE Séfirin	Associate Professor	On duty
18	JATSA BOUKENG Hermine spouse MEGAPTCHE	Associate Professor	On duty
19	LEKEUFACK FOLEFACK Guy B.	Associate Professor	On duty
20	MEGNEKOU Rosette	Associate Professor	On duty
21	MONY Ruth spouse NTONE	Associate Professor	On duty
22	NGUEGUIM TSOFACK Florence	Associate Professor	On duty
23	TOMBI Jeannette	Associate Professor	On duty
24	ALENE Désirée Chantal	Lecturer	On duty
25	ATSAMO Albert Donatien	Lecturer	On duty
26	BELLET EDIMO Oscar Roger	Lecturer	On duty
27	DONFACK Mireille	Lecturer	On duty
28	ETEME ENAMA Serge	Lecturer	On duty
29	GOUNOUE KAMKUMO Raceline	Lecturer	On duty
30	KANDEDA KAVAYE Antoine	Lecturer	On duty
31	MAHOB Raymond Joseph	Lecturer	On duty
32	MBENOUN MASSE Paul Serge	Lecturer	On duty
33	MOUNGANG Luciane Marlyse	Lecturer	On duty
34	MVEYO NDANKEU Yves Patrick	Lecturer	On duty
35	NGOUATEU KENFACK Omer Bébé	Lecturer	On duty
36	NGUEMBOK	Lecturer	On duty
37	NJUA Clarisse Yafi	Lecturer	*Head Div. UBA*
38	NOAH EWOTI Olive Vivien	Lecturer	On duty
39	TADU Zephyrin	Lecturer	On duty

40	TAMSA ARFAO Antoine	Lecturer	On duty
41	YEDE	Lecturer	On duty
42	BASSOCK BAYIHA Etienne Didier	Assistant lecturer	On duty
43	ESSAMA MBIDA Désirée Sandrine	Assistant lecturer	On duty
44	KOGA MANG DOBARA	Assistant lecturer	On duty
45	LEME BANOCK Lucie	Assistant lecturer	On duty
46	YOUNOUSSA LAME	Assistant lecturer	On duty

3- DEPARTMENT OF BIOLOGY AND VEGETAL PHYSIOLOGY (BVP) (31)

1	AMBANG Zachée	Professor	*Head of Division/UYII*
2	BELL Joseph Martin	Professor	On duty
3	DJOCGOUE Pierre François	Professor	On duty
4	MBOLO Marie	Professor	On duty
5	MOSSEBO Dominique Claude	Professor	On duty
6	YOUMBI Emmanuel	Professor	Head of Department
7	ZAPFACK Louis	Professor	On duty
8	ANGONI Hyacinthe	Associate Professor	On duty
9	BIYE Elvire Hortense	Associate Professor	On duty
10	MALA Armand William	Associate Professor	On duty
11	MBARGA BINDZI Marie Alain	Associate Professor	*TA/MINESUP*
12	NDONGO BEKOLO	Associate Professor	*CE/MINRESI*
13	NGODO MELINGUI Jean Baptiste	Associate Professor	On duty
14	NGONKEU MAGAPTCHE Eddy L.	Associate Professor	On duty
15	TONFACK Libert Brice	Associate Professor	On duty
16	TSOATA Esaïe	Associate Professor	On duty
17	DJEUANI Astride Carole	Lecturer	On duty
18	GOMANDJE Christelle	Lecturer	On duty
19	MAFFO MAFFO Nicole Liliane	Lecturer	On duty
20	MAHBOU SOMO TOUKAM. Gabriel	Lecturer	On duty
21	NGALLE Hermine BILLE	Lecturer	On duty
22	NNANGA MEBENGA Ruth Laure	Lecturer	On duty
23	NOUKEU KOUAKAM Armelle	Lecturer	On duty
24	ONANA JEAN MICHEL	Lecturer	On duty
25	GODSWILL NTSOMBOH NTSEFONG	Assistant lecturer	On duty
26	KABELONG BANAHO Louis-Paul-Roger	Assistant lecturer	On duty
27	KONO Léon Dieudonné	Assistant lecturer	On duty
28	LIBALAH Moses BAKONCK	Assistant lecturer	On duty
29	LIKENG-LI-NGUE Benoit C	Assistant lecturer	On duty
30	TAEDOUNG Evariste Hermann	Assistant lecturer	On duty
31	TEMEGNE NONO Carine	Assistant lecturer	On duty

4- DEPARTMENT OF INORGANIC CHEMISTRY (IC) (33)

1	AGWARA ONDOH Moïse	Professor	*Head of Department*
2	DJOUFAC WOUMFO Emmanuel	Professor	On duty
3	Florence UFI CHINJE spouse MELO	Professor	*Rector Univ.Ngaoundere*
4	GHOGOMU Paul MINGO	Professor	*Minister in Charge of Miss.PR*
5	NANSEU Njiki Charles Péguy	Professor	On duty
6	NDIFON Peter TEKE	Professor	*TA MINRESI*

7	NDIKONTAR Maurice KOR	Professor	*Vice-Dean Univ. Bamenda*
8	NENWA Justin	Professor	On duty
9	NGAMENI Emmanuel	Professor	*Dean FS Uds*
10	NGOMO Horace MANGA	Professor	*Vice Chancelor/UB*
11	ACAYANKA Elie	Associate Professor	On duty
12	BABALE born DJAM DOUDOU	Associate Professor	*Mission Officer P.R.*
13	EMADACK Alphonse	Associate Professor	On duty
14	KAMGANG YOUBI Georges	Associate Professor	On duty
15	KEMMEGNE MBOUGUEM Jean C.	Associate Professor	On duty
16	KONG SAKEO	Associate Professor	On duty
17	NDI NSAMI Julius	Associate Professor	On duty
18	NJIOMOU C. spouse DJANGANG	Associate Professor	On duty
19	NJOYA Dayirou	Associate Professor	On duty
20	TCHAKOUTE KOUAMO Hervé	Associate Professor	On duty
21	BELIBI BELIBI Placide Désiré	Lecturer	*CS/ENS Bertoua*
22	CHEUMANI YONA Arnaud M.	Lecturer	On duty
23	KENNE DEDZO GUSTAVE	Lecturer	On duty
24	KOUOTOU DAOUDA	Lecturer	On duty
25	MAKON Thomas Beauregard	Lecturer	On duty
26	MBEY Jean Aime	Lecturer	On duty
27	NCHIMI NONO KATIA	Lecturer	On duty
28	NEBAH born NDOSIRI Bridget NDOYE	Lecturer	*TA/MINFEM*
29	NYAMEN Linda Dyorisse	Lecturer	On duty
30	PABOUDAM GBAMBIE A.	Lecturer	On duty
31	NJANKWA NJABONG N. Eric	Assistant lecturer	On duty
32	PATOUOSSA ISSOFA	Assistant lecturer	On duty
33	SIEWE Jean Mermoz	Assistant lecturer	On duty

5- DEPARTMENT OF ORGANIC CHEMISTRY (OC) (40)			
1	DONGO Etienne	Professor	*Vice-Dean/DSEE FSE*
2	GHOGOMU TIH Robert Ralph	Professor	*Dir. IBAF/UDA*
3	NGOUELA Silvère Augustin	Professor	*Head of Department UDS*
4	NYASSE Barthélemy	Professor	On duty
5	PEGNYEMB Dieudonné Emmanuel	Professor	*Director MINESUP/Head of Department*
6	WANDJI Jean	Professor	On duty
7	Alex de Théodore ATCHADE	Associate Professor	Vice-Dean/DPSAA
8	AMBASSA Pantaléon	Associate Professor	On duty
9	EYONG Kenneth OBEN	Associate Professor	On duty
10	FOLEFOC Gabriel NGOSONG	Associate Professor	On duty
11	FOTSO WABO Ghislain	Associate Professor	On duty
12	KEUMEDJIO Félix	Associate Professor	On duty
13	KENMOGNE Marguerite	Associate Professor	On duty
14	KOUAM Jacques	Associate Professor	On duty
15	MBAZOA born DJAMA Céline	Associate Professor	On duty
16	MKOUNGA Pierre	Associate Professor	On duty
17	MVOT AKAK CARINE	Associate Professor	On duty
18	NGO MBING Joséphine	Associate Professor	*Assistant Director MINERESI*

19	NGONO BIKOBO Dominique Serge	Associate Professor	*C.E/MINESUP*
20	NOTE LOUGBOT Olivier Placide	Associate Professor	*C.S/MINESUP*
21	NOUNGOUE TCHAMO Diderot	Associate Professor	On duty
22	TABOPDA KUATE Turibio	Associate Professor	On duty
23	TAGATSING FOTSING Maurice	Associate Professor	On duty
24	TCHOUANKEU Jean-Claude	Associate Professor	*Dean/FS/UYI*
25	TIH née NGO BILONG E. Anastasie	Associate Professor	On duty
26	YANKEP Emmanuel	Associate Professor	On duty
27	ZONDEGOUMBA Ernestine	Associate Professor	On duty
28	KAMTO Eutrophe Le Doux	Lecturer	On duty
29	NGNINTEDO Dominique	Lecturer	On duty
30	NGOMO Orléans	Lecturer	On duty
31	OUAHOUO WACHE Blandine M.	Lecturer	On duty
32	SIELINOU TEDJON Valérie	Lecturer	On duty
33	MESSI Angélique Nicolas	Assistant lecturer	On duty
34	MUNVERA MFIFEN Aristide	Assistant lecturer	On duty
35	NONO NONO Éric Carly	Assistant lecturer	On duty
36	OUETE NANTCHOUANG Judith	Assistant lecturer	On duty
37	TCHAMGOUE Joseph	Assistant lecturer	On duty
38	TSAFFACK Maurice	Assistant lecturer	On duty
39	TSAMO TONTSA Armelle	Assistant lecturer	On duty
40	TSEMEUGNE Joseph	Assistant lecturer	On duty

6- DEPARTMENT OF INFORMATIC (IN) (25)

1	ATSA ETOUNDI Roger	Professor	*Head Div.MINESUP*
2	FOUDA NDJODO Marcel Laurent	Professor	*Head Dpt ENS/Head IGA.MINESUP*
3	NDOUNDAM Réné	Associate Professor	On duty
4	ABESSOLO ALO'O Gislain	Lecturer	*Head of Department*
5	AMINOU Halidou	Lecturer	On duty
6	DJAM Xaviera YOUH – KIMBI	Lecturer	On duty
7	DOMGA KOMGUEM Rodrigue	Lecturer	On duty
8	EBELE Serge Alain	Lecturer	On duty
9	KOUOKAM KOUOKAM E. A.	Lecturer	On duty
10	MELATAGIA YONTA Paulin	Lecturer	On duty
11	MONTHE DJIADEU Valery M.	Lecturer	On duty
12	MOTO MPONG Serge Alain	Lecturer	On duty
13	OLLE OLLE Daniel Claude Delort	Lecturer	*Deputy Director Enset Ebolowa*
14	TAPAMO Hyppolite	Lecturer	On duty
15	TINDO Gilbert	Lecturer	On duty
16	TSOPZE Norbert	Lecturer	On duty
17	WAKU KOUAMOU Jules	Lecturer	On duty
18	BAYEM Jacques Narcisse	Assistant lecturer	On duty
19	EKODECK Stéphane Gaël Raymond	Assistant lecturer	On duty
20	HAMZA Adamou	Assistant lecturer	On duty
21	JIOMEKONG AZANZI Fidel	Assistant lecturer	On duty
22	MAKEMBE S. Oswald	Assistant lecturer	On duty
23	MESSI NGUELE Thomas	Assistant lecturer	On duty
24	MEYEMDOU Nadège Sylvianne	Assistant lecturer	On duty
25	NKONDOCK MI. BAHANACK N.	Assistant lecturer	On duty

7- DEPARTMENT OF MATHEMATICS (MA) (30)

1	AYISSI Raoult Domingo	Professor	*Head of Department*
2	EMVUDU WONO Yves S.	Professor	*Inspector MINESUP*
3	KIANPI Maurice	Associate Professor	On duty
4	MBANG Joseph	Associate Professor	On duty
5	MBEHOU Mohamed	Associate Professor	On duty
6	MBELE BIDIMA Martin Ledoux	Associate Professor	On duty
7	NKUIMI JUGNIA Célestin	Associate Professor	On duty
8	NOUNDJEU Pierre	Associate Professor	*Head of Programs & Diplomas*
9	TCHAPNDA NJABO Sophonie B.	Associate Professor	*Director/AIMS Rwanda*
10	TCHOUNDJA Edgar Landry	Associate Professor	On duty
11	AGHOUKENG JIOFACK Jean Gérard	Lecturer	*Head Cell MINPLAMAT*
12	CHENDJOU Gilbert	Lecturer	On duty
13	DJIADEU NGAHA Michel	Lecturer	On duty
14	DOUANLA YONTA Herman	Lecturer	On duty
15	FOMEKONG Christophe	Lecturer	On duty
16	KIKI Maxime Armand	Lecturer	On duty
17	MBAKOP Guy Merlin	Lecturer	On duty
18	MENGUE MENGUE David Joe	Lecturer	On duty
19	NGUEFACK Bernard	Lecturer	On duty
20	NIMPA PEFOUKEU Romain	Lecturer	On duty
21	POLA DOUNDOU Emmanuel	Lecturer	On duty
22	TAKAM SOH Patrice	Lecturer	On duty
23	TCHANGANG Roger Duclos	Lecturer	On duty
24	TETSADJIO TCHILEPECK M. E.	Lecturer	On duty
25	TIAYA TSAGUE N. Anne-Marie	Lecturer	On duty
26	BITYE MVONDO Esther Claudine	Assistant lecturer	On duty
27	MBATAKOU Salomon Joseph	Assistant lecturer	On duty
28	MBIAKOP Hilaire George	Assistant lecturer	On duty
29	MEFENZA NOUNTU Thiery	Assistant lecturer	On duty
30	TCHEUTIA Daniel Duviol	Assistant lecturer	On duty

8- DEPARTMENT OF MICROBIOLOGY (MIB) (18)

1	ESSIA NGANG Jean Justin	Professor	*Head of Dpartment*
2	NYEGUE Maximilienne Ascension	Professor	*VICE-Dean/DSSE*
3	NWAGA Dieudonné M.	Professor	On duty
4	ASSAM ASSAM Jean Paul	Associate Professor	On duty
5	BOYOMO ONANA	Associate Professor	On duty
6	RIWOM Sara Honorine	Associate Professor	On duty
7	SADO KAMDEM Sylvain Leroy	Associate Professor	On duty
8	BODA Maurice	Lecturer	On duty
9	BOUGNOM Blaise Pascal	Lecturer	On duty
10	ESSONO OBOUGOU Germain G.	Lecturer	On duty
11	NJIKI BIKOÏ Jacky	Lecturer	On duty
12	TCHIKOUA Roger	Lecturer	On duty

13	ESSONO Damien Marie	Assistant lecturer	On duty
14	LAMYE Glory MOH	Assistant lecturer	On duty
15	MEYIN A EBONG Solange	Assistant lecturer	On duty
16	NKOUDOU ZE Nardis	Assistant lecturer	On duty
17	SAKE NGANE Carole Stéphanie	Assistant lecturer	On duty
18	TOBOLBAÏ Richard	Assistant lecturer	On duty

9. DEPARTMENT OF PHYSIC (PHY) (44)

1	BEN- BOLIE Germain Hubert	Professor	On duty
2	DJUIDJE KENMOE spouse ALOYEM	Professor	On duty
3	EKOBENA FOUDA Henri Paul	Professor	*Vice Rector*
4	ESSIMBI ZOBO Bernard	Professor	On duty
5	KOFANE Timoléon Crépin	Professor	On duty
6	NANA ENGO Serge Guy	Professor	On duty
7	NANA NBENDJO Blaise	Professor	On duty
8	NDJAKA Jean Marie Bienvenu	Professor	Head of Department
9	NJANDJOCK NOUCK Philippe	Professor	On duty
10	NOUAYOU Robert	Professor	On duty
11	PEMHA Elkana	Professor	On duty
12	TABOD Charles TABOD	Professor	*Dean Univ/Bda*
13	TCHAWOUA Clément	Professor	On duty
14	WOAFO Paul	Professor	On duty
15	ZEKENG Serge Sylvain	Professor	On duty
16	BIYA MOTTO Frédéric	Associate Professor	DG/HYDRO Mekin
17	BODO Bertrand	Associate Professor	On duty
18	ENYEGUE A NYAM spouse BELINGA	Associate Professor	On duty
19	EYEBE FOUDA Jean sire	Associate Professor	On duty
20	FEWO Serge Ibraïd	Associate Professor	On duty
21	HONA Jacques	Associate Professor	On duty
22	MBANE BIOUELE César	Associate Professor	On duty
23	MBINACK Clément	Associate Professor	On duty
24	NDOP Joseph	Associate Professor	On duty
25	SAIDOU	Associate Professor	MINRESI
26	SIEWE SIEWE Martin	Associate Professor	On duty
27	SIMO Elie	Associate Professor	On duty
28	VONDOU Derbetini Appolinaire	Associate Professor	On duty
29	WAKATA born BEYA Annie	Associate Professor	*Director ENS/UY1*
30	ABDOURAHIMI	Lecturer	On duty
31	CHAMANI Roméo	Lecturer	On duty
32	EDONGUE HERVAIS	Lecturer	On duty
33	FOUEDJIO David	Lecturer	*Head Cell. MINADER*
34	MBONO SAMBA Yves Christian U.	Lecturer	On duty
35	MELI'I Joelle Larissa	Lecturer	On duty
36	MVOGO ALAIN	Lecturer	On duty
37	OBOUNOU Marcel	Lecturer	*DA/Univ Inter State/Sangmalima*
38	WOULACHE Rosalie Laure	Lecturer	On duty
39	AYISSI EYEBE Guy François Valérie	Assistant lecturer	On duty
40	DJIOTANG TCHOTCHOU Lucie Angennes	Assistant lecturer	On duty

41	LAMARA Maurice	Assistant lecturer	On duty
42	OTTOU ABE Martin Thierry	Assistant lecturer	On duty
43	TEYOU NGOUPOU Ariel	Assistant lecturer	On duty
44	WANDJI NYAMSI William	Assistant lecturer	On duty

10- DEPARTMENT OF EARTH SCIENCES (ES) (43)

1	BITOM Dieudonné	Professor	*Dean/FASA/UDs*
2	FOUATEU Rose spouse YONGUE	Professor	On duty
3	NDAM NGOUPAYOU Jules-Remy	Professor	On duty
4	NDJIGUI Paul Désiré	Professor	*Head of Department*
5	NGOS III Simon	Professor	On duty
6	NKOUMBOU Charles	Professor	On duty
7	NZENTI Jean-Paul	Professor	On duty
8	ABOSSOLO born ANGUE Monique	Associate Professor	*Vice-Dean/DRC*
9	BISSO Dieudonné	Associate Professor	*Director/Barrage Project Memve'ele*
10	EKOMANE Emile	Associate Professor	On duty
11	GANNO Sylvestre	Associate Professor	On duty
12	GHOGOMU Richard TANWI	Associate Professor	*CD/Uma*
13	MOUNDI Amidou	Associate Professor	*TA/ MINIMDT*
14	NGUEUTCHOUA Gabriel	Associate Professor	*CEA/MINRESI*
15	NJILAH Isaac KONFOR	Associate Professor	On duty
16	NYECK Bruno	Associate Professor	On duty
17	ONANA Vincent Laurent	Associate Professor	*Head of Maintenance & Equipment*
18	TCHAKOUNTE J. spouse NUMBEM	Associate Professor	*Head cell MINRESI*
19	TCHOUANKOUE Jean-Pierre	Associate Professor	On duty
20	TEMDJIM Robert	Associate Professor	On duty
21	YENE ATANGANA Joseph Q.	Associate Professor	*Head Div./MINTP*
22	ZO'O ZAME Philémon		*DG/ART*
23	ANABA ONANA Achille Basile	Lecturer	On duty
24	BEKOA Etienne	Lecturer	On duty
25	ELISE SABABA	Lecturer	On duty
26	ESSONO Jean	Lecturer	On duty
27	EYONG JOHN TAKEM	Lecturer	On duty
28	FUH Calistus Gentry	Lecturer	*State Sec. /MINMIDT*
29	LAMILEN BILLA Daniel	Lecturer	On duty
30	MBESSE CECILE OLIVE	Lecturer	On duty
31	MBIDA YEM	Lecturer	On duty
32	METANG Victor	Lecturer	On duty
33	MINYEM Dieudonné-Lucien	Lecturer	*CD/Uma*
34	NGO BELNOUN Rose Noël	Lecturer	On duty
35	NGO BIDJECK Louise Marie	Lecturer	On duty
36	NOMO NEGUE Emmanuel	Lecturer	On duty
37	NTSAMA ATANGANA Jacqueline	Lecturer	On duty
38	TCHAPTCHET TCHATO De P.	Lecturer	On duty
39	TEHNA Nathanaël	Lecturer	On duty
40	TEMGA Jean Pierre	Lecturer	On duty
42	FEUMBA Roger	Assistant lecturer	On duty
43	MBANGA NYOBE Jules	Assistant lecturer	On duty

Quantified distribution of teachers from the Faculty of Sciences of the University of Yaoundé 1

NUMBER OF TEACHERS					
DEPARTMENT	**Professors**	**Associate Professors**	**Lecturers**	**Assistant lecturers**	**Total**
BCH	8 (01)	14 (10)	13 (05)	3 (02)	**38 (18)**
BAP	15 (01)	8 (06)	18 (05)	05 (02)	**46 (14)**
BVP	07 (01)	9 (01)	8 (06)	07 (01)	**31 (9)**
IC	10 (01)	10 (02)	10 (02)	03 (0)	**33 (5)**
OC	6 (0)	21 (06)	05 (02)	08 (02)	**40 (10)**
IN	2 (0)	1 (0)	14 (01)	08 (01)	**25 (2)**
MAT	2 (0)	8 (0)	15 (01)	05 (02)	**30 (3)**
MIB	3 (0)	4 (02)	05 (01)	06 (02)	**18 (5)**
PHY	15 (0)	14 (02)	09 (03)	06 (01)	**44 (6)**
ES	7 (1)	15 (01)	18 (05)	02 (0)	**42 (7)**
Total	**75 (5)**	**104 (29)**	**115 (31)**	**53 (13)**	**347 (79)**

A total of	**347 (79)** with:
-Professors	**75 (5)**
-Associate Professors	**104 (29)**
-Lecturers	**115 (31)**
-Assistant lecturers	**53 (13)**
( ) = Number of Women	**79**

CERTIFICAT

I, the undersigned, NGOUELA Silvere Augustin (Professor), certify that the work presented in this thesis and entitled "Chemical constituents and antiplasmodial activity of *Dacryodes edulis* (G.Don) H.J.Lam (Burseraceae) and *Celtis adolphi-friderici* Engl. (Cannabaceae)" was carried out by Mrs DONGMO JUMETA Johane Kevine (Master in Organic Chemistry, Registration number 16X5884), in the Laboratory of Natural Products and Organic Synthetic, University of Yaoundé I.

This work has not yet been the subject of any submission for the acquisition of any academic degree.

Student	**Supervisor**
DONGMO JUMETA J. Kevine	**NGOUELA Silvère Augustin**

DEDICATION

To my parents

ACKNOWLEDGEMENTS

I thank the Almighty GOD for all the grace, the wonders which He never ceases to fill me.

The accomplisment of this work is obviously linked to various contributions that I have benefited. I therefore express my sincere thanks and my deep gratitude to all those who directly or indirectly contributed to it. Above all, I address my sincere thanks:

to my supervisor, **Professor Silvère A. NGOUELA**, Head of the Laboratory of Natural Products and Organic Synthetic, for welcoming me in his laboratory. I am extremely grateful, for his availability, his guidance and good discussion we had during my research work. I also thank him for, his encouragement, his dynamism, his advice and above all his scientific rigor which was very decisive in the realization of this work;

to **Professor Bruno N. LENTA**., Coordinator of the YaBiNaPA project in Cameroon to have giving me the opportunity to work in YaBiNaPA project. I also thank him for all the facilities (financial and materials) used in the achievement of the work, his sense of humor and his enthusiasm in promoting natural products, as well as the various scientific collaboration. I equally address my sincere thanks to him for his patience, for the scientific training that he gave us through this period of research work;

to **Professor Norbert SEWALD**, Coordinator of YaBiNaPA project in Germany for his advice and efforts done to manage the project so well;

to **Professor Emmanuel D. PEGNYEMB,** Head of Department of Organic Chemistry at the University of Yaoundé I, for his dynamism, dedication and availability in the good running of the Department. Professor, received my deep respect;

to the **lecturers of the Department of Organic Chemistry** and the **Department of Chemistry of the University of Yaoundé I** and **University of Dschang,** respectively and to all the **member of YaBiNaPA Graduate School** for the high quality of the training;

to **Professors Leon TAPONDJOU** and **Bertrand TEPONNO** who guided my first steps in research and for always encouraging, supporting me and providing excellent suggestions during my research work;

to **Professors Diderot T. NOUNGOUE, Jean J. K. BANKEU** and **Angelbert AWANTU**, for their daily help, their great sympathy, their availability and many advice throughout this research work;

to **Doctors Brice MBA'NING, Yannick S. F. FONGANG, Beaudelaire PONOU, Aimée TCHUENTE, Rosine F. NGAMGWE, Jules NGATCHOU, Joël ATEBA, Flaure**

ESSOUNG, Donald K. KAGHO and **Mrs Christine Claire WALEGUELE, Mr Maxime THIENEHOM, Mrs Linda MATCHI** for their advice, encouragement and critical readings;

to my Lab mates and all my classmates, particularly: **Clemence GOUNI, Suzy CHOUNA, Kelly WONKAM, Armelle TSAKOU, Jean GARBA, Leonel TAGUIMJEU, Maxime NANGMO, Ruland NGUENGANG, Hermine NONO, Fabiola MADAHA, Desmond KHAN** for their contributions their support and friendship;

to **Doctors Bosco JOUDA, Billy TCHEGNITEGNI, Cyril NGOUFACK** and **Gabin BITCHAGNO** for their advice, help and encouragement;

to **Mr. Victor NANA** of the National Herbarium of Cameroon for the identification of the plant material;

to my lovely mother **Sabine TAJONA**. A deeply thanks for your permanent affection and determination in work. You send me to school and supported me at the cost of unforgettable sacrifices. Thank you such much mom;

to **Fabrice KAMMI** for his unconditional love, various support and his encouragement;

to **KENNE** and **TIEUMENA families**, for their advice, their various support and their unconditional love;

to **MO'O TEJIOLEKO family** for their unconditional support and the family warmth;

to my friends **Ida TCHUMMEGNE**, **Viviane KAMSO** and **Angele NKINGUE** for their collaboration, their friendship and the good times shared together .

to **DAAD** (German Academic Exchange Service) with funding from the Federal Ministry for Economic Cooperation and Development (BMZ) for the financial support granted to "the Yaoundé-Bielefeld Graduate School of Natural Products with Antiparasite and Antibacterial activities" (**YABINAPA**, www.yabinapa. de), No. 57316173, that enable me to receive stipend and to have access to differents facilities for four years;

to the **International Center for Chemical and Biological Sciences (ICCBS)**, University of Karachi, Pakistan for the chemical analysis and biological screening of same samples.

TABLE OF CONTENTS

OFFICIAL LIST OF THE LECTURERS OF THE FACULTY OF SCIENCE ---------- i

LIST OF PERMANENT TEACHING STAFF ---------- i

CERTIFICAT ---------- x

DEDICATION ---------- xi

ACKNOWLEDGEMENTS ---------- xii

TABLE OF CONTENTS ---------- xiv

ABBREVIATIONS AND SYMBOLS ---------- xviii

LIST OF TABLES ---------- xx

LIST OF FIGURES ---------- xxii

LIST OF SCHEMES ---------- xxv

ABSTRACT ---------- xxvi

RESUME ---------- xxviii

GENERAL INTRODUCTION ---------- 1

CHAPTER I: LITERATURE REVIEW ---------- 3

I.1 BOTANICAL STUDY ON THE BURSERACEAE AND CANNABACEAE FAMILY ------- 3

I.1.1 Overview on the Burseraceae family ---------- 4

I.1.1.1 Overview on *Dacryodes* genus ---------- 4

I.1.1.2 Overview on *D. edulis* ---------- 5

I.1.2. Overview on the Cannabaceae family ---------- 8

I.1.2.1 Overview on the *Celtis* genus ---------- 8

I.1.2.2 Ethnomedicinal uses of species of the *Celtis genus* ---------- 9

I.1.2.3 Overview on *C. adolphi-friderici* ---------- 10

I.1.2.4 Economical uses of species of the *Celtis* genus ---------- 11

I.2 PREVIOUS PHARMACOLOGICAL AND CHEMICAL STUDIES ON THE STUDIED SPECIES ---------- 11

I.2.1 Previous pharmacological studies on *D. edulis* ---------- 11

I.2.2 Previous chemical investigation on the *D. edulis* ---------- 12

I.2.3 Previous pharmacological studies of *Celtis* genus ---------- 15

I.2.4 Previous chemical investigation on the *Celtis* genus ---------- 16

I.3. OVERVIEW ON SOME SECONDARY METABOLITES ---------- 19

I.3.1 Cerebrosides ---------- 19

I.3.1.1 Definition and general structure ---------- 19
I.3.1.2 The Biosynthesis of cerebrosides ---------- 19
I.3.1.3 Biological activities of cerebrosides ---------- 21
I.3.1.4 General method for the structure elucidation of cerebrosides ---------- 21
I.3.2. Phenolic amides ---------- 24
I.3.2.1 Definition and general structure ---------- 24
I.3.2.2 Biosynthesis of phenolic amides ---------- 24
I.3.2.3 Biological activities ---------- 25
I.3.2.4 General method for identification of avenanthramides ---------- 26
I.4 OVERVIEW ON MALARIA ---------- 27
I.4.1 Definition ---------- 27
I.4.2 History of malaria and discovery of the parasite ---------- 28
I.4.3 Geography and incidence ---------- 29
I.4.4 Malaria parasite, mosquito vector and Life-cycle ---------- 30
I.4.4.1 Malaria parasite, mosquito vector ---------- 30
I.4.4.2 Life cycle of Plasmodium parasites ---------- 31
I.4.5 Signs and symptoms of malaria ---------- 32
I.4.6 Malaria situation in Cameroon ---------- 33
I.4.7 Malaria diagnosis, treatment and vaccine ---------- 34
CHAPTER II: RESULTS AND DISCUSSION ---------- 37
II.1. CHEMICAL STUDY OF *Dacryodes edulis* AND *Celtis adolphi-friderici* Engl. ----- 39
II.1.1. Plant material, extraction and isolation of compounds ---------- 39
II.1.1.1 *D. edulis* ---------- 39
II.1.1.2. *C. adolphi-friderici Engl*. ---------- 41
II.1.2 Structures determination of isolated compounds ---------- 42
II.1.2.1 Structure determination of CAF2 ---------- 42
II.1.2.2 Structure identification of phenolic amides ---------- 51
II.1.2.3 Structure identification of dicarboxylic acids ---------- 58
II.1.2.4 Structure identification of CAF10 ---------- 62
II.1.2.5 Structure identification of fatty acids ---------- 64
II.1.2.6 Structure identification of CAF15 ---------- 68
II.1.2.7 Structure identification of CAF16 ---------- 71
II.1.2.8 Structure identification of phenolic compounds ---------- 73

II.1.2.9 Structure identification of triglycerids ---------- 78
II.1.2.10 Structure identification of xanthones ---------- 83
II.1.2.11 Structure identification of ellagic acids derivatives ---------- 88
II.1.2.12 Structure identification of DF3 ---------- 97
II.1.2.13 Structure identification of DE7 ---------- 100
II.1.2.14 Structure identification of DF6 ---------- 104
II.1.2.15 Structure identification of triterpenes ---------- 106
II.2 CHEMOPHENETIC SIGNIFICANCE OF THE ISOLATED COMPOUNDS --- 117
II.3 EVALUATION OF BIOLOGICAL ACTIVITIES OF EXTRACTS, FRACTIONS AND PURE COMPOUNDS OBTAINED FROM *D. edulis* AND *C. adolphi friderici.* - 118
II.3.1 Results and discussion of the in vitro antiplasmodial activities ---------- 118
II.3.2 Acute oral toxicity study of aqueous extract of the leaves of D. edulis (DEF) - 122
II.3.3 Other biological activities on C. adolphi friderici ---------- 124
II.4 PRE-FORMULATION ASSAY ---------- 126
CONCLUSION AND PERSPECTIVES ---------- 129
CHAPTER III: GENERAL EXPERIMENT ---------- 132
III.1 GENERALITY ---------- 133
III.1.1 Chromatography techniques ---------- 133
III.1.1.1 Thin layer chromatography ---------- 133
III-1.1.2 Column chromatography ---------- 133
III.1.2 Physico-chemical methods and apparatus ---------- 133
III.1.2.1 Mass spectra ---------- 133
III.1.2.2 Nuclear Magnetic Resonance (NMR) ---------- 133
III.1.2.3. Instruments ---------- 134
III.1.3 Chemical characterization tests ---------- 134
III.1.3.1 Ferric chloride test ---------- 134
III.1.3.2 Liebermann-Burchard test ---------- 134
III.1.3.3 Molish test ---------- 134
III.1.3.4 $NaHCO_3$ (sodium bicarbonate) ---------- 134
III.2. EXTRACTION AND ISOLATION ---------- 134
III.2.1. Plant material ---------- 134
III.2.1.1 *Celtis adolphi-friderici* Engl ---------- 134
III.2.1.2 *Dacryodes edulis* (G.Don) ---------- 135
III.2.2 EXTRACTION ---------- 135

III.2.2.1 Preparation of extract from *C. adolphi friderici* Engl ---------- 135

III.2.2.2 Preparation of extracts from *D. edulis* (G.Don) ---------- 135

III.2.3 Isolation of compounds---------- 135

III.2.3.1 Isolation of compounds from *C. adolphi-friderici* Engl.---------- 135

III.2.3.2 Isolation of compounds from MeOH extract of the stem bark of *D. edulis* ------ 138

III.3 CHEMICAL TRANSFORMATION---------- 141

III.4 EVALUATION OF BIOLOGICAL ACTIVITIES ---------- 141

III.5 PROTOCOL OF PRE-FORMULATION OF PHYTOMEDICINE FROM HYDROETHANOLIC LEAVES EXTRACT ---------- 145

III.6 PHYSICAL AND SPECTROSCOPIC DATA FOR COMPOUNDS ISOLATED FROM *C. adolphi friderici* Engl and *D. edulis* ---------- 146

REFERENCES ---------- 155

ANNEXE---------- 172

ABBREVIATIONS AND SYMBOLS

LDL	:	Low Density Lipoprotein
FAD	:	Flavin Adenine Dinucleotide
CC	:	Column Chromatography
TLC	:	Thin Layer Chromatography
IC_{50}	:	50% Inhibitory Concentration
δ	:	Chemical shift in ppm
d	:	doublet
dd	:	doublet of doublet
s	:	singlet
LCB	:	Long-chain Base
DEPT	:	Distortionless Enhancement by Polarization Transfer
DMSO	:	Dimethylsulfoxide
DMDS	:	Dimethyl disulfide
DPPH	:	Diphenyl-2,2 picryl-1 hydrazyl
COSY	:	Correlation Spectroscopy
HMBC	:	Heteronuclear Multiple Bond Correlation
HSQC	:	Heteronuclear Single Quantum Correlation
Hz	:	Hertz
HR-EI-MS	:	High Resolution Electron Impact Mass Spectrum
HR-ESI-MS	:	High Resolution ElectroSpray Ionization Mass Spectrometry
HR-FAB-MS	:	High Resolution Fast Atom Bombardment Mass Spectrometry
HPLC	:	High-Performance Liquid Chromatography
GC	:	Gas Chromatography
GC-MS	:	Gas Chromatography-Mass Spectrometry
IR	:	Infra Red
UV	:	Ultraviolet
MS	:	Mass Spectrometry
J	:	Coupling constant
m	:	multiplet
MHz	:	Megahertz
NOESY	:	Nuclear Overhauser Effect Spectroscopy

mp	:	Melting point
ppm	:	Part per million
^{13}C NMR	:	Carbone 13 Nuclear Magnetic Resonance spectroscopy
^{1}H NMR	:	Proton Nuclear Magnetic Resonance spectroscopy
NADH	:	Nicotinamide adenine dinucleotide
WHO	:	World Health Organization
UDP	:	Uridine 5-Diphosphate
NGF	:	Nerve Growth Factor
AVAs	:	Avenanthramides
4CL	:	4-Coumarate-CoA Ligase
CCoAOMT	:	Caffeoyl-CoA O-MethylTransferase
PAL	:	Phenylalanine Ammonia Lyase
C4H	:	Cinnamic acid 4-Hydroxylase
HHT	:	Hydroxyanthranilate N-HydroxycinnamoylTransferase
OECD		Organisation for Economic Co-operation and Development

LIST OF TABLES

Table 1: Some areas in Cameroon where *D. edulis* is highly distributed ---------- 6
Table 2: The traditional uses of *D. edulis* ---------- 7
Table 3: Classification of *C. adolphi-friderici* ---------- 9
Table 4: Traditional uses of some medicinal plants from genus *Celtis* ---------- 9
Table 5: Biological activities reported on *D. edulis* ---------- 12
Table 6: Compounds isolated from *D. edulis* ---------- 12
Table 7: Some identified compounds from *D. edulis* using GC-MS analysis ---------- 13
Table 8: Biological activities reported on *Celtis* species ---------- 15
Table 9: Some amide alkaloids from *Celtis* species ---------- 16
Table 10: Some phenolics compounds from *Celtis* species ---------- 17
Table 11: Some triterpenoids from *Celtis* species ---------- 17
Table 12: ^{1}H and ^{13}C-NMR Data of CAF2 ---------- 45
Table 13: ^{1}H and ^{13}C-NMR data of CAF14 and *trans-N*-feruloyloctopamine ---------- 52
Table 14: ^{1}H and ^{13}C-NMR data of CAF7 and *trans-N*-feruloyltyramine ---------- 55
Table 15: ^{1}H and ^{13}C-NMR data of CAF8 and *trans-N*-coumaroyltyramine ---------- 57
Table 16: ^{1}H-NMR data of CAF9 and azelaic acid ---------- 59
Table 17: ^{1}H-NMRdata of CAF13 ---------- 61
Table 18: ^{1}H and ^{13}C-NMR data of CAF10 and indole 3-carboxaldehyde ---------- 63
Table 19: ^{1}H-NMR data of CAF12 ---------- 65
Table 20: ^{1}H-NMR data of CAF3 ---------- 67
Table 21: ^{1}H-NMR data of CAF15 and allantoin ---------- 69
Table 22: ^{1}H and ^{13}C-NMR data of CAF16 ---------- 72
Table 23: ^{1}H and ^{13}C-NMR data of CAF5 and vanillin ---------- 74
Table 24: ^{1}H and ^{13}C-NMR data of CAF11 and Parahydroxybenzoic acid ---------- 75
Table 25: ^{1}H and ^{13}C-NMR data of DE22 and 3,4-dihydroxybenzoic acid ---------- 77
Table 26: ^{1}H and ^{13}C-NMR data of CAF4 ---------- 79
Table 27: ^{1}H and ^{13}C-NMR data of DF5 and glyceryl-1-tetracosanoate ---------- 81
Table 28: ^{1}H and ^{13}C-NMR data of DE2 and lichexanthone ---------- 84
Table 29: ^{1}H and ^{13}C-NMR data of DE10 ---------- 86
Table 30: ^{1}H and ^{13}C-NMR data of DE4 and 3,3′,4-tri-*O*-methylellagic acid ---------- 89
Table 31: ^{1}H-NMR data of DE3 and 3,3'-di-*O*-methylellargic acid ---------- 92
Table 32: ^{1}H and ^{13}C-NMR data of DE21 and 3,3″-di-*O*-methylellargic acid 4-*O*-(3″-galloyl)-*β*-*D*-xylopyranoside ---------- 94
Table 33: ^{1}H and ^{13}C-NMR data of DF3 and auranthiamide acetate ---------- 98
Table 34: ^{1}H and ^{13}C-NMR data of DE7 and confluentic acid ---------- 102
Table 35: ^{1}H and ^{13}C-NMR data of DF6 and ethyl gallate ---------- 105
Table 36: ^{1}H and ^{13}C-NMR data of DE5 and masticaidenonic acid ---------- 107
Table 37: Comparison of ^{13}C-NMR data of DE16 and DE14 with those of *β*-amyrin and *β*-amyrin acetate ---------- 112
Table 38: ^{1}H and ^{13}C-NMR data of CAF1 and friedelin ---------- 114

Table 39: Results of antiplasmodial screening against *Pf*3D7 and *Pf*Dd2 and selectivity on Raw cells lines ---------- 120
Table 40: Effects of administration in rats of DEF extract at a dose of 2000 mg/kg/BW --- 122
Table 41: Antioxidant activity, lipoxygenase, urease and butyrylcholinesterase inhibition of compounds from *C. adolphi-friderici Engl*..---------- 125
Table 42: Chromatogram of fraction F1 ---------- 136
Table 43: Chromatogram of fraction F2 ---------- 136
Table 44: Chromatogram of fraction A1---------- 137
Table 45:Chromatogram of fraction A2 ---------- 137
Table 46: Chromatogram of fraction A3---------- 138
Table 47: Chromatogram of fraction F3 ---------- 138
Table 48: Chromatogram of the *n*-hexane fraction from the stem bark of *D. edulis* --------- 139
Table 49: Chromatogram of the DCM fraction from the stem bark of *D. edulis* ---------- 139
Table 50: Chromatogram of the EtOAc fraction from the stem bark of *D. edulis*---------- 140
Table 51: Chromatogram of the EtOAc fraction from the leaves of *D. edulis* ---------- 141

LIST OF FIGURES

Figure 1: Leaves and fruits of *D. edulis* (a), *D. klaineana* (b) *D. igaganga* (c) and *D. vahl* (d) 5
Figure 2: A map showing the distribution of *D.edulis* in Africa 6
Figure 3: Tree and fruits of *D. edulis* 7
Figure 4: Tree and stem bark of *C. adolphi-friderici* Engl 11
Figure 5: Estimated number of malaria cases 29
Figure 6: Estimated number of malaria deaths 29
Figure 7: Countries with cases in 2000 and their status by 2019. 30
Figure 8: Life-cycle of malaria parasite. 32
Figure 9: HR-ESI (negative mode) mass spectrum of CAF2 47
Figure 10: IR spectrum of CAF2 47
Figure 11: UV spectrum of CAF2 47
Figure 12: ^{1}H-NMR spectrum of CAF2 48
Figure 13: Expanded ^{1}H-NMR spectrum of CAF2 48
Figure 14: ^{13}C-NMR spectrum of CAF2 48
Figure 15: COSY spectrum of CAF2 49
Figure 16: HMBC spectrum of CAF2 50
Figure 17: ESI Mass Spectrum of CAF2 50
Figure 18: GC-MS analysis of FAME from of CAF2 50
Figure 19: EI mass spectrum of CAF14 53
Figure 20: ^{1}H-NMR spectrum of CAF14 53
Figure 21: ^{13}C-NMR spectrum of CAF14 54
Figure 22: HMBC spectrum of CAF14 54
Figure 23: EI mass spectrum of CAF7 56
Figure 24: ^{1}H-NMR spectrum of CAF7 56
Figure 25: EI mass spectrum of CAF8 58
Figure 26: ^{1}H-NMR spectrum of CAF8 58
Figure 27: HR-ESI mass spectrum of CAF9 60
Figure 28: ^{1}H-NMR spectrum of CAF9 60
Figure 29: EI mass spectrum of CAF13 61
Figure 30: ^{1}H-NMR spectrum of CAF13 62
Figure 31: ^{1}H-NMR spectrum of CAF10 63
Figure 32: ^{13}C NMR spectrum of CAF10 64
Figure 33: HMBC spectrum of CAF10 64
Figure 34: EI mass spectrum of CAF12 65
Figure 35: ^{1}H-NMR spectrum of CAF12 66
Figure 36: EI spectrum of CAF3 67
Figure 37: ^{1}H-NMR spectrum of CAF3 67
Figure 38: EI mass spectrum of CAF15 69
Figure 39: ^{1}H-NMR spectrum of CAF15 69
Figure 40: HSQC spectrum of CAF15 70

Figure 41: COSY spectrum of CAF15 70
Figure 42: HMBC spectrum of CAF15 71
Figure 43: EI mass spectrum of CAF16 72
Figure 44: ^{1}H NMR spectrum of CAF16 72
Figure 45: HMBC spectrum of CAF16 73
Figure 46: ^{1}H-NMR spectrum of CAF5 74
Figure 47: HMBC spectrum of CAF5 74
Figure 48: EI mass spectrum of CAF11 76
Figure 49: ^{1}H NMR spectrum of CAF11 76
Figure 50: ^{1}H-NMR spectrum of DE22 77
Figure 51: ^{13}C-NMR spectrum of DE22 78
Figure 52: EI mass spectrum of CAF4 79
Figure 53: ^{1}H-NMR spectrum of CAF4 80
Figure 54: HR-ESI mass spectrum of DF5 81
Figure 55: ^{1}H NMR spectrum of DF5 82
Figure 56: ^{13}C-NMR spectrum of DF5 82
Figure 57: HMBC spectrum of DF5 82
Figure 58: HR-ESI mass spectrum of DE2 84
Figure 59: ^{1}H-NMR spectrum of DE2 85
Figure 60: ^{13}C-NMR spectrum of DE2 85
Figure 61: HMBC spectrum of DE2 85
Figure 62: ESI mass spectrum of DE10 87
Figure 63: ^{1}H-NMR spectrum of DE10 87
Figure 64: Comparative ^{13}C NMR spectra of DE2 and DE10 88
Figure 65: HR-ESI Mass spectrum of DE4 90
Figure 66: ^{1}H-NMR spectrum of DE4 90
Figure 67: ^{13}C-NMR spectrum of DE4 90
Figure 68: HMBC spectrum of DE4 91
Figure 69: HR-ESI mass spectrum of DE3 92
Figure 70: ^{1}H-NMR spectrum of DE3 93
Figure 71: HR-ESI mass spectrum of DE21 95
Figure 72: ^{1}H-NMR spectrum of DE21 96
Figure 73: ^{13}C-NMR spectrum of DE21 96
Figure 74: COSY spectrum of DE21 96
Figure 75: HMBC spectrum of DE21 97
Figure 76: HR-ESI mass spectrum of DF3 99
Figure 77: ^{1}H NMR spectrum of DF3 99
Figure 78: COSY spectrum of DF3 99
Figure 79: HMBC spectrum of DF3 100
Figure 80: HR-ESI mass spectrum of DE7 103
Figure 81: ^{1}H-NMR spectrum of DE7 103
Figure 82: COSY spectrum of DE7 104
Figure 83: HMBC spectrum of DE7 104
Figure 84: ^{1}H-NMR spectrum of DF6 106

Figure 85: HR-ESI mass spectrum of DE5 107
Figure 86: ^{1}H-NMR spectrum of DE5 108
Figure 87: ^{13}C-NMR spectrum of DE5 108
Figure 88: HMBC spectrum of DE5 108
Figure 89: HR-ESI Mass spectrum of DE14 110
Figure 90: ^{1}H-NMR spectrum of DE14 110
Figure 91: ^{13}C NMR spectrum of DE14 110
Figure 92: COSY spectrum of DE14 111
Figure 93: ^{1}H-NMR spectrum of DE16 113
Figure 94: EI mass spectrum of CAF1 115
Figure 95: ^{1}H-NMR spectrum of CAF1 115
Figure 96: ^{13}C-NMR spectrum of CAF1 115
Figure 97:^{1}H NMR spectrum of DE8 116
Figure 98: ^{13}C NMR spectrum of DE8 117
Figure 99: Effects of the aqueous extract of DEF on the weight development in acutely toxic rats 123
Figure 100: Effects of aqueous DEF extract on the relative weight of organs in acute toxicity 124
Figure 101: Pre-formulation of a phytodrug against malaria 128

LIST OF SCHEMES

Scheme 1: The basic mechanism for the biosynthesis of sphinganine sphingamine (dihydrosphingamine) 20
Scheme 2: Process to transform sphinganine to ceramide 20
Scheme 3: Process from ceramide to cerebroside 21
Scheme 4: The complete biosynthetic pathway of three major avenanthramides in oat 25
Scheme 5: Extraction and isolation of compounds from stem bark of *D. edulis* 40
Scheme 6: Extraction and isolation of compounds from leaves of *D. edulis* 40
Scheme 7: Extraction and isolation of compounds from the roots of *C. adolphi-friderici* 42
Scheme 8: Methanolysis of CAF2 45

ABSTRACT

Pending the development of an effective vaccine for everyone, antimalarials remain the only way to fight against the mortality and morbidity generated by parasites. Despite the antimalarial arsenal currently on the market, the problems of parasite resistance to drugs make research and development of new active ingredients permanent. Previous research has shown that medicinal plants are an important source of active ingredients. These active ingredients in their different forms (extracts, fractions, pure compounds) could be used to justify the use of the plants from which they are derived in traditional pharmacopoeia or to suggest other valuation axes. They could also be used as a raw material for the development of phytomedicines or in the case of isolated pure compounds, as candidates for drug development or as a source of inspiration for their designs. It is in this spirit that, within the framework of this thesis, we undertook the chemical study and the evaluation of the antiplasmodial activity of two Cameroonian medicinal plants: *D. edulis* (G. Don) HJ Lam (Burseraceae) and *C. adolphi- friderici* Engl (Cannabaceae). *D. edulis* is used in traditional medicine to treat fever, headache, malaria, while *C. adolphi-friderici* is used to treat cough, fever, headache, tuberculosis and eye pain. The study of the different parts of these two plants by liquid-liquid, solid-liquid partition and column chromatography has led to the isolation of thirty-one compounds, including a new cerebroside. Structural elucidation was performed mainly by high resolution mass spectrometry and nuclear magnetic resonance spectroscopy 1D (^{1}H and ^{13}C) and 2D (COSY, HMQC, HSQC, HMBC and NOESY). The isolated compounds were grouped into different classes including 1 cerebroside, 5 triterpenoids, 2 steroids, 2 xanthones, 3 derivatives of ellagic acid, 1 depside, 2 dicarboxylic acids, 6 phenolic compounds (including 3 phenolic amides), 1 auranthiamide acetate, 2 triglyceryls, 2 fatty acids, 1 gallic acid derivative, 1 indole alkaloid, 1 carbamide, 1 amino acid. From the stem bark of *D. edulis*, lichexanthone, griseoxanthone C, 3,3'-di-*O*-methylellagic acid, 3,3',4-tri-*O*-methylellagic acid, 3,3″-di-*O*-methylellagic 4-*O*-(3″-galloyl)-*β*-*D*-xylopyranoside acid, 3,4-dihydroxybenzoic, confluentic acid, 3-oxo-lanosta-7,24-*Z*-dien-26-oic, *β*-amyrin, *β*-amyrin acetate, and the mixture of *β*- and *α*-amyrin were isolated. In addition, ethyl gallate, auranthiamide acetate, glyceryl-1-tetracosanoate, mixture of *β*-sitosterol and stigmasterol, *β*-sitosterol-3-*O*-*β*-*D*-glucopyranoside were isolated from the leaves of *D. edulis*. A new cerebroside: eloundemnoside and fourteen known compounds including vanillin, hydroxybenzoic acid, allantoin, azelaic acid, sebacic acid, *trans*-*N*-feruloyloctopamine, *trans*-*N*-feruloyltyramine, *trans*-*N*-coumaroyltyramine, friedeline, glycerol 1-octadecanoate, indole 3-carboxaldehyde, aspartic acid, heptacosanoic

acid and laceroid acid have been isolated from the roots of *C. adolphi-friderici*. It is important to note that all compounds except steroids were isolated from *D. edulis* for the first time. Likewise, the compounds isolated from *C. adolphi-friderici* are obtained for the first time from this species. In addition, lichexanthone, griseoxanthone C, confluentic acid, auranthiamide acetate , glyceryl-1-tetracosanoate and 3,3″-di-*O*-methylellagic 4-*O*-(3″-galloyl)-*β*-D-xylopyranoside acid were isolated for the first time from the Burseraceae family. The crude extracts, the fractions and some isolated compounds were tested on the *3D7* sensitive strains and the *Dd2* multiresistant strains to chloroquine of *P. falciparum* (using the protocol described by Smilkstein and collaborators in 2004). The methanolic extract of the stems bark of *D. edulis* showed moderate antiplasmodial activity with IC_{50} values of 9.62 and 6.32 μg/mL, respectively, on *Pf3D7* and *PfDd2*, while the hydroethanolic leaves extract of *D. edulis* showed good antiplasmodial activity with IC_{50} values of 3.10 and 3.56 μg / mL, respectively, on the two strains. The EtOAc fraction of the methanolic extract of the stem bark of *D. edulis* showed the best activity (IC_{50} = 1.44 μg/mL) and led to the isolation of the most active compound: 3,3′,4-tri-*O*-methylellagic acid (IC_{50} = 0.63 μg/mL on the *Dd2* strain). The hexane fraction of the hydroethanolic leaves extract of *D. edulis* also showed good activity (IC_{50} = 2.70; 2.98 μg/mL on *3D7* and *Dd2* strains, respectively). The purification of the EtOAc fraction of the hydroethanolic leaves extract of *D. edulis* led to the isolation of ethyl gallate which exhibited an interesting antiplasmodial activity with IC_{50} values of 1.15 and 2.86 μg/mL on *Dd2* and *3D7* strains, respectively. The acetone extract of *C. adolphi-friderici* roots showed good antiplasmodial activity on *Pf3D7* and *PfDd2* with IC_{50} values of 6.91 and 6.03 μg/mL, respectively. *Trans-N*-feruloyltyramine from *C. adolphi-friderici* showed antiplasmodial activity with an IC_{50} of 23.53 and 18.43 μg/mL, respectively on *Pf3D7* and *PfDd2* the strains. An acute oral toxicity study of the aqueous extract of the leaves of *D. edulis* was carried out in order to verify its safety. The extract was found to be no toxic. The results obtained in the study of these two plants constitute evidence to justify their use in the traditional pharmacopoeia for the treatment of malaria. The preformulation of an antimalarial syrup was carried out on the basis of the results obtained.

Keywords: Malaria, Burseraceae, Cannabaceae, *Dacryodes edulis*, *Celtis adolphi-friderici*, antiplasmodial, eloundemnoside.

RESUME

En attendant le développement d'un vaccin éfficace pour tous, les antipaludéens restent l'unique moyen de lutte contre la mortalité et la morbidité générées par les plasmodies. Malgré l'arsenal antipaludéen actuellement sur le marché, les problèmes de résistance des parasites aux médicaments, rend la recherche et le développement de nouveaux principes actifs permanent. Les travaux de recherches antérieures ont montré que les plantes médicinales constituaient une source importante de principes actifs. Ces principes actifs sous leurs différentes formes (extraits, fractions, composés purs) pourraient permettre, de justifier l'utilisation des plantes dont elles sont issues dans la pharmacopée traditionnelle ou de suggérer d'autres axes de valorisation. Ils pourraient aussi être utilisés comme matière première pour l'élaboration des phytomédicaments ou dans le cas de composés purs isolés, comme candidats pour le développement de médicaments ou comme source d'inspiration pour leurs conceptions. C'est dans cet esprit que nous avons dans cadre de cette thèse entrepris l'étude chimique et l'évaluation de l'activité antiplasmodiale de deux plantes médicinales camerounaises : *D. edulis* (G. Don) H. J. Lam (Burseraceae) et *C. adolphi-friderici* Engl (Cannabaceae). *D. edulis* est utilisé en médecine traditionnelle pour traiter le paludisme, la fièvre, les maux de tête, tandis que *C. adolphi-friderici* est exploité pour le traitement de la toux, de la fièvre, des maux de tête, de la tuberculose et des douleurs oculaires. L'étude des différentes parties de ces deux plantes par partition liquide-liquide, solide-liquide et chromatographie sur colonne, a conduit à l'isolement de trente-un composés dont un nouveau cérébroside. L'élucidation structurale a été réalisée principalement par spectrométrie de masse à haute résolution et spectroscopie de résonance magnétique nucléaire 1D (^{1}H et ^{13}C) et 2D (COSY, HMQC, HSQC, HMBC et NOESY). Les composés isolés ont été regroupés en différentes classes dont 1 cérébroside, 5 triterpénoïdes, 2 stéroïdes, 2 xanthones, 3 dérivés d'acide ellagique, 1 depside, 2 acides dicarboxyliques, 6 composés phénoliques (dont 3 amides phénoliques), 1 acétate d'auranthiamide, 2 triglycéryl, 2 acides gras, 1 dérivé d'acide gallique, 1 alcaloïde indolique, 1 carbamide, 1 acide aminé. À partir de l'écorce de tige de *D. edulis*, la lichexanthone, la griséoxanthone C, les acides 3,3'-di-*O*-méthylellagique, 3,3',4-tri-*O*-méthylellagique, 3,3″-di-*O*-méthylellagique 4-*O*-(3″-galloyl)-*β*-D-xylopyranoside, 3,4-dihydroxybenzoïque, confluentique, 3-oxo-lanosta-7,24-*Z*-dien-26-oique, la *β*-amyrine, l'acétate de *β*-amyrin, et le mélange de *β*- et *α*- amyrin ont été isolé. En outre, le gallate d'éthyle, l'acétate d'auranthiamide, le glycéryl-1-tétracosanoate, le mélange de *β*-sitostérol et stigmastérol, le *β*-sitostérol-3-O-*β*-*D*-glucopyranoside ont été isolés des feuilles de *D. edulis*. Un nouveau cérébroside: l'éloundemnoside et quatorze composés connus dont le vanilline, l'acide hydroxybenzoïque, l'allantoïne, l'acide azélaïque, l'acide sébacique, la *trans*-*N*-feruloyloctopamine, la *trans*-*N*-féruloyltyramine, la *trans*-*N*-coumaroyltyramine, la friedeline, le 1-octadécanoate de

glycérol, le 3-carboxaldéhyde d'indole, les acides aspartique, heptacosanoïque et lacéroïque ont été isolés des racines de *C. adolphi-friderici*. Il est important de noter que tous les composés, à l'exception des stéroïdes, ont été isolés de *D. edulis* pour la première fois. De même les composés isolés de *C. adolphi-friderici* sont obtenus pour la première fois de cette espèce. En outre, la lichexanthone, la griséoxanthone C, l'acide confluentique, l'acétate d'auranthiamide, le glycéryl-1-tétracosanoate et l'acide 3,3″-di-*O*-méthylellagique 4-*O*- (3″-Galloyl)-*β*-*D*-xylopyranoside ont été isolés pour la première fois de la famille des Burseraceae. Les extraits bruts, les fractions et certains composés isolés ont été testés sur la souche sensible *3D7* et la souche multi résistantes *Dd2* à la chloroquine de *P. falciparum* (en utilisant le protocole decrit par Smilkstein *et al*., 2004). L'extrait méthanolique des écorces du tronc de *D. edulis* a montré une activité antiplasmodiale modérée avec des valeurs CI_{50} de 9,62 et 6,32 μg/mL respectivement, sur *Pf3D7* et *PfDd2*, tandis que l'extrait de feuilles hydroéthanolique de *D. edulis* a présenté une bonne activité antiplasmodiale avec des valeurs CI_{50} de 3,10 et 3,56 μg/mL, respectivement, sur les deux souches. La fraction à EtOAc de l'extrait méthanolique des écorces du tronc de *D. edulis* a présenté la meilleure activité (CI_{50} = 1,44 μg/mL) et a conduit à l'isolement du composé le plus actif : l'acide 3,3',4-tri-*O*-méthylellagique (CI_{50} = 0,63 μg/mL sur la souche *Dd2*). La fraction à l'hexane de l'extrait hydroéthanolique des feuilles de *D. edulis* a également présenté une bonne activité (CI_{50} = 2,70 ; 2,98 μg/mL sur les souches *3D7* et *Dd2*, respectivement). La purification de la fraction EtOAc de l'extrait hydroéthanolique des feuilles de *D. edulis* a conduit à l'isolement du gallate d'éthyle qui a présenté une activité antiplasmodiale intéressante avec des valeurs de CI_{50} de 1,15 et 2,86 μg/mL sur les souches *Dd2* et *3D7*, respectivement. L'extrait à l'acétone des racines de *C. adolphi-friderici* a présenté une bonne activité antiplasmodiale sur *Pf3D7* et *PfDd2* avec des valeurs CI_{50} de 6,91 et 6,03 μg/mL, respectivement. La *trans*-*N*-féruloyltyramine de *C. adolphi-friderici* a montré une activité antiplasmodiale avec des valeurs CI_{50} de 23,53 et 18,43 μg/mL, respectivement sur les souches *Pf3D7* et *PfDd2*. Une étude de toxicité orale aiguë de l'extrait aqueux des feuilles de *D. edulis* a été réalisée afin de vérifier son innocuité. L'extrait s'est avéré être non toxic. Les résultats obtenus lors de l'étude de ces deux plantes constituent des éléments permettant de justifier leur utilisation dans la pharmacopée traditionnelle pour le traitement du paludisme. La préformulation d'un sirop antipaludique a été réalisée sur la base des résultats obtenus.

Mots clés: Paludisme, Burseraceae, Cannabaceae, *Dacryodes edulis*, *Celtis adolphi-friderici*, antiplasmodial, éloundemnoside.

GENERAL INTRODUCTION

Since time immemorial, plants have been used as food for the animals and humans that inhabit the earth. But beside this nutritional value, Man discovered many other functions that plants could provide, notably the healing power. Indeed, plants have very interesting biological properties, which find applications in various fields such as medicine, pharmacy, cosmetics and agriculture (Teixeira de silva, 2004). Therefore, plants remain an important source of curative substances to humans in the fight against multiple diseases plaguing his existence on planet earth. Traditionally, medicines were prepared from plants in the past centuries by different scholars or researchers and from various time periods to obtain medicinal cures with good properties. The use of plants in traditional medicine systems has been extensively documented by different cultures in the world (Cragg *et al*., 2011). The plant-based system is continuously playing a significant role in the healthcare sector in Africa and the world at large. In 2015, WHO has estimated that, about 80% of the world's population relies on traditional medicines. For hundreds of years now, plants have been the basis of traditional medicine systems and recently natural products have been a reliable source of compounds for drug development. A good example of this plant-based medicine against malaria is quinine, which was isolated from *Cinchona officinalis* bark and was used as a template for the synthesis of chloroquine and mefloquine (Witchi and Anton, 2003). Recently, artemisinin isolated from a Chinese plant *Artemisia annua*, has been used successfully against chloroquine-resistant *Plasmodium falciparum* strains (Schwikkard and Van-Heerden, 2006). Plants are used in the treatment of ailments such as cancer, fever, skin diseases, dysentery and malaria (Ominyi *et al*., 2018). Among these ailments malaria is one of the most plaguing ailments in Africa today (Arjen *et al*., 2017).

Malaria is a life-threatening disease caused by parasites transmitted to humans by infected female mosquito bites. WHO in 2019 has estimated that, there were 229 million cases of malaria in the world as compared to the previous year's audit. Malaria has been responsible of the death of more than 409,000 people each year, largely in Africa. It remains the leading cause of morbidity in Cameroon, and among the top five causes of mortality, malaria represents in 2019 approximately 25.8% of health consultations, and 14.3% of death (NMCP, 2020).

Unfortunately, many drugs used for the treatment of malaria have been reported to face parasites resistance which leading to treatment failure in significant number of cases. Despite extensive efforts to control and roll back malaria, thousands of people continue to die from

malaria. This control became difficult due to the increase of resistance that vectors and parasites developed towards the currently used molecules (Kamkumo *et al*., 2012). There is a constant need to develop new drugs which new mechanism of action for the treatment of malaria. Because of this resistance or due to their socio-cultural conveniences many populations used medicinal plants for their primarily healthcare. In order to validate the use of those medicine plants in the treatment of malaria, researchers worldwide focused their research on their chemical compositions and their pharmacological properties. In the same research line, we are interested in Cameroonian medicinal plants used in the treatment of malaria.

In Cameroon pharmacopeia, plants are widely used in the treatment of malaria and several other diseases, particularly in areas where access to conventional medicine is limited (Kuete and Efferth, 2010). Bark, fruits and leaves of *C. adolphi-friderici* Engl, are taken in folk medicine in Cameroon to treat severe cough, fever, headache, tuberculosis, and sore eyes (Poorter *et al.*, 2004). *D. edulis* is a species widely distributed in Cameroon, it is used in traditional medicine for the treatment of fever/headaches and malaria (Uhunmwangho *et al*., 2018; Zofou et al., 2013) and leprosy (Miguel et al., 2017).

The choice of these plants was motivated by the fact that *D. edulis* has been reported to display a significant antiplasmodial activity on *PfDd2* strain with an IC_{50} value of 6.43 $\mu g/mL$ (Zofou *et al*., 2013). Species from *Celtis* genus (*Celtis tessmannii*) are used against malaria in Cameroonian folk medicine (Titanji *et al*., 2008). And only a few chemical studies have so far been carried out on *D. edulis* and *C. adolphi-friderici*.

The general objective of this work was to obtain active and no toxic extracts and/or fractions which can be used as a raw material for the preparation of phytomedicines and to isolate their secondary metabolites that can be used as leads for the development of new drugs against malaria.

More specifically, this work consisted to :

- prepare extracts and to screen them for their antiplasmodial activities;
- perform fractionation and screen the fractions for the antiplasmodial activity;
- Isolate, characterize secondary metabolites and evaluate their antiplasmodial activity;
- Evaluate the toxicity of the most active extract**.**

In the first chapter, we will present a literature review on the studied plant as well as on malaria an overview on cerebrosides. The second chapter will disclose the results and discussion while the last chapter will summarize the methodology used for the study.

CHAPTER I: LITERATURE REVIEW

I.1 BOTANICAL STUDY ON THE BURSERACEAE AND CANNABACEAE FAMILY

I.1.1 Overview on the Burseraceae family

Burseraceae is a family of flowering plants mostly distributed throughout the tropical or subtropical regions of the world, composed of about 19 genera of resinous trees and shrubs comprising around 700 species (Murthy *et al*., 2016). The trees and shrubs of Burseraceae family have in their stem bark prominent vertical schizogenous resin ducts, containing various secondary metabolites (Murthy *et al*., 2016). A majority of available ethnomedicinal information is limited to Asiatic and African genera, such as *Commiphora*, *Canarium*, *Boswellia*, *Bursera*, *Protium* and *Dacryodes* (Veiga *et al*., 2007). Burseraceae family is mostly represented by the genus *Protium* in the neotropics with about 135 species (Veiga *et al*., 2007).

I.1.1.1 Overview on *Dacryodes* genus

The genus name *Dacryodes* comes from the Greek word "Dakruon" that means tear. Most of these species are entirely woody, small to large trees but few are shrubs (Murthy *et al*., 2016). They are flowering plants, widely distributed throughout the tropical or subtropical regions of the world. In its natural habitat in Africa, these species start flowering from January to April followed by the major fruiting season between May and October, the minor fruiting season is between November and March. Their trees/shrubs are about 10-70 m height (Figure 1) (Orwa *et al*., 2009).

There are approximately 142 species from the genus *Dacryodes* with around 70 species distributed in the humid tropical forests of America (22 species and 14 species which have not yet been described), South and Central Africa (18 species) and South-East Asia (18 species) (Tee *et al*., 2014). We can list *D. edulis* (a), *D. klaineana* (b) *D. igaganga* (c) and *D. excelsa vahl* (Figure 1).

Figure 1: Leaves and fruits of *D. edulis* (a), *D. klaineana* (b) *D. igaganga* (c) and *D. vahl* (d) (https:\\www.wikiwand.com/en/Dacryodes/)

I.1.1.2 Overview on *D. edulis*

I.1.1.2.1 Botanical description of *D. edulis*

D. edulis is a dioeciously shade loving species of non-flooded forests in the humid tropical zone. It is locally called "native pear, bush butter tree, African plum and African pear" by the English speaking and "safoutier or prunier" by the French speaking (Jecinta *et al*., 2015). The Cameroonian species is an evergreen fruit tree, of medium-size reaching 18-40 m in forest but not exceeding 12 m in farm. It is generally branched from low down with a deep dense crown. The fruit is red, turning blue-black when ripe with unpleasant turpentine smell. The leaves are pinnate with leaflets measuring 3 to 4 cm by 23 cm. The leaflets are glabrous narrowly oblong and elliptic (Figure 3) (Orwa *et al*., 2009).

I.1.1.2.2 Systematic position of *D. edulis* in Africa.

D. edulis is a fruit tree that grows naturally in the rainforests of Central Africa, Gulf of Guinea and the Congo Basin regions (Miguel *et al*., 2017). The popularity of "safou" fruit (boiled or roasted for consumption) has led to its widespread cultivation, extending its area of distribution to Sierra Leone in the West, Uganda in the East and Angola in the South. The species occurs mainly throughout Gabon especially towards the Atlantic Coast, Equatorial Guinea and mostly in the forests of South and South-West Cameroon (Todou *et al*., 2013). The

African distribution is as shown in figure 2 and the presence of this species in Cameroon is resumed in table 1.

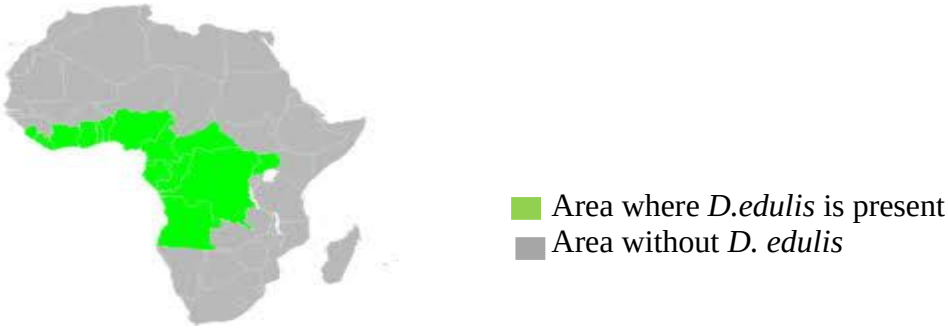

Figure 2: A map showing the distribution of *D.edulis* in Africa (https:\\www.wikiwand.com)

Table 1: Some areas in Cameroon where *D. edulis* is highly distributed (Todou *et al*., 2013)

Administrative unit	Location
South region	Bipindi (Ngovayang forest) Kribi
Center region	Eséka, Makenene
Littoral region	Yingui and Yabassi
East region	Reserve of Dja Reserve forest of Mokoko Rhumpi mounts
South-West region	Mamfe Bakossi
North-west region	Bali
West region	In all the departments

I.1.1.2.3 Systhematic classification of *D. edulis* (Miguel *et al*., 2017).

The plant *D. edulis* is classified as shown below.

Kingdom: Plantae– Plants

Superdivision: Angiospermatophyta– Seed plants

Division: Magnoliophyta– Flowering plants

Class: Magnoliopsida– Dicotyledons

Subclass: Rosidae

Order: Sapindales

Family: Burseraceae

Genus: *Dacryodes*

Species: *Dacryodes edulis* (G. Don) H.J. Lam


Figure 3: Tree and fruits of *D. edulis* (picture taken by DONGMO in 2018)

I.1.1.2.4 Ethnomedicinal uses of *D. edulis*

D. edulis is a versatile plant in African traditional medicine, as its various parts are employed for the treatment of several diseases. Table 2 shows some uses.

Table 2: The traditional uses of *D. edulis*

***D.* edulis**	**Used part**	**Preparation and treatment (Reference)**	**Country**
D. edulis	Leaves	- Leaves are chewed with kola nut as an antivomiting (Bouquet *et al*., 1969). - The leaf sap is used as ear drop to treat ear problem and vapour produced by leaf decoction is used to treat fever and headache (Bouquet *et al*., 1969).	Democratic Republic of Congo
	Bark	-The bark resin is used in Nigeria to treat parasitic skin disease (Jecinta *et al*., 2015)	Nigeria
	Leaves	-The leaves are often crushed and juice is used to treat generalized skin diseases such as ringworm, scabies, rashes jiggers (Jecinta *et al*., 2015)	
	Stem	-Stem and stem twigs are used as chewing sticks for oral hygiene (Igoli *et al*., 2005)	
	Bark	-The Bark is used for treating wounds (Jecinta *et al*., 2015).	Gabon
		-The Bark is crushed and used in concoctions against dysenteries and toothache (Uhunmwangho *et al*., 2018)	Cameroon
	Leaves and stem bark	- Leaves and the stem bark are boiled with leaves of *Cymbopogon citratus* and *Mangifera indica* in water to give a decoction against malaria (Zofou *et al*., 2013).	
	Leaves	The leaves are boiled in combination *with Lantana camara*, *Cymbopogon citratus* and *Persea americana*	

		yielding a steam bath taken to treat fever/headaches and malaria (Uhunmwangho *et al*., 2018)	Democratic Republic of Congo
	Bark	-The decoction of the bark is used in the treatment of leprosy (Miguel *et al*., 2017)	
	Leaves	-The leaves are crushed and used as plaster to treat snake bites (Miguel *et al*., 2017; Agbo *et al*., 2017).	Cameroon

I.1.1.2.5 Social-economic and nutritional importance of *D. edulis*

The fruits of *D. edulis* are delicious and good source of lipids. There are sold in local markets and have attracted international trade. Its wood is generally used for carpentry, tool handles such as axe, holes etc, and occasionally for construction (Ajibesin. 2011). The stem exudates serve as glue, cosmetic components, or for lighting. Essential oils from the fruit are rich in amino acids, triglycerids and can increase common household oils. Ikhuoria and collaborators in 2007, reported that at the level of international markets, African pear fruits imported to Europe are generally intended for nationals of the exporting countries with the volume increasing since 1982. Thus, it serves as source of income for exporting countries (Zofou *et al*., 2013).

I.1.2. Overview on the Cannabaceae family

Cannabaceae is a large family of flowering plants containing about 15 genera and approximately 200 species of trees and shrubs distributed throughout the temperate and tropical regions of the world (Zavada, 1983). Members of this family can be trees, erect herbs or twining herbs (Zhou *et al*., 2003).

Leaves are often more or less palmately lobed and always bear spitules. Flowers are actinomorphic and not showy as these plants are pollinated by the wind. These flowers are grouped to form cymes (Zhou *et al*., 2003). Cannabaceae has many genus including *Cannabis*, *Aphananthe*, *Humulus* and *Celtis*.

I.1.2.1 Overview on the *Celtis* genus

The genus *Celtis* has a large number of synonyms and is distributed in the tropics, extending to temperate regions (Berg and Dahlberg, 2001; Yang *et al*., 2013). Species are distributed in Africa, Asia, and the Neotropical region from Texas (USA) to Argentina (Sattarian, 2006). This genus is represented by about 60-70 species including: *C. australis*, *C. integrifotia*, *C. adolphi-friderici*. The table 3 below resumes the classification of *C. adolphi-friderici*.

Table 3: Classification of *C. adolphi-friderici* (Poorter *et al*., 2004)

Kingdom: Plantae– Plants

Superdivision: Spermatophyta

Division: Magnoliophyta

Class: Magnoliopsida

Subclass: Hamamelididae

Order: Urticales

Family: Ulmaceae

Genus: *Celtis*

Species: *Celtis adolphi-friderici*

I.1.2.2 Ethnomedicinal uses of species of the *Celtis* genus

Plants belonging to *Celtis* genus are used in traditional medicine for the treatment of many diseases table 4 summarizes some uses.

Table 4: Traditional uses of some medicinal plants from genus *Celtis*

Celtis species	Used part	Preparation and treatment (reference)	Country
C. tessmannii R.	Bark	Bark decoction are used to treat dysentery (Ngueyem, 2008).	Cameroon
	Leaves	Leaves are used to treat malaria (F.A.O, 1999).	
C. australis	Leaves and fruits	Decoction of both leaves and fruits is used in the treatment of amenorrhea, heavy menstrual and inter-menstrual bleeding, diarrhea, dysentery and peptic ulcers (Showkat *et al*., 2012).	Indian
	Bark	Paste obtained from the bark is considered as an important remedy for bone fracture and also applied on pimples, contusions, sprains and joint pains (Gaur *et al*., 1999).	
	All parts	It is commonly called "Taghzaz" and it is mainly used to treat gastro-intestinal ailments (Bellakhdar, 1997).	Morocco
C. africana Burm.	Leaves	Leaves are used as a traditional human and veterinary medicine for the treatment of indigestion and edema (Krief *et al*., 2005).	South Africa
		The sun-dried bark and roots are powdered and infused in water or milk and taken orally every	

	Bark and roots	day by the patients for the treatment of cancer (Koduru et al., 2007).	
C. mildbraedi	Bark	Bark decoctions are used as wash to invigorate seriously weakened babies (Oyen, 2012).	Cameroon
	Root	Root ash mixed with palm oil is applied to scarifications as a treatment of headache (Oyen, 2012).	
C. occidentalis	Wood	Wood decoction is used for the treatment of jaundice (Metcalfe *et al*., 1950)	North America
C. eriocarpa Decne.	Leaves	Decoction of leaves is used against amenorrhoea (AHMED *et al*., 2018)	Indo-Pak subcontinent
	Fruits	They are used against colic (AHMED *et al*., 2018)	
	Bark	Powdered bark is used to treat pimples, sprain, and joint pain (AHMED *et al*., 2018)	
C. adolphi-friderici	Bark	Decoction of the bark is taken to treat general malaise, severe cough, fever and headache (Poorter *et al.*, 2004)	West African
	Fruits	They have been used to treat tuberculosis (Poorter *et al.*, 2004)	

I.1.2.3 Overview on *C. adolphi-friderici*

C. adolphi-friderici Engl is a semi-deciduous tree, usually growing up to 35 m tall, but with specimens up to 50 m which have been recorded. The straight, cylindrical bole of up to 30 m. tall and 100 cm diameter can be unbranched; it has wide spreading buttresses up to 2 m high (Figure 4). The tree is harvested from the wild, mainly for local use as a medicine and source of wood. The wood is occasionally exported (Burkil H. M., 1985). It is commonly known in Center region of Cameroon as “odou” by the Ewondo tribe. It is a widespread common semi-deciduous tree in Cameroon where its bark, fruits and leaves are taken in folk medicine to treat severe cough, fever, headache, tuberculosis, and sore eyes (Poorter *et al*., 2004).

Figure 4: Tree and stem bark of *C. adolphi-friderici* Engl (picture taken by DONGMO in 2019)

I.1.2.4 Economical uses of species of the *Celtis* genus

The wood of *C. mildbraedii*, traded as "African Celtis", is used for a variety of purposes. Traditionally, it is used for poles in house building and for pestles, tool handles and spoons. The wood is suitable for heavy construction, flooring, joinery, interior trim, mine props, railway sleepers, ship building, vehicle bodies, furniture, ladders, sporting goods, boxes, crates, agricultural implements, veneer, plywood, hardboard, and particle board. It is an excellent firewood, burning slowly (Oyen, 2012). In China, oil obtained from the seed of *C. philippensis* is edible (Keeler and Harriet, 2005).

The wood of *C. adolphi-friderici* is used for the fabrication of boxes of matches (Oyen, 2012).

I.2 PREVIOUS PHARMACOLOGICAL AND CHEMICAL STUDIES ON THE STUDIED SPECIES

Plants belonging to *Dacryodes* and *Celtis* genus are widely used in traditionnal medecine for the treatment of many diseases. Given this fact, several researchers around the world have undertaken biological and chemical studies on these species.

I.2.1 Previous pharmacological studies on *D. edulis*

Previous pharmacological studies on *D. edulis* have shown several biological activities such as antimalarial, antifungal, antidiabetic, antioxidant, antibacterial etc. Table 5 summarizes some activities.

Table 5: Biological activities reported on *D. edulis*

Species	Used part	Biological activities	References
D. edulis	Leaves	Antimicrobial	Nwokwonkwo *et al*., 2014
		Antibacterial	Nna *et al*., 2017.
		Antidiabetic	Zofou *et al*., 2013
		Antioxidant	Anyam *et al*., 2015
	Bark	Anticancer	Tee *et al*., 2014
		Antimalarial	Zofou *et al*., 2013
	Resin	Antidrepanocytary activity	Agbo *et al*., 2017
		Antiulcer	Nna *et al*., 2017
	Root/bark	Antifungal	

I.2.2 Previous chemical investigation on the *D. edulis*

Previous chemical screening of the methanol extracts obtained from stem bark of *D. edulis* resulted in the identification of alkaloids, steroid/triterpenoids, phenols, reducing sugars, cardiac glycosides, flavonoids, saponins, tannins, and anthraquinones (Nna *et al*., 2017; Ogboru *et al*., 2015). The table 6 shows the isolated compounds from the methanol extracts obtained from stem bark of *D. edulis* and table7, some identified compounds from *D. edulis* using GC-MS analysis.

Table 6: Compounds isolated from *D. edulis*

Classes	Structures/ names	References
Flavonoids	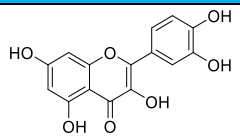 **1**: Quercetin	Zofou *et al*., 2013
	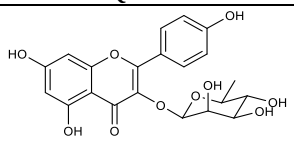 **2**: Afzelin	
	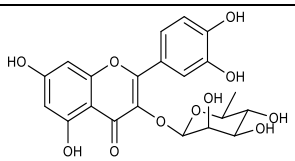 **3**: Quercitrin	

Steroids	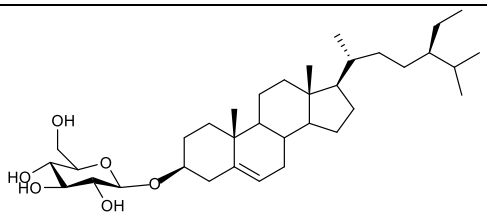 **4**: *β*-sitosterol-3-*O*-*β*-*D*-glucopyranoside	Zofou *et al.*, 2013
Phenols	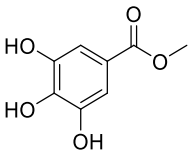 **5**: Methyl 3,4,5-trihydroxybenzoate	

Table 7: Some identified compounds from *D. edulis* using GC-MS analysis

Classes	Structures/ Names	References
Carboxylic acid	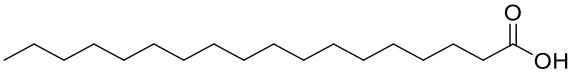 **6**: Stearic acid	Okwu *et al.*, 2009; Ochuko *et al.*, 2017
	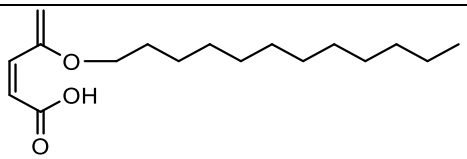 **7**: (*Z*)-4-(dodecyloxy)penta-2,4-dienoic acid	Okwu *et al.*, 2009
	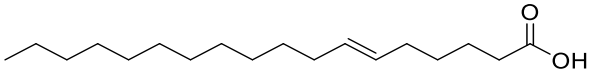 **8**: (*E*)-Octadec-6-enoic acid	
Alkane	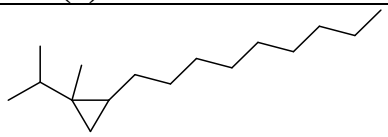 **9**: 1-Isopropyl-1-methyl-2-nonylcyclopropane	
Alkene	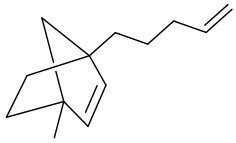 **10**: 1-Methyl-4-(pent-4-enyl)bicyclo[2.2.1]hept-2-ene	
	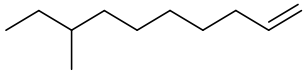 **11**: 8-Methyldec-1-ene	
	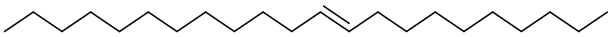 **12**: (E)-Docos-10-ene	
Ketone	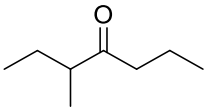 **13**: 3-Methylheptan-4-one	

Alkaloid	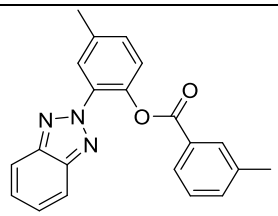 **14**: 2-(2H-1,2,3-Benzotriazo 1-2-yl)-4-methyl phenyl-3-benzoate	Okwu *et al.*, 2009
Triterpenoid	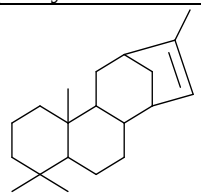 **15**: Kaur-15-ene	Ochuko *et al.*, 2017
	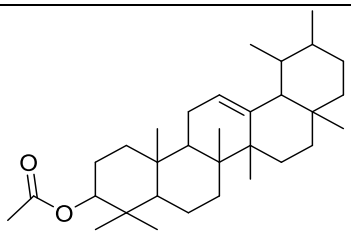 **16**: *α*-Amyrin acetate	
	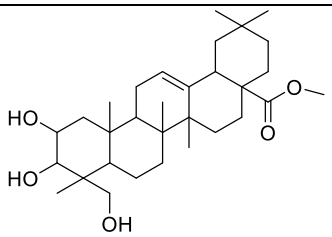 **17**: 2,3,23-Trihydroxyolean-12-en-28-oic acid methylester	
Sterol	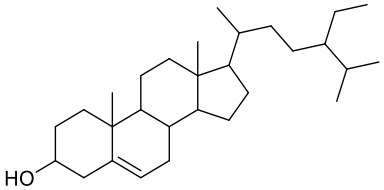 **18**: Sitosterol	
Xanthone	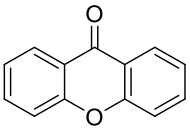 **19**: Xanthone	
	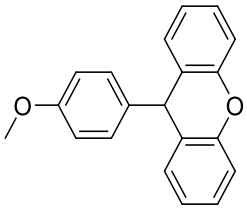 **20**: 9-(4-Methoxyphenyl)xanthene	

Esther	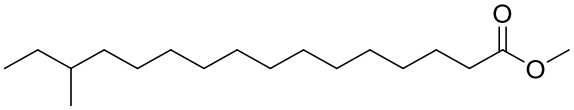 **21**: 14-methylhexadecanoate methyl ester	Ochuko *et al*., 2017
	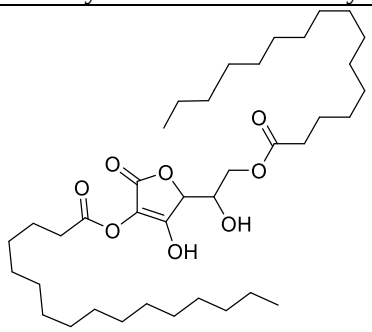 **22**: (+) L-Ascorbic acid,2,6-dihexadecanoate	Okwu *et al*.,2009 and Ochuko *et al*., 2017
Alcohol	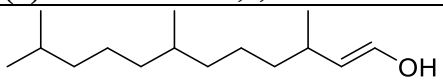 **23**: (*E*)-3,7,11-Trimethyldodec-1-en-1-ol	Ochuko *et al*., 2017
	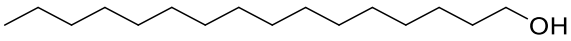 **24**: Hexadecan-1-ol	Okwu *et al*.,2009
Alcohol	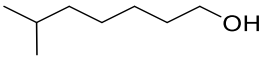 **25**: 6-Methylheptan-1-ol	

I.2.3 Previous pharmacological studies of *Celtis* genus

Previous pharmacological study on *Celtis* genus have showed several biological activities such as antioxidant, antimicrobial, anti-inflammatory etc. Those activities are summarized in the table 8.

Table 8: Biological activities reported on *Celtis* species

***Celtis* species**	**Used part/ compounds**	**Biological activities**	**References**
C. africana	*trans*-*N*-coumaroyltyramine (**26**) *trans*-*N*-feruloyltyramine (**27**) *trans*-*N*-caffeoyltyramine (**28**)	Antioxidant Antiinflammatory	Al-Taweel *et al*., 2012
	Leaves and stems	Antioxydant	Adedapo *et al*., 2009
C. australis	Vanillic acid (**31**), *β*-sitostérol-3-*O*-glucoside (**71**), *β*-sitostérol (**4**)	Antioxidant Antimicrobial	Filali-Ansari *et al*., 2016
	Leaves (ethanolic extract)	Antioxydant	El-Alfy *et al*., 2011
C. occidentalis	Leaves (ethanolic extract)	Antioxydant	

		Anticancer	
	Leaves (aqueous extract)	Anticancer	
C. toka	Leaves (ethanol extract)	Antioxidant	Alioune *et al.*, 2017
C. iguanaea	Leaves (hexane extract)	anti-ulcerogenic	Martins *et al.*, 2014
C. testimanii	Stem bark	antiplasmodial	Kagho *et al.*, 2020

I.2.4 Previous chemical investigation on the genus *Celtis*

Previous chemical studies done on *Celtis* species have led to isolation of many compounds belonging to many classes of compounds such as steroid/triterpenoids, phenolics compounds, flavonoids, phenolic amides, ceramids, fatty acids and lignans.

I.2.4.1 Phenolic amides

They are groups with proto alkaloids which do not have heterocyclic ring with nitrogen, but also derived from amino acid (Mondal S, 2019). The table 9 below shows some amide alkaloids from *Celtis* species

Table 9: Some amide alkaloids from *Celtis* species

Compounds	Nouns	Species	References
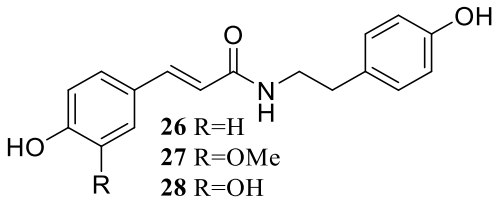	**26**: *trans-N-* coumaroyltyramine **27**: *trans-N-* feruloyltyramine **28**: *trans-N-* caffeoyltyramine	*C. africana* *C. sinensis*	Al-Taweel *et al.*, 2012 ; Kim *et al.*, 2005
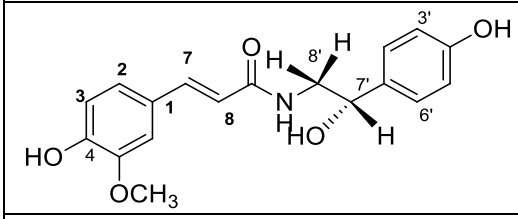	**29**: trans-*N-* feruloyloctopamine	*Acorus tatarinowii Schott*	Ge *et al.*, 2014.
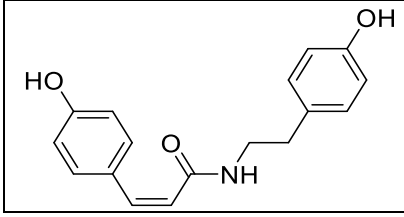	**30**: *Cis-N-* coumaroyltyramine	*C. sinensis*	Kim *et al.*, 2005

I.2.4.2 Phenolics compounds

Phenolic compounds are the main class of secondary metabolites in plants. They are aromatic rings with attached hydroxy groups in their structures (Minatel *et al.*, 2016). Table 10 shows some phenolics compounds from *Celtis* species

Table 10: Some phenolics compounds from *Celtis* species

Compounds	Nouns	Species	References
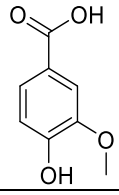	**31**: vanillic acid	*C. australis*	Filali-Ansari *et al.*, 2016
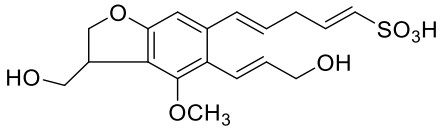	**32**: Celtisanine	*C. australis*	Badoni *et al.*, 2010
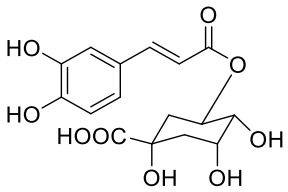	**33**: Chlorogenic acid		

I.2.4.3 Triterpenoids

Triterpenoids are biosynthetically made of six isoprene units and share in common the C_{30} acyclic precursor squalene. Different types of ring closure in skeletal types of triterpenoids. In fact, over 4000 natural triterpenoids have been isolated and more than 40 skeletal types have been identified. The triterpenoids can be divided into two main classes: the tetracyclic and the pentacyclic compounds (Shashi and Ashoke, 1991). Table 11 shows some triterpenoids from *Celtis* species

Table 11: Some triterpenoids from *Celtis* species

Compounds	Nouns	Species	References
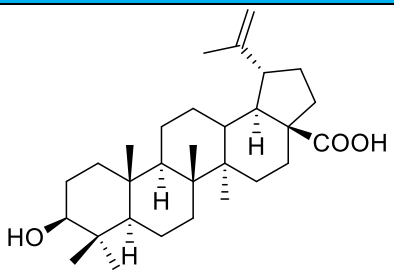	**34**: Betulinic acid	*C. sinensis*	Siddiqui *et al.*, 1988
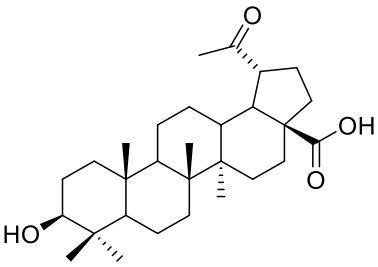	**35**: Platanic acid	*C. phillipensis*	Fujioka *et al.*, 1994

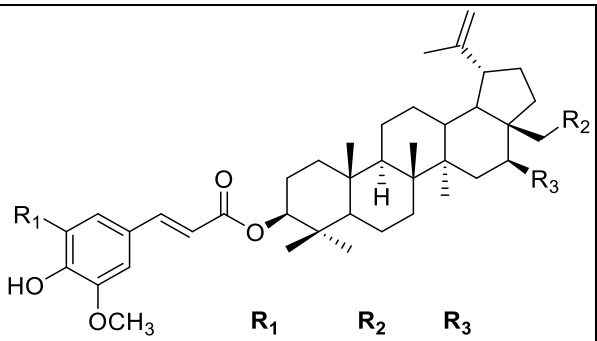 **R1** **R2** **R3** **36** OCH3 OH H **37** H H OH	**36**: 3*β*-*trans*-sinapoyloxylup-20(29)-èn-28-ol **37**: 3*β*-*trans*-feruloyloxy-16*β*-hydroxylup-20(29)-ène	*C. phillipensis*	Hwang *et al.*, 2003
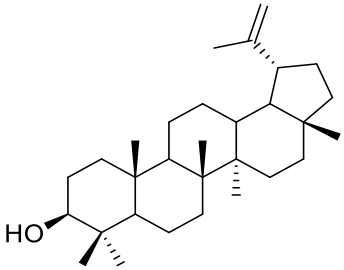	**38**: Lupeol	*C. africana*	Al-Taweel *et al.*, 2012
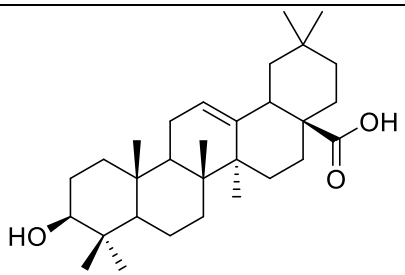	**39**: Oleanolic acid		
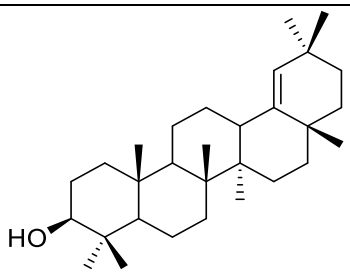	**40**: Germanicol	*C. sinensis*	Kim *et al.*, 2005
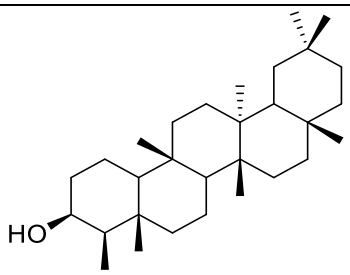	**41**: Epifriedelanol		

Previous works done on these species have led to the isolation of many classes of compounds, we will give a brief overview on some classes of compounds (cerebrosides and phenolic amides).

I.3. OVERVIEW ON SOME SECONDARY METABOLITES

I.3.1 Cerebrosides

I.3.1.1 Definition and general structure

Glycolipids are lipids that contain a sugar moiety. The sugar can be a monosaccharide, oligosaccharide, or polysaccharide (Halter *et al*., 2007). In many cases, the sugar and fatty acid moities are attached to a glycerol or sphingosine backbone to form glyceroglycolipids or glycosphingolipids, respectively. There are four main classes of glycosphingolipids: cerebrosides, sulfatides, globosides and gangliosides. Glycolipids are grouped in the Golgi apparatus by various glycosyltransferases and embedded in the surface of a vesicle. The vesicle is then transported to the cell membrane where it fuses with the cell membrane and is exocytosed out of the cell (D'Angelo *et al*., 2008).

Cerebrosides are family of lipid molecules. Also, called glycosphingolipids, they consist of a ceramide with a single sugar moiety at the 1-hydroxy moiety. The sugar moiety can be either glucose or galactose; the two major types are therefore called glucosylceramides and galactosylceramides. Cerebrosides are called monoglycosylceramides when they have only one sugar (Tan and Chen, 2003). Galactocerebrosides are typically found in neutral tissue, while glucocerebrosides are found in other tissue.

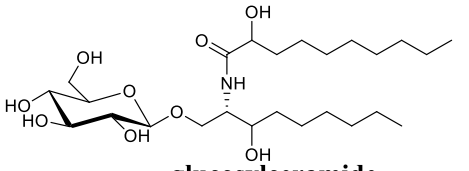

glucosylceramide

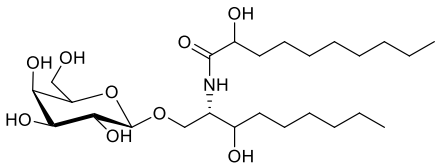

galactosylceramide

I.3.1.2 The Biosynthesis of cerebrosides

Cerebrosides, the simplest neutral glycolipids/glycosphingolipids, have a single sugar that is linked to ceramide (Tan and Chen, 2003). We will first describe the formation of a ceramide following by the formation of the cerebroside.

The condensation of serine and palmitoyl CoA by serine palmitoyl transferase (3-ketosphinganine synthase) produces 3-ketosphinganine (Scheme 1). This is followed by NADPH-dependent reduction of the ketone group of 3-ketosphinganine to form sphinganine. The reaction is catalyzed by the enzyme 3-ketosphinganine reductase. In the next step, sphinganine is condensed with an acetyl CoA molecule to form *N*-acylsphinganine

(dihydroceramide) in a reaction catalyzed by sphinganine *N*-acyltransferase or dihydroceramide desaturase. *N*-acylsphinganine is finally oxidized by *N*-acylsphinganine reductase to form ceramide (*N*-acylsphingosine) (Scheme 2), using FAD as a cofactor. Ceramide is the intermediate from which other sphingolipid subclasses are synthesized (Tafesse *et al*., 2006).

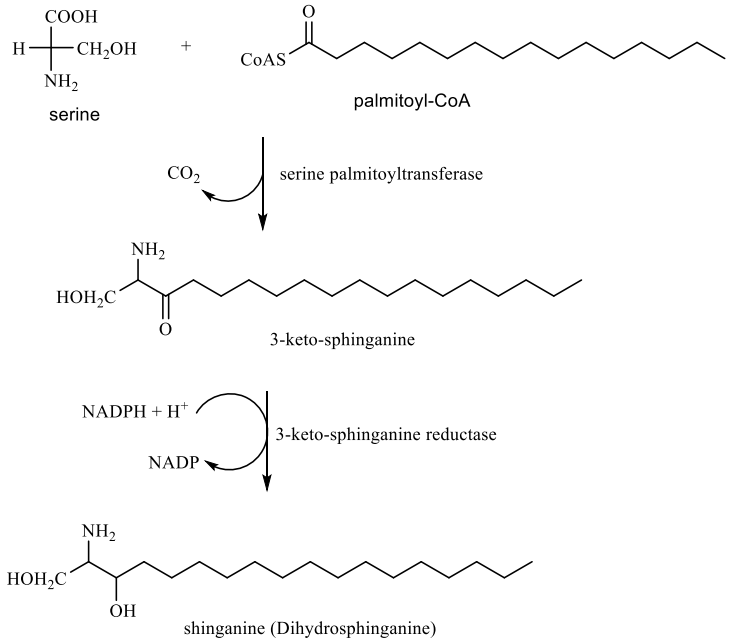

Scheme 1: The basic mechanism for the biosynthesis of sphinganine (Kolter and Sandhoff, 1999) sphingamine (dihydrosphingamine)

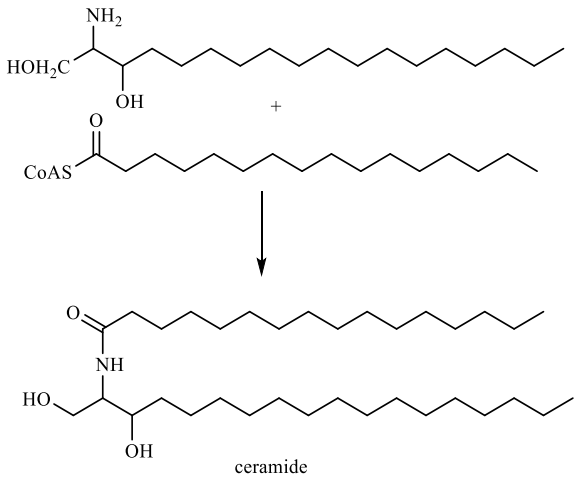

Scheme 2: Process to transform sphinganine to ceramide (Kolter and Sandhoff, 1999).

Most common examples are galactosylceramide (galactocerebroside) and glucosylceramide (glucocerebroside) with *β-D*-galactose and *β-D*-glucose as the monosaccharide unit, respectively. Prior to the biosynthesis, the sugar is activated through condensation with uridine diphosphate (UDP) as shown in scheme 3.

Cerebroside = Ceramide + UDP-hexose

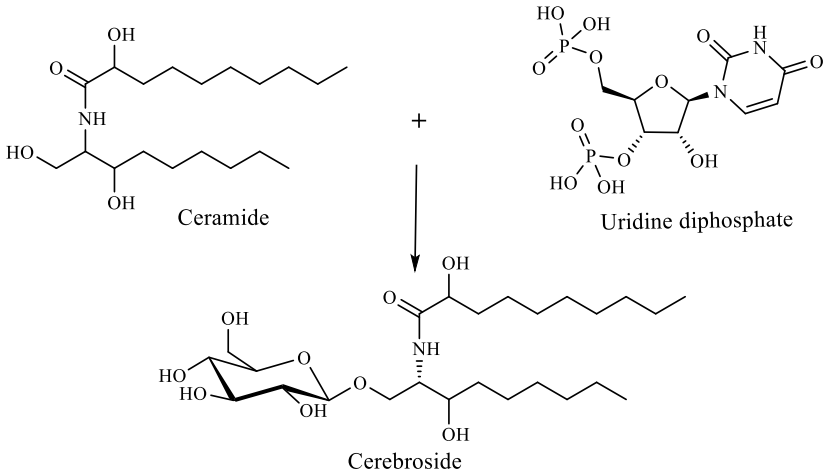

Scheme 3: Process from ceramide to cerebroside

I.3.1.3 Biological activities of cerebrosides

Biologically, some cerebrosides have been proven to serve as structural support and texture determinants of cell membranes, and act as mediators of biological events such as activation, cell agglutination, intracellular communication and cell development, most likely through protein binding (Barrett *et al*., 2000). Moreover, cerebrosides in cellular membranes play important biological roles such as cell surface antigens and receptors (Hakomori *et al*., 1981). In particular, a growing collection of evidence has indicated that cerebrosides have a wide range of biological functions (Schmidt, 1989). For example, the nerve growth factor (NGF), a biomacromolecule is the first and the best characterized neurotrophic factor that regulates the growth, differentiation and survival of neurons, and is thought to be a candidate for drugs for treating Alzheimer's disease (Hefti and Weiner., 1986; Hefti *et al*., 1989). Accordingly, the NGF-like lowmolecular-weight compounds as represented by cerebrosides are thus considered to be more promising for the treatment of Alzheimer's disease.

I.3.1.4 General method for the structure elucidation of cerebrosides

Cerebrosides consist of a ceramide with a single or many sugar(s) residue at the 1-hydroxy moiety, their chemical structure can be defined when the pattern (long-chain base, fatty acid chain and sugar moiety) of each of its constituents is determined. Apart from some discrepancies observed in ^{1}H-NMR and ^{13}C-NMR due to the presence of sugar moiety, techniques used in the structure establishment of ceramides are close to those used in the structure determination of cerebrosides. Spectral data for both long-chain fatty acid and long chain base are almost the same as observed for ceramides. Due to the sugar moiety, additional signals are observed.

I.3.1.4.1 Infra-red spectroscopy

Infrared analysis is usually used to determine the presence of secondary amide, hydroxy group, fatty acid, and olefinic function. Therefore, the typical absorptions around 3400 and 1660 suggest an amide linkage (Kagho *et al*., 2020). In addition, IR absorption bands closer to 3600 cm^{-1} indicate the presence of hydroxy group (Yasunori *et al*., 2001). Furthermore, the absorption bands near to 2940-2850 cm^{-1} (aliphatic) suggest the presence of fatty acid amide. In addition, an absorption band around 1630 cm^{-1} is due to the olefinic function (Viqar *et al*., 2004; Yasunori *et al*., 2001).

I.3.1.4.2 Mass spectrometry

Mass spectrometry analysis has a salient role in the determination of the structure of cerebrosides. It permits to determine the molecular formula and the degree of unsaturation in the molecule. It helps to determine the length of the two carbons chains, the position of olefinic bond and the present of the sugar. This is possible with the help of the mass fragmentation pattern (Muralidhar *et al*., 2005). To obtain this information, different mass spectrometry methods are used including, High Resolution Fast Atomic Bombardment Mass Spectrometry (HR-FAB-MS) and High Resolution Electrospray Ionisation Mass Spectrometry (HR-ESI-MS).

I.3.1.4.3 Proton nuclear magnetic resonance spectroscopy

Proton nuclear magnetic resonance (^{1}H-NMR) spectroscopy has been widely employed as a method for cerebrosides structure determination. The ^{1}H-NMR spectrum appears in the range of 0-10 ppm downfield from the reference signal of tetramethysilane. This spectrum shows some characteristic signals: the resonance of the primary methyl groups (-CH_3) of both side chains appear as triplet around δ_H 0.86 with the coupling constant between 7.0-7.8 Hz depending on the solvent (Muralidhar *et al*., 2005; Eyong *et al*., 2005). A peak at about δ_H 4.95 (d, J = 8.2 Hz) is due to the anomeric proton (Neeraj *et al*., 2006). This value also suggests a β-configuration of the sugar unit (Chen *et al*., 2002; Neeraj *et al*., 2006). Many multiplets between δ_H 3.60 and 4.90 due to protons of sugar are also observed on this spectrum (Chen *et al*., 2002; Neeraj *et al*., 2006). The resonances of methylene groups (CH_2-) associate with the chain appear as a broad singlet between δ_H 1.23-1.30 (Muralidhar *et al*., 2005; Naveen *et al*., 2002). The Ha and Hb resonances of the hydroxymethylene at position 1 appear as a pair of doublet of doubled (dd) around δ_H 4.50 and 4.40 (J = 10.5, 6.0 Hz) respectively, in pyridine. Also, it appears close to δ_H 3.95 and 3.70 (J = 11.0, 4.0 Hz) in $CDCl_3$ (Eyong *et al*., 2005; Naveen *et al*., 2002). These values depend on the chemical environment around carbon C-1. The resonances of the olefinic protons appear as a pair of doublets of triplets or as multiplets near to δ_H 5.52 and 5.48 (Cateni

et al., 2003). If one of the *J*-values of these protons is around 15.0 Hz, it reveals the *E*-orientation. A proton attached to the amide nitrogen resonates as a doublet around δ_H 8.55 with the coupling constant in the range 8.8-9.1 Hz in pyridine (Takahiro *et al*., 2006). A proton vicinal to amide group usually appears in the range of 5.00-5.23 ppm. However, these values can slightly change depending upon the type of solvent and the chemical environment.

I.3.1.4.3. Carbon nuclear magnetic resonance spectroscopy

The decoupled ^{13}C-NMR spectrum of cerebrosides permits ready differentiation between cerebrosides containing double bonds and cerebrosides lacking the double bonds. Signals of olefinic carbons appear in the range of 127.0-135.0 ppm (Yasunori *et al*., 2001; Viqar *et al*., 2004). The ^{13}C-NMR of cerebrosides also shows some characteristic signals. The resonance of amide carbonyl appears at about δ_C 176.0 (Yasunori *et al*., 2001; Masanori *et al*., 1997). The anomeric carbon appears at about δ_C 105.5 (Pendyala *et al*., 2005; Pittaya *et al*., 2003). The hydroxy containing methine carbons appear between δ_C 61.0 and 77.0 and reveal the presence of sugar (Pendyala *et al*., 2005; Naveen *et al*., 2002).

The signal of the methine carbon linked to the amide nitrogen appears at about δ_C 53.0 (Yasunori *et al*., 2001; Viqar *et al*., 2004). The signal of a downfield methylene bearing the hydroxy function appears at about δ_C 62.1 (Yasunori *et al*., 2001). Methylenes of both side chains show their signals between δ_C 23.0-30.0 $(-CH_2-)_n$ (Yasunori *et al*., 2001). Hydroxylated carbons appear at about δ_C 76.0 (Muralidhar *et al*., 2005). Primary methyls of both side chains appeared around δ_C 14.3 ($-CH_3$) (Muralidhar *et al*., 2005). It is important to know that all these values depend on the nature of solvent and the chemical environment of molecules involved. Therefore, these shifts can slightly change.

I.3.1.4.4 Heteronuclear multiple bond connectivity (HMBC) and ^{1}H–^{1}H correlation spectroscopy (COSY) techniques

These two techniques are of great importance in the structure determination of cerebrosides. They help specifically in the determination of the positions of hydroxy groups, the double bonds and the sugar in some cerebrosides. More especially, HMBC technique is very helpful in the determination of the stereochemistry of the double bonds in the molecule. The connectivities between the olefinic protons of the double bond and the adjacent carbons to this double bond give the crucial information on its geometry. It is known that the geometry of the double bond in the long-chain alkene can be determined on the basis of the ^{13}C-NMR chemical shift of the ethylene carbon adjacent to the olefinic carbon, which is observed at $\delta \approx 27$ in *Z* configuration and at $\delta \approx 32$ in *E* configuration (Bankeu *et al*., 2017).

I.3.1.4.5 Chemical degradative methods in the structure determination of cerebrosides

The nature of each of the constituents of ceramides is determined through the methanolysis with methanolic hydrochloric acid. The fatty acid methyl ester (FAME) obtained together with a long-chain base (LCB) from the methanolysis is extracted with *n*-hexane and this layer is concentrated and subjected to GC-MS analysis to determine the nature of FAME (Bankeu *et al*., 2017). Especially in the case of ceramides containing double-bond, an additional reaction is required to determine the position of the double bond on one of the long chains. This produces the dimethyl disulfide (DMDS) derivatives of ceramides. The FAB mass spectrum in the positive of the DMDS derivatives of ceramides shows a remarkable fragment ion peak due to cleavage of the bond between the carbons bearing a methylthio group. These data indicate the position of the double-bond in the LCB or in the FAME of ceramides (Bankeu *et al*., 2017).

I.3.2. Phenolic amides

I.3.2.1 Definition and general structure

Phenolic amides, also named avenanthramides (AVAs), are a group of *N*-cinnamoylanthranilic acids, with health-promoting properties mainly found in oat (*Avena sativa L*.). These phenolic amides have antioxidant properties and potential therapeutic benefits including antiinflammatory, antiproliferative, antigenotoxic effects and skin anti-irritant properties (Eudes *et al*., 2011).

Avenanthramides are a group of *N*-cinnamoylanthranilic acids comprising anthranilic acid and cinnamic acid linked by an amide bond (Collins *et al*., 1988). Due to the presence of various substituted groups on the two components, more than 25 different types of avenanthramides have been detected in oat grains. However, the most abundant ones are three comprising esters of 5-hydroxyanthranilic acid conjugated with caffeic acid (as avenanthramide-C or AVA-C), *p*-coumaric acid (as avenanthramide-A or AVA-A) or ferulic acid (as avenanthramide-B or AVA-B) (Collins *et al*., 1988).

I.3.2.2 Biosynthesis of phenolic amides

Although the health-promoting properties of avenanthramides are well known, the biosynthetic mechanism was not completely understood. We identified three different types of enzymes involved in the biosynthesis of the major avenanthramides in oat: 4CL (4-coumarate-CoA ligase) in activating hydroxycinnamates to their thioesters prior to the condensation, HHTs catalyzing the condensation in the biosynthesis of AVA-A and AVA-C, and CCoAOMT (caffeoyl-CoA O-methyltransferase) enzyme for the methylation of AVA-C to AVA-B. Particularly, we demonstrated that oat HHTs are only responsible for the biosynthesis of AVA-

A and AVA-C, but not for AVA-B, which is synthesized by a new mechanism, the methylation of AVA-C catalyzed by CCoAOMT enzyme. For the complete biosynthesis of the three major avenanthramides in oat, *p*-coumaric acid is initially derived from phenylalanine catalyzed by phenylalanine ammonia lyase (PAL) and cinnamic acid 4-hydroxylase (C4H). *P*-coumaric acid can be activated into its CoA thioesters by 4CL, which can then be condensed with 5-hydroxyanthranilic acid to AVA-A by HHT (hydroxyanthranilate *N*-hydroxycinnamoyltransferase). On the other hand, *p*-coumaroyl-CoA is often converted to *p*-coumaroyl shikimate/quinate first, which is then possibly hydroxylated by p-coumaroyl CoA ester 30-hydroxylase, a cytochrome P450 enzyme (CYP98) (Schoch *et al*., 2001; Bassard *et al*., 2012). Caffeoyl-CoA can then be condensed with 5-hydroxy anthranilic acid to AVA-C by HHT. Finally, AVA-C is methylated to AVA-B by CCoAOMT enzyme (scheme 4). The scheme below shows the complete biosynthetic pathway of three major avenanthramides in oat.

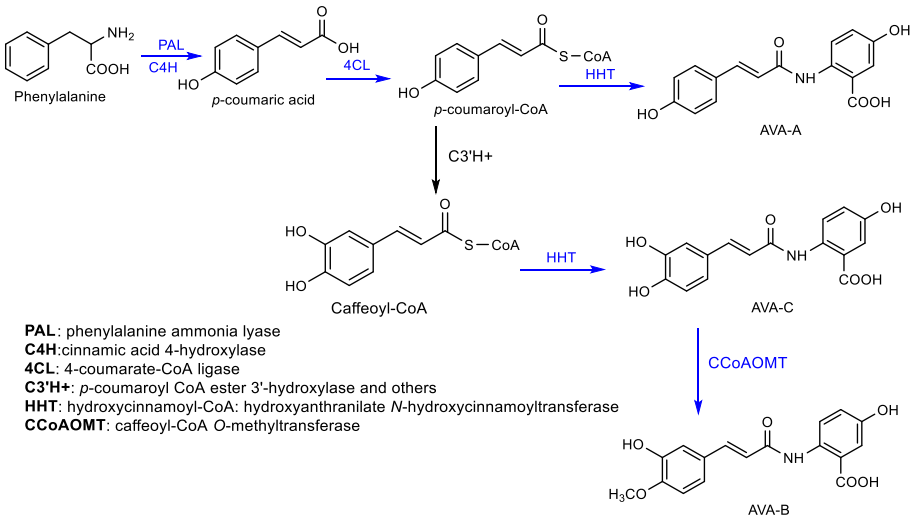

Scheme 4: The complete biosynthetic pathway of three major avenanthramides in oat

I.3.2.3 Biological activities

The whole grain cereals such as oats are important sources of phenolic compounds. Phenolic compounds are of interest because of their high antioxidant capacity and potential health benefits. Especially in recent years, there has been interest in oats and oat products as bioactive high-value sources for human health in industries such as food, pharmaceutical, and cosmetic (Chu *et al*., 2013; Orozco-Mena *et al*., 2014).

Oats and oats products are generally considered healthy and the consumption of oat bran is believed to lower LDL cholesterol (Brown *et al*., 1999; Liu *et al*., 2004; Singh *et al*., 2013). AVAs helps in preventing free radicals from damaging LDL cholesterol (Singh *et al*., 2013) and AVAs-enriched extract of oats combined with vitamin C synergistically inhibits LDL oxidation *in vitro* (Meydani, 2009). Both animal studies and human clinical trials confirmed

that oat antioxidants have the potential of reducing cardiovascular risks by lowering serum cholesterol, inhibiting LDL cholesterol oxidation and peroxidation (Cook and Samman, 1996; Ji *et al*., 2003; Inglett and Chen, 2012). Therefore, it is emphasised that the consumption of oats and oats products is extremely important to reduce the risk of cardiovascular disease (Bazzano *et al*., 2003; Chen *et al*., 2004, 2007; Singh *et al*., 2013). Another study has indicated that the consumption of oats and oat brands may reduce the risk of colon cancer not only because of their high fiber contents but also due to AVAs (Guo *et al*., 2010).

In a study on laboratory animals, the supplementation of the diet of rats with AVAs enriched extract of oats at 100 mg/kg diet were reported to increase superoxide dismutase activity in skeletal muscle, liver, and kidneys, and to enhance glutathione peroxidase activity in heart and skeletal muscles (Ji *et al*., 2003; Meydani 2009). Liu *et al*., (2004) indicated that oats AVAs provide another potential protective mechanism by which the consumption of oats may contribute to the reduction of the risk of atherosclerosis through the inhibition of vascular smooth muscle cells proliferation. AVAs enriched oat extracts and synthetic dihydroavenanthramide-D and AVA-C methyl ester (CH_3-AVA-C) have been shown to inhibit the activation of the NFκ-B transcription factor, which is the master regulator of infection and inflammation (Eudes *et al*., 2014). NFκ-B inhibitory and other functional properties of AVAs make it a candidate for supplementation in the cause of decreasing inflammation and muscle damage in post-menopausal women (Koenig *et al*., 2014).

I.3.2.4 General method for identification of avenanthramides

On the basis of their chemical structures, AVAs represent amides of different hydroxycinnamic acids with different anthranilic acids (Mattila *et al*., 2005; Singh *et al*., 2013; Ortiz-Robledo *et al*., 2013). All the three contain 5-hydroxyanthranilic acid while hydroxycinnamic acids involved are *p*-coumaric acid for AVA-A, ferulic acid for AVA-B, and caffeic acid for AVA-C (Koenig *et al*., 2011; Koenig, 2012). There is a small fraction of anionic, nitrogen-containing, covalently linked hydroxycinnamic acid compounds in their structures (Ji *et al*., 2003). It has been stated that they have a structure decorated with pharmaceutically antioxidant tranilast (Sur *et al*., 2008; Lee-Manion *et al*., 2009). Predominant AVAs in oats are esters of 5-hydroxyanthranilic acid with *p*-coumaric, caffeic, or ferulic acids (Collins and Mullin., 1988; Collins *et al*., 1991; Singh *et al*., 2014).

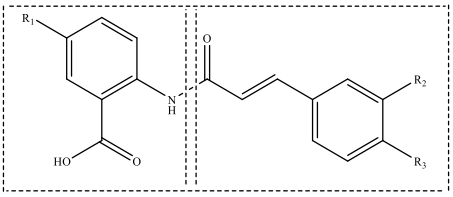

Anthranilic acid Cinnamic acid

Compound	R_1	R_2	R_3	Anthranilic acid	Cinnamic acid
AVA-A	OH	H	OH	5-hydroxyanthranilic acid	*p*-coumaric acid
AVA-B	OH	OCH_3	OH	5-hydroxyanthranilic acid	ferrulic acid
AVA-C	OH	OH	OH	5-hydroxyanthranilic acid	caffeic acid

The most commonly used solvents for the extraction of AVAs are methanol, ethanol, acetonitrile, formic acid, and their combinations. For the determination of the AVAs amounts various chromatographics technics are used such as: high-performance liquid chromatography (HPLC) (Bryngelsson *et al*., 2002; Skoglund *et al*., 2008; Ishihara *et al*., 2014), liquid chromatography-mass spectrometry (LC-MS) (Okazaki *et al*., 2004), liquid chromatography-mass/mass spectrometry (LC-MS/MS) (Ishihara *et al*., 2014), and ion-exchange chromatography (Collins, 1989). HPLC currently represents the most popular technique for the analysis of AVAs.

As previously mentionned, species of *Celtis* and *Dacryodes* are used in traditionnal medicine for the treatment of many parasitics diseases including leishmania and malaria. Thus, is the reason why within the framework of this work, we undertook to give a brief literature on malaria.

I.4 OVERVIEW ON MALARIA

I.4.1 Definition

Malaria is a life-threatening infectious disease characterized by a febrile illness and caused by a parasitic protozoan belonging to the genus *Plasmodium*. It is transmitted through the bites of infected female Anopheles mosquitoes. Malaria is a preventable and curable disease. As per the WHO fact sheet, the mortality rate from malaria has fallen by 47% globally and 54% in African region since 2000, but the disease still plays a major role in global health issues. Every minute a child dies from malaria in Africa. In 2015 WHO reported that, the global incidence of malaria was 198 million cases in 2013 with an estimated 584,000 deaths mostly among the African children (Rodriguez-Morales *et al*., 2015). But in 2019, the number of malaria cases increased to 229 million with an estimated 409,000 deaths (WHO, 2020). Malaria is mostly prevalent in tropical and sub-tropical regions and presents a huge burden on economic

development of malaria endemic countries by having an impact on population growth, absenteeism, workforce productivity, medical costs and mortality (Sachs and Malaney, 2002).

I.4.2 History of malaria and discovery of the parasite

Historically, malaria has been around for a long time and was described in China about 5000 years ago (Cui *et al*., 2015). Ancient Greeks were familiar with the disease since 500 BC. Hippocrates is known to have described the disease and its symptoms as early as 46 BC and Columella (AD 116) characterized it as a disease caused by germs breeding around swamps. The English word of malaria was 'Ague' and has been mentioned in eight of William Shakespeare's plays. Malaria was known to be indiscriminate in choosing its casualties. Famous victims include Hadrian, Vespasian, Titus, S^{t}. Augustine and Alexander the Great. The term malaria comes from the Italian 'mala aria' which means 'bad air', a reference to the presence of a peculiar sulphurous odour produced by anaerobic bacterial flora in brackish mud along river estuaries where the disease was more prevalent, reflecting the ecology and distribution of the mosquito vectors (Reiter, 2000).

In 1880, a French Army doctor, Charles Louis Alphonse Laveran observed the presence of parasites in the red blood cells of malaria-infected people while working in the military hospital in Constantine, Algeria. He proposed that malaria was caused by an organism, a protozoan he named it *Haemamoeba malariae*. His discovery was initially meet with scepticism but was gradually accepted and confirmed by other publications. He was awarded the Breant Prize by the Academy of Sciences in 1889 for his discovery and later a Nobel Prize in 1907 for his works on protozoans causing diseases (Ferri, 2009). In 1877, Patrick Manson, considered by many as the father of tropical medicine, discovered the role of mosquitoes in transmission of filarial parasites and drawing inference. From this, Albert Freeman Africanus King in 1883 suggested the possibility of malaria also being transmitted by mosquitoes (Cook and Webb, 2000). In 1881, Carlos Jan Finlay provided evidence of the role of mosquitoes in transmission of diseases in humans. Manson himself believed that malaria was transmitted by mosquitoes and formulated a hypothesis which he later called 'Mosquito Malaria theory' (Capanna, 2006).

In 1892, a British physician Sir Ronald Ross started a study on malaria and meet Manson in London in 1894, who proposed and illustrated for the first time the life cycle of the malaria parasite (Chernin, 1988). Manson demonstrated the presence of parasitic bodies as described by Laveran in the blood films of malaria infected patients and teaches Ross with the knowledge he desperately sought (Ferri, 2009). While working in India, Ross conducted experiments to prove the hypothesis of the role of mosquitoes in transmission of malaria. He initially used the

Culex mosquitoes and his research bore no results. Ross later conducted research on other species of mosquitoes found in highly malaria areas and discovered single large cells in the stomach walls of the mosquitoes fed on malaria-infected patients. These cells increased in diameters with each passing day thus demonstrating growth. Ross was able to show that the parasite reproduced sexually in the stomach of the mosquito. He continued his research on transmission of malaria in birds and noted the passage of parasites from stomach to salivary glands of the infected mosquito, from where it then passed into the bloodstream of the healthy bird when bitten by such mosquitoes. In 1902, Ross received the Nobel Prize in medicine for demonstrating the life cycle of the malaria parasite and establishing the mosquito species *Anopheles* as the vector of malaria (Chernin, 1988; Ferri, 2009).

I.4.3 Geography and incidence

Malaria was widely prevalent in Medieval Europe until the breeding habits of the mosquito vectors were disrupted by land reclamation, building of well-lit and ventilated houses, and improved drainage. Today, Malaria is mainly a disease of tropical and sub-tropical regions. Implementation of malaria control programmes and increased financing has seen a huge reduction in the malaria incidence and mortality since 2010 (Mita and Jombart, 2015). The figures 5 and 6, respectively, show the trend in the estimated cases and deaths due to malaria since 2000. The past few years have seen little progress in the fight against malaria (WHO, 2018).

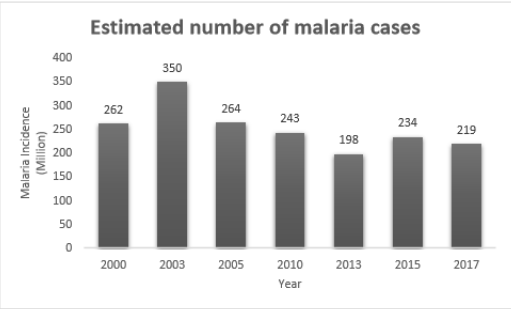

Figure 5: Estimated number of malaria cases (WHO, 2018)

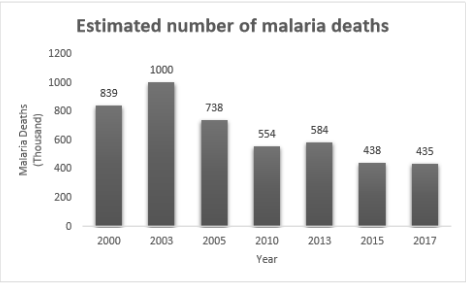

Figure 6: Estimated number of malaria deaths (WHO, 2018)

Climate plays an important role in the life cycle of malaria parasites as rainfall, humidity and ambient temperatures determine the survival of the mosquito vector. Warm tropical and subtropical temperatures are ideal for the parasite to complete the growth cycle. At temperatures 15°C for *Plasmodium vivax* and 20°C for *P. falciparum* the growth cycle is not completed and thus the transmission of malaria is difficult (Ecology of malaria, 2015). The ecological conditions required for the more efficient mosquito vectors of malaria to thrive, determined the intensity of the disease and its distribution (Gallup and Sachs, 2001). There is a compelling correlation between malaria and poverty. Human societies have prospered least in areas where malaria has prospered most (Rodriguez-Morales *et al*., 2015). Cases and deaths from malaria started to increase globally since 1990 and reached a peak in 2003 with more than 350 million cases and more than 1 million deaths (WHO, 2005). A decrease in child mortality rates has been observed in the sub-Saharan region since 2004, while the malaria mortality rate has been on a steady decline since 1990 in regions outside of Africa (Murray *et al*., 2014). Artemisinin-based combination therapies (ACT) have played a major role in decreasing the global burden of malaria but the emergence and potential spread of strains of malaria parasites resistant to artemisinin in Southeast Asia and variations in sensitivities to artemisinin partner drugs is a major cause of concern (Cui *et al*., 2015). Figure 7 shows countries with cases in 2000 and their status by 2019.

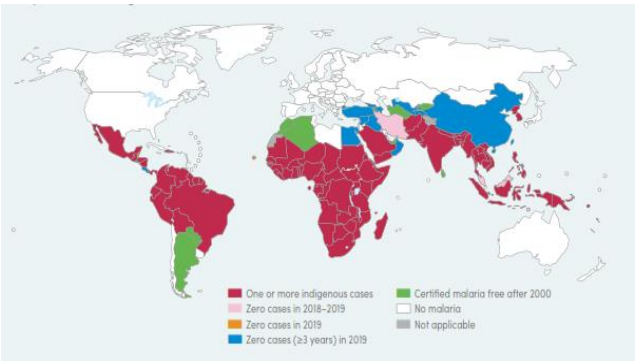

Figure 7: Countries with cases in 2000 and their status by 2019.

I.4.4 Malaria parasite, mosquito vector and Life-cycle

I.4.4.1 Malaria parasite, mosquito vector

Malaria disease is caused by a protozoan parasite belonging to one of the following four *Plasmodium* species: *P. falciparum*, *P. vivax*, *P. ovale* and *P. malariae* (Franco-Paredes and Santos-Preciado, 2006). *P. knowlesi* is a zoonotic parasite and is known to cause infections in humans. Recently, *P. simium* emerged as another potential species to infect humans (Brasil *et al*., 2017).

The malaria parasite is transmitted to humans through the bites of female *Anopheles* mosquitoes. The ability to transfer malaria parasite differs among the various species of *Anopheles*. Some female *Anopheles* species have an inclination towards human blood for their meals (anthropophilic) whereas some others prefer animals (zoophilic). Some have indoor biting habits (endophagic) whereas the others have outdoor (exophagic). All the other factors being equal, the better vectors for malaria transmission are the species with anthropophilic, endophagic habits as they tend to have more frequent contacts with humans. A field study observed that *P. falciparum* alters the behavioral patterns of the mosquito vector host *gambiae* and increases the frequency of multiple feeding, thereby facilitating a more rapid spread and increase in the transmission in humans (Koella *et al*., 1998). There are many countries which have eliminated malaria, but the *Anopheles* mosquito is still present in these countries and presents a potential for reintroduction of malaria through cases in returning travelers or immigrants (imported malaria), if such cases are not treated promptly (Odolini *et al*., 2012).

I.4.4.2 Life cycle of *Plasmodium* parasites

The malaria parasite requires two hosts to complete the life cycle: humans and the female *Anopheles* mosquito. In the human host the parasite presents different antigens throughout the several life stages which are useful targets for vaccine development (Florens *et al*., 2002). The mosquito transmits the disease from one human to another but itself does not suffer from the presence of parasites. The different stages are the following:

- *Plasmodium* parasites in the form of sporozoites are introduced into the bloodstream of human hosts by bites of infected female *Anopheles* mosquitoes. These sporozoites reach the liver and over the period of 7 to 10 days, the sporozoites are multiplied asexually producing no symptoms (pre-erythrocytic stage);
- the parasites, in the form of merozoites are released in the bloodstream where they infected the red blood cells (erythrocytes) and multiplied further. The erythrocytes burst releasing the merozoites which invade more erythrocytes thus repeating the cycle and causing fever each time there is the release of merozoites from the erythrocytes (erythrocytic stage);
- some of these merozoites leaved the asexual cycle and developed into the sexual forms called gametocytes.
- these gametocytes enter the mosquito during a blood meal when it bites an infected human and develops into mature sex cells called gametes;
- ookinetes are formed on fertilization of the female gamete. The ookinetes actively move through the midgut wall of the mosquito and developed into an oocyst inside

which several thousands of sporozoites are formed. These sporozoites are released into the body cavity when the oocyst burst;

- The sporozoites then travel to the mosquito's salivary gland and the cycle is completed when the infected mosquito bites a human (Soulard *et al*., 2015).

The figure 8 below shows the life cycle of malaria parasite. Sexual and asexual stages of malaria parasite life cycle (Osta *et al*., 2002).

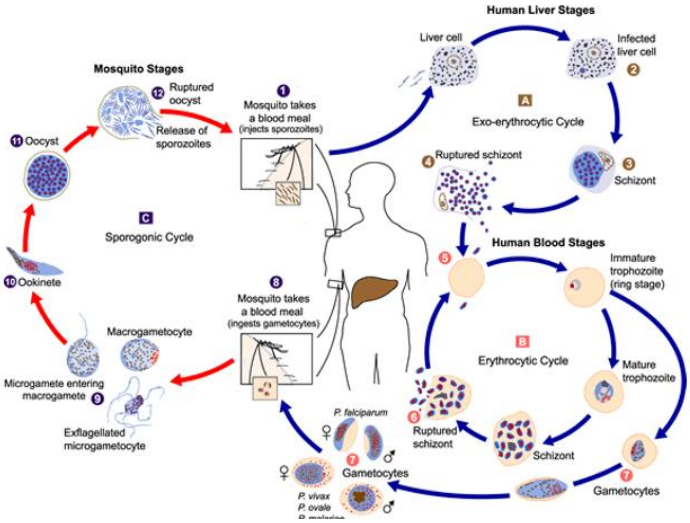

Figure 8: Life-cycle of malaria parasite.

P. vivax and *P. ovale* have stages in their asexual life cycle in humans (hypnozoites) wherein they remain in a dormant state in liver and can reactivate later. They can invade the bloodstream causing relapses. Vertical transmission through the mother (congenital malaria), shared needles, organ transplantation or transfusion are rare modes of malaria transmission from person to person without the involvement of the mosquito vector (Zoller *et al*., 2009).

I.4.5 Signs and symptoms of malaria

Incubation period of malaria is between 9 to 30 days depending on the *Plasmodium* species and the patient usually presents a non-specific flu-like syndrome with fever, malaise, headache, nausea, vomiting, sometimes diarrhoea or jaundice. Diagnosis or exclusion of malaria should be confirmed by microscopic examination of blood films (Bartoloni and Zammarchi, 2012). There are three stages in the classical malaria paroxysm lasting for 6 to 10 hours and usually beginning in afternoon or evening:

- the cold stage in which the patient feels cold and may shiver. The phase usually lasts up to 10-30 minutes and the temperature begins to gradually rise usually to 39°C to 41°C;

- the hot stage in which the shivering stops, and the temperature may rise further to hyperpyrexia levels. The skin is hot and dry, the face appears flushed, and patient, may suffer

from vomiting, diarrhoea, retro-orbital headache, altered consciousness. Convulsions might occur in children. The phase lasts for 2 to 6 hours (Bartoloni and Zammarchi, 2012);

- the sweating stage which is characterized by profuse sweating and rapid fall in temperature. The patient feels better but is usually tired and the stage lasts for 2 to 3 hours. Fever is usually synchronized with schizogony and occurs every alternate day (Tertian) in *P. vivax*, *P. ovale* or *P. falciparum* malaria and every third day (Quartan) in *P. malariae* malaria (Ferri, 2009).

P. falciparum is the only species causing severe malaria leading to death by causing acidosis, respiratory distress, severe anemia, acute renal failure, hemoglobinuria, severe anemia or shock, encephalopathy and coma due to cerebral malaria (Bartoloni and Zammarchi, 2012; Krungkrai *et al*., 2010). This occurs due to the ability of the *P. falciparum* parasites to sequester in brain and various other organs (Greenwood *et al*., 2008).

I.4.6 Malaria situation in Cameroon

Cameroon is situated in Central Africa, within the Gulf of Guinea at a latitude between 2–13°N and a longitude between 9–16°E. It has a surface area of 475442 km^2 with a population of about 24 million who live in malaria endemic areas, with 71% living in high transmission areas (> 1 case per 1,000 population), and 29% living in low transmission settings (0-1 case per 1,000 population). Cameroon has three malaria transmission zones that vary by geographic region and transmission intensity. The equatorial forest zone in the south is a hot and humid climate with abundant precipitation. This zone has perennial malaria transmission of 7 to 12 months and an entomological inoculation rate of 100 infective bites per person per month. The tropical/Sudanian zone includes parts of central and northern Cameroon, particularly the North and Adamawa regions, and has an intense seasonal malaria transmission season of four to six months. This zone has an entomologic inoculation rate of 10 infective bites per person per month. The Sahelian zone is comprised of the Far North region and has a hot and dry tropical climate where malaria transmission lasts only one to three months. The entomologic inoculation rate during this short transmission season is roughly 10 infective bites per person per month (Antonio-Nkondjio *et al*., 2019).

According to annual report 2019 of the National Malaria Control Program, a total of 2,139,482 cases of malaria were confirmed by diagnostic test. Of these, 50.01% were classified as severe malaria. These cases represent 25.8% of all medical consultations at health facilities, and 14.3% of deaths. Malaria parasite prevalence among children under five years of age in the Adamaoua, Far North, and North regions accounts for 32%, 22%, and 26%, respectively. There

were 3,263 malaria deaths reported in health facilities, which represented 13.9% of all causes of death. The proportion of death due to malaria is highest in the Far North and North regions, where the malaria season is shortest (Serafini *et al*., 2011).

I.4.7 Malaria diagnosis, treatment and vaccine

- **Diagnosis of malaria**

- **Clinical diagnosis**

The initial symptoms of malaria (most often fever, chills, sweats, headaches, muscle pains, nausea and vomiting) are often non-specific and can also be found in other diseases (e.g. influenza and other common viral infections). Likewise, the physical findings are often non-specific (elevated temperature, sweating and tiredness). However, in severe malaria (mostly caused by P. falciparum), the clinical findings of confusion, coma, convulsions, severe anaemia, respiratory difficulties are more specific and may increase the index of suspicion for malaria.

- **Laboratory diagnosis**

For all cases of suspected malaria, the health-care provider should conduct an initial workup and arrange for a malaria parasitological test either via a quality assured Rapid Diagnostic Tests (RDT) or a microscopic examination of blood smear slide. Either test, or both, can be used as a primary diagnostic tool for the confirmation and management of suspect clinical malaria in all epidemiological situations, including areas of low transmission. For microscopy, thick blood smears are more sensitive to detecting the presence of malaria parasites while thin smears allow for better species identification.

- **Treatment of malaria**

Malaria can be a severe, potentially fatal disease (especially when caused by *P. falciparum*), and treatment should be initiated as soon as possible.

Quinolines are the oldest class of antimalarial. Quinine the first drug in this group is an alkaloid isolated from the bark of the Cinchona tree. Quinine and its derivatives are currently used for the treatment of malaria and several years after its discovery (Greenwood D, 1992). Artemisinin is a potent and rapidly acting blood schizontocide, which is active against all Plasmodium species. Artemisinin was originally isolated from the plant Artemisia annua, an herb employed in Chinese traditional medicine. It has an unusually broad activity against asexual parasites, killing all stages from young rings to schizonts (Krishna *et al*., 2010).

If you clinically suspect a diagnosis of malaria, and the lab result of the malaria test is not available for more than 2 hours, treatment of malaria should be started presumptively based on the probability that the illness is malaria, and reviewed later based on the test results. If the

patient has signs and symptoms of severe malaria, presumptive treatment should be initiated immediately regardless of laboratory test results (WHO, 2018).

- **Uncomplicated *P. falciparum* malaria**

Adults with uncomplicated *P. falciparum* malaria should be treated with one of the following recommended artemisinin-based combination therapies (ACT) for 3 days. The benefits of ACTs are their high efficacy, fast action and the reduced likelihood of resistance development (Bousema *et al*., 2006). In 2014, the Ministry of Health of Cameroon reconsidered its policy and shifted to artemisinin-based combination therapy (ACT) used as a first-line treatment for uncomplicated malaria (artesunate-lumefanthrine, artesunate-mefloquine, …) (Antonio-Nkondjio *et al*., 2019). Some combinaison are :

1- 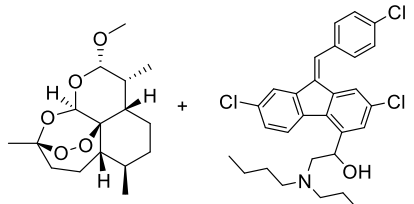

,twice daily for 3 days

2- 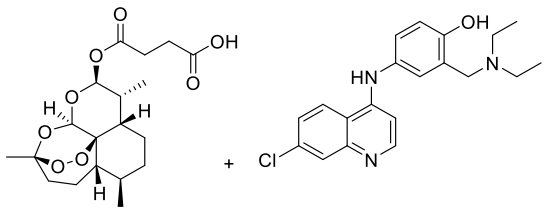

, once daily for 3 days

3- 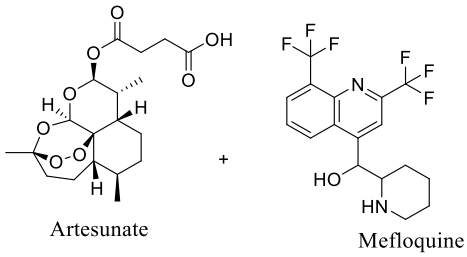

, once daily for 3 days

4- 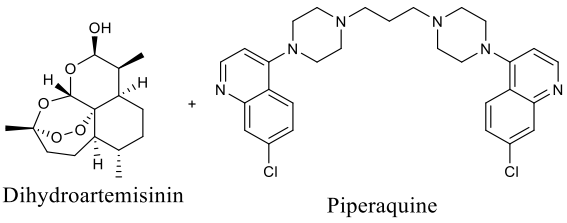

,once daily for 3 days

- **Uncomplicated *p. vivax, p. ovale, p. malariae* or *p. knowlesi* malaria**

If the malaria species is not known, treat as uncomplicated *P. falciparum* malaria. In areas with chloroquine susceptible infections, treat uncomplicated *P.vivax*, *P. ovale*, *P. malariae*, or *P. knowlesi* with either chloroquine or ACT (WHO, 2018). In areas with chloroquine-resistant

infections, treat uncomplicated *P. vivax*, *P. ovale*, *P. malariae* or *P. knowlesi* malaria with ACT (Nosten F and White N. J., 2007).

- **Uncomplicated malaria in pregnancy**

Artemisinin combination treatments should be used to treat malaria in pregnant women. The combination artesunate + sulfadoxine/pyrimethamine (SP) should not be given in the first trimester because SP is contraindicated in this period of pregnancy (WHO, 2018).

- **Severe malaria**

Severe malaria is defined as confirmed malaria with at least one of the following: impaired consciousness, prostration, multiple convulsions, respiratory distress, severe anaemia, significant bleeding, or jaundice. Treat patients with severe malaria with intravenous or intramuscular artesunate for at least 24 hours until they can tolerate oral medication. For adults, artesunate should be administered and if artesunate is not available, use artemether in preference to quinine for treating severe malaria (WHO, 2018). In the fight against this disease, a vaccin has been approved by WHO on October 6, 2021 (WHO, 2021).

- **Malaria vaccine**

The World Health Organization has recommended the use of the RTS,S malaria vaccine, which is produced by GlaxoSmithKline. This vaccine is used in addition to the prevention already implemented, such as taking medication and protective measures against mosquito bites. It is the first malaria vaccine which has proven to be effective. RTS, S (trade name Mosquirx) is given in four doses to children aged 5 to 17 months; the first three doses are given every month, the fourth, a booster dose, is given between 15 and 17 months. The efficacy is around 40% against the development of malaria and 30% against severe forms (Alonso *et al*., 2004).

Considering the limit of the current treatment against malaria and the malaria vaccine, the various uses in traditional medicine of plants of the genera *Dacryodes* and *Celtis*, the structural diversity of the compounds isolated from plants of the burseraceae and cannabaceae families, their potential scientific here presented, we undertook a chemical and biological study on the stem bark and leaves of *Dacryodes edulis* and roots of *C. adolphi-friderici*.

CHAPTER II:
RESULTS AND DISCUSSION

II.1. CHEMICAL STUDY OF *Dacryodes edulis* AND *Celtis adolphi-friderici* Engl.

II.1.1. Plant material, extraction and isolation of compounds

II.1.1.1 *D. edulis*

Leaves and stem bark of *D. edulis* were collected in April 2018 at Batcham (GPS coordinates: Latitude: 5° 31' 59.99" N, Longitude 10° 13' 60.00" E), a village in the West Region of Cameroon and identified at the National Herbarium-Yaoundé (where a voucher specimen was deposited under the reference N° 45713 HNC) by Mr. NANA Victor, a botanist at the National Herbarium Cameroon.

The air-dried stem bark (4.5 kg) and leaves (1.5 kg) of *D. edulis* were each ground and macerated (thrice at room temperature, within 72 hours in 15 L solvent) separately with MeOH and ethanol-water (70-30). The filtrate was freed from solvent to give 239.8 g and 205.5 g of methanol and hydroethanol extract for leaves and stem bark, respectively. The methanolic extract from the stem bark of *D. edulis* displayed good antiplasmodial activity on both *Pf3D7* and *PfDd2* with IC_{50} values of 9.62 and 6.32 μg/mL, respectively. The hydroethanolic leaves extract from *D. edulis* exhibited pronounced antiplasmodial activity with IC_{50} values of 3.10 and 3.56 μg/mL on both *Pf3D7* and *PfDd2* strains, respectively. These extracts were suspended in water and successively partitioned with *n*-hexane, dichloromethane, EtOAc, MeOH and *n*-BuOH to afford eight fractions labeled DEH (25.5 g), DEC (5.3 g), DEA (40.5 g), DEN (110.7 g), DFH (25.7 g), DFC (17.5 g), DFA (20.3 g) and DFM (102.3 g). Each fraction was subjected to successive column chromatography over silica gel or sephadex LH-20. Eleven and five compounds were obtained, respectively, from the methanol and hydroethanolic extracts of the stem bark and the leaves. The protocol of extraction and isolation of compounds from the two extracts is resumed in the scheme below.

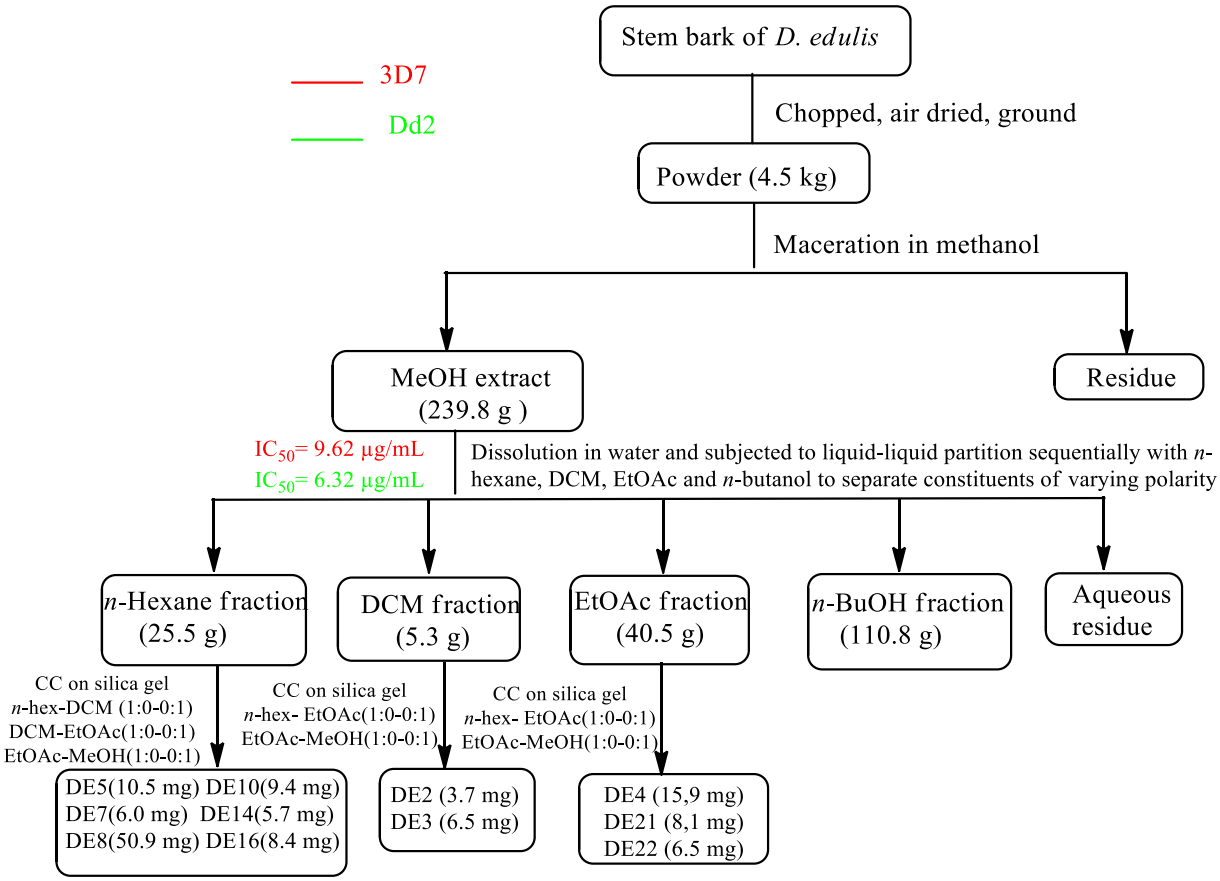

Scheme 5: Extraction and isolation of compounds from stem bark of *D. edulis*

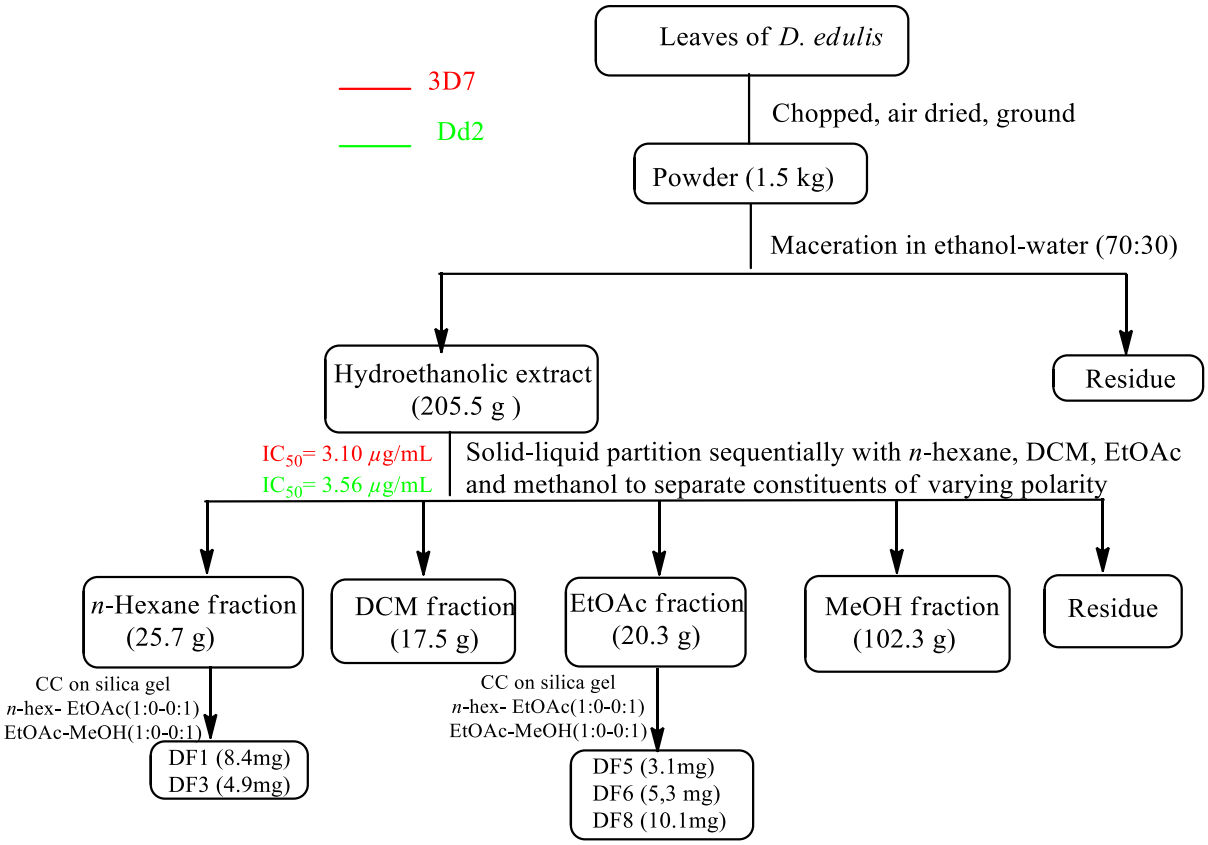

Scheme 6: Extraction and isolation of compounds from leaves of *D. edulis*

II.1.1.2. *C. adolphi-friderici* Engl.

The roots of *C. adolphi-friderici* were collected in December 2013 at mount Eloundem (GPS coordinates: Latitude: 3° 49' 42" N, Longitude 11° 26' 18" E), a locality in the Center Region of Cameroon. The plant material was identified by Mr. Victor Nana, Botanist at the National Herbarium of Cameroon, Yaoundé, by comparison with voucher specimens formerly kept at the National Herbarium under the registration number 34804 HNC.

The air-dried and powdered roots (1.5 kg) were macerated with acetone (repeated three times, within 48h in 10 L) at room temperature (around 27°C). The extract was freed from solvent under vacuum at low temperature (40°C) to afford 70.1 g of brown crude extract. This extract presented a good activity with an IC_{50} of 6.91 and 6.03 μg/mL on both *Pf3D7* and *PfDd2* strains, respectively. The extract was dissolved in the mixture of MeOH-H_2O (1:2) and subjected to liquid-liquid extraction with different solvents to give four fractions including the *n*-hexane fraction (F1, 24.4 g), the dichloromethane fraction (F2, 15.0 g), the ethyl acetate fraction (F3, 17.5 g), and the water-soluble residue (F4, 10.3 g). Each fraction was subjected to successive column chromatography over silica gel or Sephadex LH-20. Fifteen compounds were obtained from this extract (Scheme 7). The protocol of extraction and isolation of compounds is resumed in scheme 7.

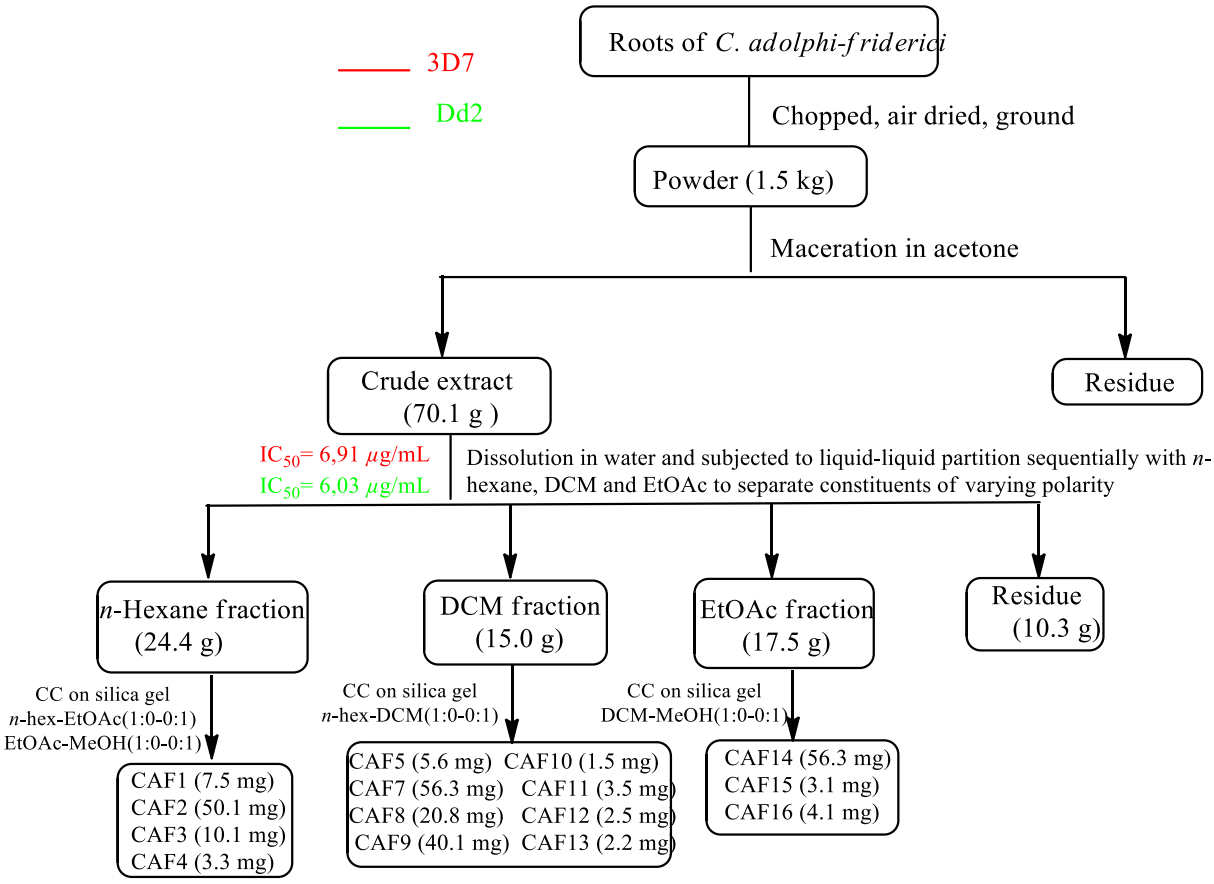

Scheme 7: Extraction and isolation of compounds from the roots of *C. adolphi-friderici*

II.1.2 Structures determination of isolated compounds

Column chromatography of the methanolic extract of the stem bark of *D. edulis* led to the isolation of eleven compounds, while hydroethanolic extract of the leaves led to the isolation of five compounds, and the acetone extract of the roots of *C. adolphi-friderici* led to the isolation of fifteen compounds. Their structures were elucidated by spectroscopic and spectrometric data. They belong to sixteen classes of compounds including one new cerebroside, five triterpenoids, two dicarboxylic acids, three phenolic compounds, three phenolic amides, two triglyceryl, two fatty acids, one indolic alkaloid, one carbamide, one amino acid, two xanthones, three ellagic acid derivatives, one depside, one auranthiamide acetate, one gallic acid derivative, and two steroids.

II.1.2.1 Structure determination of CAF2

Compound **CAF2** was obtained as a white amorphous powder, $[\alpha]_D^{24}$ -13.88 (*c* 0.002, MeOH). The molecular formula, $C_{40}H_{77}NO_{10}$, implying three degrees of unsaturation was deduced from its NMR data and its HRESIMS (negative mode) spectrum (Figure 9), which showed the deprotonated molecular ion peak $[M-H]^-$ at *m/z* 730.5460 (calcd. 730.5475, for

$C_{40}H_{76}NO_{10}$). The analysis of its 1D and 2D spectra combined with its mass spectrum contributed to assign the following structure to CAF2.

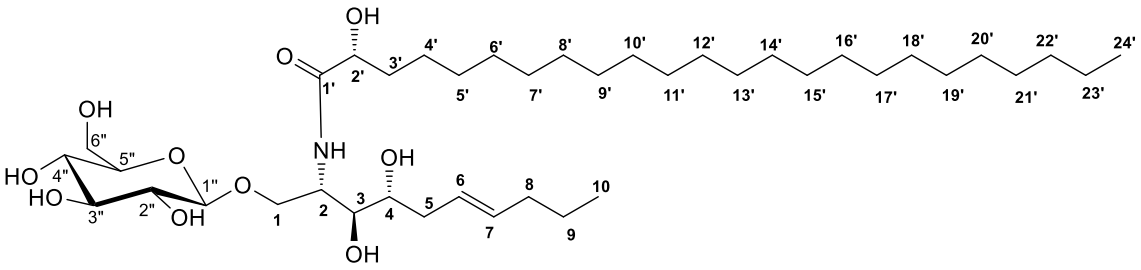

42

The IR spectrum (KBr) (Figure 10) of CAF2 showed absorption bands for hydroxy and amide functionalities (3661 and 3421 cm^{-1}), olefinic group (1634 cm^{-1}) and amide carbonyl group (1744 cm^{-1}). Its UV spectrum (Figure 11) showed absorption bands at λ_{max} 210 and 228 nm.

The ^{1}H-NMR spectrum (Figure 12) of CAF2 showed signals for an amide proton at δ_H 8.55 (1H, d, J = 9.2 Hz), two terminal methyl groups at δ_H 0.85 (6H, t, J = 5.6 Hz), two oxymethylene protons at δ_H 4.70 (1H, m, H-1a) and 4.53 (1H, d, J = 4.4 Hz, H-1b), three oxymethines at δ_H 4.56 (1H, m, H-2′), 4.27 (1H, m, H-3), and 4.18 (1H, m, H-4), and a downfield signal at δ_H 5.27 (1H, m, H-2) assigned to H-2 of sphingosine. It further exhibited resonances for hydroxy group protons at δ_H 7.67 (1H, brd, J = 4.4 Hz), 7.12 (1H, brs), 6.85 (1H, brd), 6.40 (1H, brs), and 6.04 (1H, brs), for olefinic protons at δ_H 5.50 (1H, m) and 5.44 (1H, m); and a long chain methylene protons between δ_H 1.23-2.24 (nCH_2, brs). All the above spectral data revealed that compound CAF2 was a phytosphingosine-type sphingolipid (Bankeu *et al*., 2017). Additionally, the signals for glucose moiety at δ_H 4.93 (1H, brd, J = 7.6 Hz), 4.46 (1H, dd, J = 12.4, 1.6 Hz), 4.32 (1H, dd, J = 12.0, 5.6 Hz), 4.18 (2H, brt, J = 4.4 Hz), 3.99 (1H, t, J = 8.0 Hz) and 3.85 (1H, m) suggested that compound CAF2 was a glucosphingolipid (Bankeu *et al*., 2017, Perveen *et al*., 2015).

The ^{13}C-NMR spectrum (Figure 14) of this compound exhibited carbon signals, which were sorted by DEPT and HSQC techniques into a signal for an amide carbonyl group at δ_C 175.8 (C-1′), two olefinic methine carbons at δ_C 130.5 (C-6) and 130.3 (C-7) (suggesting the presence of one double bond), two oxymethine carbons at δ_C 76.0 (C-3) and 72.5 (C-4, and C-2′), and an oxymethylene carbon at δ_C 70.4 (C-1). It equally displayed resonances for secondary amine at δ_C 51.8 (C-2), aliphatic chain in the range of δ_C 23.0-35.6. It also displayed resonnances of a sugar moiety at δ_C 105.5 (C-1″), 78.6 (C-5″), 78.5 (C-3″), 75.2 (C-2″), 71.5 (C-4″) and 62.7 (C-6″), while the two terminal methyl carbons were observed at δ_C 14.3 (C-10 and C-24′).

The long chain hydrocarbon skeleton and the substitutions at various positions were confirmed by the ^{1}H-^{1}H COSY (Figure 15) and HMBC (Figure 16) correlations. The ^{1}H-^{1}H COSY spectrum of **CAF2** showed correlations between H-1a/H-1b, H-2/H-1a, H-1b and H-3, H-3/H-4, H-4/H-5b, H-5a/H-5b and H-6, H-6/H-5a and H-7, H-7/H-6, H-8a/H-8b and H-2′/H-3′a, H-3′b. The above COSY correlations contributed in the location of the double bond and of the hydroxy groups. This was further confirmed by the HMBC spectrum which showed correlations between H-1a and H-1b /C-2, C-3 and C-1″, H-2/C-1, C-3 and C-1′, H-4/C-2, H-5a/C-6, C-4, H-6 and H-7/C-5 and C-8, H-2′/C-1′, and N-H/C-2, C-3, and C-1′.

Additionally, the location of the glucose moiety was confirmed by HMBC experiments which showed correlations between the anomeric proton H-1″ and carbons C-1 and C-3″. Furthermore, some correlations were observed between H-2″/C-1″ and C-3″, H-3″/C-4″, C-2″ and C-5″, and H-6″/ C-4″, C-5″. The sugar unit was identified as *D*-glucose using chemical shifts and coupling constants (Bubb, 2006).

Also, the linkage between the long chain base (LCB) and the fatty acid were confirmed through the HMBC correlations of H-2/C-1′ and N-H/C-2 and C-1′. The configuration of the double bond was easily determined as *E* configuration according to the carbon chemical shift of allylic methylene proton at δ_C 34.0. Bankeu *et al*. (2017) showed that the geometry of the double bond in the long-chain alkene can be determined on the basis of the ^{13}C-NMR chemical shift of the ethylene carbon adjacent to the olefinic carbon, which is observed at δ≈27 in *Z* configuration and at δ≈32 in *E* configuration

The above data, suggested that, compound CAF2 was a glucosphingolipid and it was further supported by the ESI-MS fragmentation (Figure 17), showing prominent peaks at *m/z* 568.6 due to the loss of the hexose moiety.

The fatty acid length of CAF2 was determined through the methanolysis reaction (Scheme 8). In fact, methanolysis reaction took place in the presence of methanol and hydrochloric acid, and yielded to the isolation of the fatty acid methyl ester (FAME) from the hexane layer at the end of the reaction. The GC-MS analysis (Figure 18) of the FAME showed the molecular ion peak at *m/z* 398 assigned to methyl 2-hydroxytetracosanoate. This information further confirmed the position of the double bond on the LCB moiety (Scheme 8).

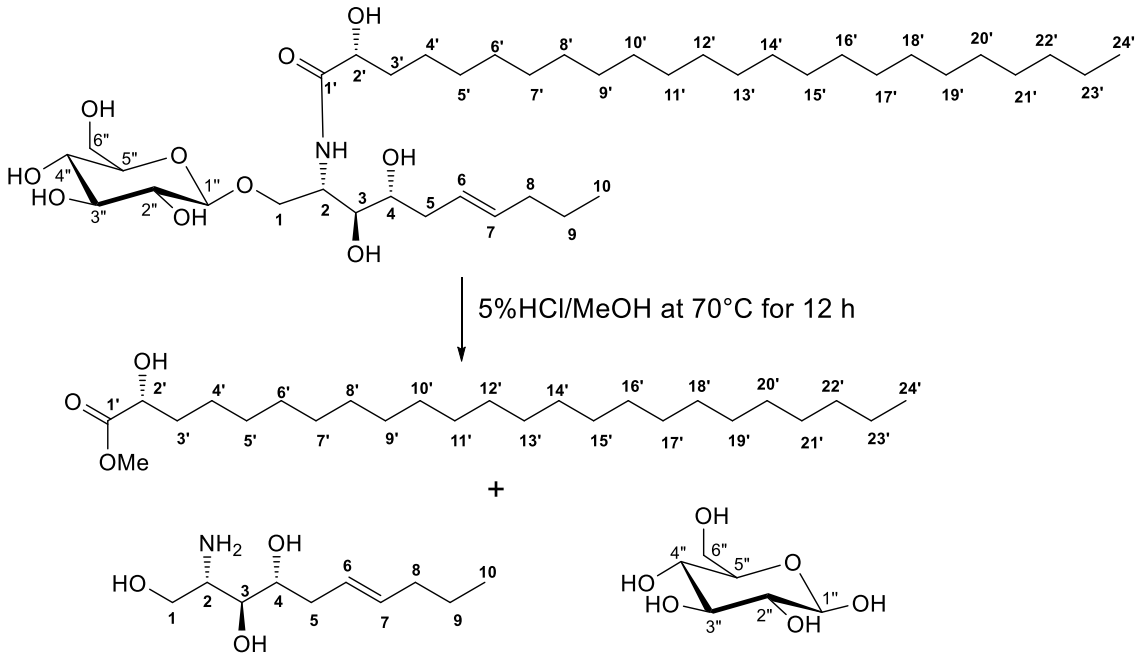

Scheme 8: Methanolysis of CAF2

The relative stereochemistry of CAF2 at C-2, C-3, C-4 and C-2′ was proposed as 2*S*, 3*S*, 4*R*, and 2*R*, respectively on the basis of ^{13}C-NMR spectrum, since the chemical shifts of C-2 (δ_C 51.8), C-3 (δ_C 76.0), C-4 (δ_C 72.5) and C-2′ (δ_C 72.5) were in agreement with those reported in the literature (Bankeu *et al*., 2017).

FAME from CAF2 was subjected to GC-MS [column temp. 100-250℃ (rate of temp. increase 5℃/min]. The result of GC-MS analysis (Figure 18) gives methyl 2-hydroxytetracosanoate, t_R = 55.058 (100), EI-MS *m/z*: 398 $[M]^+$.

Based on above evidences, the structure of the new cerebroside to which the trivial name eloundemnoside was given. It was established as 1-(*O*-*β*-*D*-glucopyranosyl)-(2*S*,3*S*,4*R*,6*E*)-2-{[(2*R*)-2-hydroxytetracosanoyl] amino} dec-6-ene-1,3,4-triol (**42**).

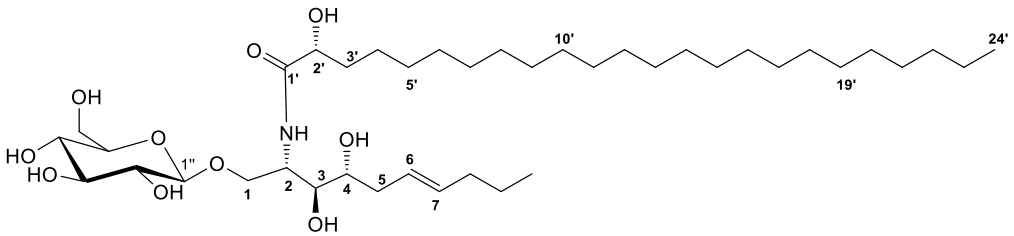

Table 12: ^{1}H (Pyridine-d_5, 600 MHz) and ^{13}C (Pyridine-d_5, 150 MHz) NMR Data of CAF2

	CAF2	
Position	δ_C	δ_H **(nH, m, *J* (Hz))**
NH	-	8.55 (1H, d, *J* = 9.2)
1a		4.70 (1Ha, m)

1b	70.4 (CH_2)	4.53 (1Hb, m)
2	51.8 (CH)	5.27 (1H, m)
3	76.0 (CH)	4.27 (1H, m)
4	72.5 (CH)	4.18 (1H, m)
5a	34.0 (CH_2)	2.15-2.24 (1Ha, m)
5b		1.89-1.96 (1Hb, m)
6	130.5 (CH)	5.50 (1H, m)
7	130.3 (CH)	5.44 (1H, m)
8a	33.0 (CH_2)	2.03-2.08 (1Ha, m)
8b		1.97-2.02 (1Hb, m)
9	30.0 (CH_2)	1.23-1.99 (2H, m)
10	14.3 (CH_3)	0.85 (3H, t, *J* = 5.6)
1′	175.8 (C=O)	-
2′	72.5 (CH)	4.56 (1H, m)
3a′	35.6 (CH_2)	2.15-2.24 (1Ha, m)
3b′		1.97-2.02 (1Hb, m)
4′-23′	23.0-34.0 $(CH_2)_n$	1.23-1.80 (m)
24′	14.3 (CH_3)	0.85 (3H, t, *J* = 5.6)
1″	105.5 (CH)	4.93 (1H, brd, *J* = 7.6)
2″	75.2 (CH)	3.99 (1H, t, *J* = 8.0)
3″	78.5 (CH)	3.85 (1H, m)
4″	71.6 (CH)	4.18 (1H, brt, *J* = 4.4)
5″	78.6 (CH)	4.18 (1H, brt, *J* = 4.4)
6″a	62.7 (CH_2)	4.46 (1Ha, dd, *J* = 12.4, 1.6)
6″b		4.32 (1Hb, dd, *J* = 12.0, 5.6)
OH-2′	-	7.67 (1H, brd, *J* = 4.4)
OH-3	-	6.85 (1H, brd)

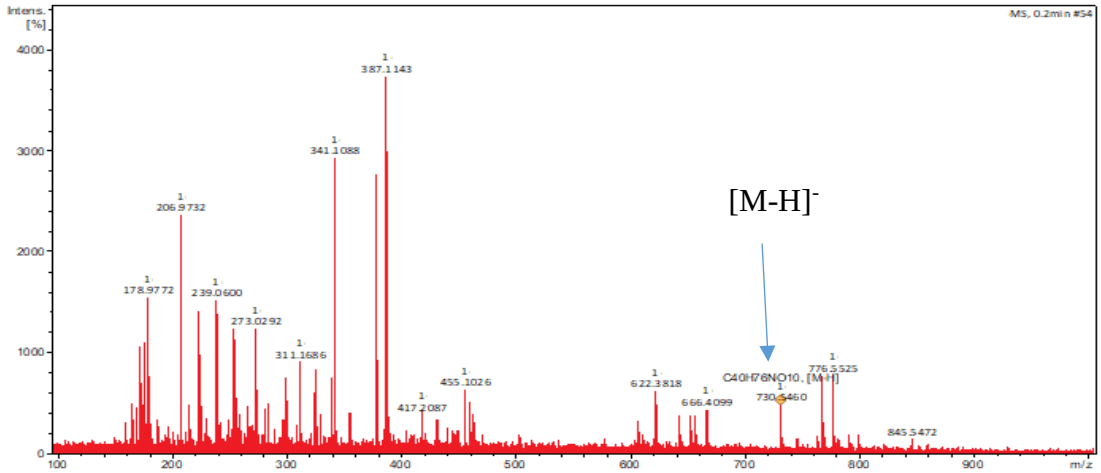

Figure 9: HR-ESI (negative mode) mass spectrum of CAF2

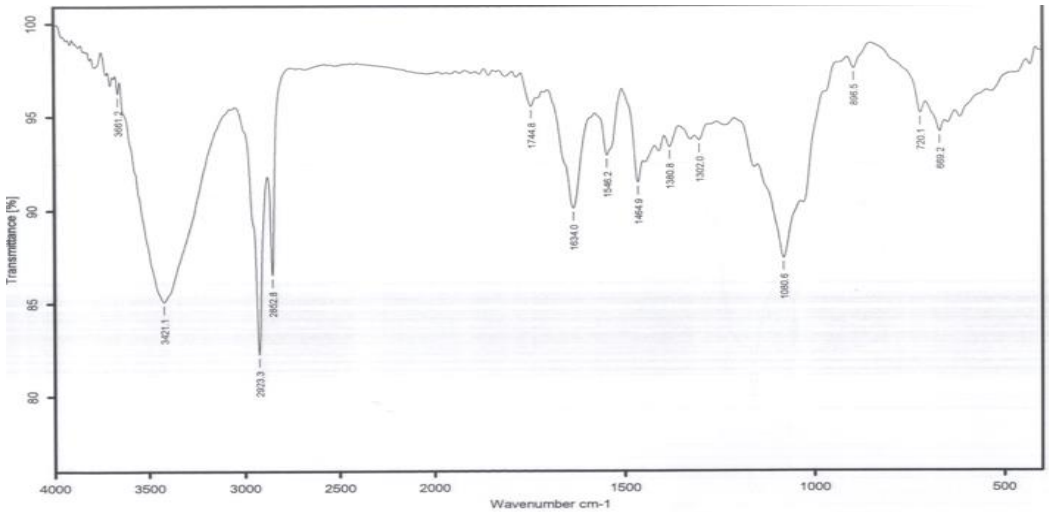

Figure 10: IR spectrum of CAF2

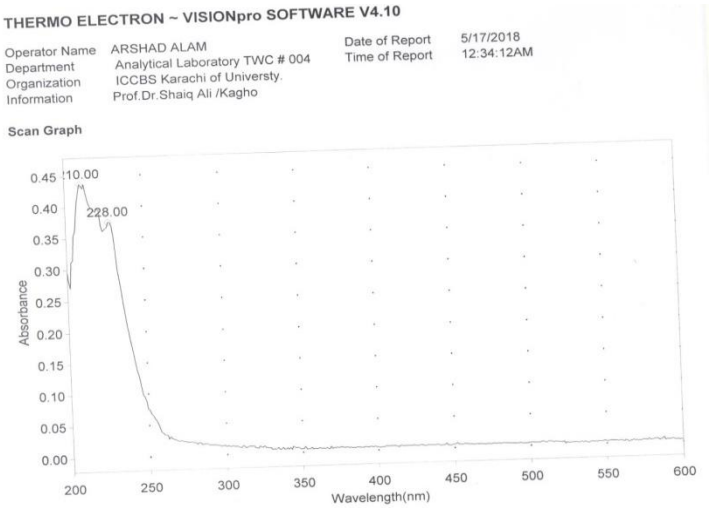

Figure 11: UV spectrum of CAF2

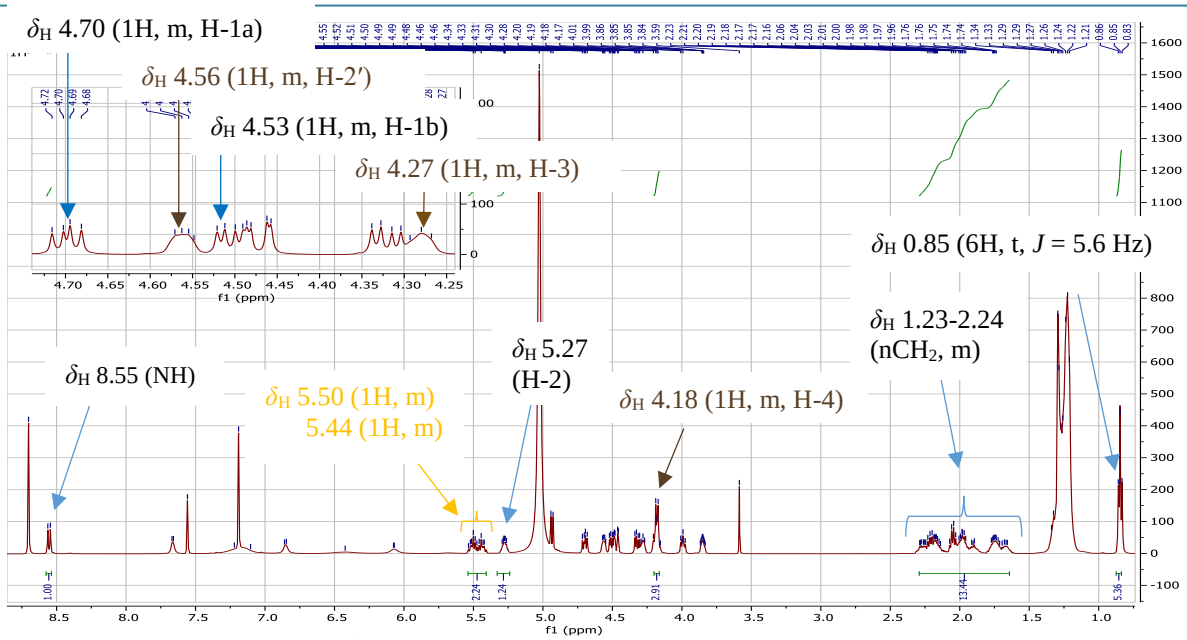

Figure 12: ^{1}H-NMR spectrum (Pyridine-d_5, 400 MHz) of CAF2

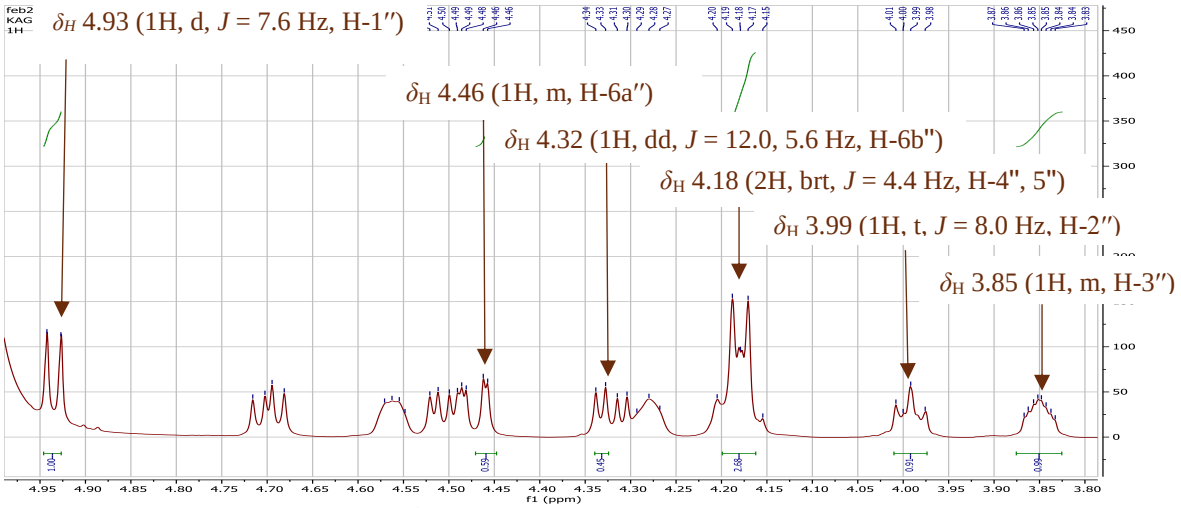

Figure 13: Expanded ^{1}H-NMR spectrum (Pyridine-d_5, 400 MHz) of CAF2

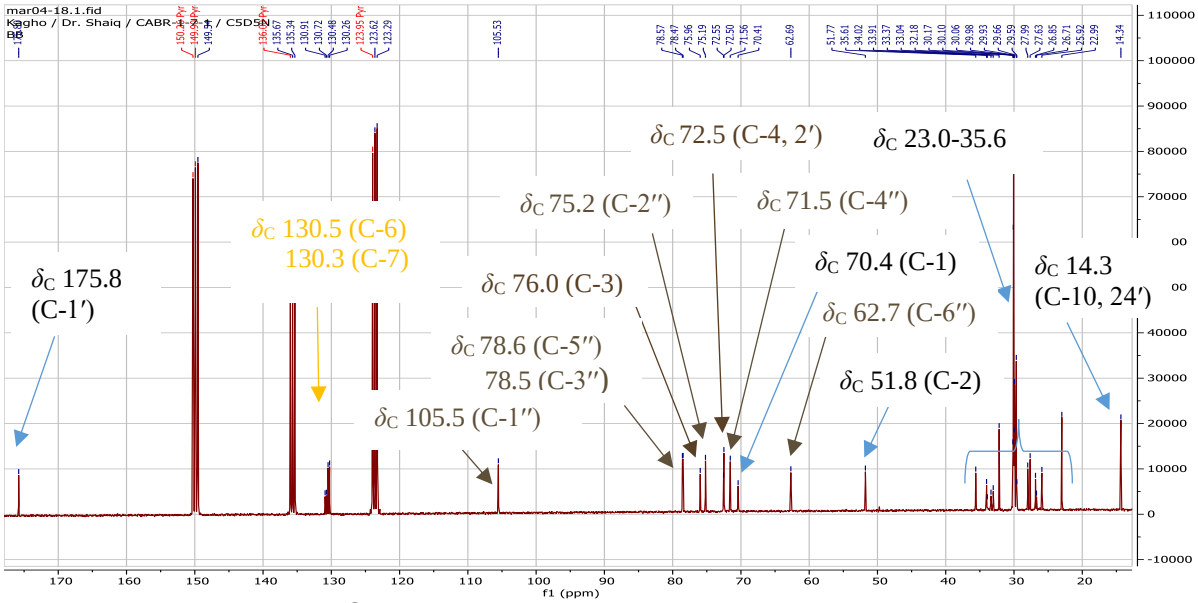

Figure 14: ^{13}C-NMR spectrum (Pyridine-d_5, 100 MHz) of CAF2

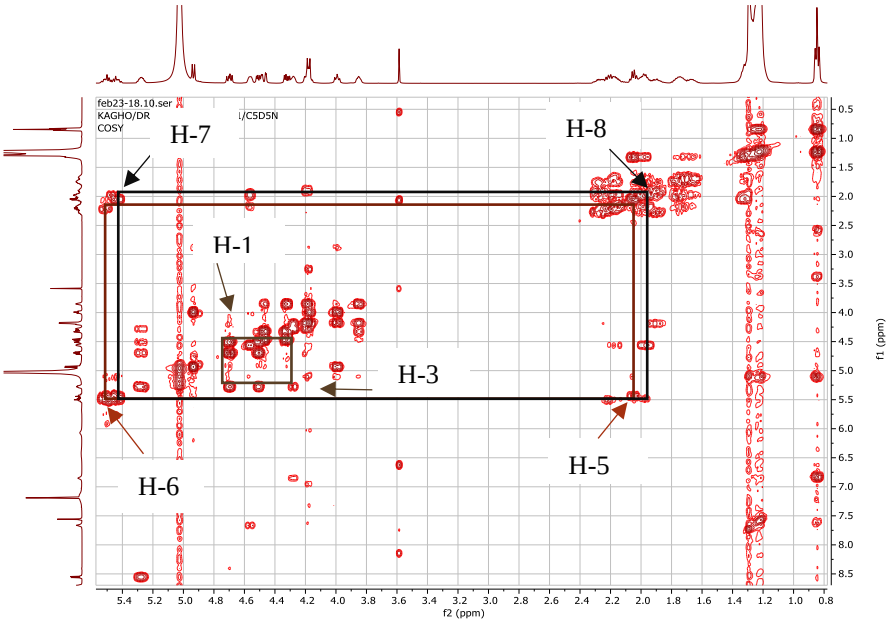

Figure 15: COSY spectrum of CAF2

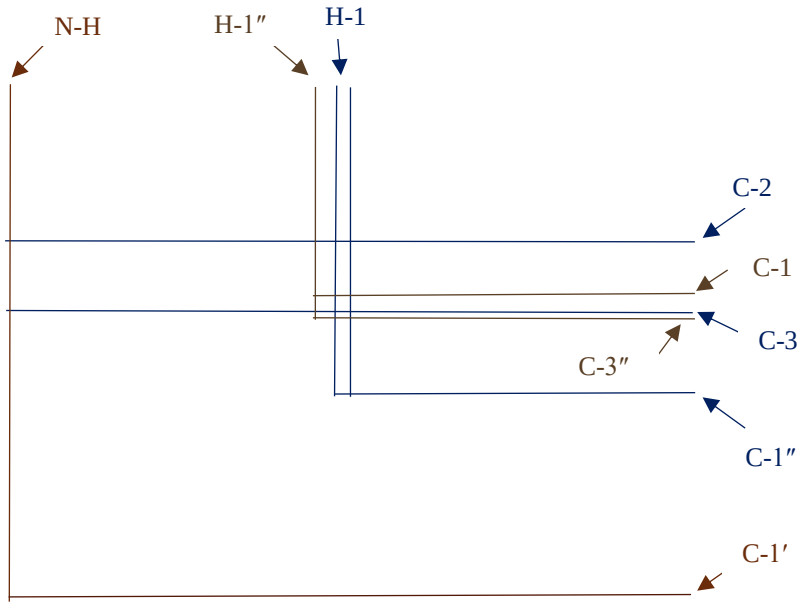

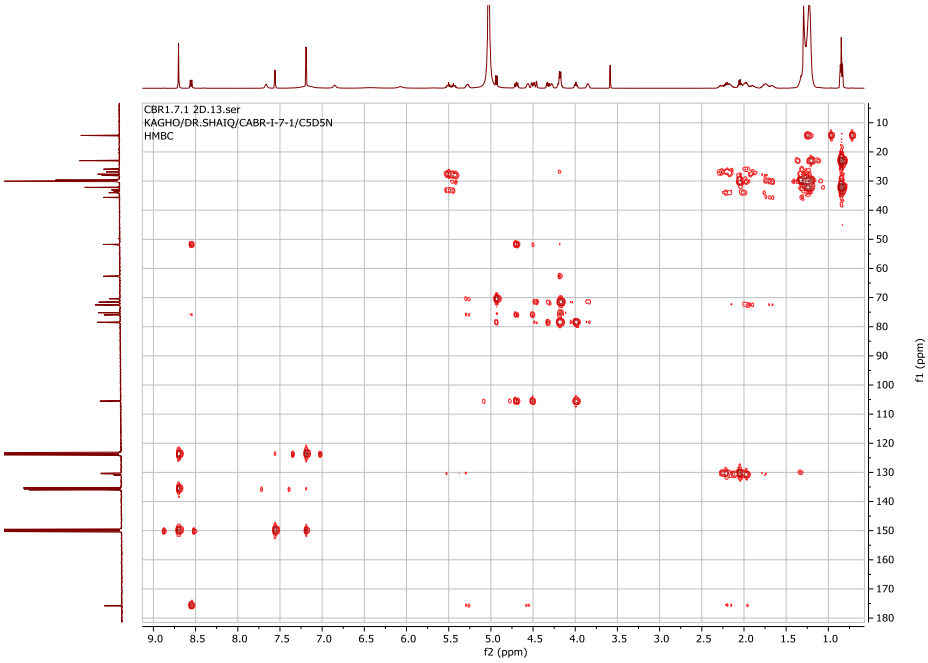

Figure 16: HMBC spectrum of CAF2

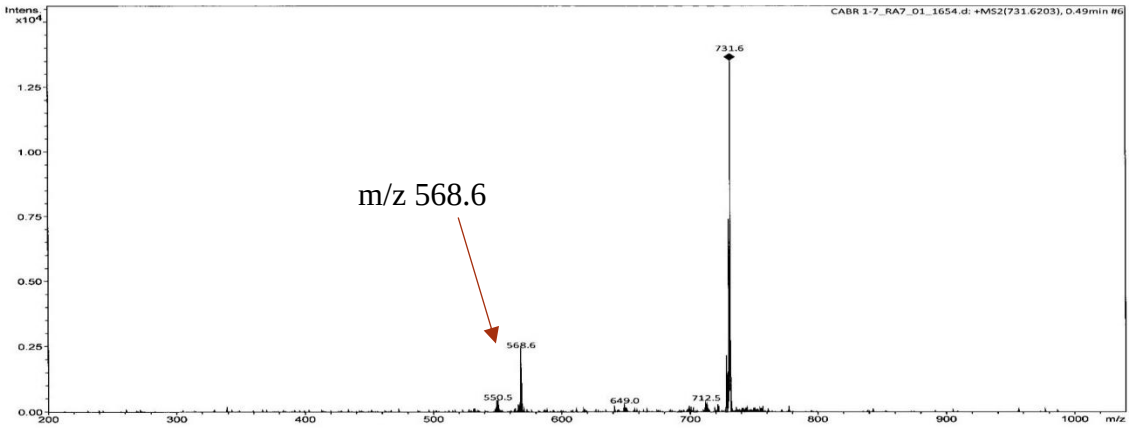

Figure 17: ESI Mass Spectrum of CAF2

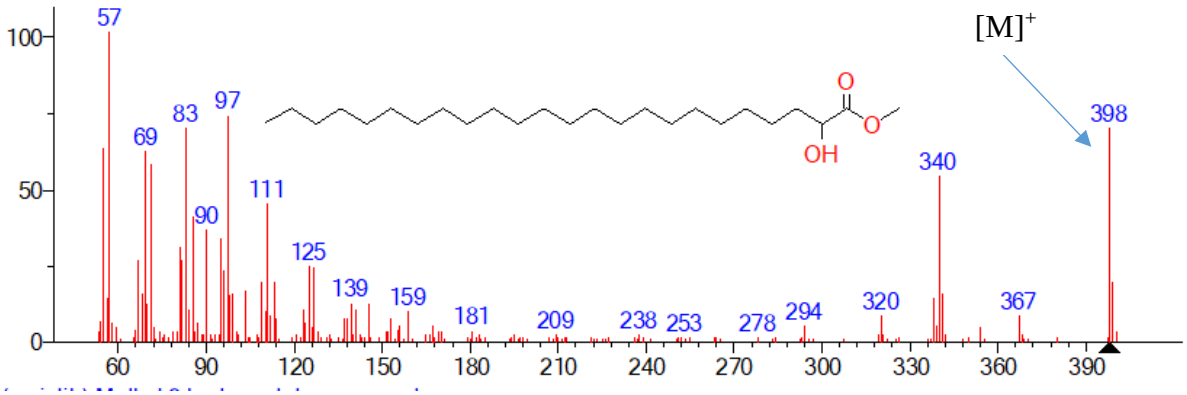

Figure 18: GC-MS analysis of FAME from of CAF2

II.1.2.2 Structure identification of phenolic amides

II.1.2.2.1 Structure identification of CAF14

CAF14 was obtained as yellow-orange powder in the mixture of dichloromethane-methanol (98:2) and was soluble in MeOH. It is positif to ferric chloride tests characteristic of phenolic compounds by the change in color to purple or blue. The analysis of its 1D and 2D spectra combined with its mass spectrum contributed to assign the following structure to CAF14.

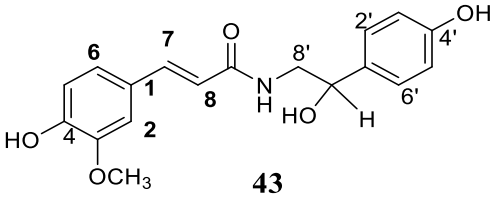

43

The molecular formula, $C_{18}H_{19}NO_5$, implying nine degrees of unsaturation was deduced from its NMR data and its EI-MS (Figure 19), which showed the peak of the dehydrated molecular ion at *m/z* 311.1 $[M-H_2O]^+$.

The ^{1}H-NMR spectrum (Figure 20) exhibited resonances of two doubles at δ_H 7.44 (1H, d, *J* =16.0 Hz, H-7) and 6.45 (1H, d, *J* = 15.6 Hz, H-8) assignable to an olefin *trans* system in the *α*-position to a carbonyl group (**SS1**) (Ge *et al*., 2014). The proton spectrum also displayed resonnances of two doublets of two aromatics protons each attributable to an AA'BB' of a parasubstituted aromatic ring (**SS2**), at δ_H 7.22 (2H, d, *J* = 8.4 Hz, H-2' and H-6') and 6.77 (2H, d, *J* = 8.4 Hz, H-3' and H-5'), three aromatic protons of an ABX system (**SS3**) at δ_H 7.10 (1H, d, *J* = 1.2 Hz, H-2); 7.01 (1H, d, *J* = 8.4 Hz, H-6) and 6.77 (1H, d, *J* = 6.8 Hz, H-5) (Ge *et al*., 2014). In addition, the proton spectrum displayed a deshielded quartet of one proton at δ_H 4.72 (1H, brd, *J* = 4.8 Hz, H-7') (assignable to an oxymethyne), a deshielded singlet of an oxymethyl at δ_H 3.85 (3H, s), and a signal of an azomethylene at δ_H 3.53 (1H, dd, *J* =13.6 and 4.8 Hz, H-8′a) and 3.43 (1H, dd, *J* = 13.6 and 8.0 Hz, H-8′b) (**SS4**). These diastereotopic protons indicate the present of a stereogenic center at position 7′.

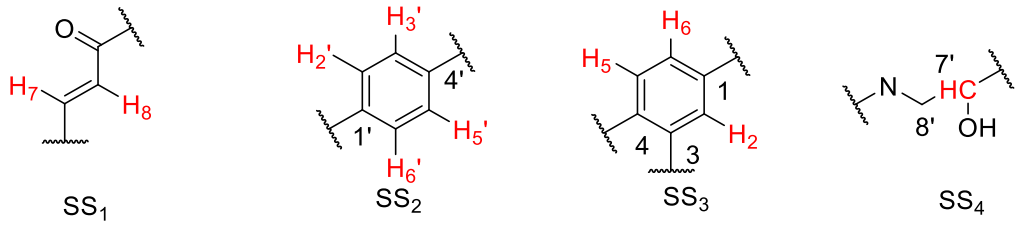

The broadband decoupled ^{13}C-NMR spectrum (Figure 21) displayed fifteen carbon signals which were sorted by DEPT techniques into:

- A methyl at δ_C 56.4 characteristic of carbons belonging to oxymethyl;

- A methylene at δ_C 48.3;

- Eight methines at δ_C 73.4; 111.5; 116.1; 116.4; 118.6; 123.3; 128.2 and 142.3;

- Six quaternary carbons including three oxygenated carbons resonnances at δ_C 158.1 (C-4′), 149.8 (C-3), 149.2 (C-4) and an amide carbonyl at δ_C 169.5 (C-9).

The connections of the different substructures SS1, SS2, SS3 and SS4 were established by the HMBC correlations (Figure 22) of:

- H-7 and carbons at δ_C 111.5 (C-2), 123.3 (C-6), and 169.5 (C-9) to connect olefin to the aromatic nucleus containing the ABX system;

- H-6 and carbons at δ_C 111.5 (C-2), 149.2 (C-4) and 142.3 (C-7) allowing methoxy to be positioned on the aromatic nucleus with the ABX system. This position was confirmed by the correlation between the methoxy proton and the C-3 carbon.

- The correlations between H-2'/H-6' protons and carbons at δ_C 158.0 (C-4') and 73.4 (C-7') of oxymethyne and finally, the correlations between the H-8' proton and the C-7', C-9 and C-1' carbons linked the combined system with azomethylene, oxymethyne and the AA'BB system.

All this data, similar to those described in the literature, *trans-N*-feruloyloctopamine **43** previously isolated from *Acorus tatarinowii* Schott by Ge *et al*., in 2014.

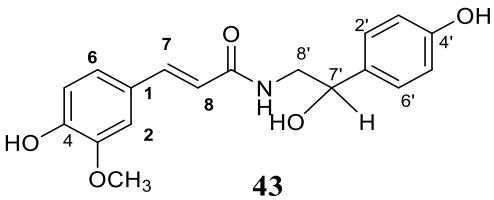

43

Table 13: ^{1}H (MeOH-d_4, 400 MHz) and ^{13}C (MeOH-d_4, 100 MHz) NMR data of CAF14 and *trans-N*-feruloyloctopamine (CD_3COCD_3, 400 MHz and 100 MHz) (Ge *et al*., 2014)

Position	CAF14		*Trans-N*-feruloyloctopamine	
	δ_C	δ_H (nH, m, *J* (Hz))	δ_C	δ_H (nH, m, *J* (Hz))
1	128.2	-	129.4	-
2	111.5	7.10 (1H, d, *J* = 1.2 Hz)	110.4	7.22 (1H, t)
3	149.8	-	147.7	-
4	149.2	-	150.6	-
5	116.4	6.77 (1H, d, *J* = 8.4 Hz)	115.2	6.83 (1H, d, *J* = 8.4 Hz)
6	123.3	7.01 (1H, d, *J* = 8.4Hz)	127.1	7.05 (1H, d, *J* = 8.4 Hz)
7	142.3	7.44 (1H, d, *J* = 16.0 Hz)	139.9	7.45 (1H, d, *J* = 15.6 Hz)
8	118.6	6.45 (1H, d, *J* = 15.6 Hz)	118.8	6.57 (1H, d, *J* = 15.6 Hz)
9	169.5	-	166.5	-
1′	134.7	-	132.8	-

2′,6′	128.5	7.22 (2H, d, *J* = 8.4 Hz)	127.3	7.13 (2H, d, *J* = 8.2 Hz)
3′, 5′	116.1	6.77 (2H, d, *J* = 6.8 Hz)	114.9	6.78 (2H, d, *J* = 8.2 Hz)
4′	158.1	-	158.3	-
7′	73.4	4.72 (1H, q, *J* = 4.8 Hz)	72.7	4.73 (1H, s)
8′	48.3	3.53 (1H, dd, *J* = 13.6, 4.8 Hz)	47.8	3.36 (1H, d)
		3.43 (1H, dd, *J* = 13.6, 8.0 Hz)		3.30 (1H, d)
O-CH_3	56.4	3.85 (3H, s)	55.3	3.87 (3H, s)

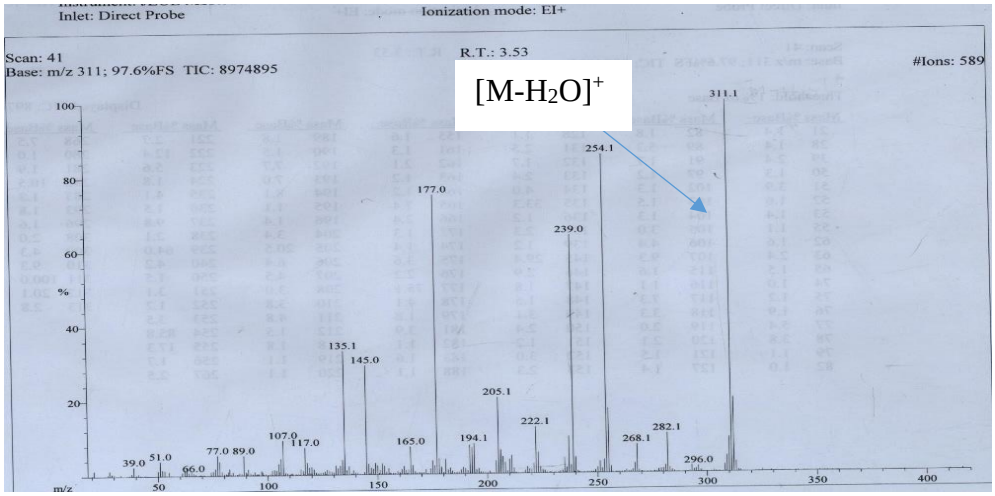

Figure 19: EI mass spectrum of CAF14

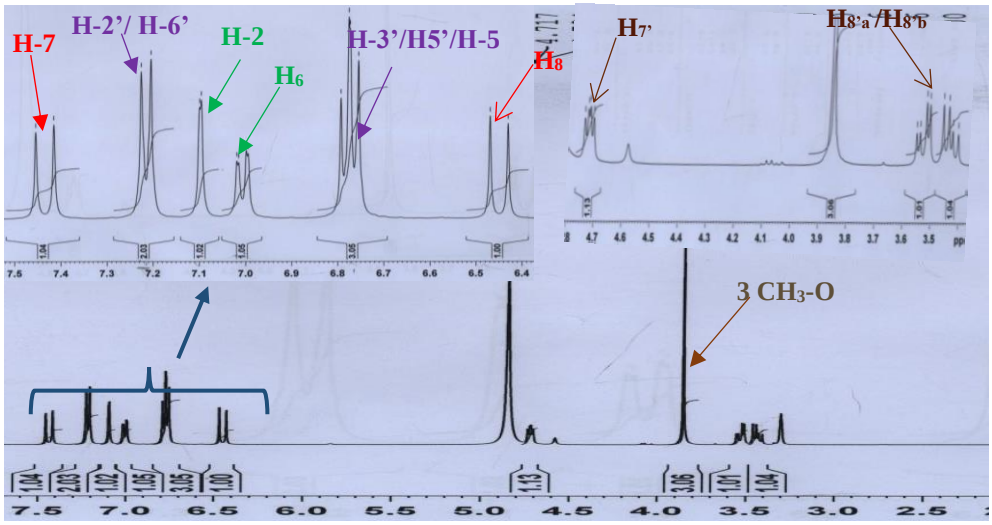

Figure 20: ^{1}H-NMR spectrum (MeOH-d_4, 400 MHz) of CAF14

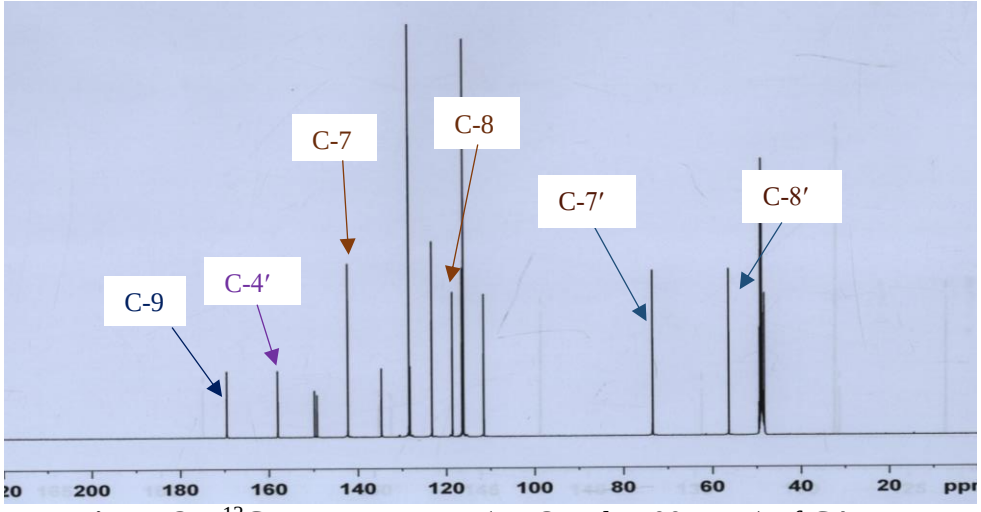

Figure 21: ^{13}C-NMR spectrum (MeOH-d_4, 100 MHz) of CAF14

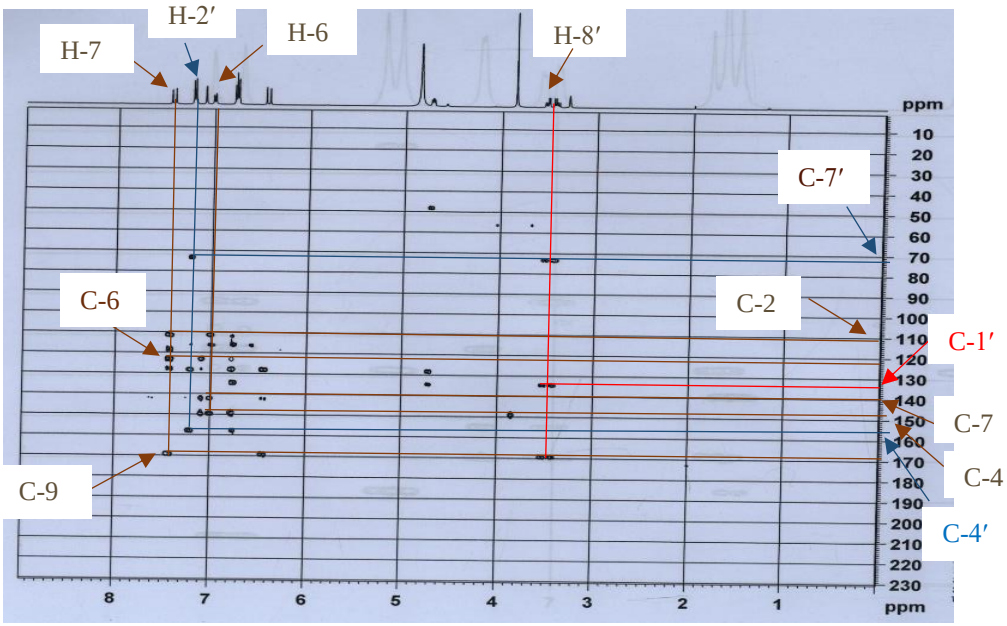

Figure 22: HMBC spectrum of CAF14

II.1.2.2.2 Structure identification of CAF7

Compound CAF7 was obtained as a yellow powder in the mixture of dichloromethane-methanol (49-1), soluble in MeOH. It is positif to ferric chloride tests characteristic of phenolic compounds by the change in color to purple or blue. The 1D and 2D spectra combined with its mass spectrum were in favour to the following structure.

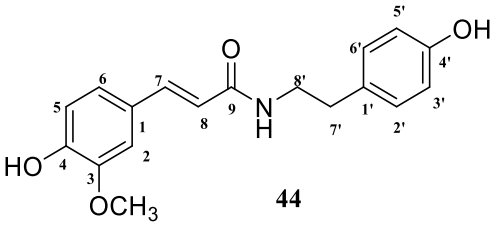

44

Its EI-MS (Figure 23) showed the molecular ion peak $[M]^+$ at *m/z* 313.2, which combined with its NMR data were in favour to the molecular formula, $C_{18}H_{19}NO_4$, containing nine degrees of unsaturation.

The spectrum ^{1}H-NMR (Figure 24) highlights:

- two doublets at δ_H 7.42 (1H, d, *J* =15.6 Hz, H-7), and 6.39 (1H, d, *J* = 15.6 Hz, H-8) attributable to a trans olefin system conjugated located in α of a carbonyl group (Al-Taweel *et al*., 2012).
- two doublets of two protons each at δ_H 7.04 (2H, d, *J* = 8.0Hz, H-2'/H-6'), and 6.71 (2H, d, *J* = 8.4 Hz, H-3'/H-5') assignable to a system AA'BB' on a 1,4-disubstituted aromatic nucleus.
-two deshielded triplets of two protons each at δ_H 3.45 (2H, t, *J* = 7.2 Hz, H-7′); 2.74 (2H, t, *J* = 7.6 Hz, H-8′).

The ^{1}H and ^{13}C-NMR spectra of CAF7 were closed to those of CAF14 with some little discrepancies. In fact, the major change in their ^{13}C-NMR spectra was the absence of the carbon resonance at δ_C 73.4 (C-7') in the carbon spectrum of CAF7 which was replaced by the carbon signal at δ_C 35.8 (C-7'), indicating the lack of the hydroxyl group at position 7′ in CAF7. This was also observed on the proton spectrum (Figure 24) where the diastereotopic protons at position 8′ were replaced by the triplet of two protons at δ_H 3.45 (2H, t, *J* = 7.2 Hz, H-8′). Based on the above spectroscopic data, CAF7 was concluded to be the *trans-N*-feruloyltyramine, previously isolated from *Celtis africana* by Al-Taweel and collaborators in 2012.

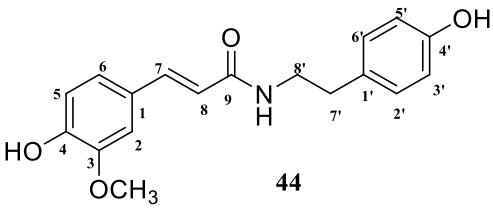

44

Table 14: ^{1}H (MeOH-d_4, 400 MHz) and ^{13}C (MeOH-d_4, 100 MHz) NMR data of CAF7 and *trans-N*-feruloyltyramine (MeOH-d_4, 500 MHz and 125 MHz) (Al-Taweel *et al*., 2012)

	CAF7		***Trans-N*-feruloyltyramine**	
Position	**δ_C**	**δ_H (nH, m, *J* (Hz))**	**δ_C**	**δ_H (nH, m, *J* (Hz))**
1	128.3	-	128.2	-
2	111.5	7.10 (1H, d, *J* = 1.2 Hz)	111.5	7.13 (1H, d, *J* = 1.2 Hz)
3	149.3	-	149.3	-
4	149.8	-	149.8	-
5	116.5	6.78 (1H, d, *J* = 8.0 Hz)	116.4	6.81 (1H, d, *J* = 8.5 Hz)
6	123.2	7.00 (1H, dd, *J* = 8.0, 1.6 Hz)	123.2	7.05 (1H, dd, *J* = 8.5;1.2 Hz)
7	142.0	7.42 (1H, d, *J* = 15.6 Hz)	142.0	7.44 (1H, d, *J* = 15.5 Hz)

8	118.7	6.39 (1H, d, *J* = 15.6 Hz	118.7	6.41 (1H, d, *J* = 15.5 Hz)
9	169.2	-	169.2	-
1'	131.3	-	131.3	-
2'/6'	130.7	7.04 (2H, d, *J* = 8.0 Hz)	130.7	7.07 (2H, d, *J* = 8.4 Hz)
3'/5'	116.3	6.71 (2H, d, *J* = 8.4 Hz)	116.2	6.73 (2H, d, *J* = 8.4 Hz)
4'	156.9	-	156.9	-
7'	35.8	2.74 (2H, t, *J* = 7.6 Hz)	35.8	2.76 (2H, t, *J* = 7.5 Hz)
8'	42.5	3.45 (2H, t, *J* = 7.2 Hz)	42.5	3.47 (2H, t, *J* = 7.5 Hz)
OCH_3	56.4	3.87 (3H, s)	56.4	3.85 (3H, s)

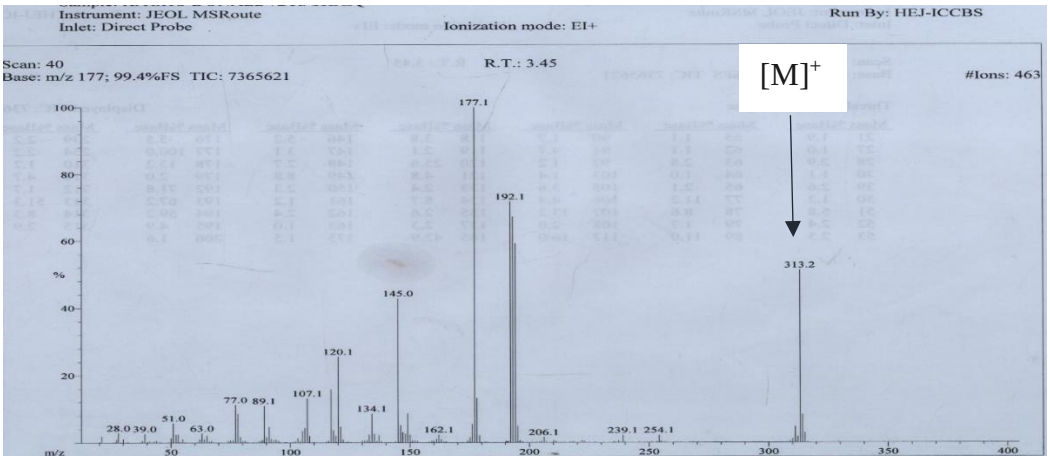

Figure 23: EI mass spectrum of CAF7

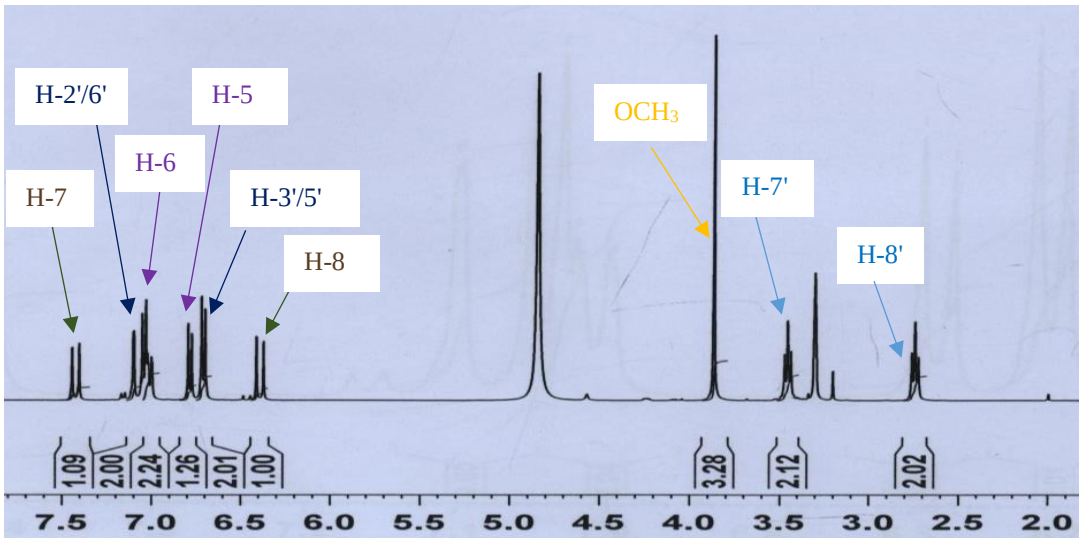

Figure 24: ^{1}H-NMR spectrum (MeOH-d_4, 400 MHz) of CAF7

II.1.2.2.3 Structure identification of CAF8

Compound CAF8 was obtained as white powder, soluble in MeOH. The interpretation of all its spectroscopic and spectrometric data led to the assignment of the following structure.

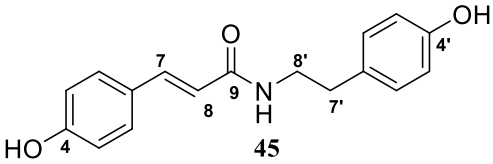

45

The molecular formula, $C_{17}H_{17}NO_3$, with nine degrees of unsaturation was deduced from its NMR data and its HR-EI-MS (Figure 25) which showed the molecular-ion peak at *m/z* 283.1184 $[M]^+$.

The ^{1}H-NMR spectrum (Figure 26) showed resonances for two sets of AA′BB′ type signals at δ_H 7.38 (2H, d, *J* = 8.4 Hz, H-2/6), 7.04 (2H, d, *J* = 8.6 Hz, H-2′/6′), 6.78 (2H, d, *J* = 8.4 Hz, H-3/5), and 6.71 (2H, d, *J* = 8.6 Hz, H-3'/5'). In addition, two coupled triplets of methylene protons appeared at δ_H 3.45 (2H, t, *J* = 7.5 Hz, H-8′) and 2.74 (2H, t, *J* = 7.5 Hz, H-7′) attributable to an azomethylene and a methylene, respectively.

The ^{1}H and ^{13}C-NMR spectra of CAF8 were equally closed to those of CAF7 with some little discrepancies. The main difference was the absence of the methoxy group protons and the carbon signals on both the ^{1}H and ^{13}C NMR spectrum, respectively. In addition, the ABX system found in the proton spectrum of CAF7 is replaced by an additional AA′BB′ system with signals at δ_H 7.38 (2H, d, *J* = 8.4 Hz, H-2, 6), 7.04 (2H, d, *J* = 8.6 Hz, H-2′, 6′), 6.78 (2H, d, *J* = 8.4 Hz, H-3, 5) and 6.71 (2H, d, *J* = 8.6 Hz, H-3', 5') in CAF8 (Figure 26).

The above data led to the identification of CAF8 as *trans*-*N*-coumaroyltyramine previously isolated from *C. africana* by Al-Taweel and collaborators in 2012.

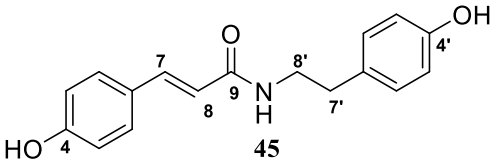

45

Table 15: ^{1}H (MeOH-d_4, 400 MHz) and ^{13}C (MeOH-d_4, 100 MHz) NMR data of CAF8 and *trans*-*N*-coumaroyltyramine (MeOH-d_4, 500 MHz and 125 MHz) (Al-Taweel *et al*., 2012)

Position	**CAF8**		***Trans*-*N*-coumaroyltyramine**	
	δ_C	δ_H **(nH, m, *J* (Hz))**	δ_C	δ_H **(nH, m, *J* (Hz))**
1	127.7	-	127.7	-
2/6	130.6	7.38 (2H, d, *J* = 8.4 Hz)	130.5	7.41 (2H, d, *J* = 8.4 Hz)
3/5	116.2	6.78 (2H, d, *J* = 8.4 Hz)	116.2	6.80 (2H, d, *J* = 8.4 Hz)
4	160.6	-	160.5	-
7	141.8	7.37 (1H, d, *J* = 15.6 Hz)	141.8	7.44 (1H, d, *J* = 15.5 Hz)
8	118.3	6.32 (1H, d, *J* = 15.6 Hz)	118.4	6.38 (1H, d, *J* = 15.5 Hz)
9	169.2	-	169.2	-

1'	131.3	-	131.3	-
2'/6'	130.7	7.04 (2H, d, *J* = 8.4 Hz)	130.5	7.06 (2H, d, *J* = 8.6 Hz)
3'/5'	116.7	6.71 (2H, d, *J* = 8.4 Hz)	116.7	6.73 (2H, d, *J* = 8.6 Hz)
4'	156.9	-	156.9	-
7'	35.8	2.74 (2H, t, *J* = 7.2 Hz)	35.8	2.75 (2H, t, *J* = 7.5 Hz)
8'	42.6	3.45 (2H, t, *J* = 7.2 Hz)	42.5	3.46 (2H, t, *J* = 7.5 Hz)

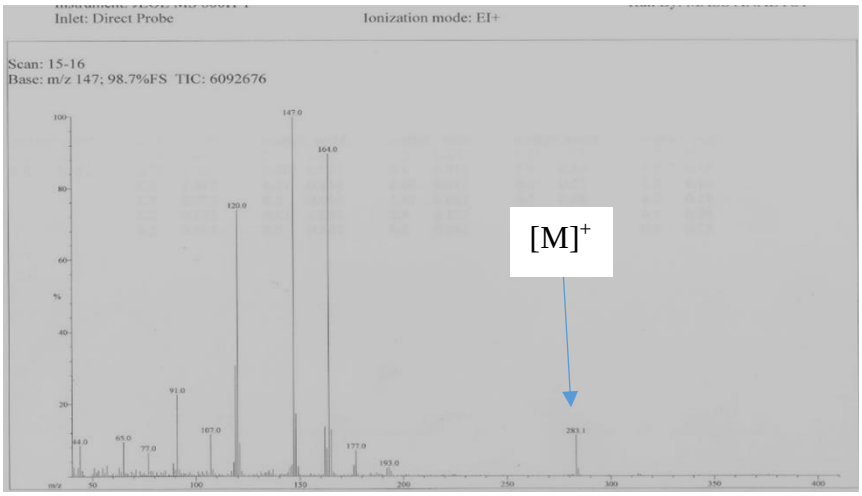

Figure 25: EI mass spectrum of CAF8

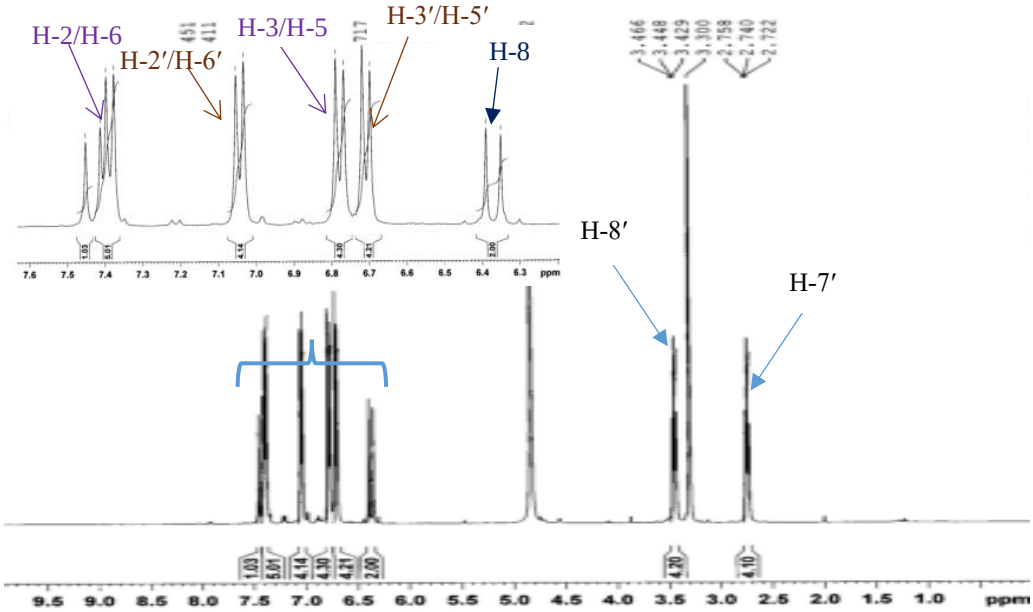

Figure 26: ^{1}H-NMR spectrum (MeOH-d_4, 400 MHz) of CAF8

II.1.2.3 Structure identification of dicarboxylic acids

II.1.2.3.1 Structure identification of CAF9

Compound CAF9 was obtained as a white powder in the mixture of methylene chloride-methanol (99:1). It is soluble in DMSO and responds positively to the carboxylic acid test. The

combinaison of its NMR data with its mass spectrum data led to the attribution of the following structure to CAF9.

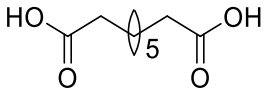

46

The molecular formula, $C_9H_{16}O_4$, which indicated two degrees of unsaturation with two hydrogens deficiency was deduced from its NMR data and its HR-ESI-MS in positive mode (Figure 27) which showed the protonated molecular ion peak $[M+H]^+$ at *m/z* 189.1121 (calcd for 188.1049).

The ^{1}H-NMR spectrum (figure 28) exhibited:

- A singlet of two protons at δ_H 11.95 (2H, s) attributable to protons of a carboxylic acid function;
- Two triplets of four protons at δ_H 2.17 (4H, t, J=14.4 Hz, H-2 and H-8) and 1.46 (4H, t, J = 13.2 Hz, H-3 and H-7), where the most deshielded one corresponds to the methylene at α-position to the carboxyl groups.
- A broad singlet of protons at δ_H 1.23 (nH, s), which was assigned to methylene protons of an aliphatic chain.

The length of the chain was determined using the mass spectrum data (Figure 27).

Based on the above data, CAF9 was identified as azelaic acid previously prepared, characterized, and theoretical studies by Kadhum and collaborators in 2012. The table 16 below resumes these data.

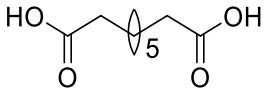

46

Table 16: ^{1}H-NMR (DMSO-d_6, 400 MHz) data of CAF9 and azelaic acid (DMSO-d_6, 200 MHz) (Kadhum *et al*., 2012)

Position	**CAF9**	**azelaic acid**
	δ_H (nH, m, J (Hz))	**δ_H (nH, m, J (Hz))**
1	11.95 (1H, s)	
2/8	2.17 (4H, t, J=14.4Hz)	2.4
3/7	1.46 (4H, t, J=13.2Hz)	1.8
4/5/6	1.23 (6H, brs)	1.3

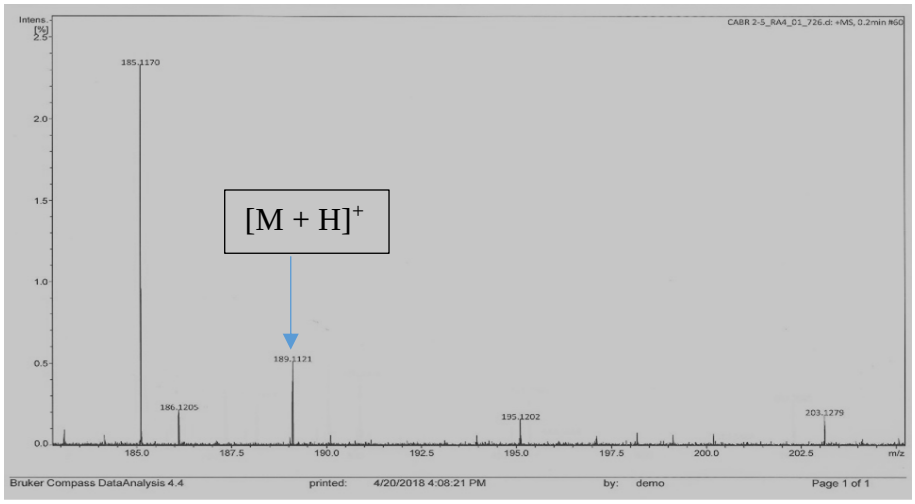

Figure 27: HR-ESI mass spectrum of CAF9

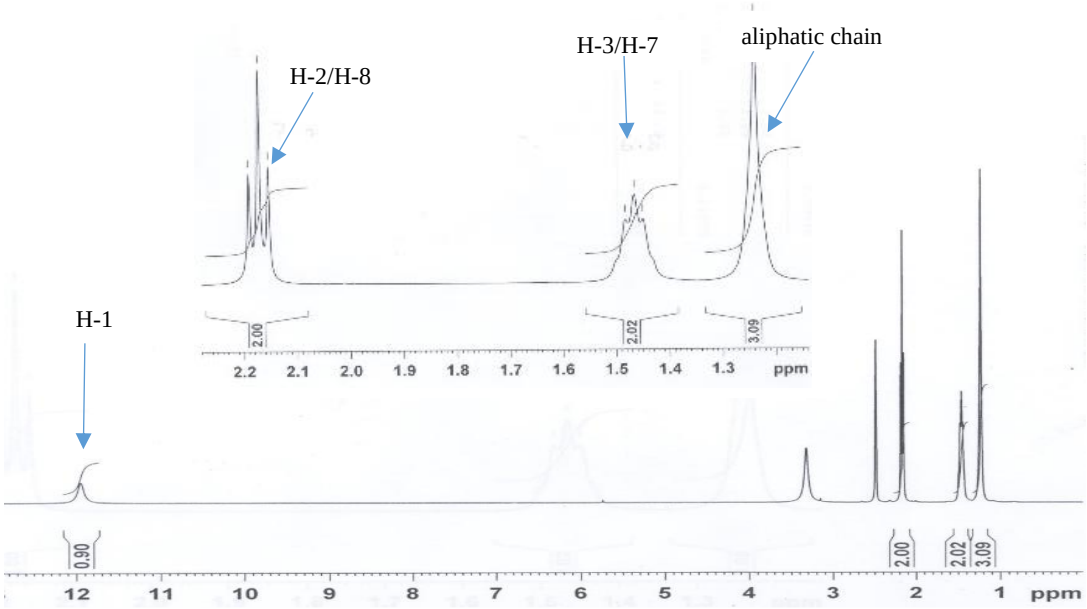

Figure 28: ^{1}H-NMR spectrum (DMSO-d_6, 400 MHz) of CAF9

II.1.2.3.2 Structure identification of CAF13

Compound CAF13 was obtained as a white powder in the (96:4) mixture of methylene chloride-methanol. It was soluble in MeOH+$CDCl_3$ and responded positively to the carboxylic acid test. The combinaison of its NMR data with its mass spectrum data led to assignement of the following structure to CAF13.

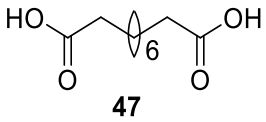

47

The molecular formula, $C_{10}H_{18}O_4$, with two degrees of unsaturation was obtained from its NMR and EI-MS data (Figure 29), which showed the peak of a dehydroxylated molecular

ion peak [M - OH]$^+$ at *m/z* 185.1. This mass suggested that CAF13 differ from CAF9 by 14 Uma corresponding to one additional methylene group

This observation was futher supported by the similarities observed in the ^{1}H-NMR spectrum (Figure 28 and Figure 30) of both compound CAF9 and CAF13. In fact, the main difference observed in the two proton spectra was due to the type of solvent used in dissolving the two compounds during the recording of their NMR spectra. Hence, the proton spectrum of CAF13, which was recorded in the protic solvent, MeOD, did not give rise to the signal of exchangeable hydroxy protons of the carboxylic acid groups.

Based on the above evidences, CAF13 was concluded to be sebacic acid previously synthesized by Otte and collaborators in 2017, and hence, isolated from the first time from natural sources.

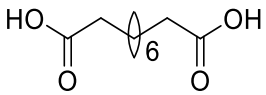

47

Table 17: ^{1}H NMR (MeOH+CDCl$_3$, 400 MHz) data of CAF13

Position	CAF13 δ_H (nH, m, *J* (Hz)
2/9	2.28 (4H, t, *J* = 14.8 Hz)
3/8	1.58 (4H, t, *J* = 8 Hz)
4/5/6/7	1.32 (2H, s)

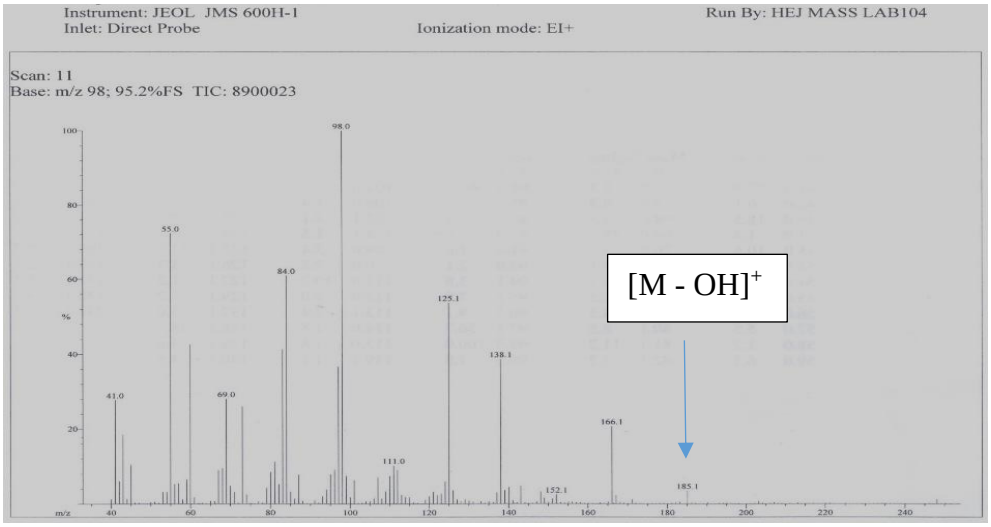

Figure 29: EI mass spectrum of CAF13

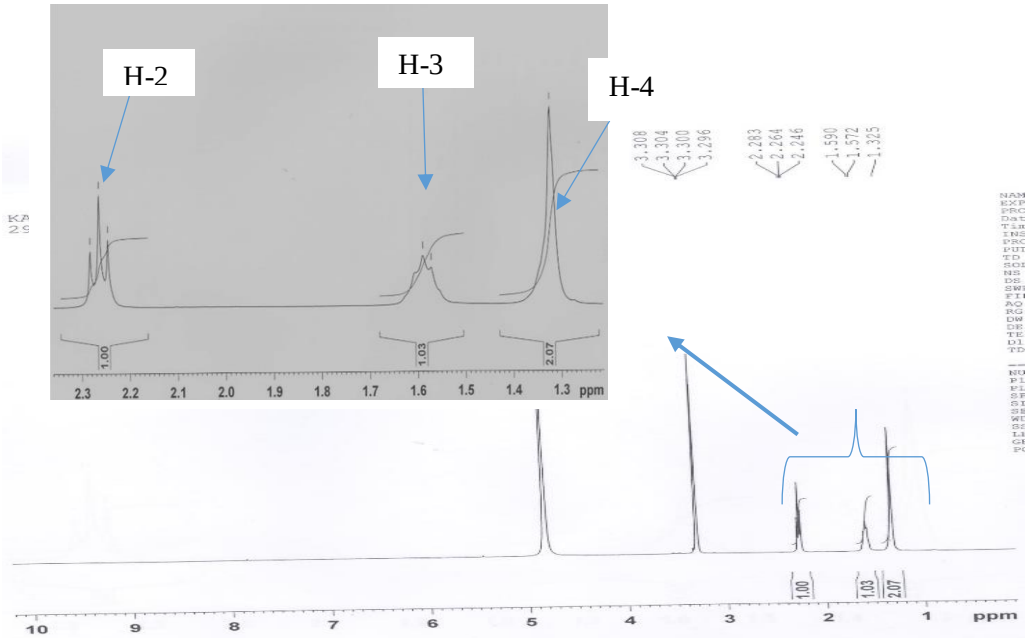

Figure 30: ^{1}H-NMR spectrum (MeOH+$CDCl_3$, 400 MHz) of CAF13

II.1.2.4 Structure identification of CAF10

Compound CAF10 was obtained as a white powder nature in the mixture of *n*-hexane-methylene chloride (4-1). It was soluble in $CDCl_3$. The combinaison of its NMR and mass spectrum data were in favour of the following structure.

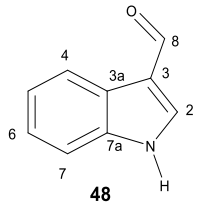

48

The ^{1}H-NMR spectrum (Figure 31) of CAF10 exhibited resonances for aromatic protons at δ_H 7.43 (1H, m, H-7), 8.31 (1H, m, H-4), 7.31 (1H, m, H-5/ H-6), and at 7.83 (1H, d, J = 3Hz, H-2). It also exhibited resonance downfield for a carbonyl proton at δ_H 10.10 (1H, s, J = 10.06 Hz, H-8). Finally, it exhibited a resonance for a broad singlet peak of one proton at δ_H 8.67 (1H, brd s, J = 8.63 Hz, NH-1), suggesting an unsubstituted ring of indole skeleton (shigemori *et al.*, 2003).

The broadband decoupled ^{13}C-NMR spectrum (Figure 32) displayed 9 carbon signals, which were sorted by DEPT and HSQC techniques into three quaternary carbons at δ_C 119.8 (C-3), 124.4 (C-3a), and 125.6 (C-7a), six methine carbon signals at δ_C 122.4 (C-4), 123.1 (C-5), 124.3 (C-6), 111.4 (C-7), 135.1 (C-2), and 185.1 (C-8).

The HMBC spectrum (Figure 33) of CAF10 showed correlations between H-7/C-3a, H-4/C-3a; H-2/ C-3, and C-3a; and H-8/ C-3a.

Based on the above evidences, CAF10 was identified as indole 3-carboxaldehyde (**48**), previously isolated from *Pseudomonas syringae* pv. by Evidente and Surico in 1986.

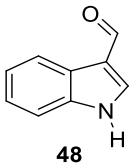

48

Table 18: ^{1}H ($CDCl_3$, 500 MHz) and ^{13}C ($CDCl_3$, 125 MHz) NMR data of CAF10 and indole 3-carboxaldehyde (CD_3OD, 270MHz) (Evidente and Surico, 1986)

Position	CAF10 δ_C	CAF10 δ_H (nH, m, *J* (Hz)	Indole 3-carboxaldehyde δ_H (nH, m, *J* (Hz)
1			
2	135.1	7.83 (1H, d, *J* = 3Hz)	8.09(s)
3	119.8		
4	122.4	8.31 (1H, m)	8.16 (1H, dd, *J*=8.0, 1.5 Hz)
5	123.1	7.31 (1H, m)	7.23 (ddd, *J*=8.0, 8.0, 1.5 Hz)
6	124.3	7.31 (1H, m)	7.28 (ddd, *J*=8.0, 8.0, 1.5 Hz)
7	111.4	7.43 (1H,m)	7.48 (dd, *J*=8.0, 1.5 Hz)
8	185.1		
3a	124.4		
7a	125.6		

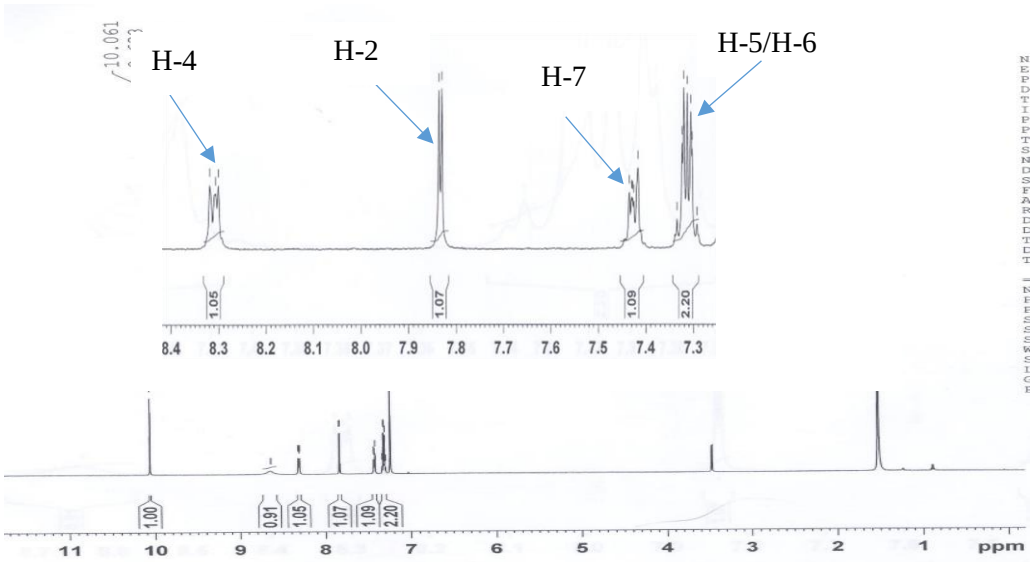

Figure 31: ^{1}H-NMR spectrum ($CDCl_3$, 500 MHz) of CAF10

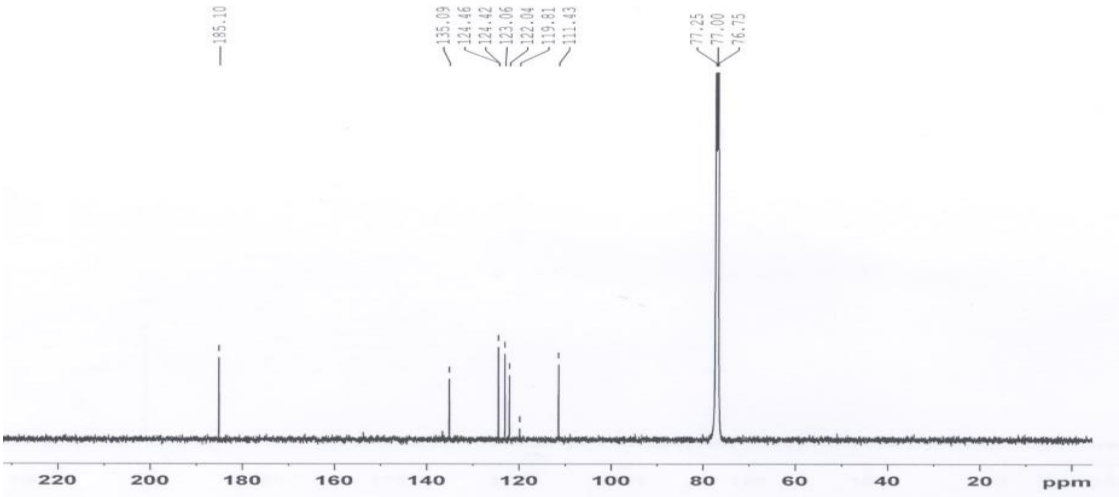

Figure 32: ^{13}C NMR spectrum ($CDCl_3$, 125MHz) of CAF10

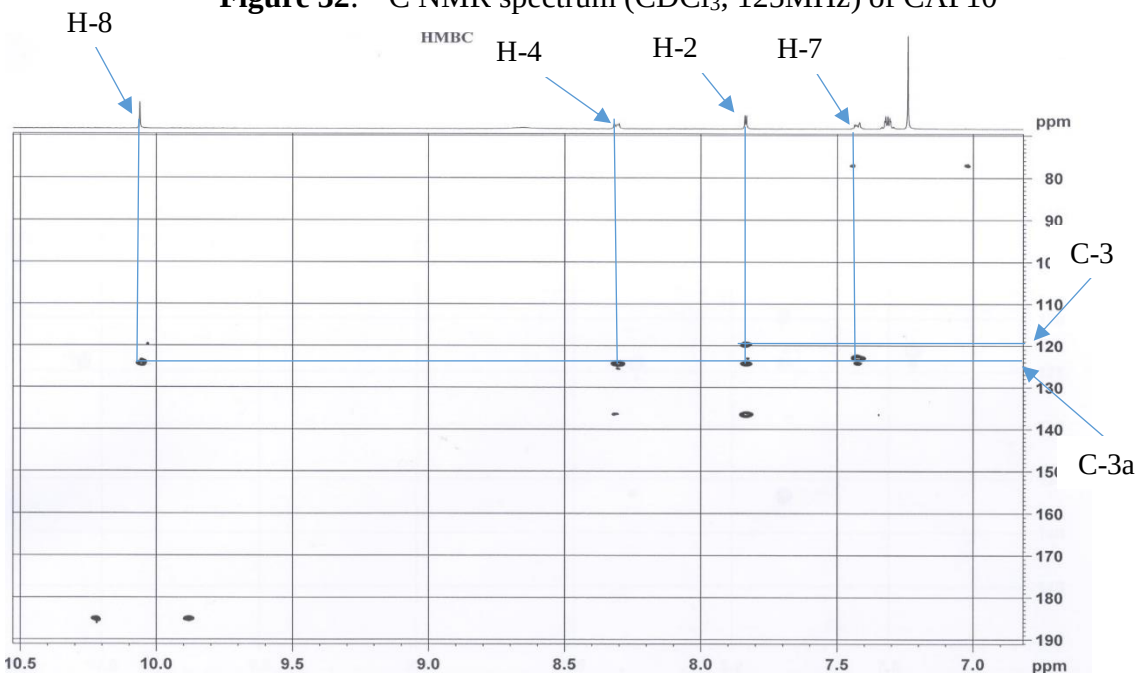

Figure 33: HMBC spectrum of CAF10

II.1.2.5 Structure identification of fatty acids

II.1.2.5.1 Structure identification of CAF12

Compound CAF12 was obtained as a white oil in the mixture *n*-hexane-methylene chloride (50%). It was soluble in chloroform. The combinaison of its NMR data with its mass spectrum permitted us to attribute the following structure.

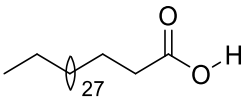

49

The molecular formula, $C_{32}H_{64}O_2$, implying one degree of unsaturation, was deduced from its NMR and its EI-MS data (Figure 34), which showed the molecular ion peak $[M]^+$ at *m/z* 480.2.

The ^{1}H-NMR spectrum (Figure 35), displayed resonances of the following:

- a triplet at δ_H 2.23 (2H, t, J = 7.6 Hz, H-2) assignable to a methylene group adjacent to a carbonyl group;
- a multiplet of 2 protons at δ_H 1.60 (2H, p, J = 7.2 Hz, H-3);
- a broad singlet at δ_H 1.23 (nH, brs, H-4 to H-31)assignable to the protons of an aliphatic long chain;
- and a triplet of 3 protons at δ_H 0.86 (3H, t, J = 6.4 Hz, H-32).

In addition, the EI spectrum showed a series of ion peaks separated by 14 uma, confirming the presence of the long chain in CAF12.

Based on the above data, CAF12 was concluded to be laceroic acid, previously isolated from *Limnophila polystachya* Benth by Kalimuthu and collaborators in 2011.

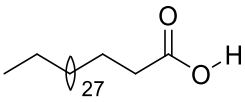

49

Table 19: ^{1}H-NMR ($CDCl_3$, 400 MHz) data of CAF12

Position	CAF12 **δ_H (nH, m, J (Hz)**
1	
2	2.33 (2H, t, J = 7.6 Hz)
3	1.60 (2H, m, J = 7.2 Hz)
4-31	1.27-1.23 (56H, m)
32	0.86 (3H, t, J = 6.4 Hz)

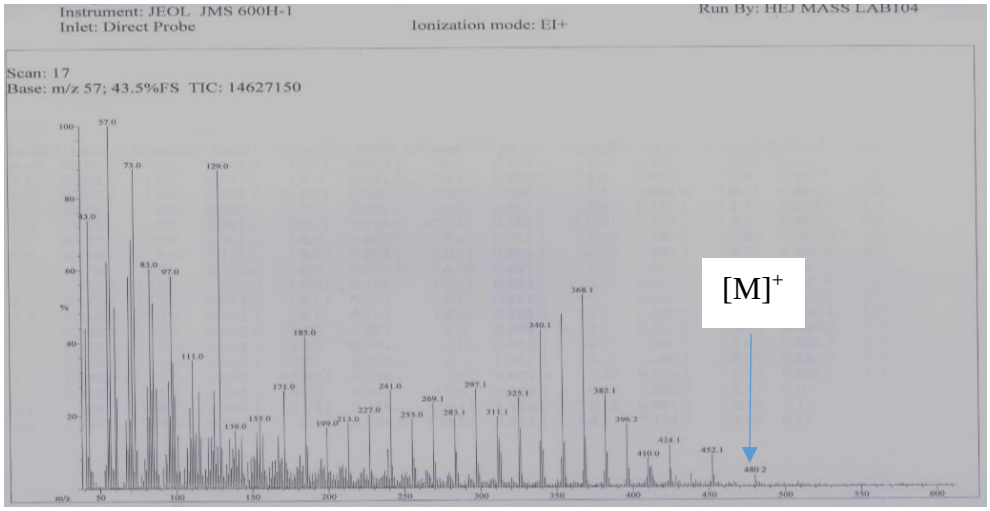

Figure 34: EI mass spectrum of CAF12

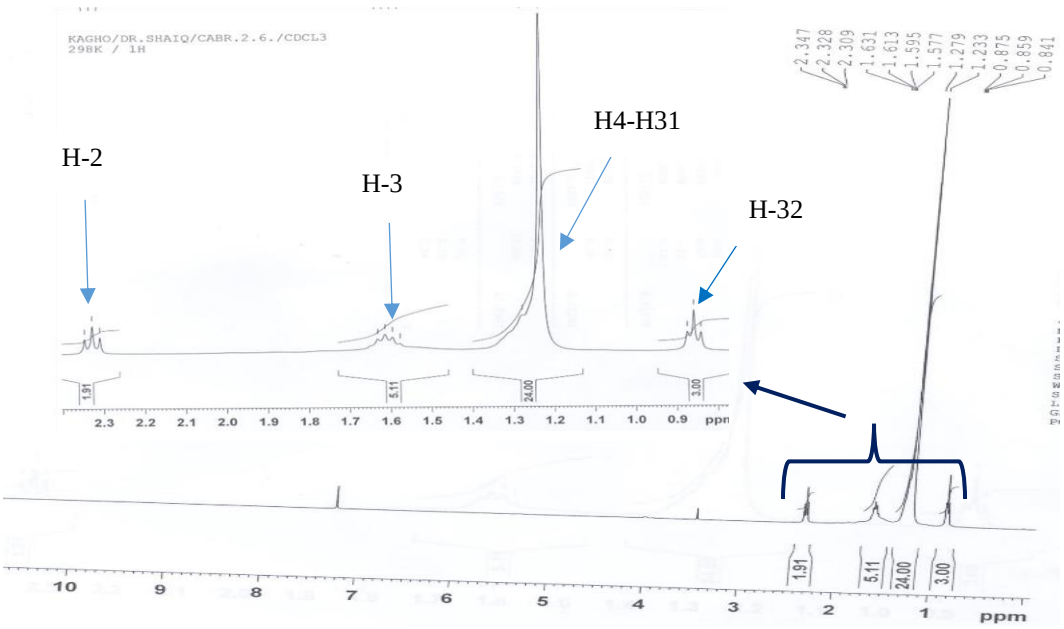

Figure 35: ^{1}H-NMR spectrum ($CDCl_3$, 400 MHz) of CAF12

II.1.2.5.2 Structure identification of CAF3

Compound CAF3 was obtained as a white amorphous powder in the mixture of *n*-hexane-EtOAc (98:2). It was soluble in pyridine. Its NMR data combined with its mass spectrum permitted us to attribute the following structure

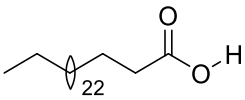

50

The molecular formula, $C_{27}H_{52}O_2$, implying one degree of unsaturation, was deduced from its NMR and its EI-MS data (Figure 36), which showed the molecular ion peak $[M]^+$ at *m/z* 410.3.

The ^{1}H-NMR spectrum of CAF3 (Figure 37), was similar to that of CAF12. Discrepancies were observed on their EI spectra. The EI-MS spectrum of CAF3 displayed the molecular ion peak at *m/z* 410.3, which differs from that of CAF12 by 70 uma, corresponding to 14×5. Therefore, CAF3 is also a fatty acid with five methylene units less as compared to CAF12, confirming the molecular formular, $C_{27}H_{52}O_2$.

CAF3 was therefore concluded to be heptacosanoic acid (Kovganko *et al*., 1999).

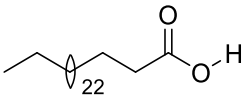

50

Table 20: ^{1}H-NMR (Pyridine-d_5, 400 MHz) data of CAF3

Position	CAF3 (δ_H (nH, m, J (Hz)) ppm
1	
2	2.54 (2H, t, J = 7.6 Hz)
3	1.82 (2H, qt, J = 7.6 Hz)
4-26	1.39-1.29 (m)
27	0.85 (3H, t, J = 6.4 Hz)

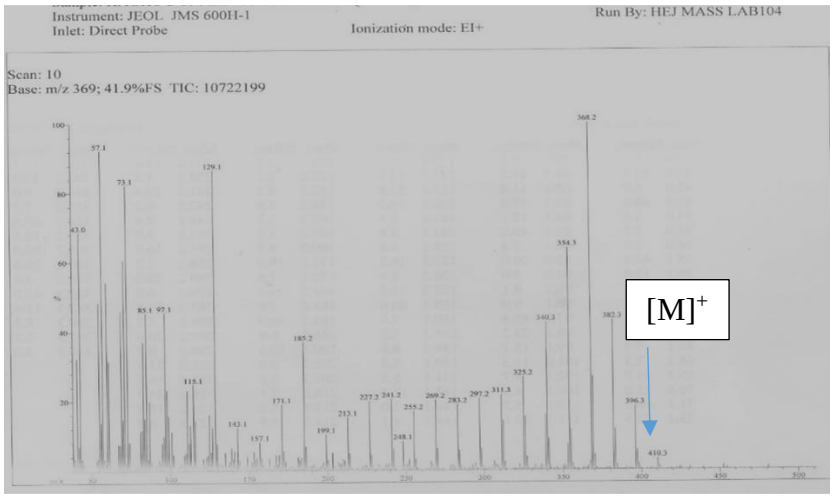

Figure 36: EI spectrum of CAF3

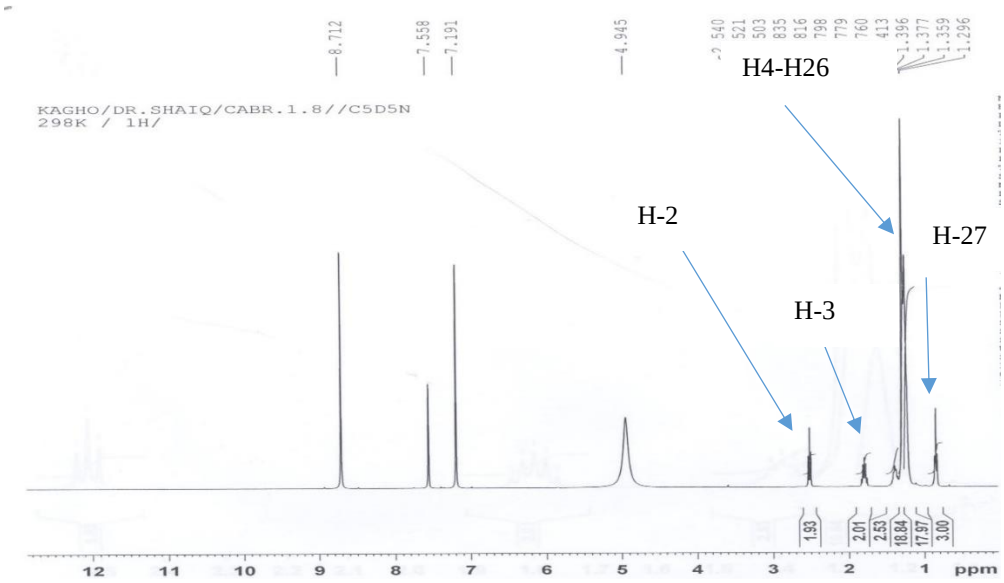

Figure 37: ^{1}H-NMR spectrum (Pyridine-d_5, 400 MHz) of CAF3

II.1.2.6 Structure identification of CAF15

Compound CAF15 was obtained as a white powder in a mixture of methylene chloride-methanol (95-5). It was soluble in DMSO. The combinaison of its NMR data with its EI-MS data led to the identification of the following structure.

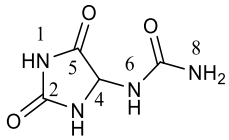

51

The molecular formula, $C_4H_6N_4O_3$, implying four degrees of unsaturation, was deduced from its NMR and its EI-MS data (Figure 38), which showed the molecular ion peak $[M]^+$ at *m/z* 158.1.

The ^{1}H-NMR spectrum (Figure 39) of CAF15 gave prominent peaks at δ_H 5.23 (1H, d, *J*= 8.00, H-4), 5.76 (2H, s, N_8-H2), 6.86 (1H, d, *J* = 8.00, N_6-H), 8.04 (1H, s, N_3-H) and 10.52 (1H, brd s, N_2-H) suggesting an imidazole alkaloid substituted skeleton (Scripathi *et al*., 2011).

The HSQC spectrum (Figure 40) of CAF15 showed only one correlation between the proton at δ_H 5.23 and the carbon signal at δ_C 62.8. Hence, the other proton signals are due to proton attached to heteroatoms.

The ^{1}H-^{1}H COSY spectrum (Figure 41) of CAF15, displayed correlations of H-4/N_6-H and N_3-H indicating that these protons are in the same viccinities. Probably a weak interaction may be present between the proton at δ_H 5.23 and the proton at δ_H 8.04.

The HMBC spectrum (Figure 42) for this compound showed correlations between proton H-4 and carbons C-2 (δ_C 157.6) and C-5 (δ_C 174.0), proton N_6-H and carbons C-4 (δ_C 62.8), and C-5 (δ_C 174.0), proton N_3-H and carbons C-4 (δ_C 62.8), C-2 (δ_C 157.6), and C-5 (δ_C 174.0); and finally protons N_1-H and carbons C-4 (δ_C 62.8) and C-2 (δ_C 157.6).

A thorough analysis of all the spectra and comparison of spectral data with those in literature revealed that compound **51** was allantoin, a heterocyclic compound previously isolated from the leaves of *Pisonia grandis* by Scripathi and collaborators in 2011.

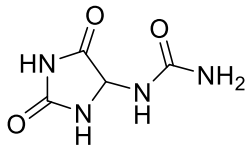

51

Table 21: ^{1}H-NMR (DMSO-d_6, 400 MHz) data of CAF15 and allantoin (Scripathi *et al*., 2011)

Position	CAF15 (δ_H (nH, m, *J* (Hz))	Allantoin (δ_H)
H-4	5.23 (1H, d, *J* = 9.2 Hz)	5.3 (1H, m)
H-N_8-H	5.76 (2H, s, N_8-H2)	5.83 (2H, s)
H-6	6.86 (1H, d, *J* = 8.0 Hz)	6.9 (1H, d)
H-3	8.04 (1H, s)	8.06 (1H,s)
H-1	10.52 (1H, brs)	10.50 (1H, brs)

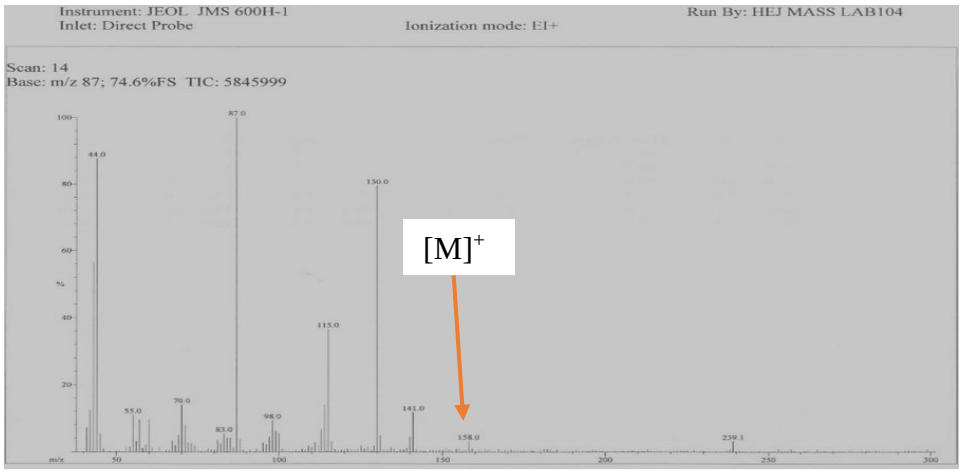

Figure 38: EI mass spectrum of CAF15

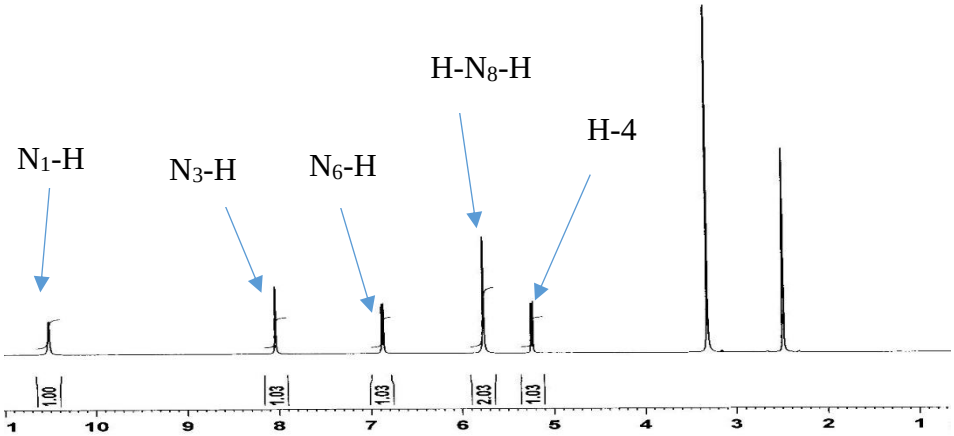

Figure 39: ^{1}H-NMR spectrum (DMSO-d_6, 400 MHz) of CAF15

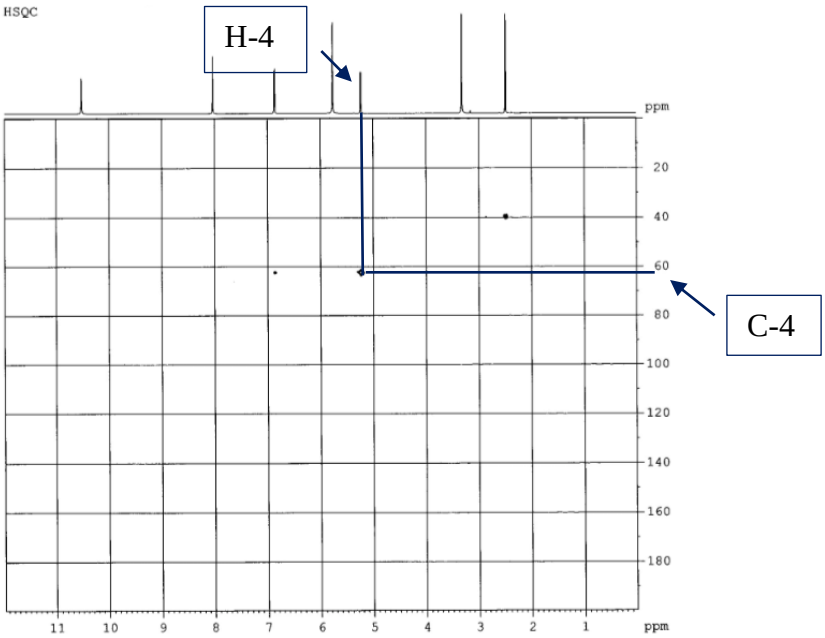

Figure 40: HSQC spectrum of CAF15

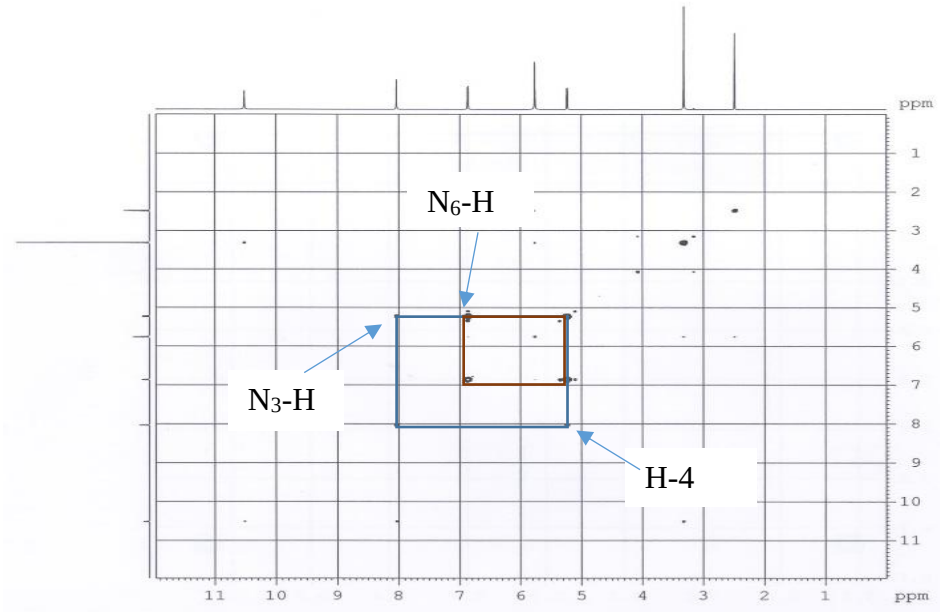

Figure 41: COSY spectrum of CAF15

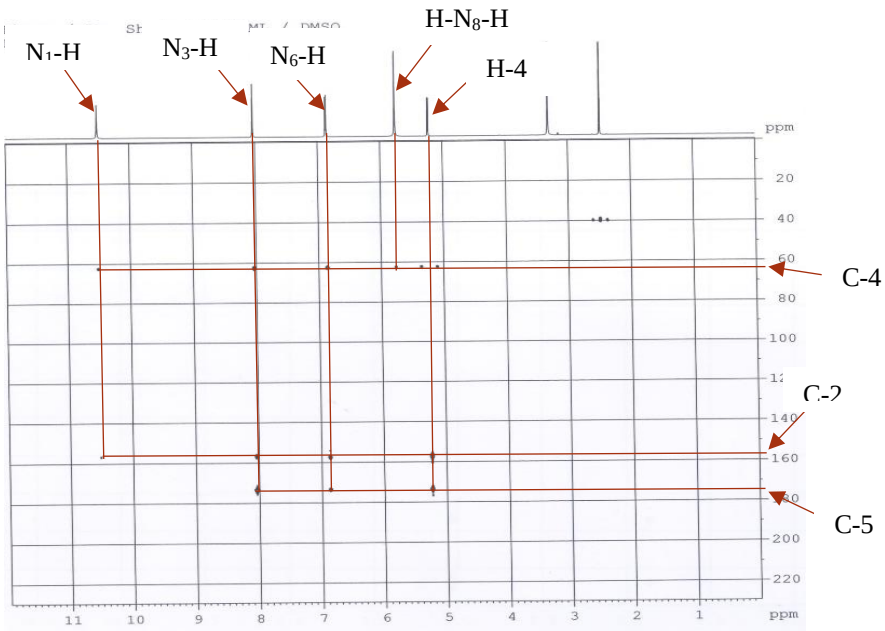

Figure 42: HMBC spectrum of CAF15

II.1.2.7 Structure identification of CAF16

Compound CAF16 was obtained as colorless crystal in the mixture of methylene chloride-methanol (95:5). It was soluble in water. The interpretation of all its spectroscopic and spectrometric data led to the assignement of the following structure.

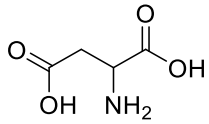

52

The molecular formula, $C_4H_7NO_4$, implying two degrees of unsaturation, was deduced from its NMR and its EI-MS data (Figure 43), which showed the molecular ion peak $[M]^+$ at *m/z* 133.0.

The ^{1}H NMR spectrum (Figure 44) of CAF16 displayed resonances of multiplets at δ_H 3.97 (1H, m, H-2) and 2.92-2.82 (2H, m, H-3).

The HMBC spectrum (Figure 45) showed correlations between proton H-2 and carbons at δ_C 37.8 (C-3) and 176.1 (C-1). There were also correlations between the proton H-3 and carbons at 53.8 (C-2) and 177.4 (C-4).

Based on the above evidences, CAF16 was concluded to be aspartic acid **(52)** previously synthesized by Dunn and Fox, 1993.

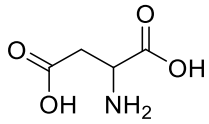

52

Table 22: ^{1}H (D_2O, 400 MHz) and ^{13}C (D_2O, 100 MHz) NMR data of CAF16

Position	CAF16 δ_C	CAF16 δ_H (nH, m, *J* (Hz)
1	176.1	
2	53.8	3.97 (1H, dd, *J* = 7.8; 4.2 Hz)
3	37.8	2.92 - 2.82 (2H, m)
4	177.4	

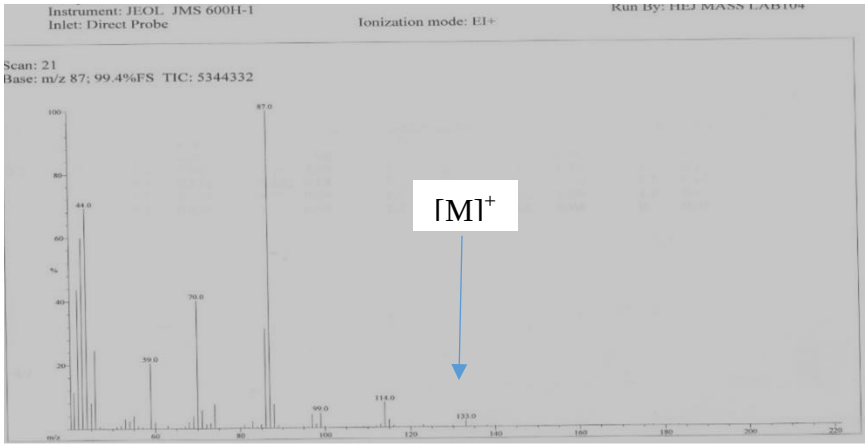

Figure 43: EI mass spectrum of CAF16

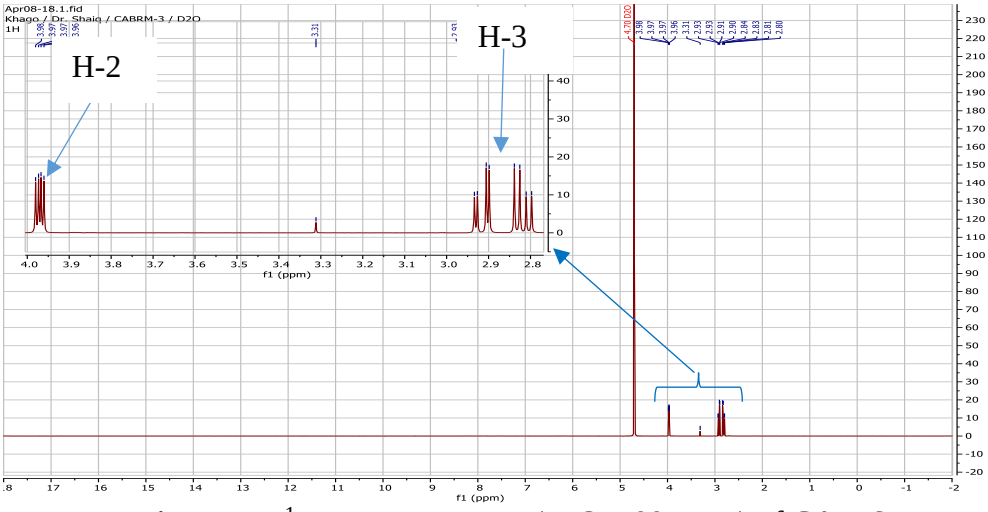

Figure 44: ^{1}H NMR spectrum (D_2O, 400 MHz) of CAF16

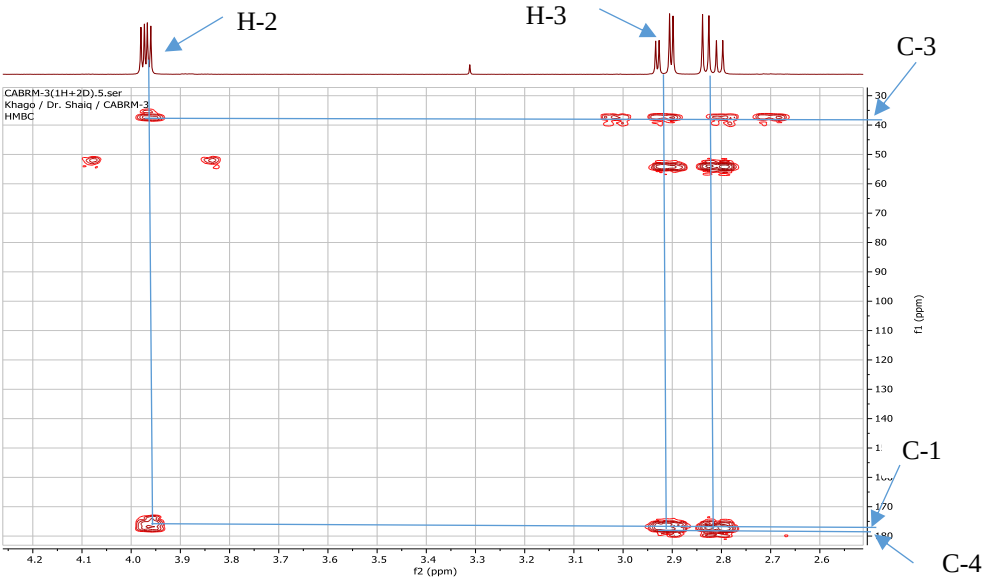

Figure 45: HMBC spectrum of CAF16

II.1.2.8 Structure identification of phenolic compounds

II.1.2.8.1 Structure identification of CAF5

Compound CAF5 was obtained as a white powder in DCM and was soluble in the same solvent. The interpretation of all its spectroscopic and spectrometric data led to the attribution of the following structure.

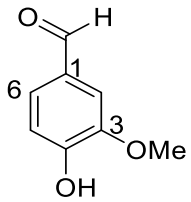

53

The ^{1}H NMR (Figure 46) spectrum of CAF5 showed signals of three aromatics protons at δ_H 7.42 (1H, m), 7.40 (1H, m) and 7.02 (1H, d, J = 8.5 Hz), assignable to a trisubstitued benzene system. It also showed resonances of 2 singlets attributable to the hydroxy group at δ_H 9.81 (H, s) and a methoxy group at δ_H 3.95 (3H, s, OCH_3).

The HMBC spectrum (Figure 47) displayed correlations of proton H-6 at δ_H 7.42 with carbons at δ_C 108.8 (C-3), 152.2 (C-4), and 191.4 (CHO). And also the correlations between the proton H-5 at δ_H 7.40 and carbons δ_C 152.2 (C-4), and 130.3 (C-1).

Based on the above mentioned data, CAF5 was concluded to be vanillin (**53)** previously isolated from *vanilla planifolia* by Bogdan and collaborators in 2002.

Table 23: ^{1}H ($CDCl_3$, 400 MHz) and ^{13}C ($CDCl_3$, 100 MHz) NMR data of CAF5 and vanillin (D_2O, 500MHz) (Bogdan *et al*., 2002)

Position		CAF5	Vanillin
	δ_C	δ_H (nH, m, *J* (Hz))	δ_H (nH, m, *J* (Hz))
1	130.3		
2	114.3	7.40 (1H, m)	7.46 (1H, m)
3	146.9		
4	152.2		
5	108.8	7.02 (1H, d, *J* = 8.5 Hz)	7.23 (1H, m)
6	127.7	7.42 (1H, m)	7.47(1H, m)
CHO	191.4	9.81 (1H, s)	9.64 (H, s)
OCH_3	56.2	3.95 (3H, s)	3.86 (3H, s)

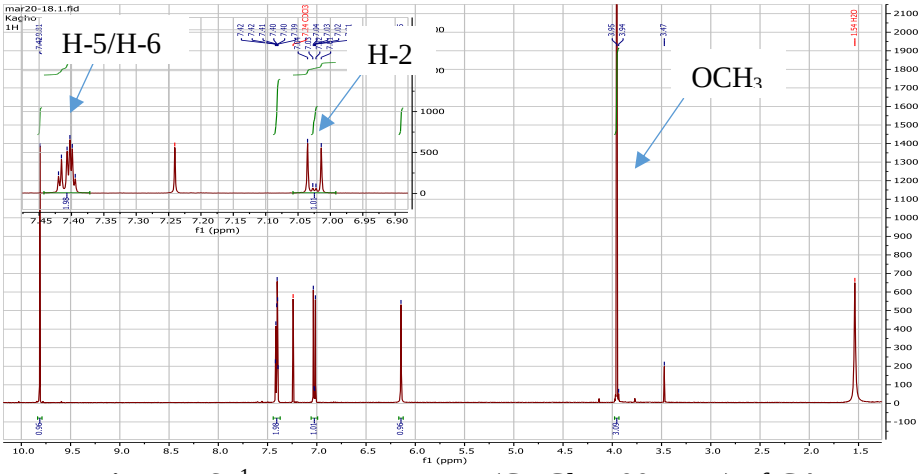

Figure 46: ^{1}H-NMR spectrum ($CDCl_3$, 400 MHz) of CAF5

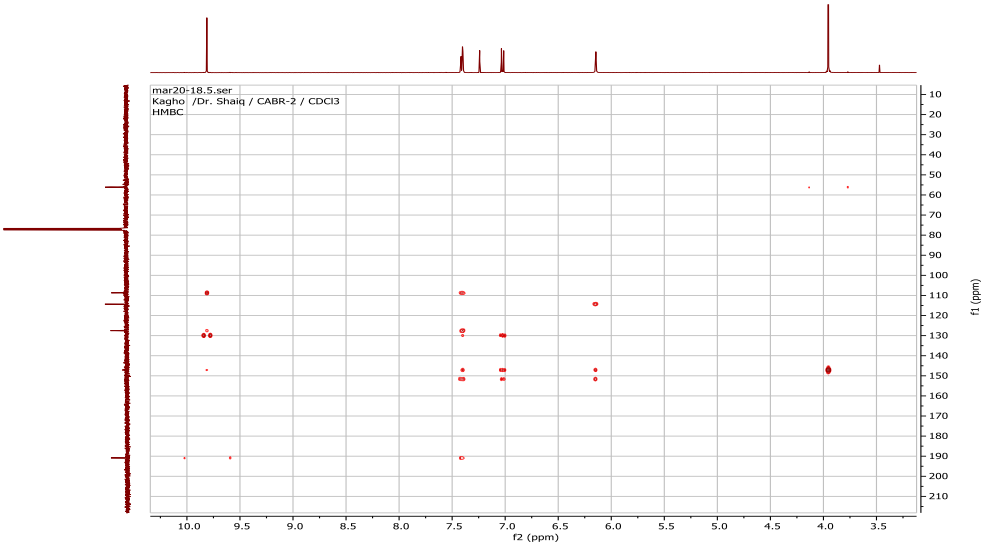

Figure 47: HMBC spectrum of CAF5

II.1.2.8.2 Structure identification of CAF11

CAF11 was obtained as a white powder in the mixture of *n*-hexane-DCM (1:1). The interpretation of all their spectroscopic and spectrometric data led to the identification of the following structure.

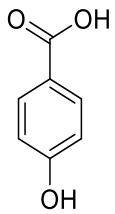

54

The molecular formula, $C_7H_6O_3$, implying five degrees of unsaturation, was deduced from the combinaison of its NMR and its EI-MS data (Figure 48), which showed the dehydroxylated molecular ion peak $[M\text{-}OH]^+$ at *m/z* 121.0.

The ^{1}H-NMR spectrum (Figure 49) of CAF11 showed resonnaces of two AA′BB′ protons at δ_H 7.79 (2H, d, J = 8.4 Hz, H-2/6) and 6.93 (2H, d, J = 8.0 Hz, H-3/5) for a para-disubstitued aromatic system. The proton spectrum also displayed signals of a carboxylic acid at δ_H 9.85 (1H, s, COOH) and that of a hydroxy group at δ_H 5.73 (1H, s, OH).

Based on the above data, CAF11 was identified as parahydroxybenzoic acid (**54)** previously isolated from the bark of *Vitex negundo L* by Ram and collaborators in 2009.

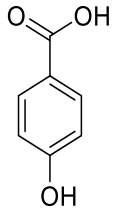

54

Table 24: ^{1}H ($CDCl_3$, 400 MHz) and ^{13}C ($CDCl_3$, 100 MHz) NMR data of CAF11 and Parahydroxybenzoic acid **(**CD_3OD, 500 and 125 MHz) (Ram *et al*., 2009)

Position	**CAF11**		**Parahydroxybenzoic acid**	
	δ_C	δ_H **(nH, m, *J* (Hz)**	δ_C	δ_H **(nH, m, *J* (Hz)**
1	124.0		122.6	
2/6	131.1	7.79 (2H, d, *J* = 8.4 Hz)	132.9	7.87 (2H, *J* = 8.80)
3/5	115.6	6.93 (2H, d, *J* = 8.0 Hz)	116.0	6.81 (2H, *J* = 8.76)
4	160.1		163.3	
COOH	170.0	9.85 (H, s)	170.1	
OH		5.73 (H, s)		

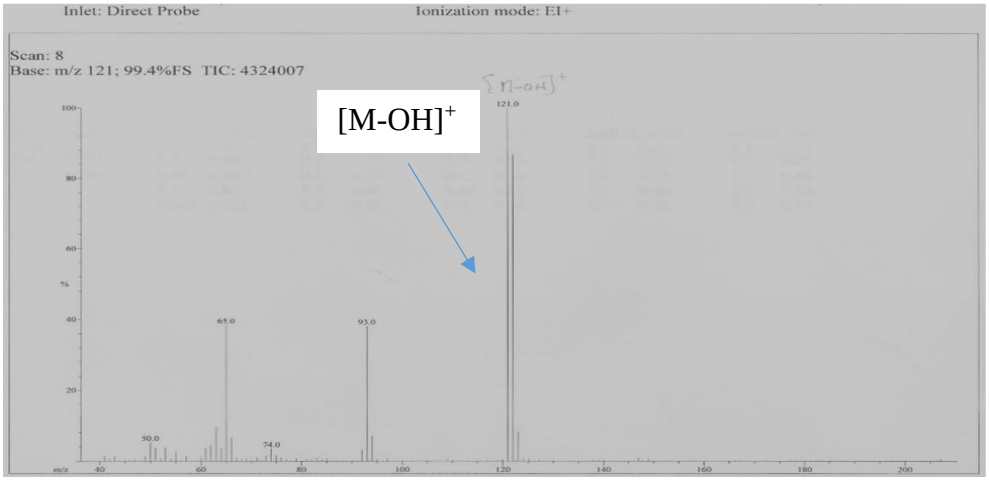

Figure 48: EI mass spectrum of CAF11

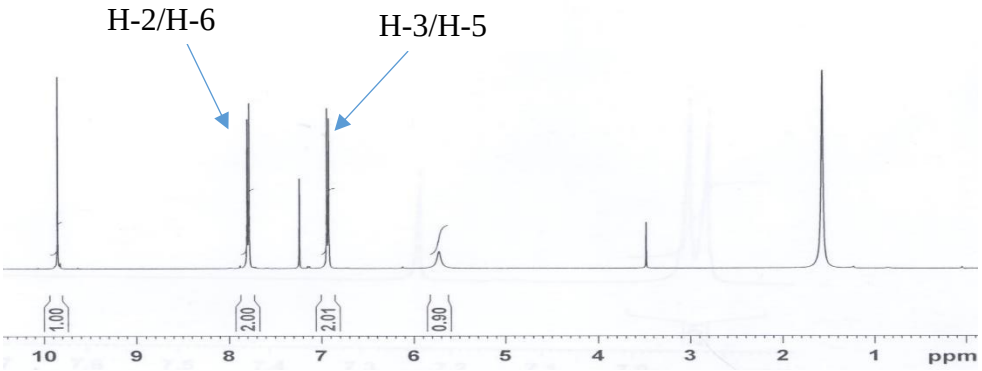

Figure 49: ^{1}H NMR spectrum ($CDCl_3$, 400 MHz) of CAF11

II.1.2.8.3 Structure identification of DE22

DE22 was obtained as a white powder, in the mixture of solvents EtOAc-MeOH (9-1). It was soluble in methanol. The interpretation of all its spectroscopic data led to the identification of the following compound (**55**).

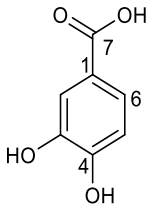

55

The ^{1}H-NMR (Figure 50) spectrum of DE22 showed signals of three aromatics protons at δ_H 7.45 (1H, d, J = 2.0 Hz, H-2), 7.44 (1H, d, J = 2.1 Hz, H-6), 6.82 (1H, d, J = 7.9 Hz, H-5).

The ^{13}C-NMR spectrum (Figure 51) revealed seven peaks attributable to nineteen carbons in the structure. These peaks were characterized as one carbonyl group at δ_C 170.0,

three methine at δ_C 122.9, 117.5, and 115.5; three quaternary carbons at δ_C 151.3, 145.9, and 123.6.

Based on the above mentioned data, DE22 was concluded to be 3,4-dihydroxybenzoic acid (**55**) previously isolated from *Maclura pomifera* by Zushang and collaborators in 2017.

Table 25: ^{1}H (MeOH-d_4, 600 MHz) and ^{13}C (MeOH-d_4, 150 MHz) NMR data of DE22 and 3,4-dihydroxybenzoic acid (MeOH-d_4, 600 MHz) (Zushang *et al*., 2017)

Position	DE22		3,4-dihydroxybenzoïc acid	
	δ_C	δ_H (nH, m, *J* (Hz))	δ_C	δ_H (nH, m, *J* (Hz))
1	123.6		123.0	
2	115.5	7.45 (1H, d, *J* = 2.0 Hz)	116.4	7.45 (1H, d, *J* = 1.98 Hz)
3	122.9		149.7	
4	151.3		144.5	
5	145.9	6.82 (1H, d, *J* = 7.9 Hz)	114.3	6.80 (1H, d, *J* = 8.22 Hz)
6	117.5	7.44 (1H, m)	122.4	7.46 (1H, dd, *J* = 8.22; 2.04 Hz)
1'	170.0		169.7	

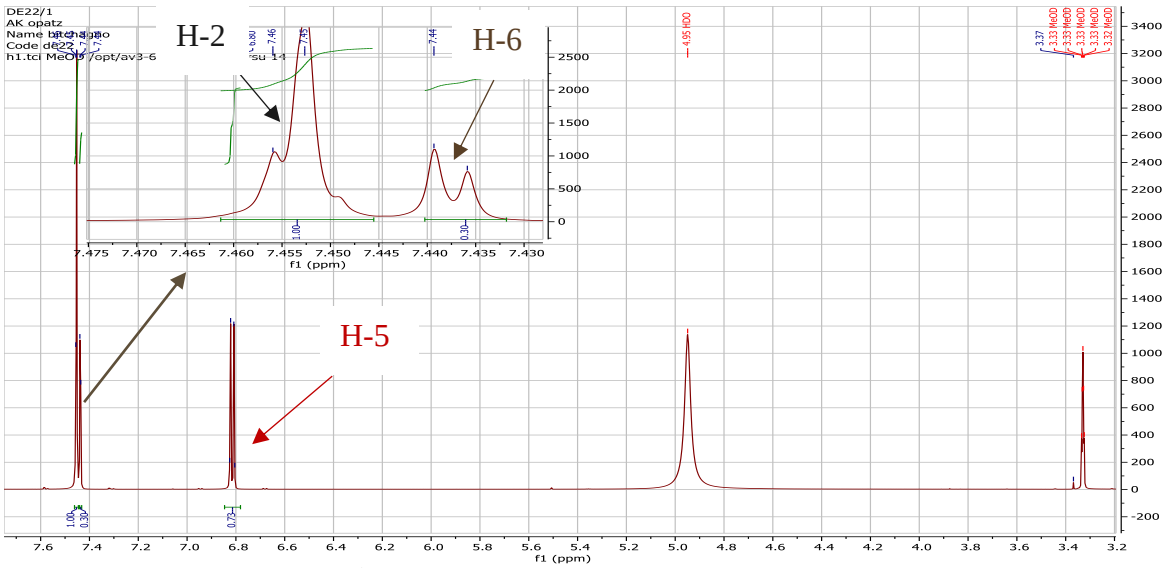

Figure 50: ^{1}H-NMR spectrum (MeOH-d_4, 600 MHz) of DE22

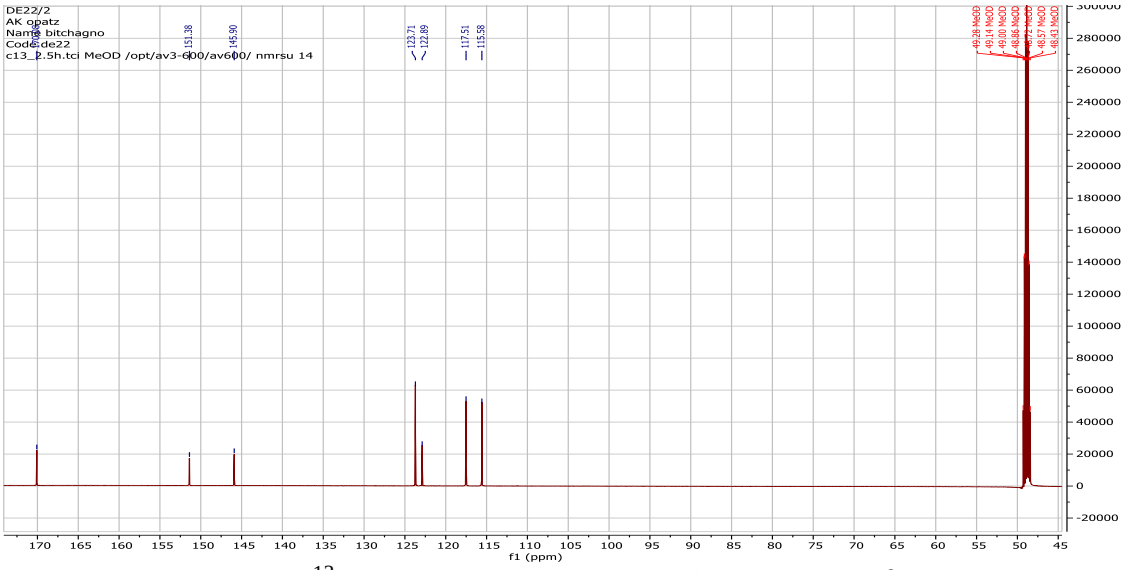

Figure 51: ^{13}C-NMR spectrum (MeOH-d_4, 150 MHz) of DE22

II.1.2.9 Structure identification of triglycerids

II.1.2.9.1 Structure identification of CAF4

Compound CAF4 was obtained as a white powder in the mixture of *n*-hexane-EtOAc (75-25). It was soluble in pyridine. The interpretation of all their spectroscopic and spectrometric data led to the identification of the following compound (**56**).

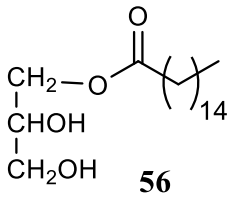

56

The molecular formula, $C_{20}H_{40}O_4$, implying one degree of unsaturation, was deduced from the combinaison of its NMR and its EI-MS data (Figure 52), which showed the dehydroxylated molecular ion peak $[M\text{-}OH]^+$ at *m/z* 327.2.

The ^{1}H-NMR spectrum (Figure 53) of CAF4 showed characteristic signal of a mono substituted glycerol, where the substituent is an allyphatic long chain ester. This was further confirmed by the data from its ^{13}C-NMR spectrum (Table 26) which displayed carbon resonances assignable to glycerol monoester at δ_C 173.8.

The location of the long chain ester was established using the HMBC correlation of methylene protons H-1a and H-1b (δ_H 4.64 and 4.71) with the C-1 (δ_C 173.8). The length of the long chain ester was determined using the mass spectrum.

Based on these evidences, CAF4 was concluded to be glycerol 1-octadecanoate, previously synthesized by Yu and collaborators in 2003.

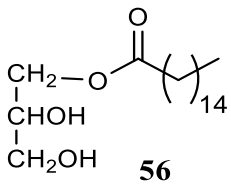

56

Table 26: ^{1}H (Pyridine-d_5, 400 MHz) and ^{13}C (Pyridine-d_5, 100 MHz) NMR data of CAF4

Position	CAF4	
	(δ_C / ppm)	**δ_H (nH, m, *J* (Hz)) ppm**
1	66.8	4.64 (1H, m) 4.71 (1H, m)
2	70.9	4.45 (1H, s)
3	63.3	4.13 (2H, dd, *J* = 5.7, 2.6 Hz)
1′	174.4	
2′	34.3	2.35 (2H, t, *J* = 7.6 Hz)
3′	24.9	1.63 (2H, q, *J* = 7.5 Hz)
4′-14′	29.7- 32.0	1.25 (brs)
15'	14.1	0.88 (3H, t, *J* = 7.0 Hz)

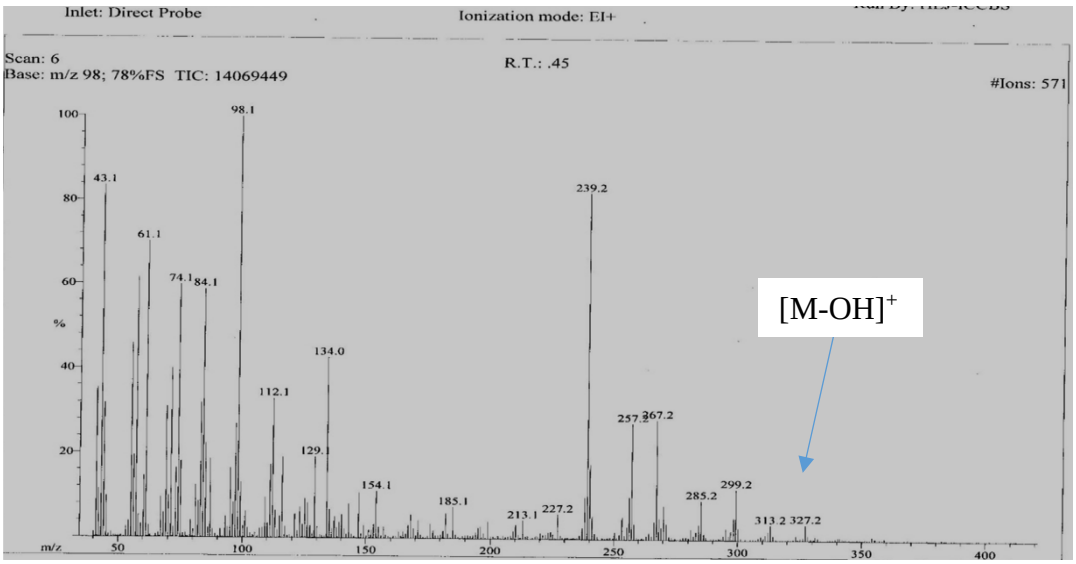

Figure 52: EI mass spectrum of CAF4

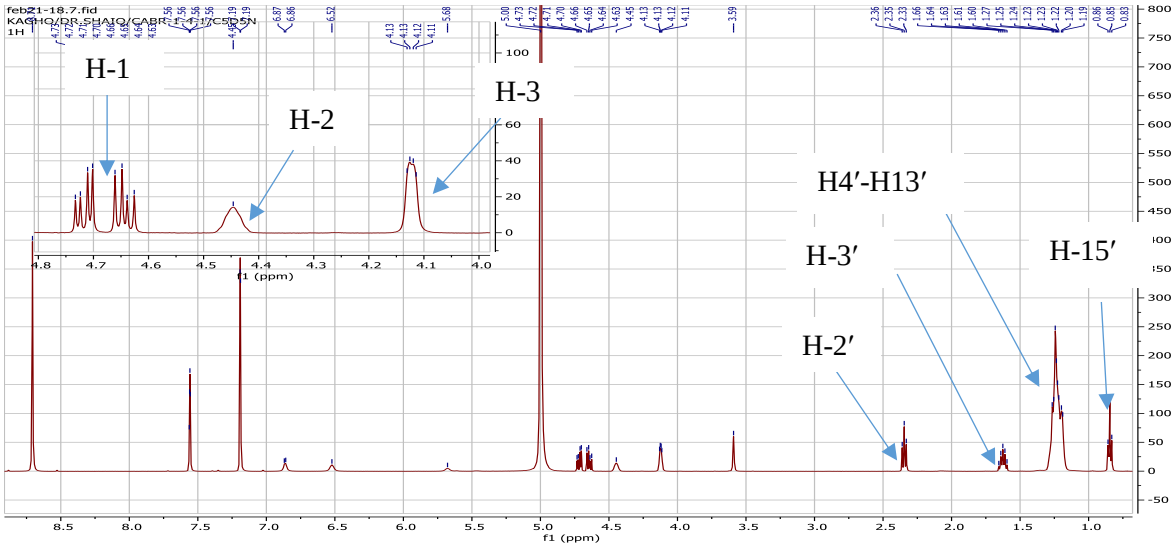

Figure 53: ^{1}H-NMR spectrum (Pyridine-d_5, 400 MHz) of CAF4

II.1.2.9.2 Structure identification of DF5

DF5 was obtained as a white powder, in the mixture of solvents *n*-hexane-EtOAc (45-5). It was soluble in dichloromethane. The interpretation of all its spectroscopic and spectrometric data led to the identification of the following compound **57**.

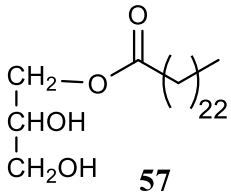

57

The molecular formula, $C_{27}H_{54}O_4$, implying one degree of unsaturation, was deduced from its NMR and its HR-ESI-MS data (Figure 54), which displayed the sodium adduct peak $[M+Na]^+$ at *m/z* 465.4395 (calcd for 442.4022).

The ^{1}H-NMR spectrum (Figure 55) of DF5 showed characteristic signal of a mono substituted glycerol, where the substituent is an allyphatic long chain ester. This was further confirmed by the data from its ^{13}C-NMR spectrum (Table 27) which displayed carbon resonances assignable to glycerol monoester at δ_C 174.4.

The location of the long chain ester was established using the HMBC correlation of methylene protons H-1a and H-1b (δ_H 4.15, 4.21) with the C-1 (δ_C 174.4). The length of the long chain ester was determined using the mass spectrum.

Based on these evidences, DF5 was concluded to be glyceryl-1-tetracosanoate, previously isolated from the aerial parts of *Eriostemon rhomboideus* by Sultana *et al*., 1999.

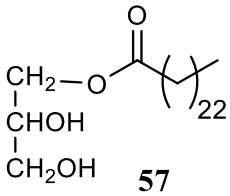

57

Table 27: ^{1}H ($CDCl_3$, 600 MHz) and ^{13}C ($CDCl_3$, 150 MHz) NMR data of DF5 and glyceryl-1-tetracosanoate ($CDCl_3$+CD_3OD, 400 and 100 MHz) (Sultana *et al*., 1999)

Position	DF5		Glyceryl-1-tetracosanoate	
	δ_C	δ_H (nH, m, *J* (Hz))	δ_C	δ_H (nH, m, *J* (Hz))
1	65.2	4.21 (1H, dd, *J* = 4.5, 11.7 Hz) 4.15 (1H, dd, *J* = 6.2, 11.7 Hz)	65.4	4.23 (dd, *J* = 4.6, 11.6 Hz) 4.17 (dd, *J* = 6.1, 11.6 Hz)
2	70.2	3.93 (1H, m)	70.5	3.94 (q, 5.9)
3	63.3	3.69 (1H, dd, *J* = 4.0, 11.4 Hz) 3.60 (1H, dd, *J* = 5.8, 11.4 Hz)	63.6	3.71 (dd, *J* = 4.0, 11.4 Hz) 3.60 (dd, *J* = 5.8, 11.4 Hz)
1′	174.4		174.6	
2′	34.3	2.35 (2H, t, *J* = 7.6 Hz)	34.4	2.35 (t, *J* = 7.48 Hz)
3′	24.9	1.63 (2H, q, *J* = 7.5 Hz)	25.2	1.64 (q, *J* = 7.12 Hz)
4′-23′	29.7- 32.0	1.25 (brs)	29.5-32.3	1.29 (brs)
24'	14.1	0.88 (3H, t, *J* = 7.0 Hz)	14.3	0.90 (t, *J* = 7.04)

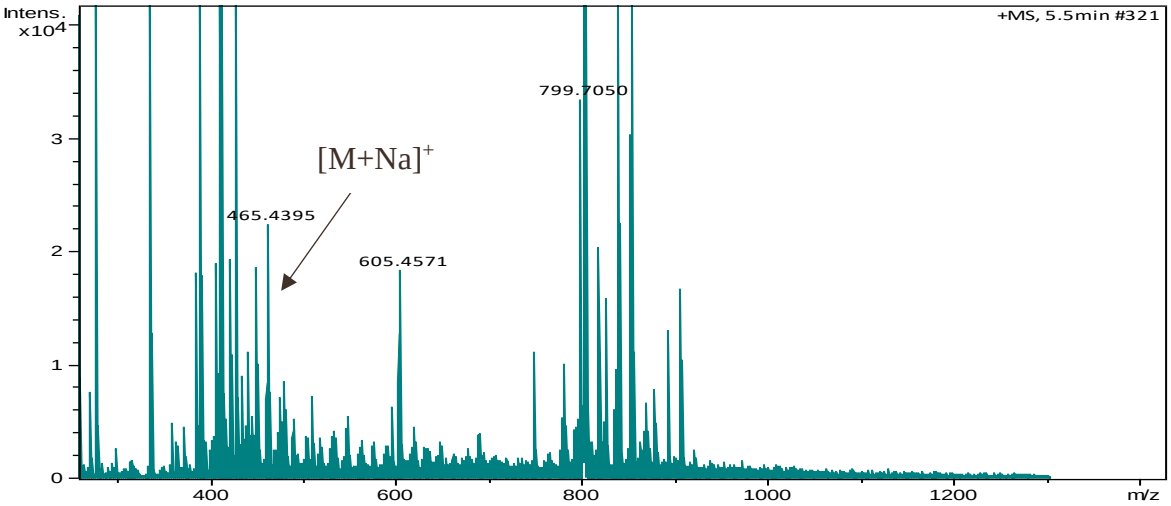

Figure 54: HR-ESI mass spectrum of DF5

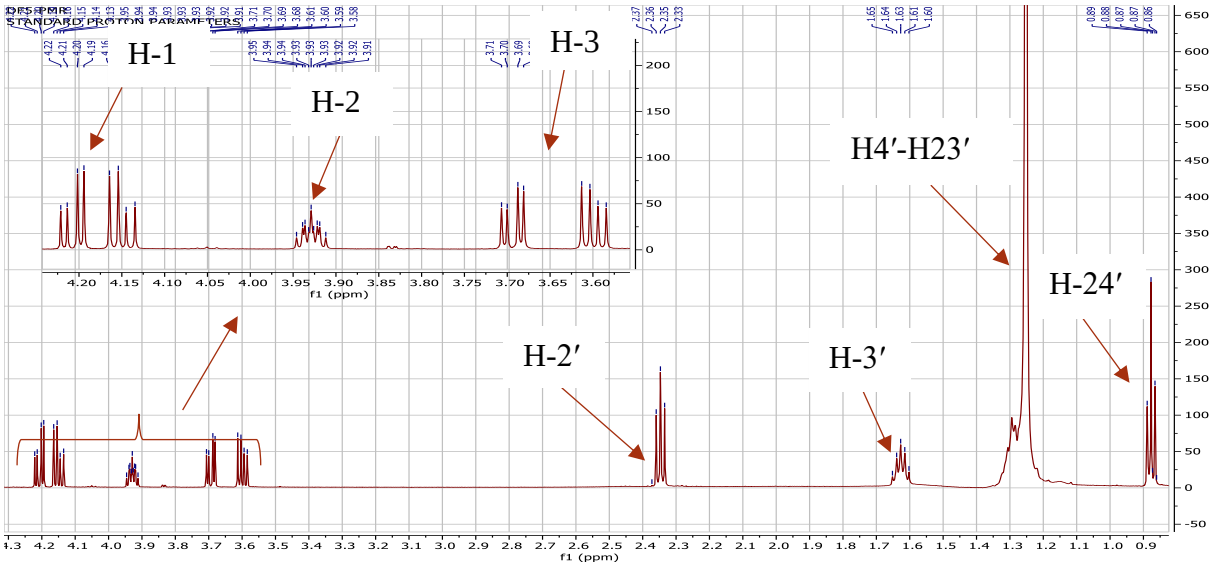

Figure 55: ^{1}H NMR spectrum ($CDCl_3$, 600 MHz) of DF5

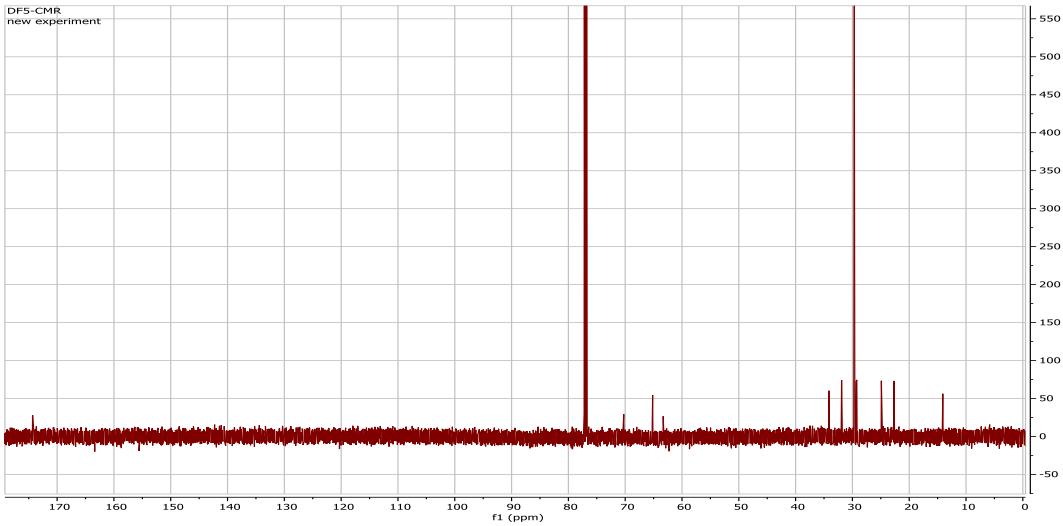

Figure 56: ^{13}C-NMR spectrum ($CDCl_3$, 150 MHz) of DF5

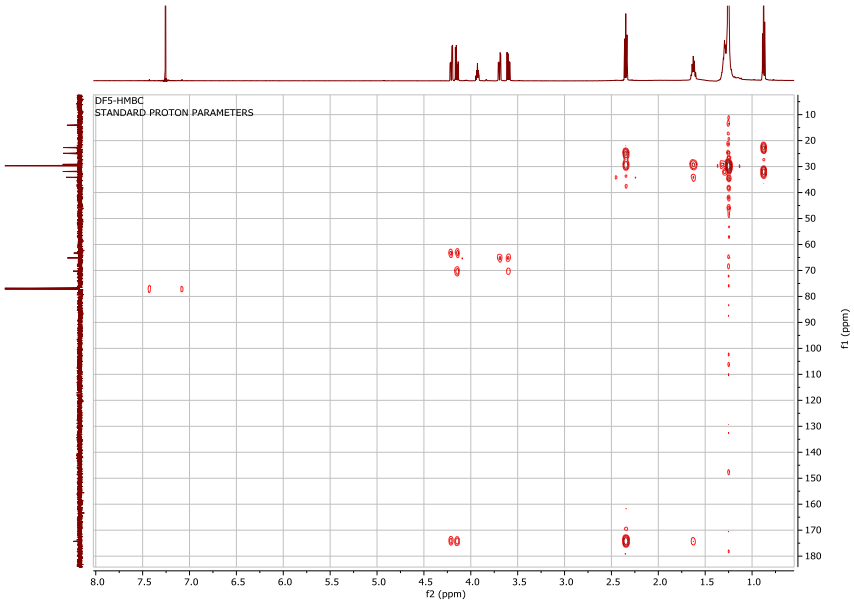

Figure 57: HMBC spectrum of DF5

II.1.2.10 Structure identification of xanthones

II.1.2.10.1 Structure identification of DE2

DE2 was obtained as a white powder in the mixture of *n*-hexane-EtOAc (4-1). It was soluble in pyridine. The interpretation of its spectroscopic and spectrometric data led to the identification of the following compound (**58**).

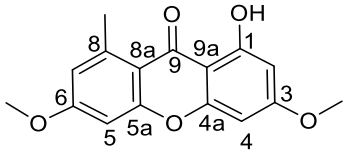

58

The molecular formula, $C_{16}H_{14}O_5$, implying ten degrees of unsaturation, was deduced from its NMR and its HR-ESI-MS (Figure 58) which displayed the protonated molecular ion peak $[M+H]^+$ at *m/z* 287.0935 (calcd for 286.0841).

The ^{1}H-NMR spectrum (Figure 59) exhibited signals characteristic of four *meta* coupling aromatics protons at δ_H 6.60 (1H, d, J = 2.1 Hz, H-4), 6.55 (1H, d, J = 2.1 Hz, H-2), 6.79 (1H, d, J = 2.4 Hz, H-5), 6.86 (1H, d, J = 2.2 Hz, H-7). The spectrum also displayed resonnaces of two methoxy group at δ_H 3.78 (3H, s), 3.81 (3H, s), one methyl group at δ_H 2.91 (3H, s), and one chelated proton at δ_H 13.91(1H, s, OH-1).

The ^{13}C-NMR spectrum (Figure 60), showed sixteen carbons resonances which were sorted into one carbonyl carbon at δ_C 183.0 (C-9), one methyl group at δ_C 23.8, two methoxy group at δ_C 56.23 and 56.21, and four methylene groups carbons at δ_C 92.8 (C-4), 97.8 (C-2), 99.5 (C-5) and 116.3 (C-7).

The location of the methyl, the two methoxy groups and the chelated hydroxyl group was determined using the HMBC spectrum (Figure 61), which showed correlations of CH_3 with carbons at δ_C 113.4 (C-8a), 116.3 (C-7), and 143.8 (C-8), 6-OCH_3 with carbon at δ_C 164.8 (C-6), and 3-OCH_3 with carbon at δ_C 166.8 (C-3). The OH group located at C-1 was confirmed by the correlation between the proton at δ_H 13.91 with carbons δ_C 164.8 (C-1), 97.8 (C-2) and 104.7 (C-9a).

Based on the above data evidences, and by comparison with data from the literature, DE2 was identified as lichexanthone (**58**) previously isolated from *Vismia baccifera* (Guttiferae) by (Buitrago *et al*., 2010).

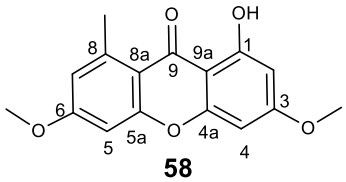

58

Table 28: ^{1}H (Pyridine-d_5, 600 MHz) and ^{13}C (Pyridine-d_5, 150 MHz) NMR data of DE2 and lichexanthone (DMSO, 600 and 150 MHz) (Buitrago *et al*., 2010)

Position	DE2		Lichexanthone	
	(δ_C / ppm)	δ_H (nH, m, *J* (Hz)) ppm	(δ_C /ppm)	δ_H (nH, m, *J* (Hz)) ppm
1	164.8	-	163.8	-
2	97.8	6.55 (1H, d, *J* = 2.1Hz)	96.8	6.49 (1H,m)
3	166.8	-	165.9	-
4	92.8	6.60 (1H, d, *J* = 2.1Hz)	92.1	6.58 (1H, m)
5	99.5	6.79 (1H, d, *J* = 2.4Hz)	98.5	6.79 (1H, m)
6	164.7	-	163.7	-
7	116.3	6.86 (1H, d, *J* = 2.2Hz)	115.4	6.82 (1H, m)
8	143.8	-	143.8	-
9	183.0	-	182.7	-
4a	160.0	-	159.5	-
5a	157.7	-	157.0	-
9a	104.7	-	104.3	-
8a	113.4	-	113.0	-
3-OCH_3	56.2	3.78 (3H, -OCH_3)	55.6	3.86 (3H,-OCH_3)
6-OCH_3	56.2	3.81 (3H, -OCH_3)	55.7	3.89 (3H, -OCH_3)
-CH_3	23.8	2.91 (3H, s, -CH_3)	23.4	2.84 (3H, -CH_3)
1-OH		13.91 (-OH)		13.39 (-OH)

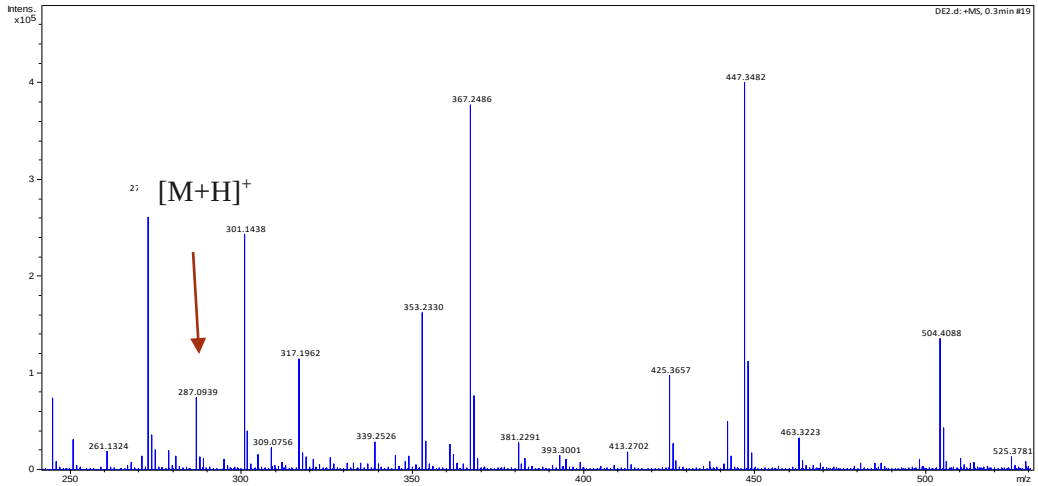

Figure 58: HR-ESI mass spectrum of DE2

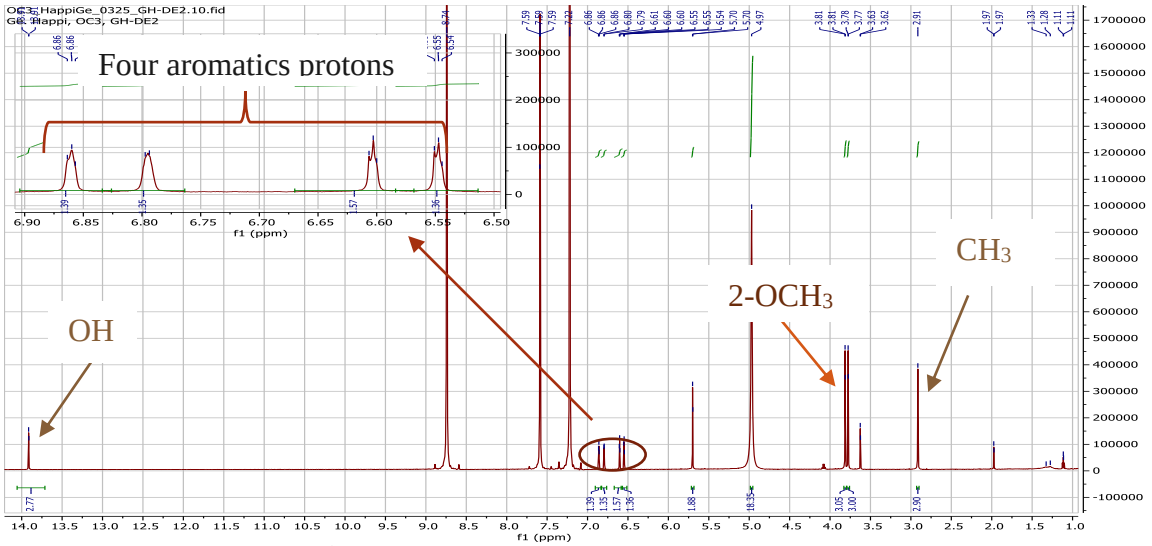

Figure 59: ^{1}H-NMR spectrum (Pyridine-d_5, 600 MHz) of DE2

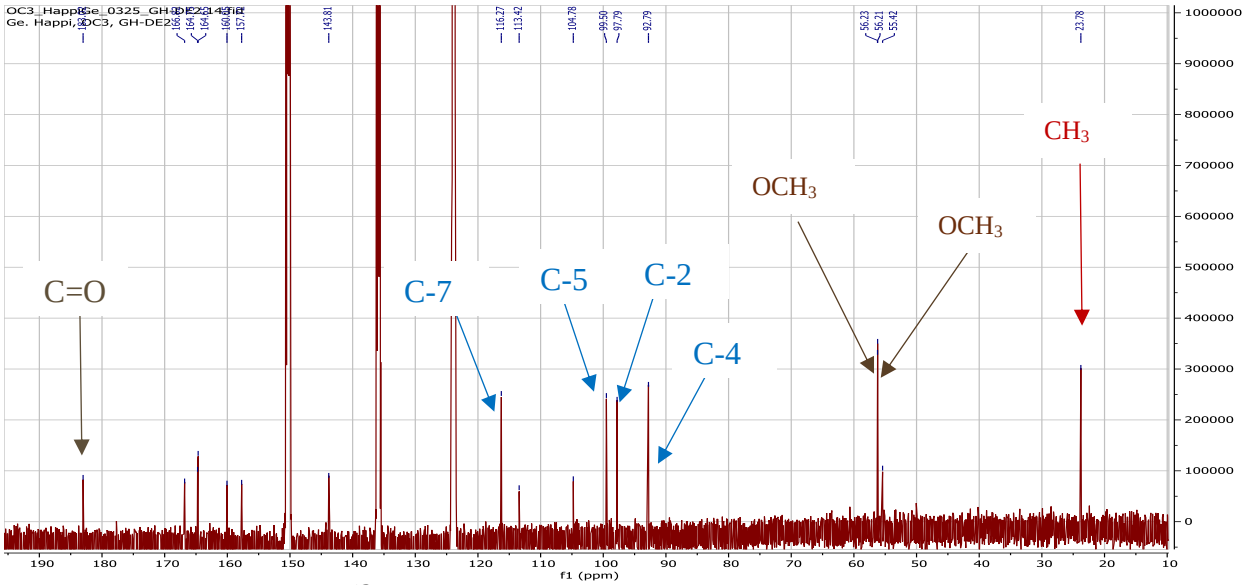

Figure 60: ^{13}C-NMR spectrum (Pyridine-d_5, 150 MHz) of DE2

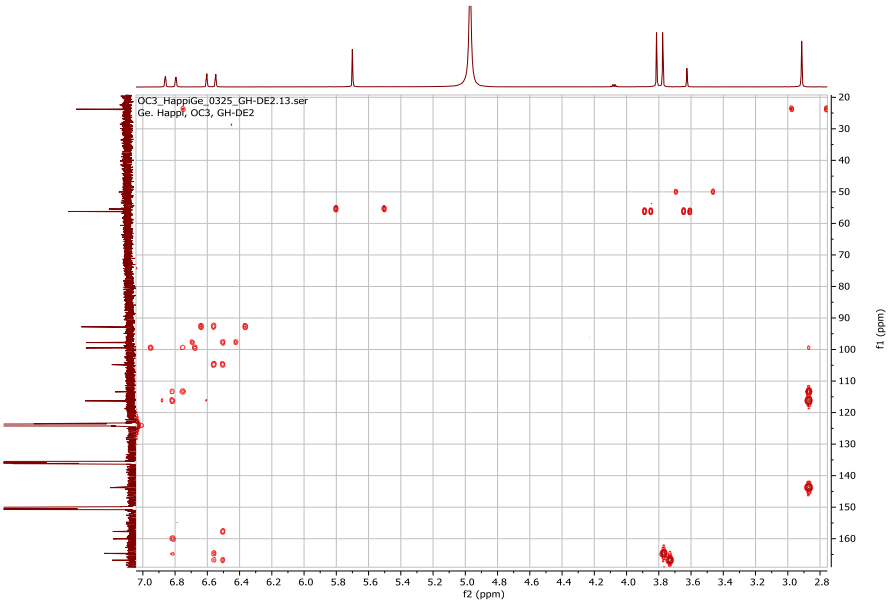

Figure 61: HMBC spectrum of DE2

II.1.2.10.2 Structure identification of DE10

DE10 was obtained as white powder, soluble in dichloromethane. The combinaison of its 1D and 2D spectral data with its mass spectrum data led to the identification of the following structure (**59**).

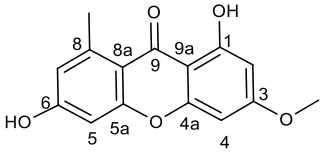

59

The molecular formula, $C_{15}H_{12}O_5$, implying ten degrees of unsaturation, was deduced from its NMR and its ESI-MS (Figure 62), which displayed the diprotonated molecular ion peak $[M+2H]^+$ peak at *m/z* 274.4.

Compared to DE2, the ^{1}H-NMR spectrum (Figure 63) of DE10 was almost superimposable except that there was one methoxy group proton lacking. This discrepancy was also observed on the comparative ^{13}C-NMR spectra (Figure 64) where one methoxy carbon signal was equally absent.

Based on the above observations, DE10 was identified as grisexanthone (**59**) previously isolated from the marine fungus *Phomopsis Sp*. (No. SK7RN3G1) (Jian *et al* ., 2013).

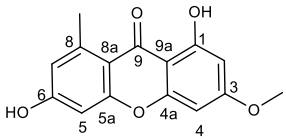

59

Table 29: ^{1}H ($CDCl_3$, 600 MHz) and ^{13}C ($CDCl_3$, 150 MHz) NMR data of DE10

Position	DE10	
	δ_C	δ_H (nH, m, *J* (Hz)
1	163.8	-
2	96.8	6.31 (1H, s)
3	165.9	-
4	92.1	6.35 (1H, s)
5	98.5	6.66 (1H, s)
6	163.7	
7	115.6	6.68 (1H, s)
8	143.5	-
9	182.6	-
4a	156.9	-
5a	159.4	-

8a	113.0	-
9a	104.2	-
3-OCH_3	55.7	3.86 (3H, brs)
-CH_3	23.6	2.88 (3H, s, -CH_3)
1-OH		13.91 (OH)

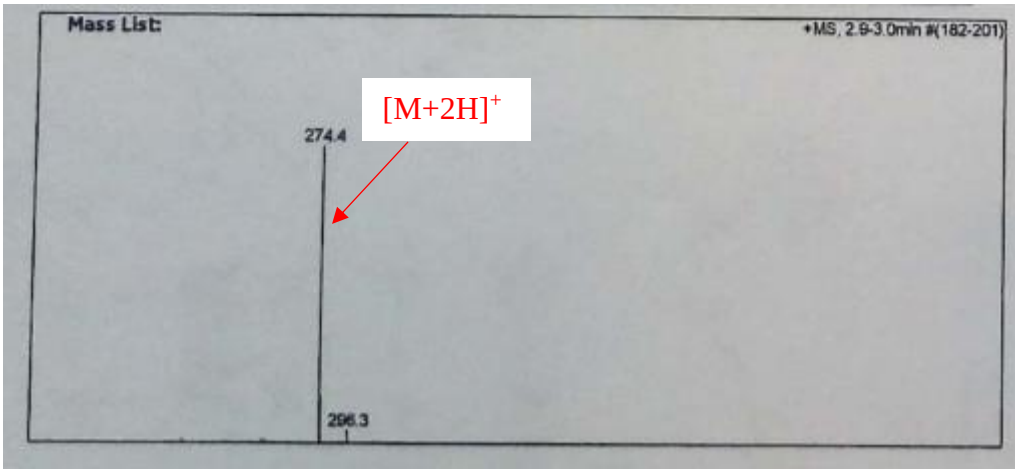

Figure 62: ESI mass spectrum of DE10

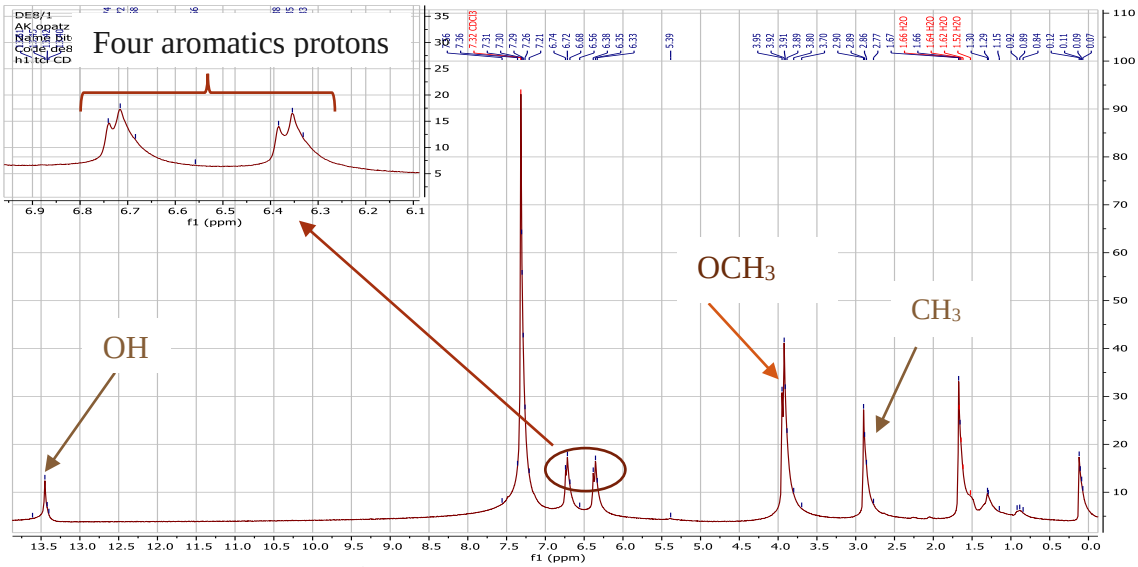

Figure 63: ^{1}H-NMR spectrum ($CDCl_3$, 600 MHz) of DE10

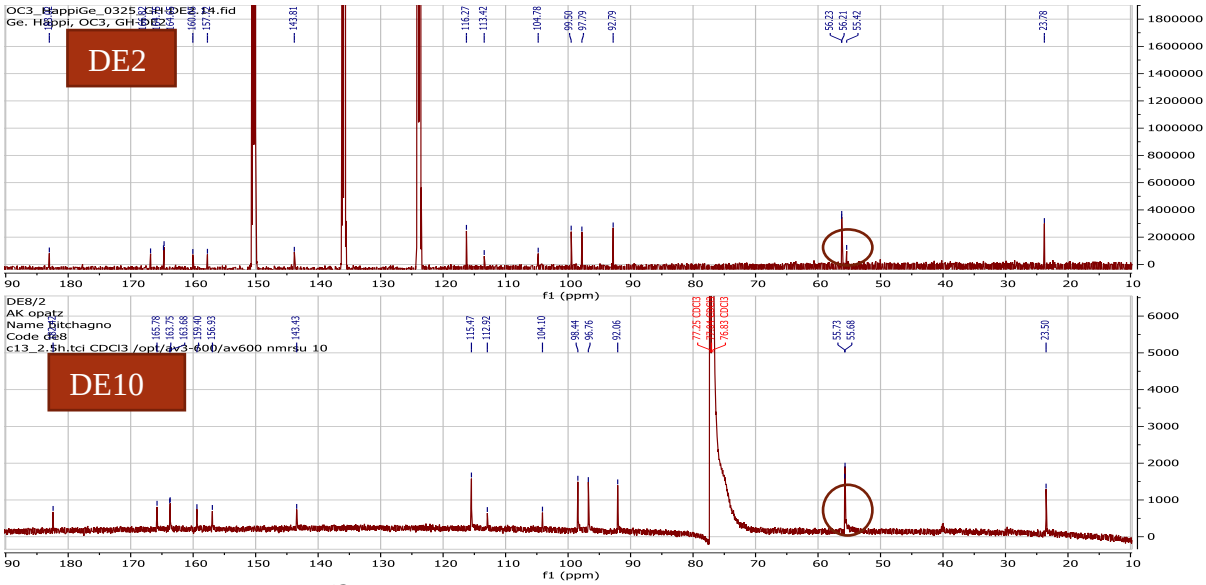

Figure 64: Comparative ^{13}C NMR spectra of DE2 (Pyridine-d_5, 150 MHz) and DE10 ($CDCl_3$, 150 MHz).

II.1.2.11 Structure identification of ellagic acids derivatives

II.1.2.11.1 Structure identification of DE4

DE4 was isolated as a white amorphous powder, in the mixture of solvents *n*-hexane-EtOAc (6-4), and was soluble in pyridine. The analysis of all its spectroscopic and spectrometric data led to the identification of DE4 as follow:

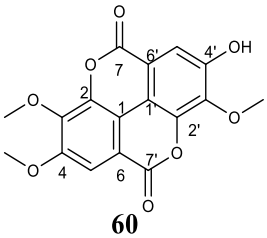

60

The molecular formula, $C_{17}H_{12}O_8$, implying twelve degrees of unsaturation, was deduced from its NMR and its HR-ESI-MS (Figure 65), which showed the sodium adduct peak $[M+Na]^+$ at *m/z* 367.0459 (cald for 344.0532).

The ^1H NMR spectrum (Figure 66) exhibited resonances for two aromatic protons at δ_H 8.03 (1H, s, H-5′) and 7.82 (1H, s, H-5). It also exhibited resonance for a hydroxy proton at δ_H 5.00 (s, -OH) characteristic of ellagic acid. It equally showed resonances of three oxymethyl groups at δ_H 4.19 (3′-OCH_3, s), 4.14 (3-OCH_3, s), and 3.85 (4-OCH_3, s). According to the low field shifted of H-5 and H-5′, both aromatic protons were then located at the *peri* position of the carbonyl groups.

The broad band decoupled ^{13}C-NMR spectrum (Figure 67) displayed 17 carbon signals which were sorted by the DEPT techniques into twelve quaternary carbons [including two

carbonyl functional group at δ_C 159.0 (C-7) and 158.9 (C-7′)], two methine carbons at δ_C 112.9 (C-5′) and 107.8 (C-5) and three methoxy group carbons at δ_C 61.3 (3-OCH_3), 61.1 (3′-OCH_3), and 56.4 (4-OCH_3).

The location of the three methoxy group on the nucleus was obtained through the HMBC (Figure 68) correlations of H-5 and carbons at δ_C 141.81 (C-3), 154.3 (C-4) which in turn were correlated to 3-OCH_3 and 4-OCH_3 respectively. In addition, the HMBC spectrum displayed correlations of H-5′ with carbons at δ_C 141.1 (C-3′) and 154.1 (C-4′) which in turn was correlating with 3′-OCH_3 (δ_H 4.19).

Based on the above data and by comparison with data from literature, DE4 was identified as 3,3′,4-tri-*O*-methylellagic acid previously isolated from *Syzygium samarangenes* (Gao *et al*., 2012).

Table 30: ^{1}H (Pyridine-d_5, 600 MHz) and ^{13}C (Pyridine-d_5, 150 MHz) NMR data of DE4 and 3,3′,4-tri-*O*-methylellagic acid (Pyridine-d_5, 400 and 100 MHz) (Gao *et al*., 2012)

Position	**DE4**		**3,3′,4-tri-*O*-methylellagic acid**	
	δ_C	**δ_H (nH, m, *J* (Hz))**	**δ_C**	**δ_H (nH, m, *J* (Hz))**
1	112.6		111.76	
2	141.1		141.0	
3	142.1		141.5	
4	154.3		153.7	
5	112.9	7.82 (1H, s)	112.5	7.52
6	114.1		113.4	
7	159.0		158.5	
1′	111.6		110.9	
2′	141.8		140.8	
3′	141.1		140.3	
4′	154.1		153.1	
5′	107.8	8.03 (1H, s)	107.4	7.91
6′	113.6		111.8	
7′	158.9		158.3	
3-OCH_3	61.3	4.14	61.3	4.04
3′-OCH_3	61.1	4.19	60.9	4.06
4-OCH_3	56.7	3.85	56.7	3.99
-OH		4.91		4.79

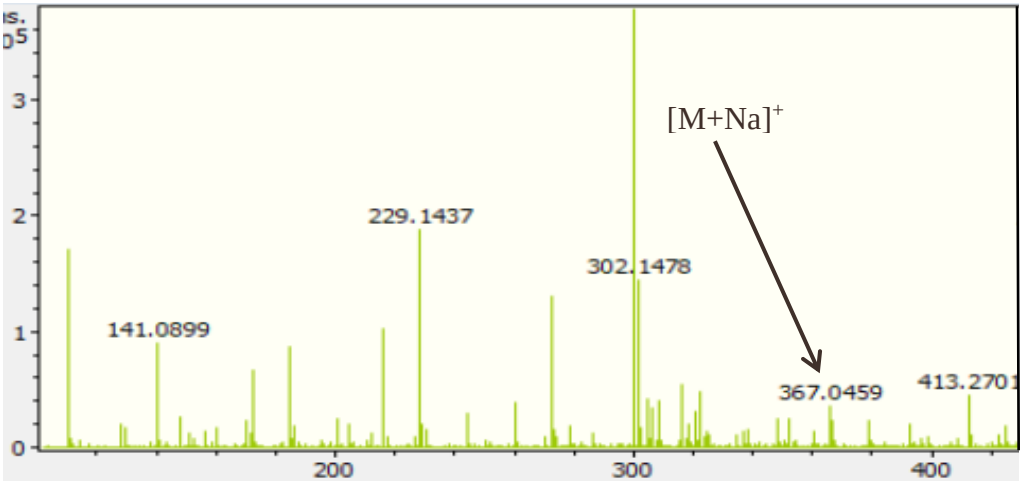

Figure 65: HR-ESI Mass spectrum of DE4

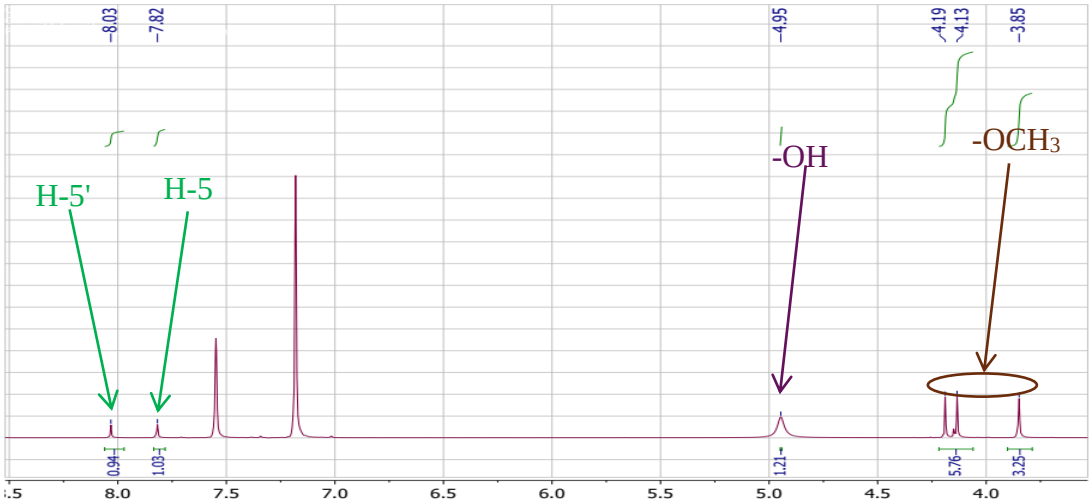

Figure 66: ^{1}H-NMR spectrum (Pyridine-d_5, 600 MHz) of DE4

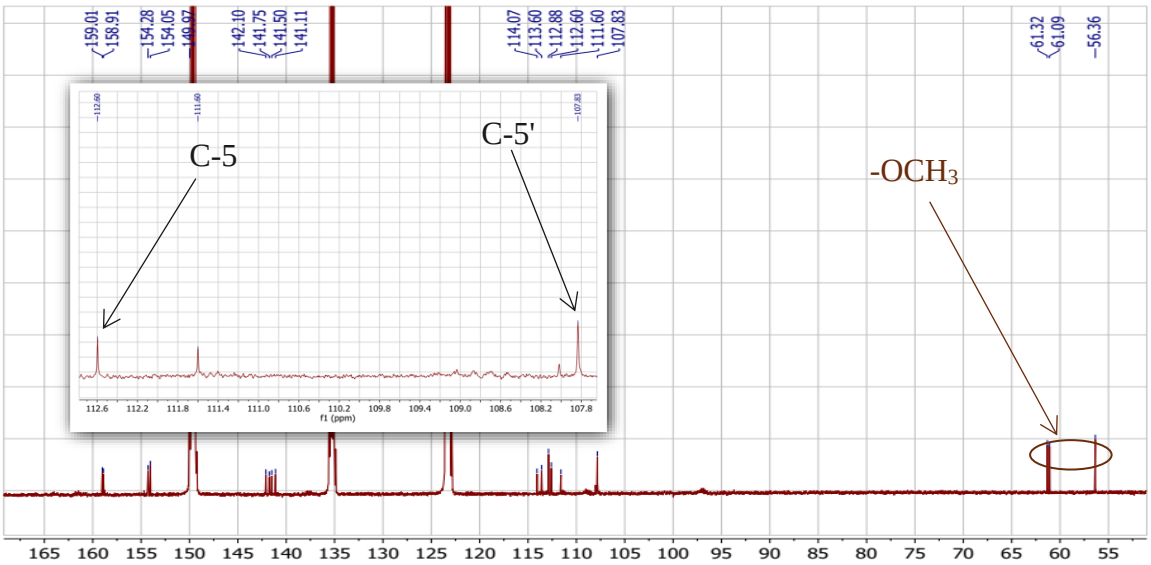

Figure 67: ^{13}C-NMR spectrum (Pyridine-d_5, 150 MHz) of DE4

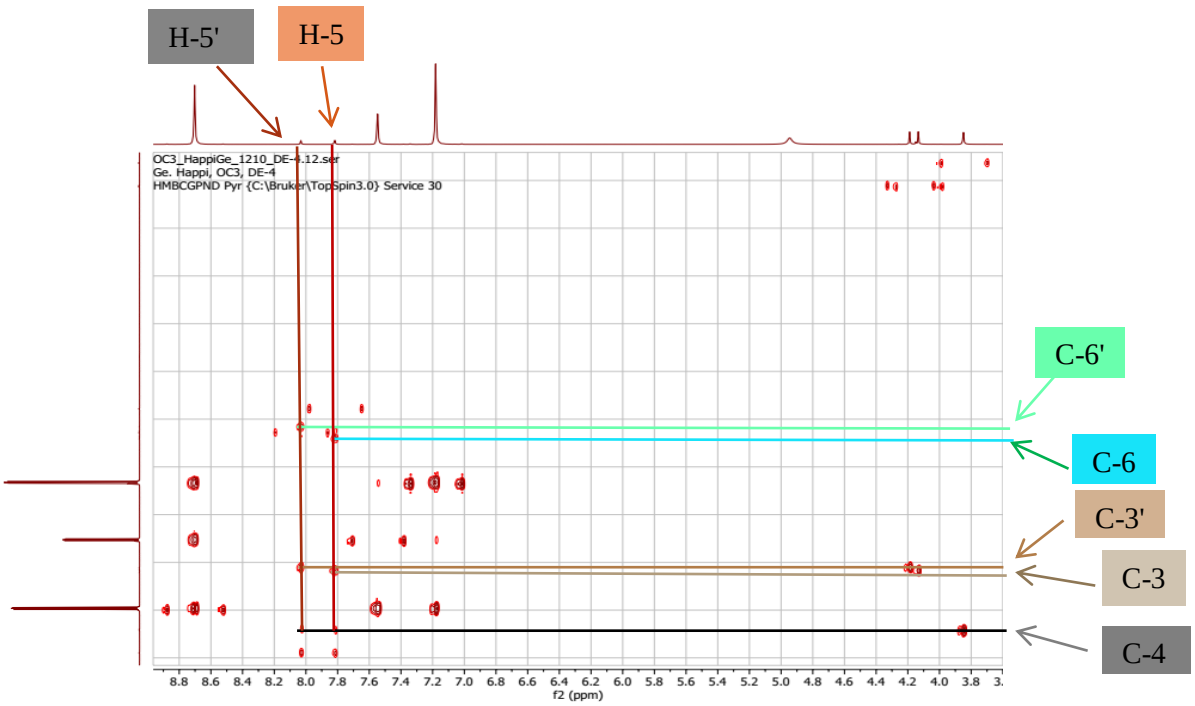

Figure 68: HMBC spectrum of DE4

II.1.2.11.2 Structure identification of DE3

DE3 was isolated as a white amorphous powder, in the mixture of solvents *n*-hexane-EtOAc (6-4). It was soluble in pyridine. The interpretation of all their spectroscopic and spectrometric data led to the identification of the following compound (**61**).

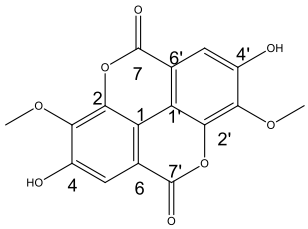

61

The molecular formula, $C_{16}H_{10}O_8$, implying twelve degrees of unsaturation, was deduced from its NMR and its HR-ESI-MS (Figure 69), which showed the sodium adduct peak $[M+Na]^+$ at *m/z* 353.2328 (cald for 330.2480).

The proton spectrum (Figure 70) of DE3 was almost similar to that of DE4, except that there was one methoxy group protons absent.

Based on this observation and by comparison of its data with those in literature DE3 was easily identified as 3,3'-di-*O*-methylellagic acid previously isolated from the *Diplopanax stachyanthus* by Khac *et al*., 1990.

Table 31: ^{1}H (Pyridine-d_5, 600 MHz) NMR data of DE3 and 3,3'-di-*O*-methylellagic acid (Khac *et al*., 1990)

Position	DE3 (δ_H)	3,3'-di-*O*-methylellagic acid (δ_H/ppm)
1	-	-
2	-	-
3	-	-
4	-	-
5	8.04	7.52
6	-	-
7	-	-
1′	-	-
2′	-	-
3′	-	-
4′	-	-
5′	8.04	7.91
6′	-	-
7′	-	-
3′-OCH_3	3.59	4.04
4-OCH_3	4.17	4.06
OH	4.99	-
OH	4.99	4.79

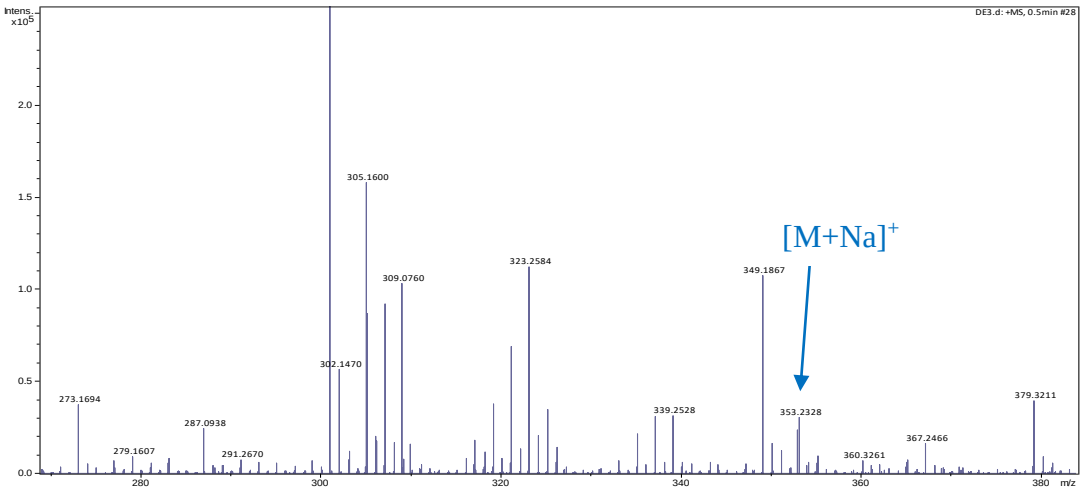

Figure 69: HR-ESI mass spectrum of DE3

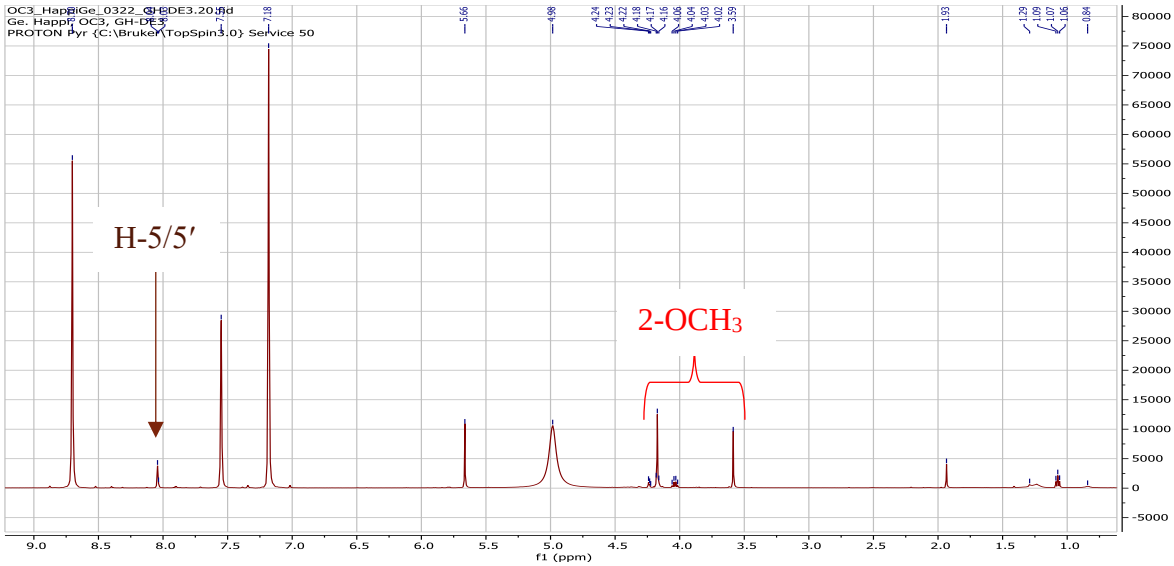

Figure 70: ^{1}H-NMR spectrum (Pyridine-d_5, 600 MHz) of DE3

II.1.2.11.3 Structure identification of DE21

DE21 was obtained as a white powder, in EtOAc (100%). It was soluble in MeOH. The interpretation of all their spectroscopic and spectrometric data contributed to the identification of DE21 as follow.

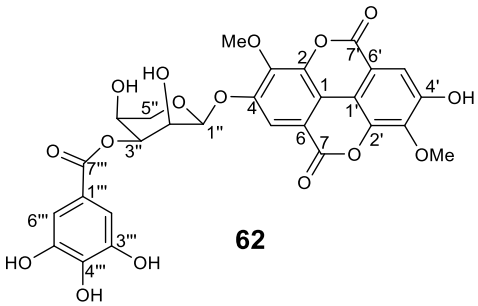

The molecular formula, $C_{28}H_{22}O_{16}$, implying ten degrees of unsaturation, was deduced from its NMR and its HR-ESI-MS (Figure 71), which showed the sodium adduct peak $[M+Na]^+$ at *m/z* 637.0797 (cald for 614.0908).

The ^{1}H-NMR spectrum (Figure 72) of DE21 displayed in addition to the signals assignable to an ellagic acid moiety at δ_H 7.66 (1H, s, H-5) and δ_H 7.36 (1H, s, H-5′), a characteristic resonance of galloyl moiety at δ_H 6.85 (2H, s, H-2‴/H-6‴). The proton spectrum of DE21 equally showed characteristic proton resonances of a xylose moiety at δ_H 5.20 (1H, d, J = 7.4 Hz, H-1″ anomeric), 4.91 (1H, d, J = 9.3 Hz, H-3″), 3.73 (1H, dd, J = 11.1; 5.2 Hz, Ha-5″), 3.53 (1H, dq, J = 9.5, 4.4 Hz, H-4″), 3.46 (1H, d, J = 6.9 Hz, H-2″), and 3.38 (1H, t, J = 10.7 Hz, Hb-5″) (Taylor *et al*., 1998).

The location of the galloyl group and the sugar moieties was established using HMBC (Figure 75) correlations of H-1″, H-5 with the carbon at δ_C 160.5 (C-4), which link ellagic acid

and the sugar. Also, correlations of H-3″, H-2‴ with the carbon δ_C 174.9 (C-7‴), which join the sugar with the galloyl group.

The COSY spectrum (Figure 74), displayed correlation between sugar hydrogens: H-5″ with H-4″, H-1″ with H-2″ which confirmed the presence of the sugar group in the molecule.

The configuration of the sugar moiety was proposed to be *β* on the basis of the coupling constant (7.4 Hz). The nature of the sugar moiety was further confirmed by the characterististic carbon signals of xylose on the ^{13}C-NMR spectrum (Figure 73) at δ_C 110.9 (C-1″), 86.7 (C-3″), 80.7 (C-2″), 76.9 (C-4″), and 72.2 (C-5″) (Taylor *et al*., 1998).

Based on the above evidences and by comparison with literature data, DE21 was concluded to be 3,3″-di-*O*-methylellagic acid 4-*O*-(3″-galloyl)-*β*-*D*-xylopyranoside previously isolated from Peruvian Rain Forest Plants (Taylor *et al*., 1998).

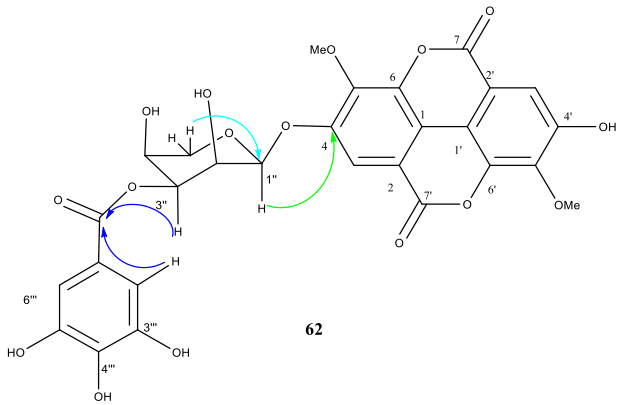

Table 32: ^{1}H (MeOH-d_4, 600 MHz) and ^{13}C (MeOH- d_4, 150 MHz) NMR data of DE21 and 3,3″-di-*O*-methylellargic acid 4-*O*-(3″-galloyl)-*β*-*D*-xylopyranoside ($CDCl_3$, 400MHz) (Taylor *et al*., 1998)

Position	DE21		3,3″-di-*O*-methylellargic acid 4-*O*-(3″-galloyl)-*β*-*D*-xylopyranoside
	δ_C	δ_H (nH, m, *J* (Hz))	δ_H (nH, m, *J* (Hz))
1	121.5	-	-
2	151.5	-	-
3	150.5	-	-
4	160.5	-	-
5	121.2	7.66 (1H, s)	7.74 (1H, s)
6	124.1	-	-
7	168.0	-	-
1′	122.6	-	-
2′	151.2	-	-

3′	149.7	-	-
4′	162.5	-	-
5′	120.6	7.36 (1H, s)	7.45 (1H, s)
6′	122.4	-	-
7′	167.9	-	-
1″	110.9	5.20 (1H, d, *J* = 7.4 Hz)	5.10 (1H, d, *J* = 5.8 Hz)
2″	80.7	3.46 (1H, d, *J* = 6.9 Hz)	3.40 (m)
3″	86.7	4.91 (1H, t, *J* = 9.3 Hz)	4.94 (1H, t, *J* = 7.3 Hz)
4″	76.9	3.53 (1H, dq, *J* = 9.5, 4.4 Hz)	3.75 (m).
5″	75.2	3.73 (1H, dd, J = 11.1; 5.2 Hz) 4.38 (1H, t, *J* = 10.7 Hz)	3.98 (1H, dd, *J* = 11; 5 Hz)
1‴	129.4	-	-
2‴	118.3	6.85 (1H, s)	6.98 (1H, s)
3‴	155.0	-	-
4‴	147.7	-	-
5‴	155.0	-	-
6‴	118.3	6.85 (1H, s)	6.98 (1H, s)
7‴	174.9	-	-
OCH_3	71.2	-	-
OCH_3	70.5	-	-

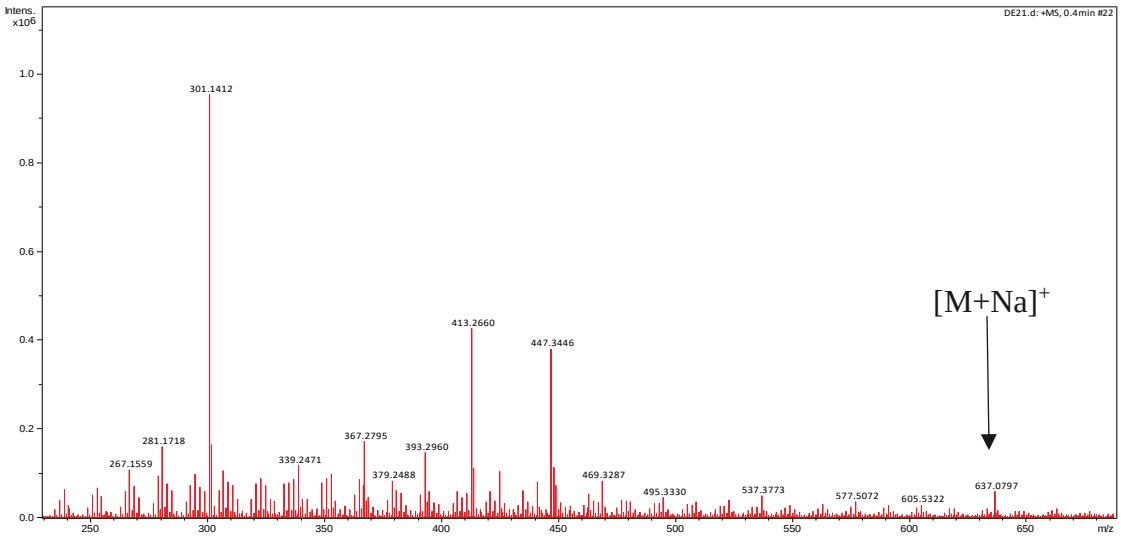

Figure 71: HR-ESI mass spectrum of DE21

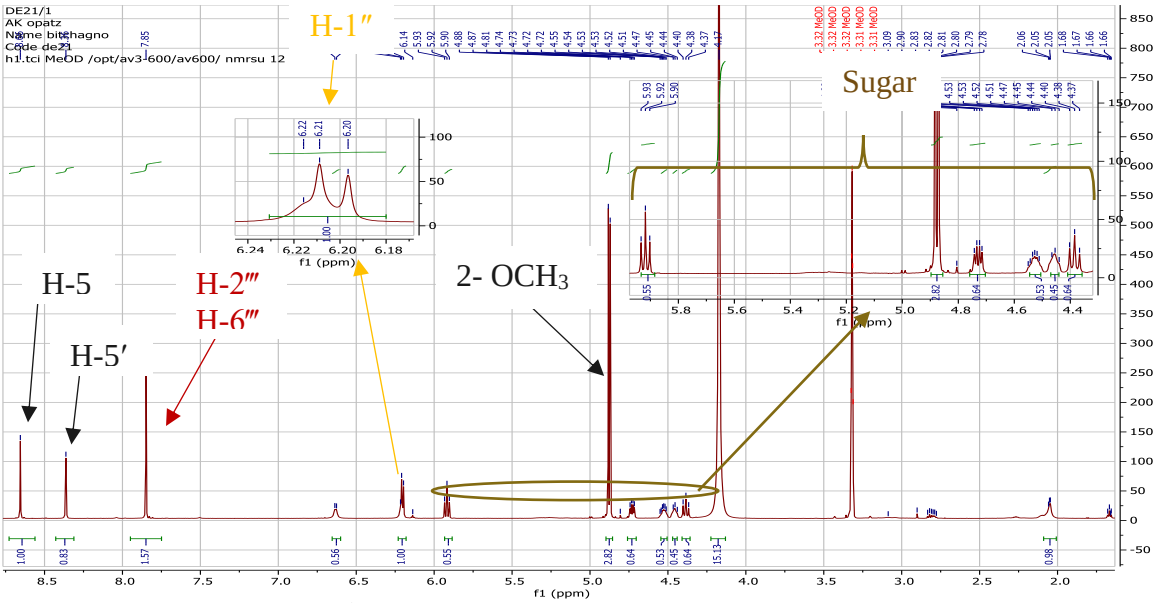

Figure 72: ^{1}H-NMR spectrum (MeOH-d_4, 600 MHz) of DE21

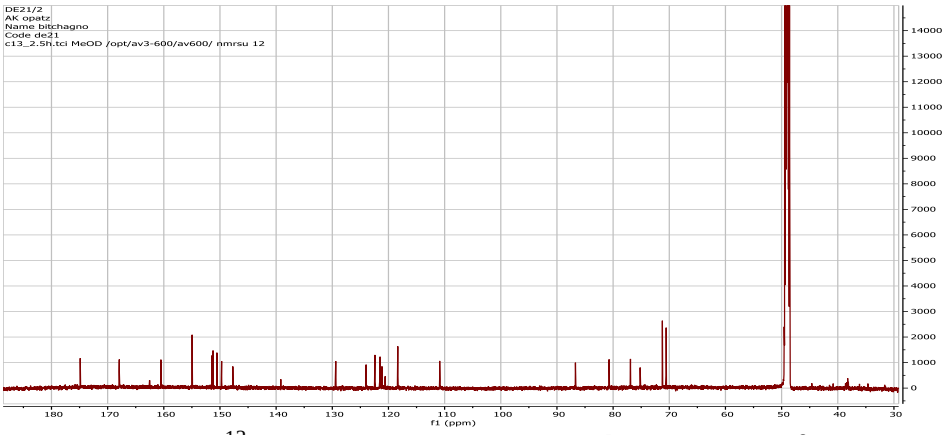

Figure 73: ^{13}C-NMR spectrum (MeOH-d_4, 150 MHz) of DE21

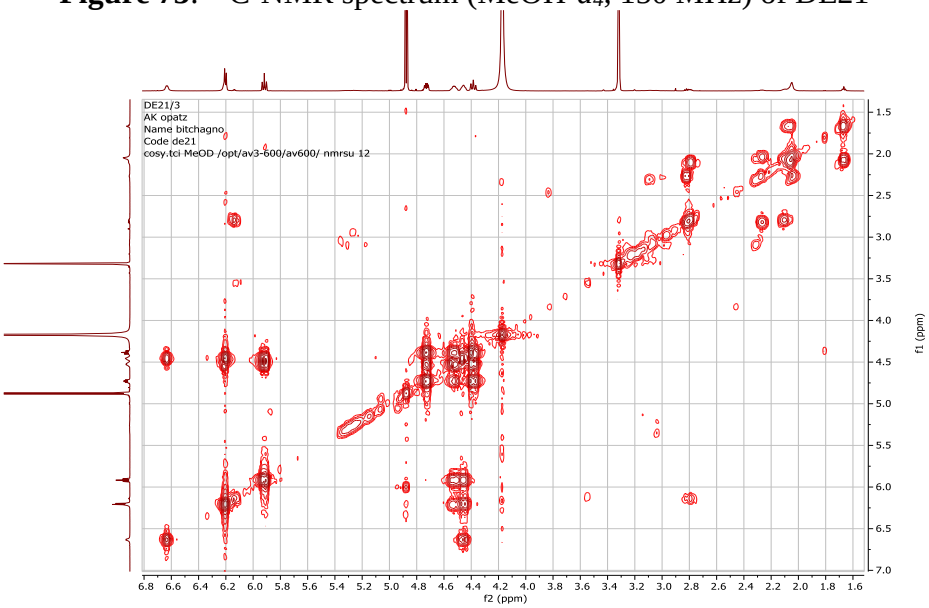

Figure 74: COSY spectrum of DE21

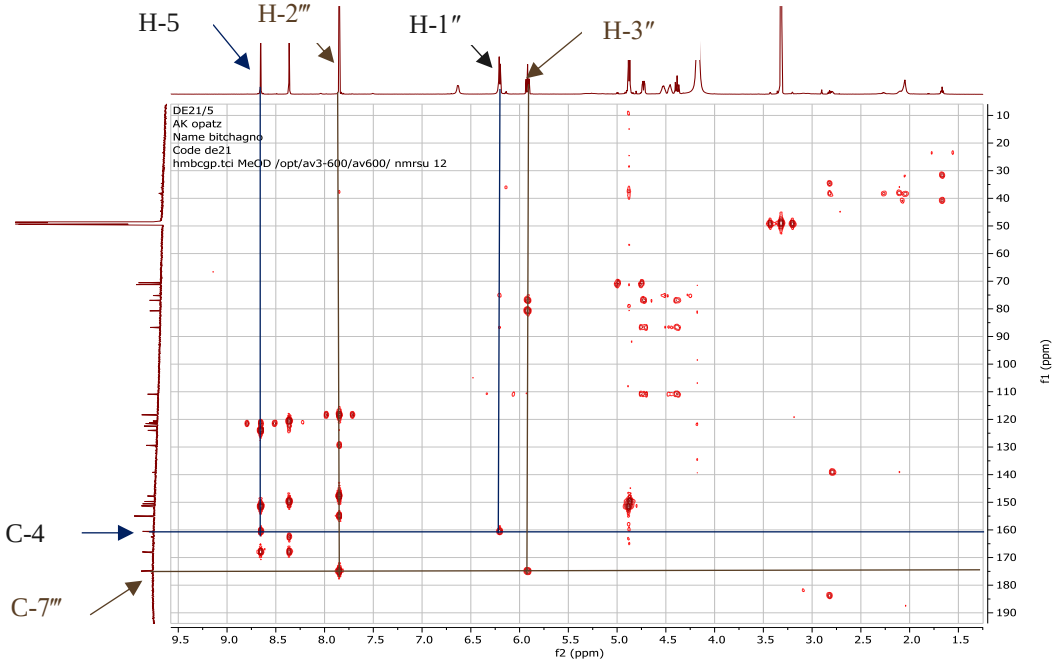

Figure 75: HMBC spectrum of DE21

II.1.2.12 Structure identification of DF3

DF3 was obtained as white powder, in the mixture of solvents *n*-hexane-EtOAc (70-30), and was soluble in dichloromethane. The interpretation of all their spectroscopic and spectrometric data contributed to the identification of DF3 as follow.

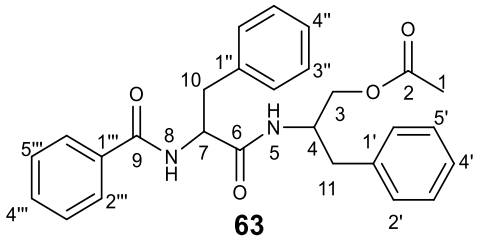

63

The molecular formula, $C_{27}H_{28}O_4N_2$, implying fifteen degrees of unsaturation, was deduced from its NMR and its HR-ESI-MS (Figure 76), which showed the protonated molecular-ion peak $[M+H]^+$ at *m/z* 445.2548 (cald for 444.2049).

The ^{1}H-NMR spectrum (Figure 77) showed the presence of two amino groups displaying the signal of their protons at δ_H 6.71 (1H, d, J = 7.6 Hz, H-8); 5.90 (1H, d, J = 8.6 Hz, H-5), many aromatic protons (δ_H 7.06-7.71), an acetoxy methyl δ_H 2.02 (3H, s, H-1) and a pair of benzylic methylenes δ_H 3.22 (1H, dd, J = 13.7, 5.9 Hz, Ha-10), 3.05 (1H, dd, J = 13.7, 8.5 Hz, Hb-10) and 2.74 (2H, m, H-11). In addition, signals due to a methylene adjacent to acetoxy group were observed at δ_H 3.93 (1H, dd, J = 11.3, 4.9 Hz, Ha-3), 3.82 (1H, dd, J = 11.3, 4.2 Hz, Hb-3). Signals at δ_H 4.78 (lH, m) and 4.35 (lH, m) were assigned to methine protons.

All this data, compared to those described in the literature, allowed give structure **63** to DF3, which is auranthiamide acetate previously isolated from the Red Alga *Acantophora Spicifera* (Wahidulla *et al*., 1991).

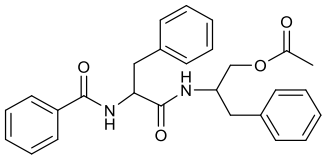

62

Table 33: ^{1}H ($CDCl_3$, 600 MHz) and ^{13}C ($CDCl_3$, 150 MHz) NMR data of DF3 and auranthiamide acetate ($CDCl_3$, 500 MHz) (Wahidulla *et al*., 1991)

Position	DF3		Auranthiamide acetate	
	δ_C	δ_H (nH, m, *J* (Hz))	δ_C	δ_H (nH, m, *J* (Hz))
1	20.8	2.02 (3H, s)	20.7	2.03 (s)
2	170.7	-	170.7	-
3	64.5	3.82 (1H, dd, *J* = 11.3, 4.2 Hz) 3.93 (1H, dd, *J* = 11.3, 4.9 Hz)	64.5	3.84 (1H, dd, *J* = 11, 5 Hz) 3.95 (1H, dd, *J* = 11, 5 Hz)
4	49.4	4.35 (lH, m)	49.5	4.2-4.47 (1H, m)
5		5.90 (1H, d, *J* = 8.6 Hz)		6.1 (1H, *d*, *J* = 7.5 Hz)
6	170.2	-	170.3	-
7	55.1	4.78 (lH, m)	54.9	4.78 (1H, m)
8		6.71 (1H, d, *J* = 7.6 Hz)		6.85 (1H, *d*, *J* = 7.5 Hz)
9	167.1		167.1	
10	37.4	3.05 (1H, dd, *J* = 13.7, 8.5 Hz) 3.22 (1H, dd, *J* = 13.7, 5.9 Hz)	37.4	3.07 (1H, dd, *J* = 14.5, 8 Hz) 3.22 (1H, dd, *J* = 15, 6 Hz)
11	38.3	2.74 (2H, m)	38.4	2.74 (2H, d, *J* = 7 Hz)
1′	136.7	-	136.7	-
2',6′	128.5	7.06-7.71 (m)	128.2	-
3′, 5′	127.0	-//-	126.7	-
4′	129.1	-//-	129.1	-
1″	136.6	-//-	136.6	-
2″, 6″	127.1	-//-	127.0	-
3″, 5″	128.6	-//-	127.1	-
4″	126.7	-//-	129.3	-
1‴	132.0	-//-	133.6	-
2‴, 6‴	128.7	-//-	128.5	-
3‴, 5‴	129.1	-//-	128.6	-
4‴	129.3	-//-	131.8	-

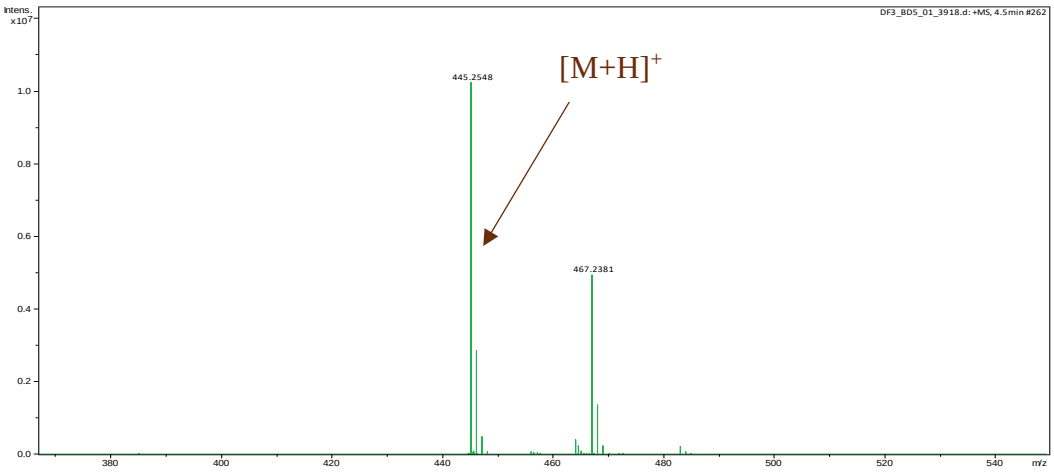

Figure 76: HR-ESI mass spectrum of DF3

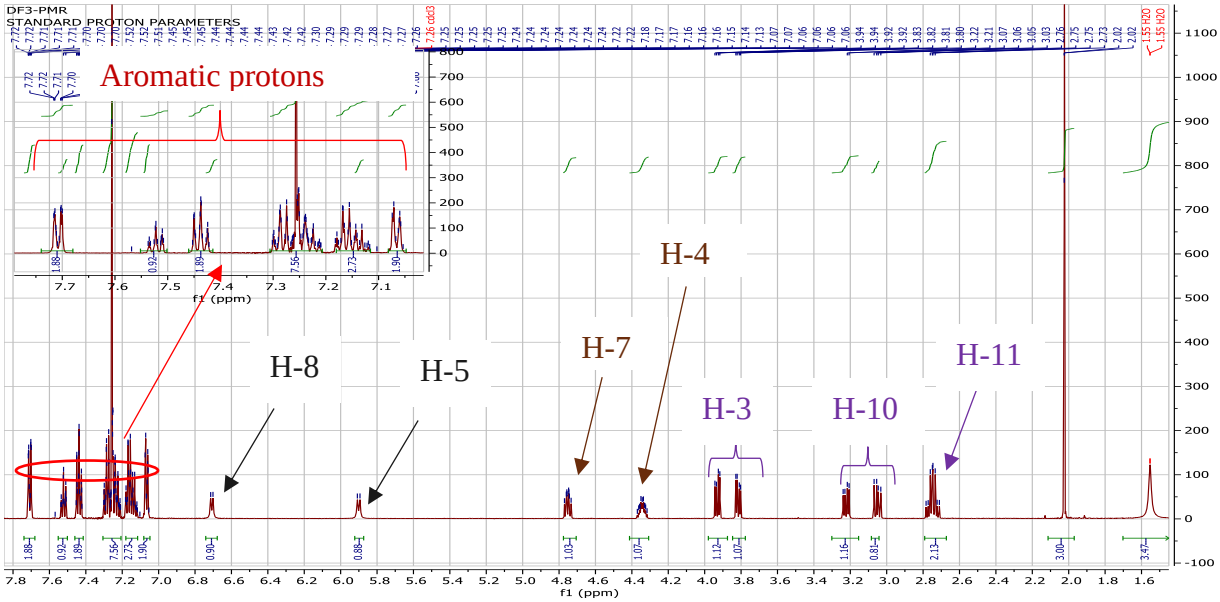

Figure 77: ^{1}H NMR spectrum ($CDCl_3$, 600 MHz) of DF3

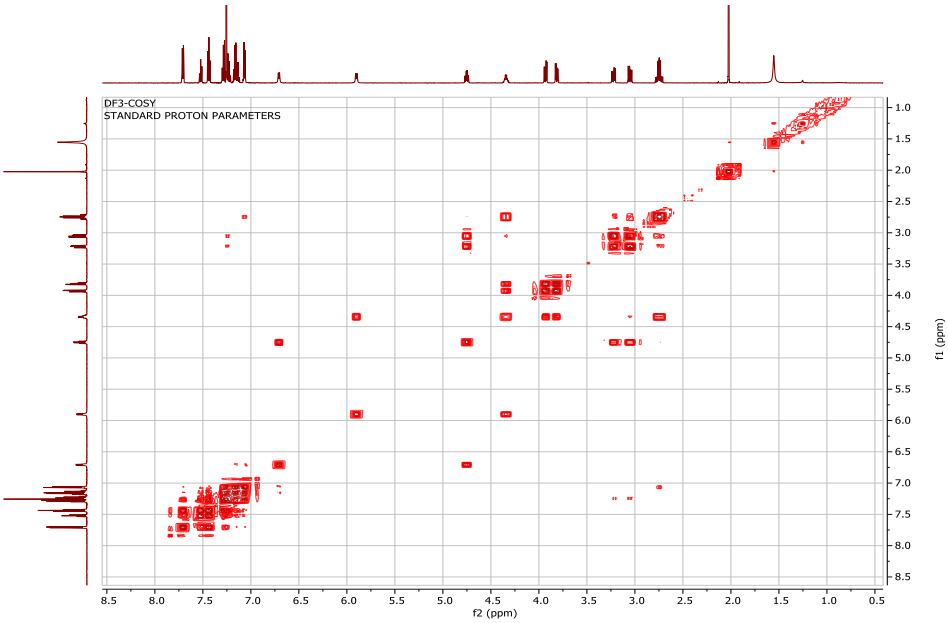

Figure 78: COSY spectrum of DF3

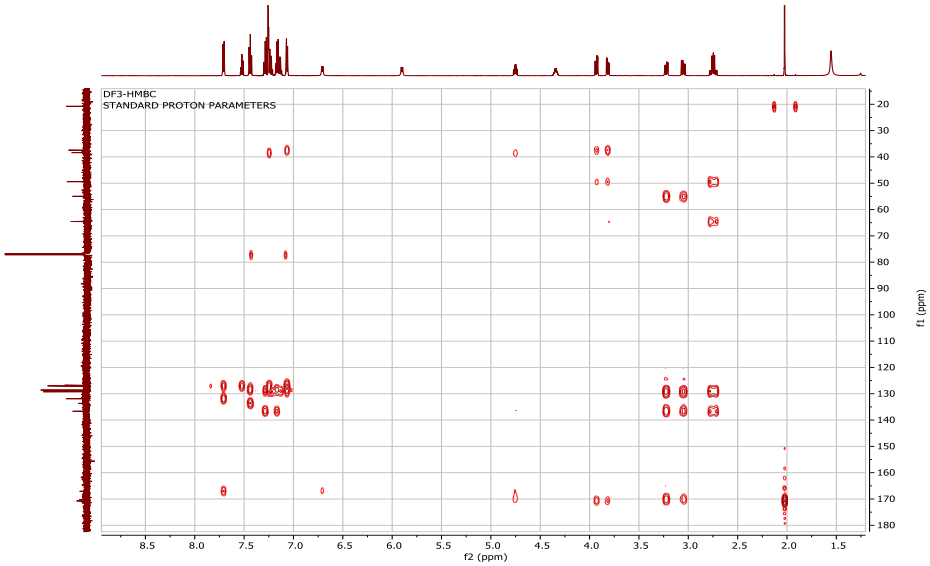

Figure 79: HMBC spectrum of DF3

II.1.2.13 Structure identification of DE7

DE7 was obtained as white powder, in the mixture of solvents DCM-EtOAc (4-1), and was soluble in methanol. The interpretation of all its spectroscopic and spectrometric data led to the identification of the following structure (**64**).

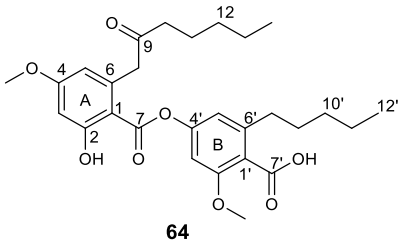

64

The molecular formula, $C_{28}H_{36}O_8$, implying eleven degrees of unsaturation, was deduced from its NMR and its HR-ESI-MS (Figure 80), which showed the the sodium adduct peak $[M+Na]^+$ at *m/z* 523.2419 (cald for 500.2410).

The ^{1}H-NMR spectrum (Figure 81) displayed signals of:

- a chelated hydroxy group at δ_H 11.36;
- four aromatic protons at δ_H 6.62 (1H, d, J = 2.0 Hz, H-5′), 6.56 (1H, d, J = 2.1 Hz, H-3′), 6.49 (1H, d, J = 2.6 Hz, H-3), and 6.32 (1H, d, J = 2.6 Hz, H-5);
- two methoxy groups at δ_H 3.90 (3H, s), and 3.87 (3H, s);
- two methylene groups that were adjacent to the benzene ring A at δ_H 4.10 (2H, s, H-8), and to benzene ring B at δ_H 2.75 (2H, m, H-8′);
- eight saturated methylene groups and two terminal methyl groups at δ_H 0.91 (3H, m, H-12′) and 0.85 (3H, t, J = 7.1 Hz, H-14).

The ring A (sub-structure1) of DE7 was established through the HMBC correlation. In fact, the HMBC spectrum (Figure 83), exhibited correlations between:

- the chelated proton of the hydroxy group OH-2 (δ_H 11.36) with carbons C-3 (δ_C 100.1), C-1 (104.2), and C-2 (167.3);

- the aromatic proton H-3 (δ_H 6.49) with carbons C-1 (δ_C 104.2), C-5 (113.4), C-4 (164.9), and C-7 (169.2);

- H-5 (δ_H 6.32) with the methylene carbon C-8 (δ_C 51.2) and with signals of aromatic carbons C-3 (δ_H 100.1), C-1 (104.2), C-4 (164.9);

- methylene protons H-10 (δ_H 2.44) with carbons C-11 (δ_C 23.9), C-12 (31.3) and with the signals of a carbonyl at C-9 (δ_C 207.1);

- and H-8 (δ_H 4.10) with carbons C-1 (δ_C 104.2), C-5 (113.7), C-6 (138.9) and C-9 (207.1).

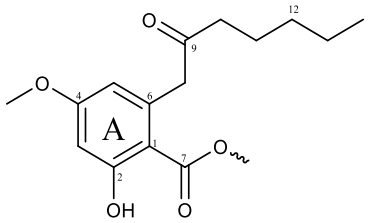

Sub-Structure 1

The ring B (sub-structure 2) of DE7 was also established through the HMBC correlations, this spectrum also displays correlations between:

- the aromatic proton H-5′ (δ_H 6.62) with the methylene carbon C-8′ (δ_C 33.6) and with signals of aromatic carbons at δ_C 103.1 (C-3′), 119.9 (C-1′), 151.4 (C-4′)

- a methylene protons H-8′ (δ_H 2.75) with carbons C-9′ (δ_C 30.7), C-5′ (115.2), C-1′ (119.9) and C-6′ (144.5).

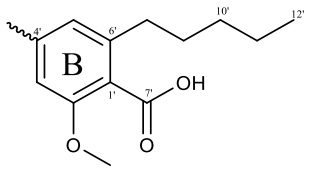

Sub-Structure 2

-This spectrum showed the correlation between methoxy signals at δ_H 3.90 and 3.87 with aromatic carbons at δ_C 156.8 and 165.2 respectively.

All these data, compared with those described in the literature, contributed to identify DE7 as confluentic acid (**64**) previously isolated from *Himatanthus sucuuba* by Yuichi and collaborators in 1994.

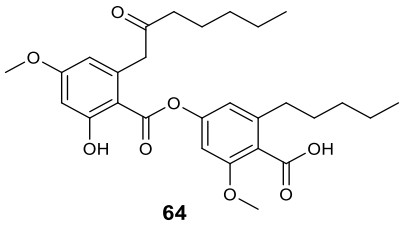

64

Table 34: ^{1}H ($CDCl_3$, 600 MHz) and ^{13}C ($CDCl_3$, 150 MHz) NMR data of DE7 and confluentic acid ($CDCl_3$, 400 and 100 MHz) (Yuichi *et al*., 1994)

Position	DE7		Confluentic acid	
	(δ_C / ppm)	δ_H (nH, m, *J* (Hz)) ppm	(δ_C /ppm)	δ_H (nH, m, *J* (Hz)) ppm
1	104.2		104.4	
2	167.3		166.6	
3	100.1	6.49 (1H, d, *J* = 2.6 Hz)	100.2	6.46 (1H, d, *J* = 2.4 Hz)
4	169.9		167.9	
5	113.4	6.32 (1H, d, *J* = 2.6 Hz)	113.4	6.30 (1H, d, *J* = 2.4 Hz)
6	138.9		140.0	
7	169.2		169.2	
8	51.2	4.10 (2H, s)	51.3	4.07 (s)
9	207.1		207.3	
10	42.6	2.44 (2H, t, *J* = 7.5 Hz)	42.5	2.41 (dd, *J* =7.3, 7.3 Hz)
11	23.4	1.55 (2H, m)	23.4	1.53 (dddd, *J* = 7.3, 7.3, 7.3, 7.3 Hz)
12	31.3	1.22 (2H, m)	31.4	1.20(m)
13	22.4	1.22 (2H, m)	22.4	1.20 (m)
14	14.0	0.85 (3H, t, *J* = 7.1 Hz)	13.8	0.83 (t, *J* = 6.8 Hz)
	51.5	3.90 (3H, s)	55.5	3.84 (s)
		11.2		11.3 (brs)
1′	119.9		120.1	
2′	156.8		157.9	
3′	103.1	6.56 (1H, d, *J* = 2.1 Hz)	103.2	6.54 (d, *J* = 2.0 Hz)
4′	151.4		151.5	
5′	115.2	6.62 (1H, d, *J* = 2.0 Hz)	115.2	6.60 (d, *J* = 2.0 Hz)
6′	144.5		144.7	
7′	170.5		169.8	
8′	33.6	2.75 (2H, m)	33.8	2.73 (dd, *J* = 7.8, 7.8 Hz)
9′	30.7	1.65 (2H, m)	30.73	1.63 (dddd, *J* = 7.8, 7.8, 7.8, 7.8 Hz)
10′	31.6	1.36 (2H, m)	31.7	1.34 (m)
11′	22.5	1.36 (2H, m)	22.4	1.34 (m)
12′	13.9	0.91 (3H, m)	14.0	0.89 (3H, m)
$-OCH_3$	55.9	3.87 (3H, s)	56.4	3.87 (3H, s)
-OH		11.36		

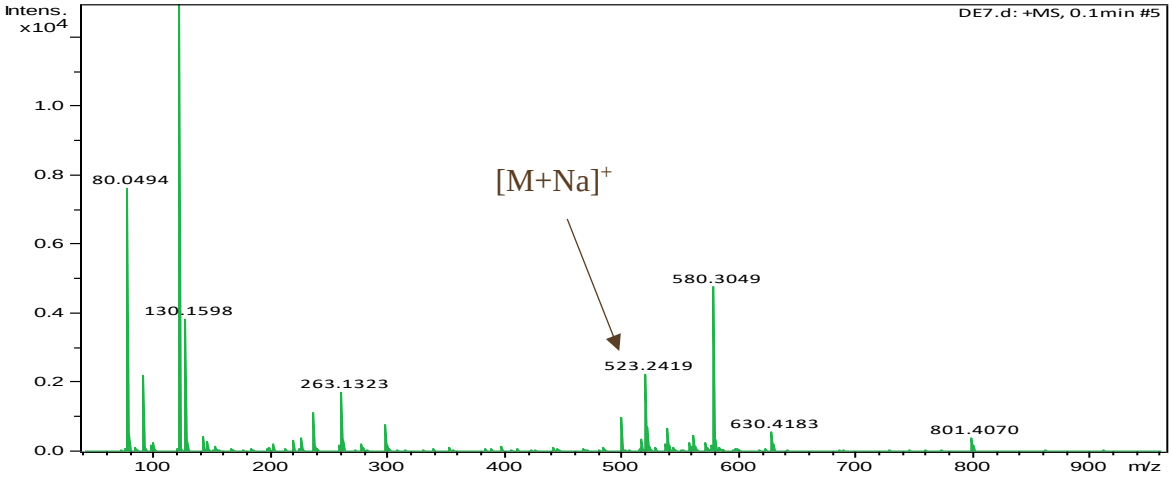

Figure 80: HR-ESI mass spectrum of DE7

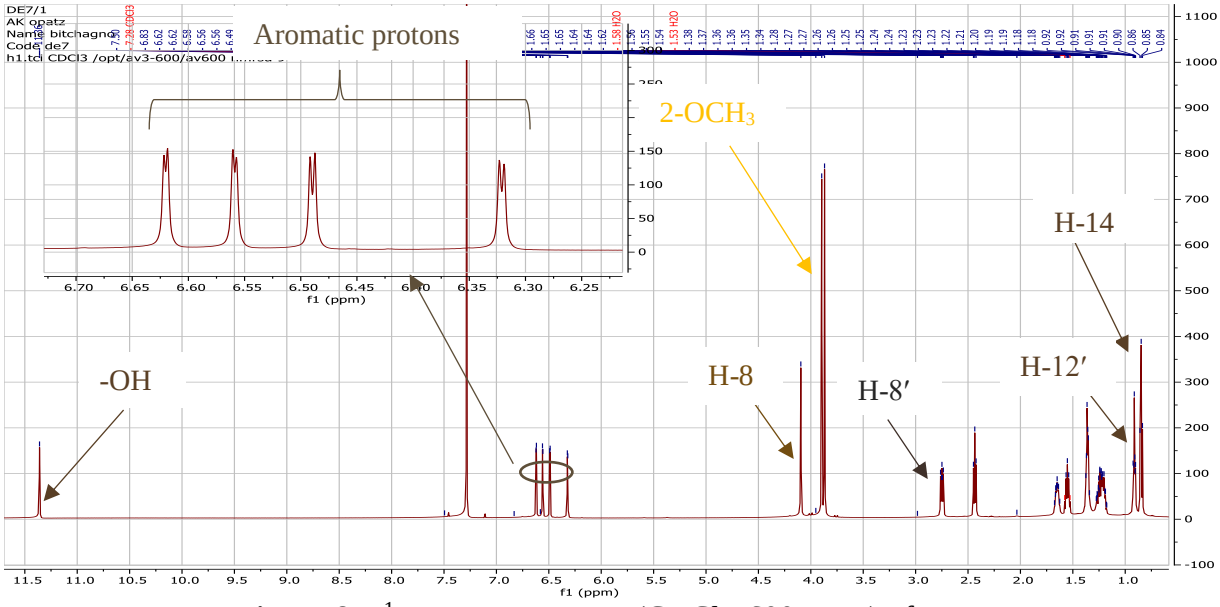

Figure 81: ^{1}H-NMR spectrum ($CDCl_3$, 600 MHz) of DE7

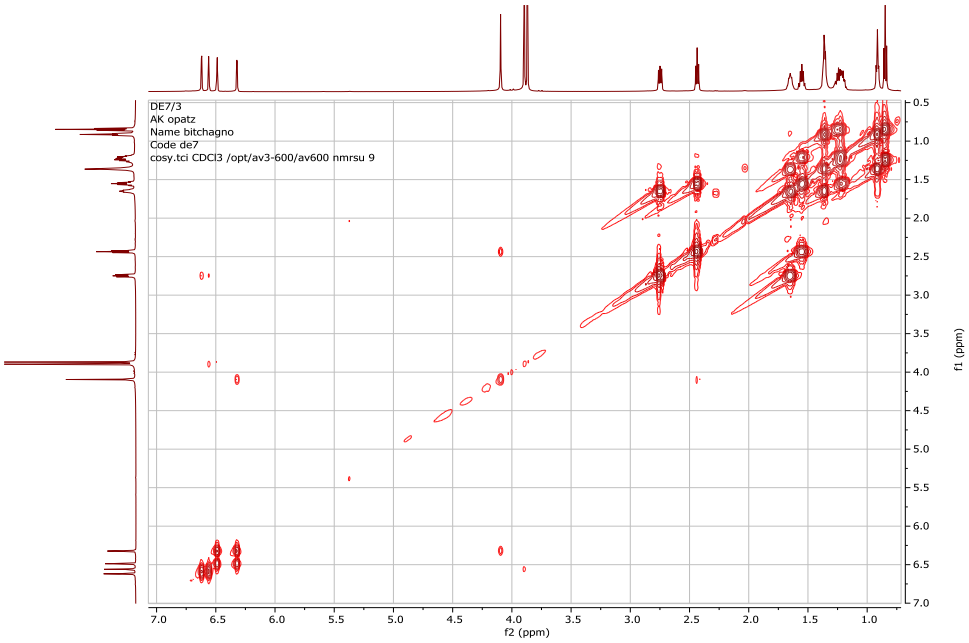

Figure 82: COSY spectrum of DE7

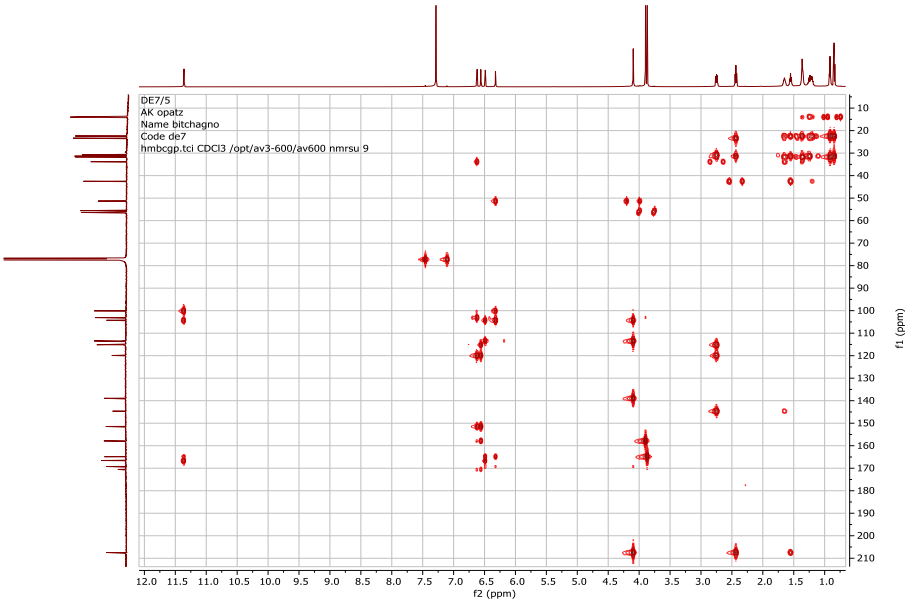

Figure 83: HMBC spectrum of DE7

II.1.2.14 Structure identification of DF6

DF6 was obtained as a white powder, in the mixture of solvents *n*-hexane-EtOAc (20-30). It was soluble in methanol. The interpretation of all its spectroscopic data led to the identification of the following compound (**65**).

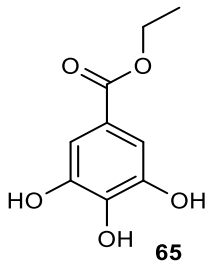

65

The ^{1}H NMR (Figure 84) spectrum of DF6 showed signals of aromatic protons at δ_H 7.06 (2H, s), an ethyl signal at δ_H 1.36 (3H, t, J = 7.1 Hz) and δ_H 4.29 (2H, q, J = 7.1 Hz). The low-field shifted of the methylene group suggested the presence of an ester group.

The ^{13}C-NMR spectrum (Table 35), confirmed the presence of two signals due to an ethyl group at δ_C 60.2 (CH_2) and 13.0 (CH_3). It also displayed four aromatic signals at δ_C 108.4 (C-2/6), 120.2 (C-1), 138.3 (C-4), and 145.1 (C-3/5); and a signal of an ester carbonyl at δ_C 167.1. Among the aromatic carbons signals, the chemical shifts at δ_C 108.4 and 120.2 were assignable to the C-H and C-C groups respectively and the remaining two signals at δ_C 138.3 and 145.1 were assignable to a C-O group, indicating the presence of a gallic acid moiety (Atsushi *et al*., 2009).

Based on the above mentioned data, DF6 was concluded to be ethyl gallate (**65**) previously isolated from *Geranium carolinianum* by Atsushi and collaborators in 2009.

Table 35: ^{1}H (MeOH-d_4, 600 MHz) and ^{13}C (MeOH-d_4, 150 MHz) NMR data of DF6 and ethyl gallate ($CDCl_3$, 500 and 125 MHz) (Atsushi *et al*., 2009)

Position	**DF6**		**Ethyl gallate**	
	δ_C	**δ_H (nH, m, J (Hz))**	**δ_C**	**δ_H (nH, m, J (Hz))**
1	120.2		121.8	
2	108.6	7.06 (1H, s)	110.0	7.04
3	145.1		146.5	
4	138.3		139.8	
5	145.1		146.5	
6	108.6	7.06 (1H, s)	110.0	7.04
1′	167.1		168.6	
2′	60.2	4.29 (2H, q, J = 7.1 Hz)	61.6	4.26
3′	13.0	1.36 (3H, t, J = 7.1 Hz)	14.6	1.33

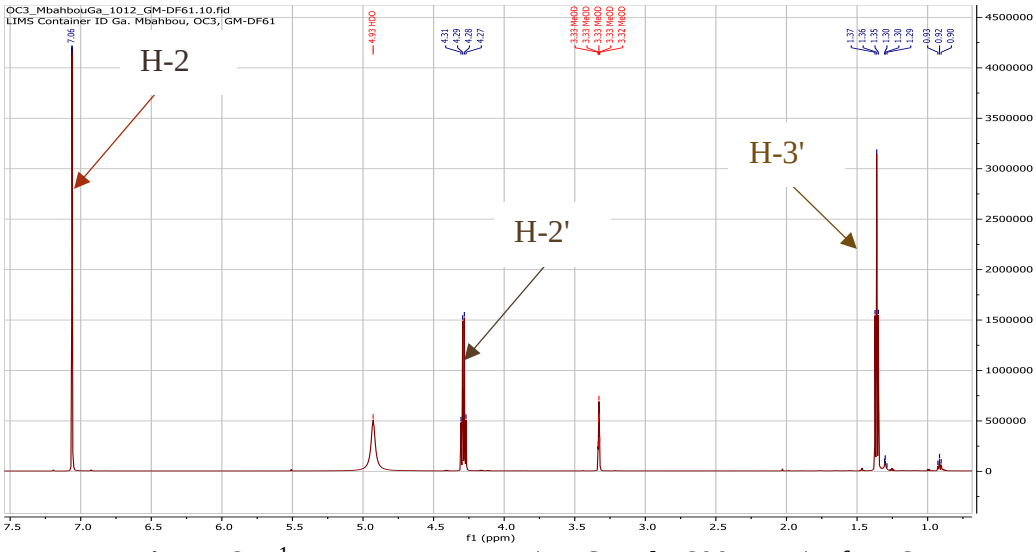

Figure 84: ^{1}H-NMR spectrum (MeOH-d_4, 600 MHz) of DF6

II.1.2.15 Structure identification of triterpenes

II.1.2.15.1 Structure identification of DE5

DE5 was obtained as a white powder, in the mixture of solvents *n*-hexane-DCM (65-35). It was soluble in dichloromethane. The interpretation of all its spectroscopic and spectrometric data led to the identification of the following compound (**66**).

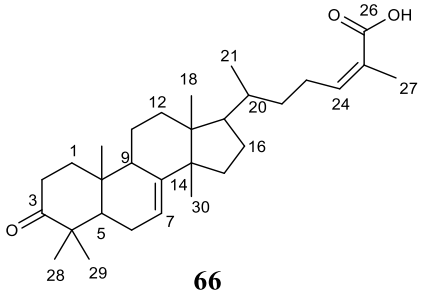

66

The molecular formula, $C_{30}H_{46}O_3$, implying eight degrees of unsaturation, was deduced from its NMR and its HR-ESI-MS data (Figure 85), which displayed the sodium adduct peak $[M+Na]^+$ at *m/z* 477.3435 (cald for 454.3447).

The ^{1}H-NMR spectrum (Figure 86), displayed 2 olefinics protons at δ_H 6.93 (H-24) and 5.67 (H-7) showing the presence of two double bonds in DE5. This spectrum also showed seven methyls characteristic triterpenes in the range of δ_H 1.87- 0.80.

The ^{13}C-NMR spectrum (Figure 87) displayed 30 signals of carbons which were sorted into: two carbonyls at δ_C 173.2 and 219.1 respectively for carbons C-26 and C-3, four olefinic carbons at δ_C 121.2-148.9 (C-7, C-8) and at δ_C 145.5-126.6 (C-24, C-25), and seven methyls. These data suggested that DE5 have the tirucallane skeleton (Barton and Seoane, 1956).

The HMBC spectrum (Figure 88) showed the correlation between the proton H-2 (δ_H 2.52) and C-3 at δ_C 219.1 which confirms the localization of the keto group at position 3. And

the correlation between the proton H-24 (δ_H 6.93) and C-26 (δ_C 173.2) which confirms the position of the keto group at position 26.

Based on the above mentioned data, DE5 was concluded to be 3-oxo-lanosta-7,24-Z-dien-26-oid acid (**66**), previously isolated from bark of *Dysoxylum pettigrewianum* by Barton and Seoane in 1956.

Table 36: ^{1}H ($CDCl_3$, 600 MHz) and ^{13}C ($CDCl_3$, 150 MHz) NMR data of DE5 and masticaidenonic acid (CD_3OD, 300MHz) (Barton and Seoane, 1956)

Position	DE5		Masticaidenonic acid	
	δ_C	δ_H (nH, m, *J* (Hz))	δ_C	δ_H (nH, m, *J* (Hz))
2	34.2	2.52	-	-
3	219.1	-	217.1	-
4	47.0	-	-	-
5	52.3	-	-	-
7	121.2	5.67	117.9	5.31
8	148.9	-	145.8	-
9	45.9	-	-	-
13	44.0	-	-	-
15	52.0	-	-	-
17	52.9	-	-	-
24	145.5	6.93	147.2	6.90
25	126.6	-	125.8	-
26	173.2	-	173.1	-
27	18.2	0.93	20.5	1.01

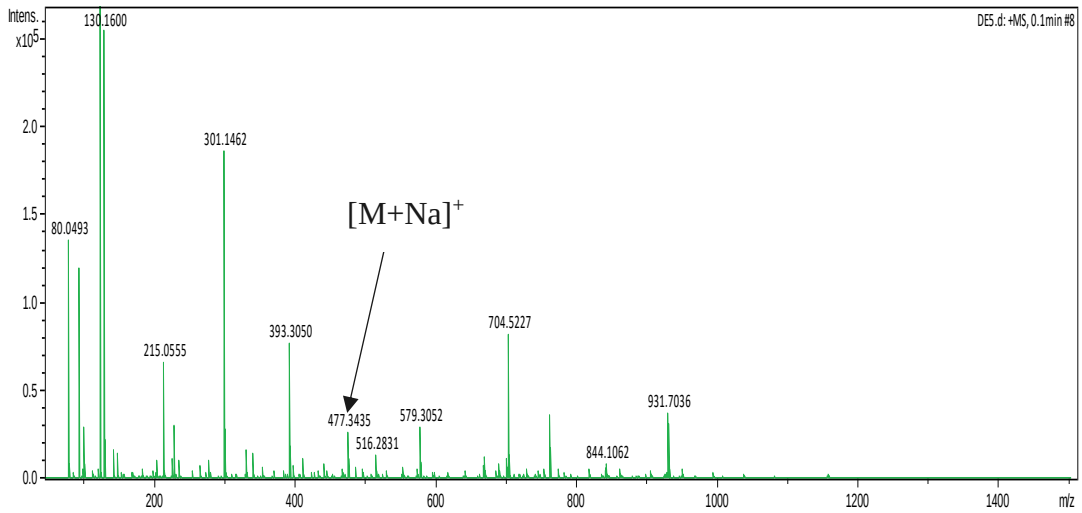

Figure 85: HR-ESI mass spectrum of DE5

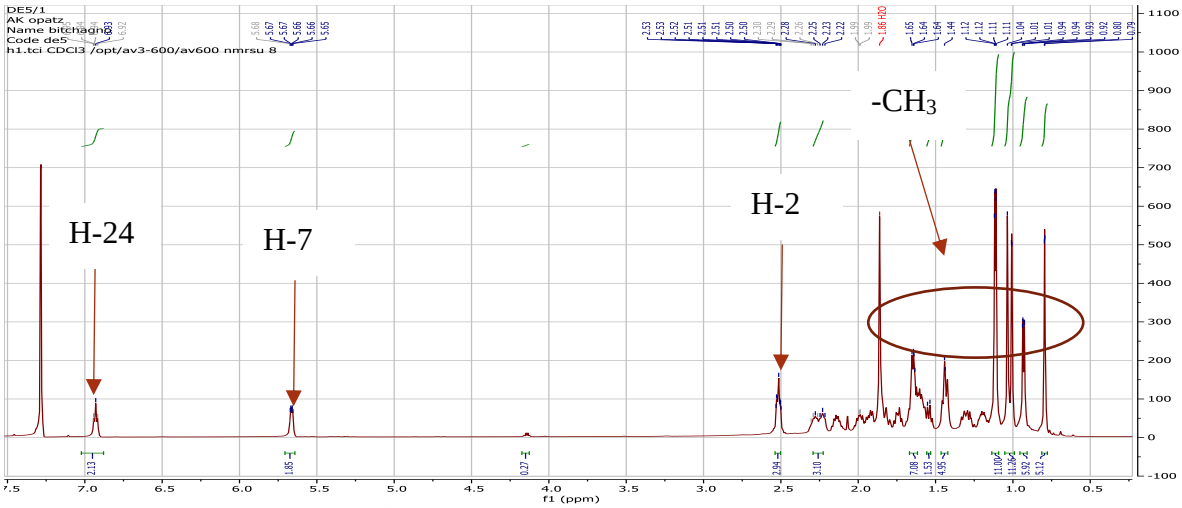

Figure 86: ^{1}H-NMR spectrum ($CDCl_3$, 600 MHz) of DE5

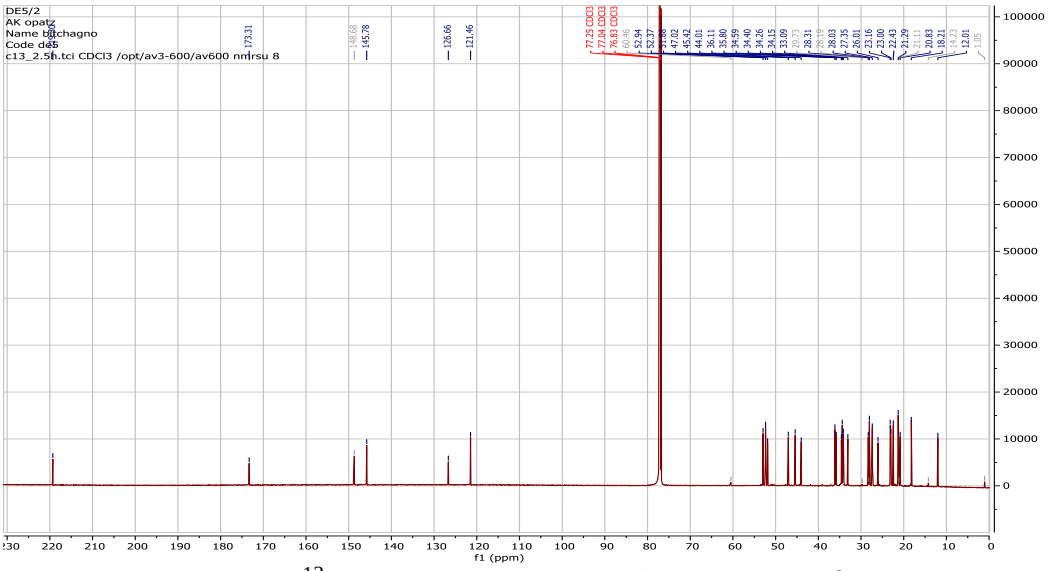

Figure 87: ^{13}C-NMR spectrum ($CDCl_3$, 150 MHz) of DE5

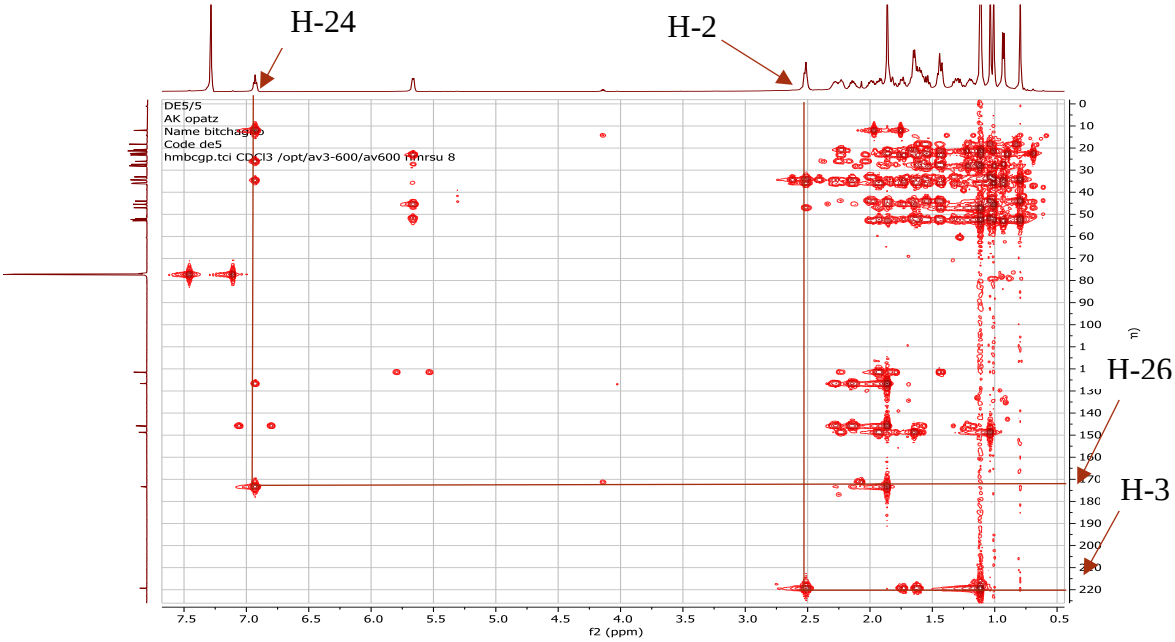

Figure 88: HMBC spectrum of DE5

II.1.2.15.2 Structure identification of DE14

DE14 was isolated as a white powder in the *n*-hexane/DCM (65-35), it was soluble in dichloromethane and reacted positively to Liebermann-Burchard's test for pentacyclic triterpenoids (pink colouration). The interpretation of all its spectroscopic and spectrometric data led to the identification as compound (**67**).

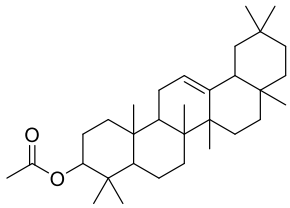

67

The molecular formula, $C_{32}H_{53}O_2$, implying seven degrees of unsaturation, was deduced from its NMR and its HR-ESI-MS data (Figure 89), which displayed the diprotonated molecular ion peak $[M+2H]^+$ at *m/z* 470.3385 (cald for 468.3967).

The ^{1}H-NMR spectrum (Figure 90) showed an olefinic proton at δ_H 5.63 (1H, brd, H-12), a proton geminal to hydroxy group at δ_H 3.47 (1H, dd, J = 4.7, 11.2 Hz, H-3), methyl protons at δ_H 1.14 (3H, s, H-26), 1.09 (3H, s, H-23), 1.04 (3H, s, H-27), 0.99 (3H, s, H-24), 0.95 (3H, s, H-28), 0.88 (3H, s, H-25), 1.16 (3H, s, H-30) and 1.00 (3H, s, H-29), suggesting the presence of an oleanane-type skeleton (Mahato and Kundu, 1994).

The broad band decoupled ^{13}C-NMR spectrum (Figure 91) displayed 32 carbon signals which were sorted into eight quaternary carbons (including the C-13 at δ_C 145.2 and a carbonyl at δ_C 171.1), five methine groups [including one olefinic methine at δ_C 121.6 (C-12) and one oxymethine at δ_C 80.9 (C-3)], ten methylene carbons and nine methyl carbons at δ_C 28.1 (C-23), 16.7 (C-24), 15.6 (C-25), 16.8 (C-26), 26.0 (C-27), 28.4 (C-28), 33.4 (C-29), 23.1 (C-30).

The COSY spectrum (Figure 92) displayed interactions between H-12 and H-11, and H-3 and H-2.

Based on the above mentioned data, DE14 was concluded to be *β*-amyrin acetate (Manguro *et al*., 2003). These data are resumed in the table 37.

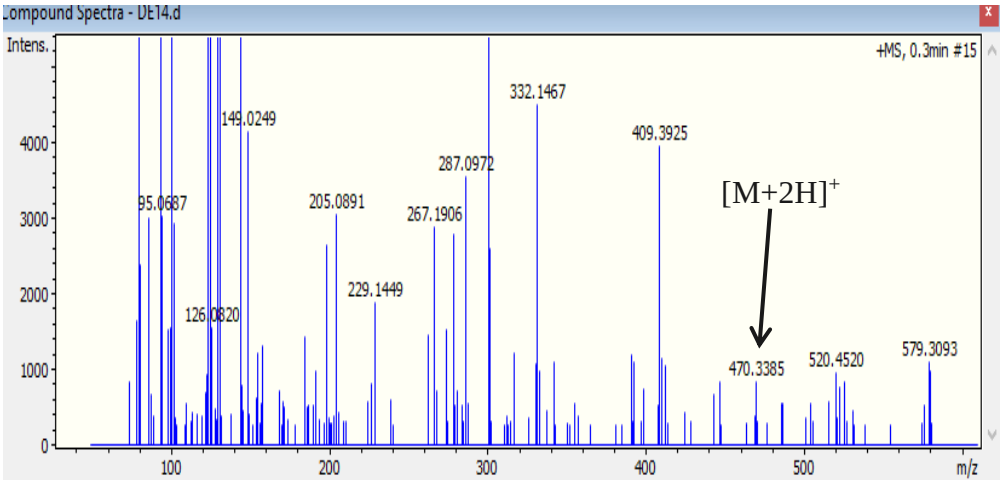

Figure 89: HR-ESI Mass spectrum of DE14

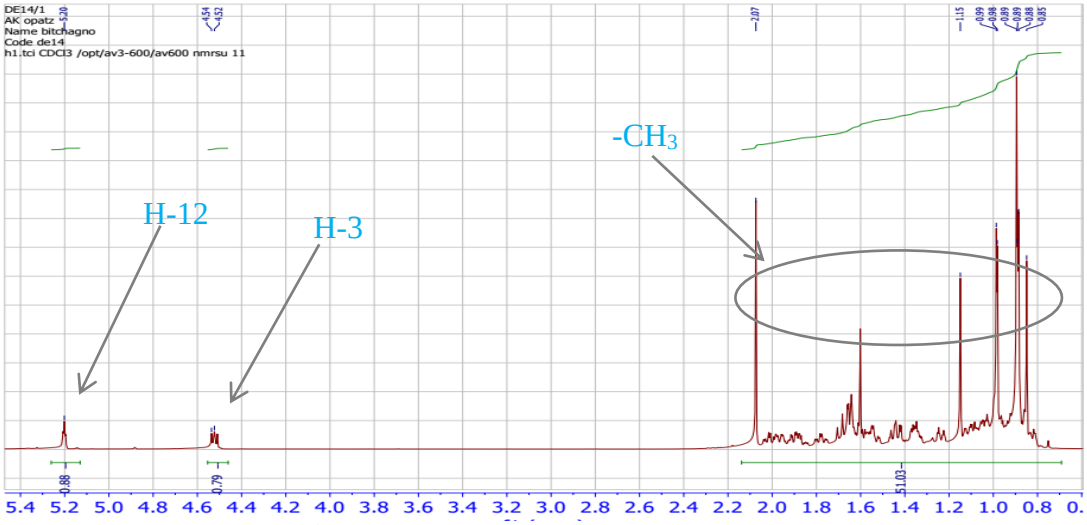

Figure 90: ^{1}H-NMR spectrum ($CDCl_3$, 600 MHz) of DE14

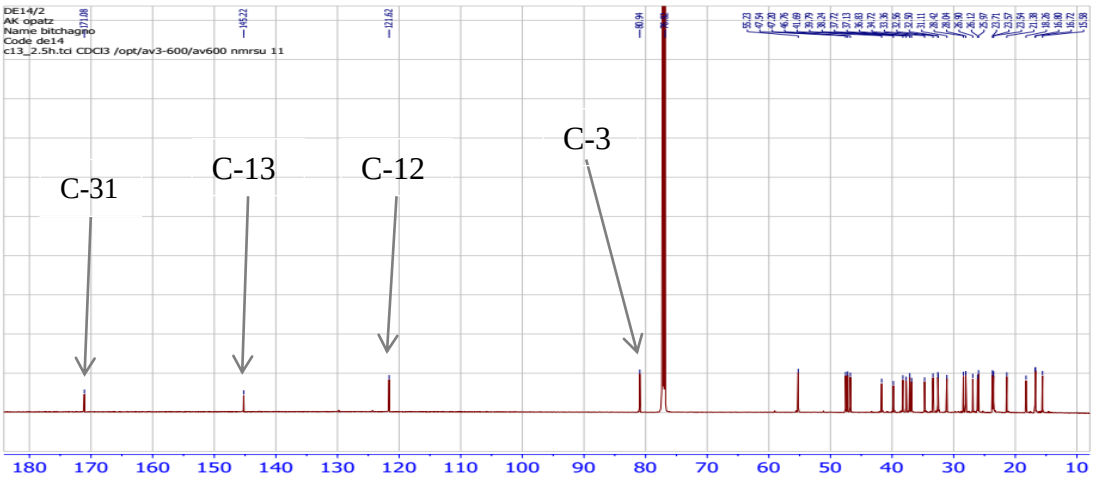

Figure 91: ^{13}C NMR spectrum ($CDCl_3$, 150 MHz) of DE14

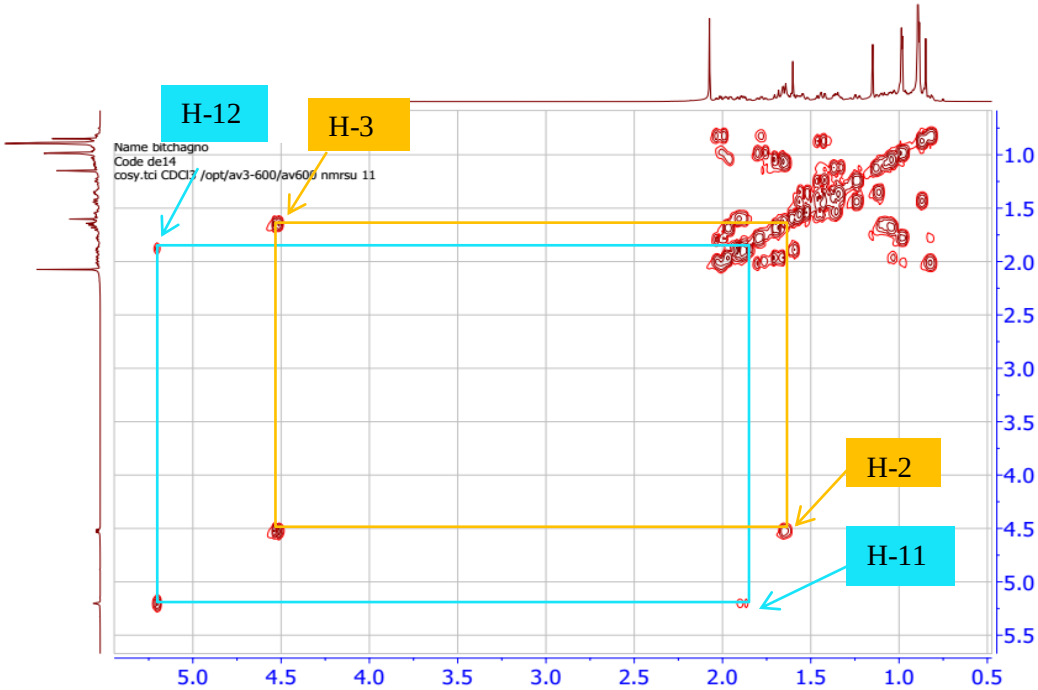

Figure 92: COSY spectrum of DE14

II.1.2.15.3 Structure identification of DE16

DE16 was isolated as a white powder in the *n*-Hex/DCM (20%) which was soluble in dichloromethane and reacted positively to Liebermann-Burchard's test for pentacyclic triterpenoids (pink colouration). The interpretation of all its spectroscopic data led to the identification of the following compound **68.**

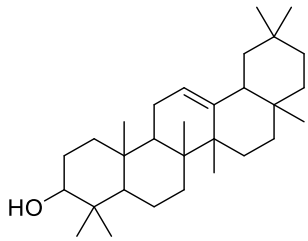

68

The ^{1}H-NMR spectrum (Figure 92) showed resonances of an olefinic proton at δ_H 5.64 (1H, brd, H-12), a proton geminal to hydroxy group at δ_H 3.49 (1H, m, H-3), and 8 singlets of three protons each between 0.77 and 1.30 ppm, assignable to characteristic protons of triterpenoids of the series (Mahato and Kundu, 1994).

This was further confirmed by the signals at δ_C 122.0 (C-12) and 141.7 (C-13) observed on the ^{13}C-NMR spectrum (table 37), characteristics of the triterpenoids of the oleanane series. Based on this evidence, DE16 was identified as β-amyrin (**68**).

Table 37: Comparison of ^{13}C ($CDCl_3$, 150 MHz) NMR data of DE16 and DE14 with those of *β*-amyrin and *β*-amyrin acetate (Manguro *et al*., 2003, (Okoye *et al*., 2014)

Position	DE16	*β*-amyrin	DE14	*β*-amyrin acetate
	δ_C	δ_C	δ_C	δ_C
1	38.3	38.7	38.2	38.7
2	26.4	27.8	28.0	27.8
3	76.4	79.0	80.9	79.0
4	36.1	38.3	38.2	38.3
5	55.0	55.3	55.2	55.3
6	19.6	18.5	18.3	18.5
7	33.1	32.8	32.6	32.8
8	38.9	38.8	39.8	38.8
9	47.5	47.7	47.2	47.7
10	36.8	37.6	37.7	37.6
11	27.8	23.6	23.6	23.6
12	122.0	121.8	121.6	121.8
13	141.7	145.1	145.2	145.1
14	39.3	41.8	41.7	41.8
15	30.1	26.2	26.1	26.2
16	28.9	27.0	26.9	27.0
17	34.5	32.5	32.5	32.5
18	46.1	47.5	47.5	47.5
19	44.9	46.9	46.8	46.9
20	32.4	31.1	31.1	31.1
21	34.6	34.8	34.7	34.8
22	35.1	37.2	37.1	37.2
23	27.6	28.2	28.1	28.2
24	14.4	15.5	16.7	15.5
25	14.2	15.6	15.6	15.6
26	16.2	16.9	16.8	16.9
27	27.3	26.0	26.0	26.0
28	28.0	28.4	28.4	28.4
29	32.5	33.3	33.4	33.3
30	23.6	23.7	23.7	23.7
31			171.1	173.2
32			21.4	22.1

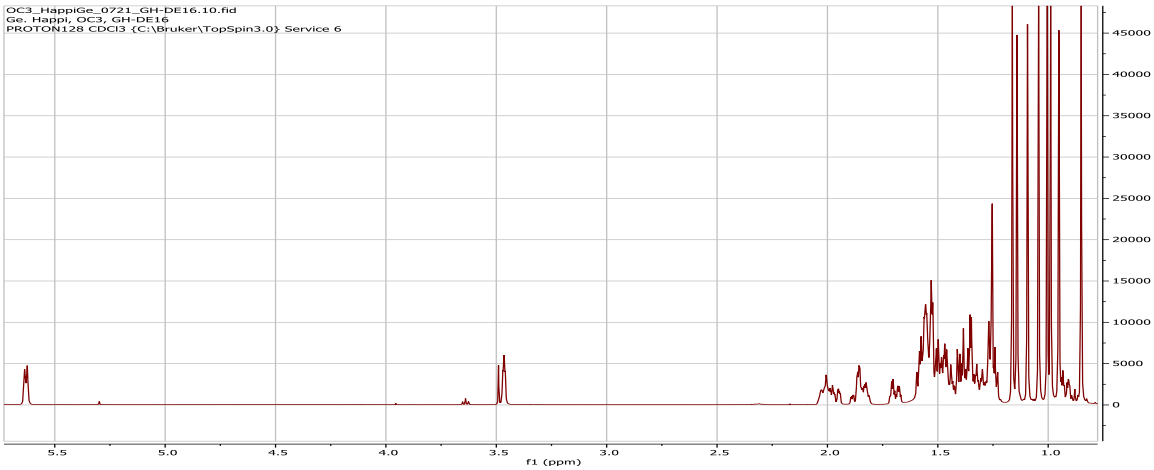

Figure 93: ^{1}H-NMR spectrum ($CDCl_3$, 600 MHz) of DE16

II.1.2.15.4 Identification of CAF1

Compound CAF1 was obtained as white powder in the system Hex/EtOAc (49:1). It was soluble in methylene chloride. It reacted positively to the Liebermann-Burchard test by giving a purplish red coloration characteristic of triterpenoids. The analysis of all its spectroscopic and spectrometric data led to the identification of the following structure (**69**).

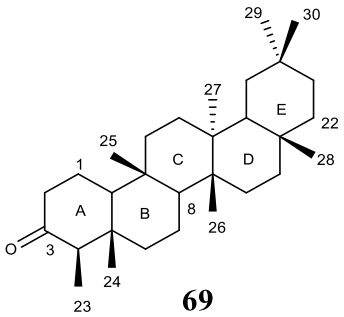

69

The molecular formula, $C_{30}H_{50}O$, implying six degrees of unsaturation, was deduced from the combinaison of its NMR and its EI-MS data (Figure 94), which displayed the molecular ion peak $[M]^+$ at *m/z* 426.3.

The ^{1}H-NMR spectrum (Figure 95) of CAF1 displayed signals of seven methyl groups including six singlets at δ_H 0.71 (3H, s, H-24), 0.85 (3H, s, H-25), 0.93 (3H, s, H-29), 0.99 (6H, s, H-26/30), 1.03 (3H, s, H-27), and 1.16 (3H, s, H-28) and a doublet at δ_H 0.86 (3H, d, J = 6.0 Hz, H-23) characteristic of the friedelane series of triterpenoids (Patra *et al*., 1990). The ^{13}C-NMR spectrum (Figure 96) exhibited resonances of 30 carbons signals which were sorted by the DEPT technique into seven quaternary carbons signals including one ketone carbonyl at δ_C 213.2, four methane carbons, eleven methylenes and eight methyl signals including one at δ_C 6.8 (C-23) confirming the friedelane series (Mahato and Kundu, 1994). Based on the above evidences, CAF1 was identified as friedelin (Sousa et al., 2012; Klass et al., 1992).

Table 38:[1]H ($CDCl_3$, 500 MHz) and ^{13}C ($CDCl_3$, 125 MHz) NMR data of CAF1 and friedelin ($CDCl_3$, 400 MHz) (Sousa *et al*., 2012; Klass *et al*., 1992).

Position	CAF1		Friedelin	
	δ_C	δ_H (nH, m, *J* (Hz)	δ_C	δ_H (nH, m, *J* (Hz)
1	22.3	1.94 (1H, m)	22.3	1.90 (1H, m)
		1.66 (1H, m)		1.65 (1H, m)
2	41.5	2.37 (1H, dq, *J* = 8.5; 3.5 Hz)	41.5	2.38 (1H, d, *J* = 7.4 Hz)
		2.36 (1H, m)		2.22 (1H, m)
3	213.3	-	212.9	-
4	58.2	2.23 (1H, q, *J* = 6.5 Hz)	58.3	2.18 (1H, q, *J* = 6.5 Hz)
5	42.1	-	42.8	-
6	41.3	1.75 (1H, m)	41.3	1.66 (1H, m)
		1.19 (1H, m)		1.21 (1H, m)
7	18.2	1.46 (1H, m)	18.3	1.45 (1H, m)
		1.32 (1H, m)		1.35 (1H, m)
8	53.1	1.32 (1H, m)	52.9	1.35 (1H, m)
9	37.4	-	37.5	-
10	59.4	1.50 (1H, m)	59.5	1.48 (1H, m)
11	35.6	1.37 (1H, m)	35.7	1.38 (1H, m)
		1.20 (1H, m)		1.19 (1H, m)
12	30.5	1.27 (1H, m)	30.5	1.31 (1H, m)
		1.26 (1H, m)		1.24 (1H, m)
13	39.7	-	39.7	-
14	38.3	-	38.3	-
15	32.7	1.24 (1H, m)	32.41	1.49 (1H, m)
		1.46 (1H, m)		1.27 (1H, m)
16	36.0	1.50 (1H, m)	36.0	1.50 (1H, m)
		1.25 (1H, m)		1.28 (1H, m)
17	30.0	-	30.0	-
18	42.8	1.56 (1H, m)	42.9	1.51 (1H, m)
19	35.3	1.33 (1H, m)	35.3	1.31 (1H, m)
		1.18 (1H, m)		1.14 (1H, m)
20	28.1	-	28.2	-
21	32.4	1.46 (1H, m)	32.7	1.42 (1H, m)
		1.33 (1H, m)		1.37 (1H, m)
22	39.2	1.44 (1H, m)	39.2	1.41 (1H, m)
		0.93 (1H, m)		0.90 (1H, m)
23	6.8	0.86 (3H, d, *J* = 6.5 Hz)	6.8	0.88 (3H, d, *J* = 6.6 Hz)
24	14.7	0.71 (3H, s)	14.7	0.72 (3H, s)
25	14.9	0.85 (3H, s)	17.9	0.87 (3H, s)
26	20.3	0.93 (3H, s)	20.2	1.01 (3H, s)
27	18.7	1.03 (3H, s)	18.7	1.05 (3H, s)
28	35.3	1.16 (3H, s)	35.0	1.18 (3H, s)
29	32.1	0.98 (3H, s)	31.9	0.95 (3H, s)
30	31.8	0.99 (3H, s)	31.7	1.00 (3H, s)

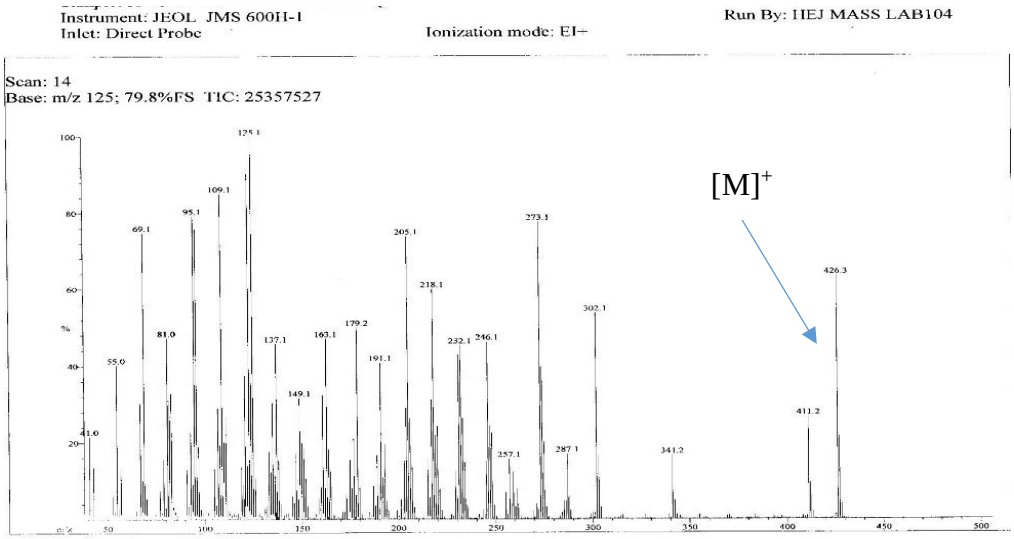

Figure 94: EI mass spectrum of CAF1

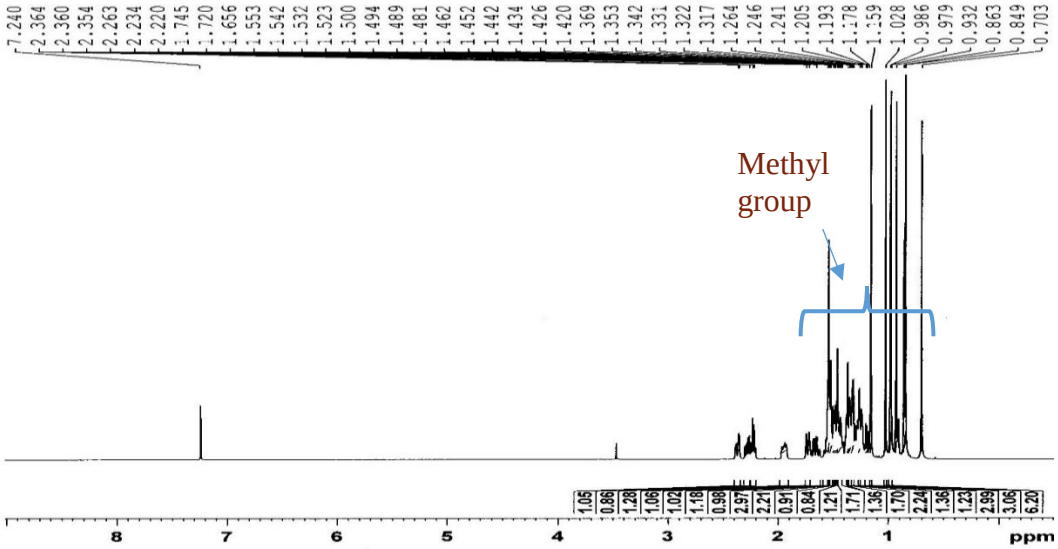

Figure 95: ^{1}H-NMR spectrum ($CDCl_3$, 500 MHz) of CAF1

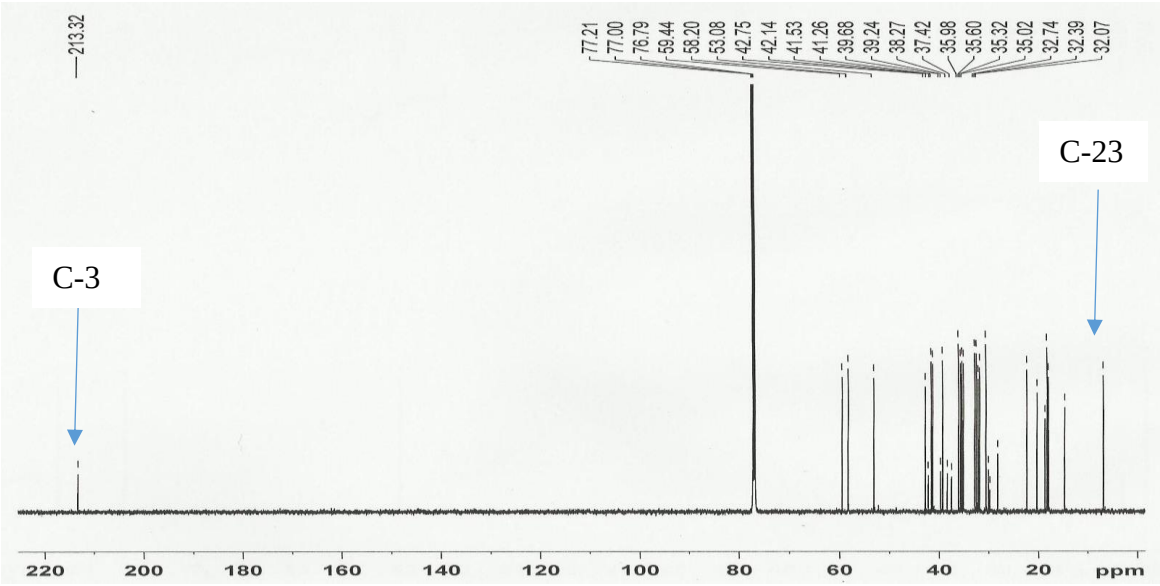

Figure 96: ^{13}C-NMR spectrum ($CDCl_3$, 125 MHz) of CAF1

II.1.2.15.5 Structure identification of DE8

DE8 was isolated as a white powder in the *n*-Hex/DCM (30%) which was soluble in dichloromethane. The analysis of all its spectroscopic and spectrometric data led to the identification of the following structure **70.**

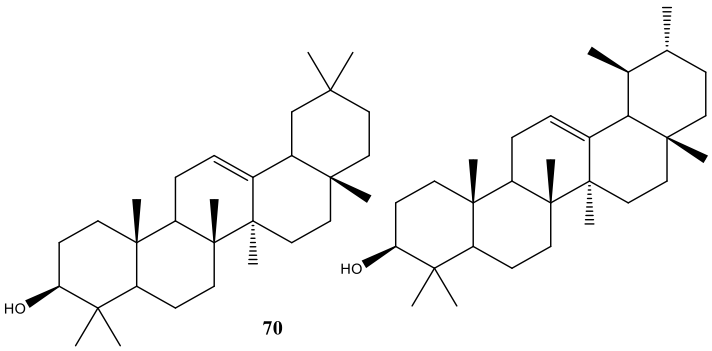

70

The ^{1}H-NMR spectrum (Figure 97) showed a group of signals in the range of δ_H 0.80-1.60 ppm which can be attributed to methyls protons of pentacyclic triterpenoids. It exhibited the presence of two olefinics protons at δ_H 5.21 and 5.15 (H-12) suggesting the presence of two double bonds in the molecule. The proton spectrum also displayed signals of two oxymethines protons at δ_H 3.26 and 3.24 which are caracteristics of proton H-3 suggesting that our compound is a mixture of triterpenoids of the type olean-12-ene and urs-12-enes. All these informations were confirmed by the presence on the ^{13}C-NMR spectrum (Figure 98) of four olefinics carbons at δ_C 145.2, 139.5, 124.4, and 121.7. Thus DE8 is a mixture of oleanolic and ursolic acids.

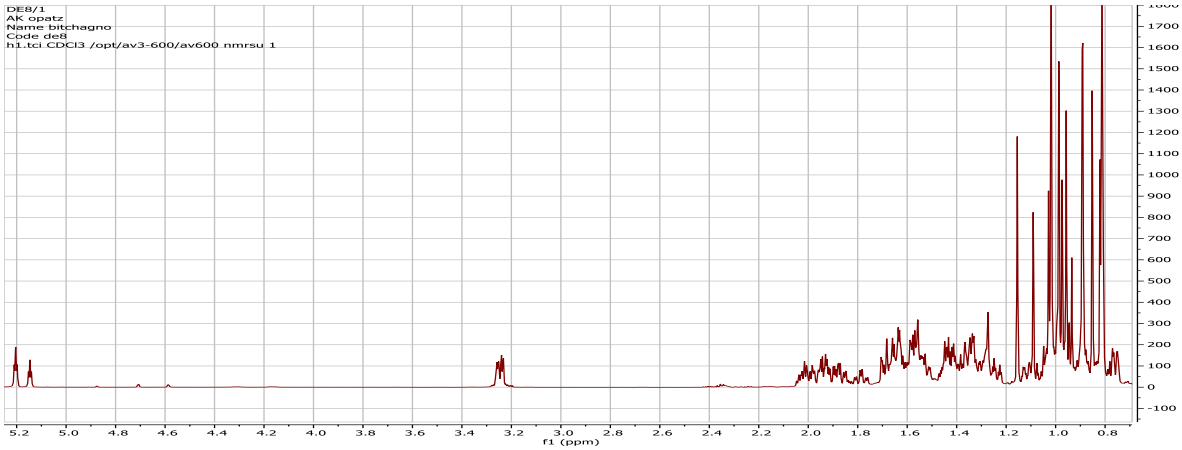

Figure 97:^{1}H NMR spectrum ($CDCl_3$, 600 MHz) of DE8

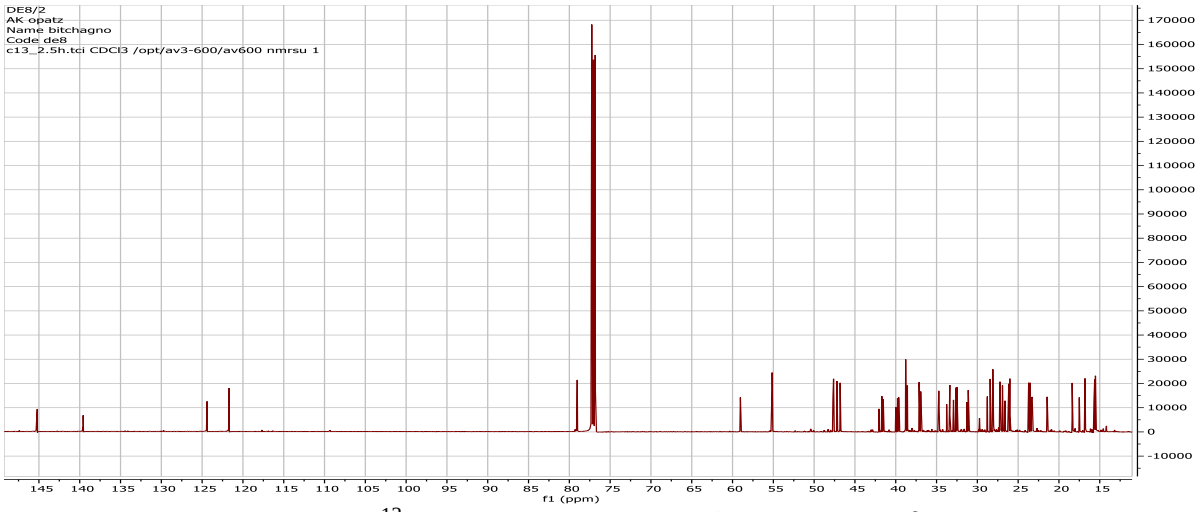

Figure 98: ^{13}C NMR spectrum ($CDCl_3$, 150 MHz) of DE8

II.2 CHEMOPHENETIC SIGNIFICANCE OF THE ISOLATED COMPOUNDS

- ***D. edulis***

Although very few studies have been carried out on plants of the genus *Dacryodes*, it belongs to the Burseraceae family which have been the subject of numerous chemical works. Some of the isolated compounds have been reported from plants of this family. It is the case of 3,4-dihydroxybenzoic acid (**55**), which has been previously isolated from *Boswellia dalzielii* Hutch (Mbiantcha *et al*., 2017), *Bursera simaruba* (Bah *et al*., 2014). Ethyl gallate (**65**) was reported from *Canarium album L* (Zhiyong *et al*., 2008), *Canarium schweinfurthii* (Sokoudjou *et al*., 2020).

Some triterpenoids such as: *β*-amyrinacetate (**67**) was isolated from *Bursera copallifera* (Romero-Estrada *et al*., 2016), *Canarium strictum* (Seethapathy *et al*., 2021), *Canarium schweinfurthii* (Koudou *et al*., 2005), *Protium paniculatum* .(Almeida *et al*., 2015). *β*-amyrin (**68**) has been previously isolated from *D. hopkinsii*, *Trattinnickia burserifolia*, *Trattinnickia rhoifolia* (Lima *et al*., 2004), *Canarium schweinfurthii* (Koudou *et al*., 2005), *Canarium strictum* (Seethapathy *et al*., 2021). Mixture of *α*-and *β*-amyrin (**70**) was isolated from *Canarium luzonicum* (Blume *et al*., 2005). The mixture of *β*-sitosterol and stigmasterol was reported from *D. hopkinsii*, *Trattinnickia burserifolia*, *Trattinnickia rhoifolia* (Lima *et al*., 2004) and the *β*-sitosterol-3-*O*-*β*-*D*-glucopyranoside was isolated from *D. edulis* (Zofou *et al*., 2013).

This work stands as the first report of the isolation of Lichexanthone (**58**), griseoxanthone C (**59**), confluentic acid (**64**), auranthiamide acetate (**63**), glyceryl-1-tetracosanoate (**57**) and 3,3″-di-*O*-methylellagic acid 4-*O*-(3″-galloyl)-*β*-*D*-xylopyranoside (**62**) in the Burseraceae family. Except steroids, the rest of compounds are isolated from *D. edulis* for the first time.

➢ *C. adolphi friderici*

To the best of our knowledge, all the compounds isolated from *C. adolphi friderici* were reported for the first time in this species. Amonst the isolated compounds, vanillin (**53**) was isolated from *Cannabis sativa* (Chen *et al*., 2012). *trans-N*-feruloyloctopamine (**43**), *trans-N*-feruloyltyramine (**44**), and *trans-N*-coumaroyltyramine (**45**) were isolated from *Celtis tournefortii* (Ibrahim., 2019), *Celtis sinensis* (Kim *et al*., 2005), *Celtis africana* (Al-Taweel *et al*., 2012), *Celtis tessmannii* Rendle (Kagho *et al*., 2020). The *β*-sitosterol-3-*O*-*β*-*D*-glucopyranoside was isolated from *Celtis australis* (Filali-Ansari *et al*.,2016). Friedelin (**69**) was isolated from *Celtis tessmannii* Rendle (Kagho *et al*., 2020). *β*-sitosterol-3-*O*-*β*-*D*-glucopyranoside and mixture of *β*-sitosterol and stigmasterol were reported from *Celtis tessmannii* Rendle (Kagho *et al*., 2020).

The presence of dicarboxylic acids azelaic acid (**46**), and sebacic acid (**47**) in the roots of *C. adolphi friderici* was not a surprise since succinic acid has been previously isolated from *Celtis tessmannii* Rendle and reported (Kagho *et al*., 2020). Also the presence of fatty acids was not a surprise since stearic acid was previously isolated from *Celtis tessmannii* Rendle and reported (Kagho *et al*., 2020). These finding enrich the chemical diversity of the *Dacryodes* and *Celtis* genus, and provide evidence for futher chemotaxonomic studies.

II.3 EVALUATION OF BIOLOGICAL ACTIVITIES OF EXTRACTS, FRACTIONS AND PURE COMPOUNDS OBTAINED FROM *D. edulis* AND *C. adolphi friderici*.

Some extracts, fractions and compounds of the two plants were assessed *in vitro* for their antiplasmodial activity and for their cytotoxicity.

II.3.1 Results and discussion of the *in vitro* antiplasmodial activities

The *in vitro* antiplasmodial activities of the methanolic and hydroethanolic extracts, fractions and isolated compounds from leaves and stem bark of *D. edulis*, the acetone extract, and some compounds of *Celtis adolphi-friderici* were evaluated against the chloroquine-sensitive *3D7* and the multidrug-resistant *Dd2* strains of *P. falciparum* by measuring the growth inhibition based on SYBR green fluorescence. Chloroquine (CQ) and artemisinin were used as reference compounds. To classify the antiplasmodial activity express as IC_{50} of tested samples, the following criteria were adopted:

- for $IC_{50} \leq 5$ μg/mL: the activity is considered to be pronounced;
- the activity is good when $5 < IC_{50} \leq 10$ μg/mL;
- the activity is moderate when $10 < IC_{50} \leq 20$ μg/mL;
- the activity is considered to be low when $20 < IC_{50} \leq 40$ μg/mL;

- and it is inactive for IC_{50} > 40 *µg*/mL (Muganza *et al*., 2016).

According to the criteria stated by Muganza and collaborators in 2016 and as shown in Table **39**, both methanolic and hydroethanolic extracts and fractions from the leaves and stem bark of *D. edulis* inhibited the growth of *P. falciparum 3D7* and *Dd2* strains with IC_{50} values ranging from 1.44 to 23.39 *µg*/mL. The methanolic extract **(DEM)** from the stem bark of *D. edulis* displayed good antiplasmodial activity on both *Pf3D7* and *PfDd2* with IC_{50} values of 9.62 and 6.32 *µg*/mL, respectively (table 39). The hydroethanolic leaves extract **(DEF)** from *D. edulis* exhibited pronounced antiplasmodial activity with IC_{50} values of 3.10 and 3.56 µg/mL on both *Pf3D7* and *PfDd2* strains, respectively. The acetone extract from the roots of *C. adolphi friderici* (**CAF**) presented also good activity with an IC_{50} of 6.91 and 6.03 µg/mL on the same strains, respectively. This suggested that, the hydroethanolic extract from leaves of *D. edulis* was the most potent extract than the methanolic extract of the stem bark of the same plant and also than the other extract. The difference observed in the antiplasmodial activity between the two extracts from the same plant could be due to the different mode of extraction or the part of plant used. Besides, four fractions obtained from the methanolic extract of the stem bark and five fractions from hydroethanolic extract of the leaves of *D. edulis* also exhibited good inhibitory activities on *P. falciparum 3D7* and *Dd2* with IC_{50} values of ranged from 1.44 to 23.39 *µg*/mL. Ethyl acetate (**DEA**) and *n*-BuOH (**DEN**) fractions from methanolic extract of the stem bark of *D. edulis* exhibited pronounced antiplasmodial activity on both sensitive and resistant strains [(DEA: IC_{50} value of 3.43 (*Pf3D7*) and 1.44 (*PfDd2*) *µg*/mL; DEN: IC_{50} value of 3.83 (*Pf3D7*) and 3.62 (*PfDd2*) µg/mL)]. Among the fractions from the hydroethanolic extract of leaves of *D. edulis*, hexene fraction (**DFH**) was the only one owing pronounced antiplasmodial activity on both strains (IC_{50} value of 2.70 and 2.98 µg/mL on *Pf3D7* and *PfDd2*, respectively). Overall, the fractionation of both extracts led to some fractions with more potent pronounced activities than the crude extracts. These results could be explained by the fact that, the phytochemical constituents responsible for the antiplasmodial activity in the crude extracts have been concentrated in potent fractions during the fractionation process. In fact, previous studies showed that, fractionation can change positively or negatively the biological properties by concentrating active ingredients into a fraction, or by sharing them between the various one (Nwodo *et al*., 2010). Among the isolated compounds from the both extracts, 3,3'-di-*O*-methylellargic acid (**61**) and ethylgallate (**65**) displayed very good antiplasmodial activity of both *Pf3D7* and *PfDd2*, they are interesting starting point for further structure-activities relationship studies. Interestingly, 3-oxo-lanosta-7,24-Z-dien-26-oid acid (**66**), the mixture of *β*- and *α*-amyrin (**70**), 3,3′,4-tri-*O*-methylellagic acid (**60**), and 3,4-dihydroxybenzoic acid (**55**)

exhibited pronounced to moderate antiplasmodial activity only on multidrug-resistant *Dd2* strain of *P. falciparum* with IC_{50} value ranging from 0.63 to 17.09 μg/mL. However, the mixture of β- and α-amyrin (**70**) and 3,3′,4-tri-*O*-methylellagic acid (**60**) were the more potent compound with IC_{50} values of 3.14 and 0.63 μg/mL, respectively. 3-oxo-lanosta-7,24-*Z*-dien-26-oid acid (**66**) and 3,4-dihydroxybenzoic acid (**55**) displayed moderate ($10 < IC_{50} \leq 20$ μg/mL) antiplasmodial activity. *Trans-N*-feruloyltyramine isolated compounds from the roots of *C. adolphi-friderici* showed an activity with an IC_{50} value of 23.53 and 18.43 μg/mL on *Pf3D7* and *PfDd2*, respectively.

Extracts, fractions and isolated compound of *D. edulis*, were also assessed *in vitro* for their cytotoxicity in order to verify their safety against mammalian cells lines.

The cytotoxicity profile showed that all active extracts, fractions and isolated compounds were non-toxic with cytotoxic concentrations 50 (CC_{50}) above 250 µg / mL for extracts and fractions and 100 µg / mL for isolated compounds. Therefore, these results highlight that *D. edulis* is a source of non-toxic molecules suitable for further investigation toward the search of antimalarial drugs. The Table 39 below summerizes the results of antiplasmodial screening against *Pf3D7* and *PfDd2* and selectivity on Raw cells lines

Table 39: Results of antiplasmodial screening against *Pf*3D7 and *Pf*Dd2 and selectivity on Raw cells lines

Extract and fractions	SYBr Green based assay			Cytotoxicity assay on Raw Cells		
	IC_{50} ± SD (μg/mL)		Resistance Index (RI)	CC_{50} (μg/mL)	SI	
	Pf3D7	***PfDd2***			***Pf3D7***	***PfDd2***
DEM	9.62 ± 0.48	6.32 ± 0.00	0.65	> 250	> 26	> 40
DEF	3.10 ± 0.09	3.56 ± 0.03	1.14	> 250	> 81	> 70
DEH	> 100	23.39 ± 0.30	-	> 250	-	> 11
DEC	1.82 ± 0.72	5.17 ± 0.10	2.84	> 250	> 137	> 48
DEA	3.43 ± 0.01	1.44 ± 0.21	0.41	> 250	> 73	>174
DEN	3.83 ± 0.17	3.62 ± 0.05	0.94	ND	-	-
DFH	2.70 ± 0.64	2.98 ± 0.22	1.31	> 250	> 93	> 84
DFC	16.92 ± 0.76	10.37 ± 0.19	0.61	> 250	> 15	> 24
DFA	3.84 ± 0.22	8.79 ± 0.10	2.28	> 250	65	>28
DFN	10.36 ± 0.98	8.47 ± 0.09	0.81	> 250	> 24	> 30
DFM	8.72 ± 1.28	4.56 ± 0.19	0.52	> 250	> 29	> 55
CAF	6,91± 0.92	6,03± 0.43				
Compounds						
3,3'-di-*O*-methylellargic acid (**61**)	1.17 ± 0.04	1.36 ± 0.14	1.16	> 100	> 85	> 74
3-oxo-lanosta-7,24-Z-dien-26-oid acid (**66**)	> 25	14.21 ± 0.11	-	> 100	-	> 7

Confluentic acid **(64)**	> 25	> 25	-	> 100	-	-
mixture *α*-and *β*- amyrin **(70)**	> 25	3.14 ± 0.09	-	> 100	-	> 32
Griseoxanthone C **(59)**	> 25	> 25	-	> 100	-	-
β-amyrinacetate **(67)**	> 25	> 25	-	> 100	-	-
β-amyrin **(68)**	> 25	> 25	-	ND	-	-
3,3′,4-tri-*O*-methylellagic acid **(60)**	> 25	0.63 ± 0.27	-	> 100	-	159
3,4-dihydroxybenzoïc acid **(55)**	> 25	17.09 ± 0.06	-	> 100	-	> 6
ethyl gallate **(65)**	1.15 ± 0.10	2.86 ± 0.07	2.48	> 100	> 87	> 35
Auranthiamide acetate **(63)**	> 25	> 25	-	> 100	-	-
3,3″-di-*O*-methylellagic acid 4-*O*-(3″-galloyl)-*β*-*D*-xylopyranoside **(62)**	1.86 ± 0.18	1.76 ± 0.14				
3,3'-di-*O*-methylellargic acid **(61)** + ethyl gallate **(65)**	6.82 ± 0.03	1.71 ± 0.09				
Glycerol 1-octadecanoate **(56)**	> 25	> 25				
trans-*N*-feruloyloctopamine **(43)**	> 25	> 25				
trans-*N*-feruloyltyramine **(44)**	23.53 ± 0.02	18.43 ± 0.23				
Allantoin **(51)**	> 25	> 25				
Hydroxybenzoic acid **(54)**	> 25	> 25				
Azelaic acid **(46)**	> 25	> 25				
trans-*N*-coumaroyltyramine **(45)**	> 25	> 25				
Artemisinin (nM)	146.6 ± 0.11	18.90 ± 0.13	0.12	-	-	-
Chloroquine (nM)	4.36 ± 0.53	133 ± 0.16	30.5	-	-	-

DEM : Methanolic extract of the stem bark of *D. edulis*, **DEF** : hydroethanolic extract of the leaves of *D. edulis*, **DEH** : Hexene fraction of DEM, **DEC** : DCM fraction of DEM, **DEA** : AcOEt fraction of DEM, **DEN** : *n*-BuOH fraction of DEM. **DFH** : Hexene fraction of DEF, **DFC** : DCM fraction of DEF, **DFA** : AcOEt fraction of DEF, **DFN** : *n*-BuOH fraction of DEF, **DFM** : methanolic fraction of DEF. CAF : acetone extract of the roots of *C. adolphi friderici*

The antiplasmodial activity of the (1:1) methylene chloride / methanol extract from *D. edulis* have already been reported by Zofou and collaborators (Zofou *et al*., 2013) and showed a significant activity against both Chloroquine-sensitive *3D7* and resistant *Dd2* strains of *P. falciparum* with an IC_{50} value of 4.34 and 6.43 μg/mL, respectively. However, the present study provides the antiplasmodial activity of methanolic stem bark extract and hydroethanolic leaves extract and underscores the fact that, no matter the solvent or the part of plant used; *D. edulis* constitute a powerful source of antiplasmodial compounds. Still in the work conducted by Zofou and collaborators, fractionation of the methylene chloride / methanol (1:1) extract led to the isolation of quercitrin (**3**), afzelin (**2**), quercetin (**1**), methyl 3,4,5-trihydroxybenzoate (**5**) and *β*-sitosterol 3-O-*β*-*D*-glucopyranoside (**4**) which displayed antiplasmodial activities with

IC_{50} values ranged from 0.37 to 18.53 *µg*/mL against both sensitive *3D7* and resistant *Dd2* strains of *P. falciparum*, respectively. This discrepancy in activities might be explained by the different extraction procedures, the part of plant used and the geographical localization of the plant, which is directly link to the quantity and quality of secondary metabolites present in the crude extract (Demain and Fang, 2000).

Knowing that the leaves of *D. edulis* are highly consummed by the population of the West Region of Cameroon, its safetyness was evaluated (Zofou *et al*., 2013).

II.3.2 Acute oral toxicity study of aqueous extract of the leaves of *D. edulis* (DEF)

The study was performed according to the protocol of OECD (2001) guideline 423. The aqueous extract of the leaves of *D. edulis* displayed the following results.

- **Effects on some clinical parameters**

The table **40** below shows the effects of administration in rats of DEF extract at a dose of 2000 mg/kg/BW (body weight) of DEF on some clinical parameters. According to the table below, we note that the plant extract was not harmless or showed no signs of toxicity with regard to the clinical parameters evaluated. Animals receiving the aqueous plant extract did not show any aggressiveness or chills. In addition, animals receiving the plant extract in the same way as normal animals receiving distilled water showed normal stool appearance, sensitivity to sound and touch, and mobility. The administration of the extract in single doses of 2000 mg/kg and 5000 mg/kg, respectively, did not cause any death either during the 24 hours after administration or during the entire duration of the experiment (14 days).

Table 40: Effects of administration in rats of DEF extract at a dose of 2000 mg/kg/BW

Parameters	**Control**			**DEF 2000 mg/kg**			**DEF 5000 mg/kg**		
	30 min	4 Hours	14 Days	30 min	4 Hours	14 Days	30 min	4 Hours	14 Days
Number of deaths	0	0	0	0	0	0	0	0	0
Shiver	-	-	-	-	-	-	-	-	-
Aggression	-	-	-	-	-	-	-	-	-
Mobility	+	+	+	+	+	+	+	+	+
Appearance of faeces	N	N	N	N	N	N	N	N	N
Horripilation	-	-	-	-	-	-	-	-	-
Touch sensitivity	+	+	+	+	+	+	+	+	+
Noise sensitivity	+	+	+	+	+	+	+	+	+

N = normal, + = Present, - = Absent

- **Effects on weight gain**

The figure **99** below shows the effects of the administration of the aqueous extract on the weight gain of rats. According to this figure, there is a non-significant variation in body weight from day 0 to day 14 in normal rats treated with plant extract at different doses of 2000 and 5000 mg/kg compared to those consuming distilled water only.

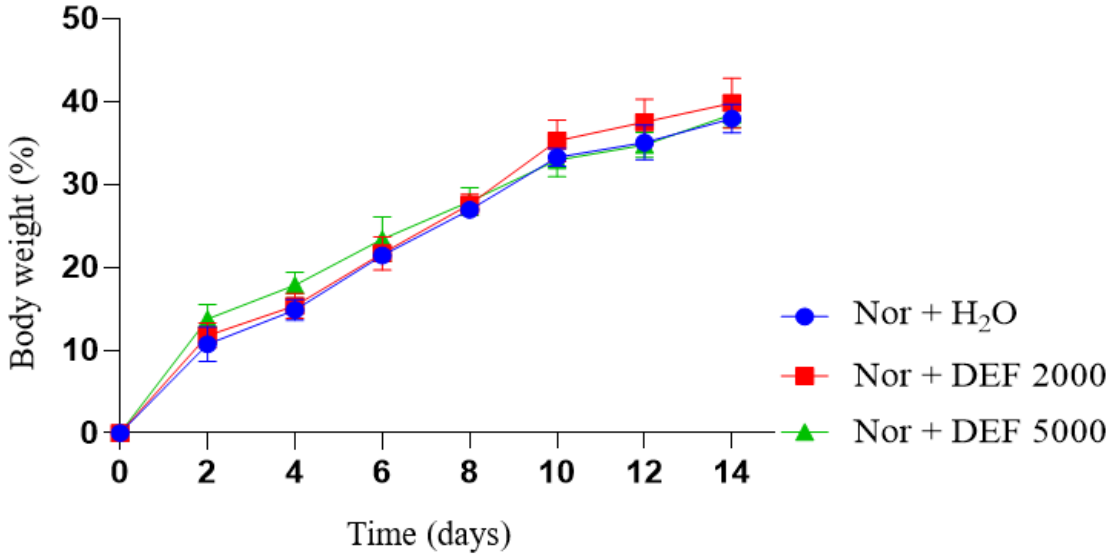

Figure 99: Effects of the aqueous extract of DEF on the weight development in acutely toxic rats

Each value represents the mean ± ESM; n = 3; Nor + H_2O: healthy rats treated with distilled water; Nor + DEF 2000, Nor + DEF 5000: rats treated with aqueous DEF extract at doses of 2000 and 5000 mg / kg, respectively.

- **Effects on the relative mass of certain organs**

The figure **100** below is an illustration of the effects of administration of the extract on the relative mass of the liver, kidney, spleen, heart and lung. According to this figure, the administration of the respective doses of 2000 mg/kg and 5000 mg/kg of plant extracts to the normal rats did not cause any significant variation in the relative mass of the various organs mentioned above for the 14 days of observation in comparison to normal animals that received distilled water.

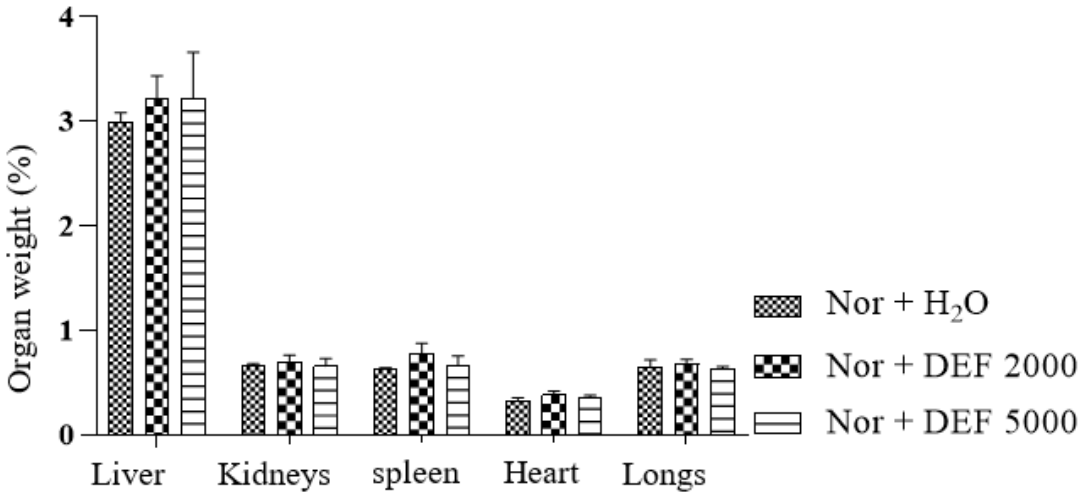

Figure 100: Effects of aqueous DEF extract on the relative weight of organs in acute toxicity

Each value represents the mean ± ESM; n = 3; Nor + H_2O: healthy rats treated with distilled water; Nor + DEF 2000, Nor + DEF 5000: rats treated with aqueous DEF extract at doses of 2000 and 5000 mg/kg, respectively.

The aqueous extract of DEF at the tested limit doses of 2000 and 5000 mg/kg did not cause any death during the 14 days of experimentation, indicating that the Lethal Dose 50 (LD_{50}) of this extract is greater than 5000 mg/kg. Furthermore, no apparent sign of toxicity, on the behavior of the animals, on their general physical appearance, on their body weight, as well as on the relative weight of the organs involved in the toxicity were noted. Moreover slight differences in color observed on the macroscopic appearance of the organs after dissection are believed to be due to the specific physiology of each animal. Indeed, WHO has shown that almost all medicinal plants are non-toxic due to their regular and common use in traditional pharmacopoeia (WHO, 2000). Our results are in close agreement with the WHO data suggesting that the aqueous extract of DEF would be classified according to the Globally Harmonized Classification System (SCGH) in category 5 of substances of little or no toxicity (OECD, 2001).

II.3.3 Other biological activities on *C. adolphi friderici*

In order to find other potentialities of *C. adolphi friderici*, we performed other biological activities

Among the compounds isolated from *C. adolphi friderici*, only 10 including eloundemnoside (**42**), azelaic acid (**46**), indole 3-carboxaldehyde (**48**), laceroic acid (**49**), heptacosanoic acid (**50**), allantoin (**51**), vanillin (**53**), hydroxybenzoic acid (**54**), friedelin (**69**), glycerol 1-octadecanoate (**56**) were assessed for the following activities.

- **Urease inhibition assay**

The 10 compounds were screened *in vitro* for urease inhibitory properties as depicted in Table 41. The IC_{50} values of the tested compounds were ranged from 15.3 to 100.0 μM, with friedelin **(69)** (IC_{50} value 15.3 μM) being the most active compound as compared to thiourea used as standard (IC_{50} value 21.6 μM).

- **DPPH radical scavenging assay**

In this assay, the tested compounds were screened *in vitro* for their antioxidant activity against DPPH radical scavenging as depicted in Table 41. The IC_{50} values of these compounds were ranged from 13.2 to 68.5 μM, with azelaic acid (**46**) (IC_{50} value 13.2 μM) being the most active compound compare to BHA (IC_{50} value 44.2 μM).

- **Lipoxygenase inhibition assay**

Tested compounds were screened *in vitro* for their lipoxygenase inhibitory properties as shown in Table 41. The IC_{50} values of all the tested compounds were ranged from 16.3 to 100.0 μM. Azelaic acid **(46)** (IC_{50} = 16.3 μM) was more active than the standard baicalein (IC_{50} value 22.6 μM).

- **Butyrylcholisnesterase inhibition assay**

All the tested compounds exhibited moderate activity with IC_{50} values ranged from 45.2 to 100.0 μM. Eserine was used as reference drug (IC_{50} 7.8 μM). It was reported in the literature that N-*p*-coumaryltyramine isolated from the twigs of *C. chinensis* showed weak AChE inhibitory activity with IC_{50} value of 122 μM (Natarajan *et al*., 2009). The table 41 below resumes these biological activities.

Table 41: Antioxidant activity, lipoxygenase, urease and butyrylcholinesterase inhibition of compounds from *C. adolphi-friderici Engl*..

Compounds	**Antioxidant IC_{50} (μM)**	**Lipoxygenase inhibition IC_{50} (μM)**	**Urease inhibition IC_{50} (μM)**	**Butrylcholinesterase inhibition IC_{50} (μM)**
Eloundemnoside (**42**)	59.1 ± 0.32	>100	38.5 ± 0.19	66.6 ± 0.92
Friedeline (**69**)	55.2 ± 0.42	>100	15.3 ± 0.77	62.3 ± 0.21
Heptacosanoic acid (**50**)	22.2 ± 0.21	39.4 ± 0.28	>100	45.2 ± 0.73
Glycerol 1-octadecanoate (**56**).	58.2 ± 0.29	>100	31.2 ± 0.82	61.1 ± 0.51
vanillin (**53**)	29.3 ± 0.48	35.2 ± 0.21	Nil	>100
Azelaic acid (**46**)	13.2 ± 0.41	16.3 ± 0.26	Nil	>100

Indole 3-carboxaldehyde (**48**)	55.2 ± 0.24	46.2 ± 0.42	71.4 ± 0.06	>100
Hydroxybenzoic acid (**54**)	58.2 ± 0.72	79.5 ± 0.09	Nil	>Nil
Laceroic acid (**49**)	59.9 ± 0.88	69.8 ± 0.11	Nil	>100
Allantoin (**51**)	56.5 ± 0.36	59.1 ± 0.26	50.2 ± 0.21	>100
BHA	44.2 ± 0.06	-	-	-
Baicalein	-	22.6 ± 0.08	-	-
Thiourea	-	-	21.6 ± 0.12	-
Eserine	-	-	-	7.8 ± 0.43

Nil : no result was observed for these sample

II.4 PRE-FORMULATION ASSAY

The objective of this work was to develop a phytomedicine with active ingredient from the plants. The evaluation of the activities of the crude extracts of different parts of the two plants studied (evaluation of the antiplasmodial activities and the acute toxicity) having led to interesting results, it seemed judicious to us to attempt a pre-formulation from the most active extract.

After carrying out the *in vitro* tests on the *p. falciparum* strains, the results obtained showed that the hydroethanolic leaves extract from *D. edulis* was a good candidates for the pre-formulation of a phytomedicine. Thus, to evolve in the ingredient selection process acute toxicity test were first performed as well as *in vivo* tests. At the end of these tests, the extract showed no sign of toxicity. To optimize the use of our plant material, we have formulated our phytomedicine using the smallest curative dose (2.08 mg / mL). The protocol used is that of Reagan-Show and collaborators, set up in 2007, entitled “Dose translation from animal to human studies revisited”. The following formula was used:

Formula for Dose Translation Based on BSA

$$\textbf{HED (mg/ kg) = Animal dose (mg/ kg)} \times \frac{\textbf{Animal Km}}{\textbf{Human Km}}$$

In the present case, animal dose was 2.08 mg/ mL. From the above formula, the Km factor is constant and known. The animal Km varies from one animal to another according to the species (Km of rat is 6 while the human Km is 37 for adult and 25 for child). Our phytodrug has been pre-formulated as a syrup (Reagan-Shaw S et al., 2007), with the consumable doses evaluated as follows. This operation has several steps:

1er step : Human effective dose calculation

HED = 2.08 × 6/ 25 = 0.499 mg/ kg.

2nd step : Calculation of the daily dose for a child

D = HED × 20 = 0.499 × 20 = 9.984 mg/ day (20 represents the average weight of a child)

3th step : Preparation of simple syrup

The standard formula for a syrup saturated is 6.7 g of sugar for 3.3 g of water. This mixture represents a total of 10 g of simple syrup. It is advisable to use demineralized or deionized water.

4th step : Determination of quantity of each ingredient

- **Extract (active ingredient)**

The daily dose is 9.984 mg for an adult. The normal concentration of the active ingredient is 1.3 mg/ mL. One teaspoon is 15 mL; i.e. a concentration of 19.5 g/15 mL. For this extract, the following was applied 9.984/3 = 3.328 mg (per dose);

(3.328/ 19500) × 100 = 0.017% of active ingredient per spoon.

- **Conservator or stabilizer (Sodium benzoate)**

It is advisable to vary the percentage of stabilizers in order to determine which stabilizes the product over a long period. This percentage varies between 0.05 and 0.5%.

- **For orange essence:** The percentage is standard for essences and is 0.5%.
- **For Aroma:** The percentage is also standard for aromas and is 0.1%.
- **Simple syrup:**

Its percentage is deducted from the percentages of the other ingredients:

% syrup = 100% - (% extract +% stabilizer +% orange essence +% flavor)

= 100% - (1.3179% + 0.3% + 0.5% + 0.1%)

= 97.8

So, in 100 mg of phytomedicine, 97.8 mg of saturated simple syrup (excipient), 1.3179 mg of crude extract (active principle), 0.3 mg of sodium benzoate (preservative), 0.5 mg of orange oil (ingredient) and 0.1 mg of flavor (ingredient) are used.

The figure 101 below is a pre-formulation of a phytodrug against malaria using the hydroethanolic extract of the leaves of *D. edulis* as the active ingredient.

Figure 101: Pre-formulation of a phytodrug against malaria

CONCLUSION AND PERSPECTIVES

The aim of this work was to obtain active and less toxic extracts and/or fractions which can be use as a raw material for the preparation of phytomedicines and to isolate their secondary metabolites that can be used as leads for the development of new drugs against malaria.

Chemical investigation on the two species led to the isolation of thirty-one compounds which were sorted into 16 classes of compounds including:

- 1 new cerebroside named: eloundemnoside;
- 5 triterpenoids including *β*-amyrin, *β*-amyrinacetate, 3-oxo-lanosta-7,24*Z*-dien-26-oid acid, friedelin and mixture of *β*- and *α*- amyrin;
- 2 steroids including the mixture of *β*-sitosterol and stigmasterol, and *β*-sitosterol-3-*O*-*β*-D-glucopyranoside
- 2 xanthones including lichexanthone, and griseoxanthone C;
- 3 ellagic acid derivatives among which 3,3'-di-*O*-methylellagic acid, 3,3′,4-tri-*O*-methylellagic acid, and 3,3″-di-*O*-methylellagic acid 4-*O*-(3″-galloyl)-*β*-D-xylopyranoside;
- 1 depside, confluentic acid;
- 2 dicarboxylic acids among which azelaic acid, and sebacic acid;
- 3 phenolic compounds including 3,4-dihydroxybenzoic acid, vanillin, and hydroxybenzoic acid;
- 3 phenolic amides among which *trans*-*N*-feruloyloctopamine, *trans*-*N*-feruloyltyramine, and *trans*-*N*-coumaroyltyramine;
- 1 auranthiamide acetate;
- 2 triglyceryl including glyceryl-1-tetracosanoate, and glycerol 1-octadecanoate;
- 2 fatty acids including heptacosanoic acid, and laceroic acid;
- 1 gallic acid derivative, ethyl gallate;
- 1 indolic alkaloid, indole 3-carboxaldehyde;
- 1 carbamide, allantoin;
- 1 amino acid, aspartic acid.

It is important to note that except for steroids, the rest of compounds are isolated from *D. edulis* for the first time. Compounds isolated from *C. adolphi-friderici* are obtained for the first time from that species. Lichexanthone, griseoxanthone C, confluentic acid, auranthiamide acetate, glyceryl-1-tetracosanoate and 3,3″-di-*O*-methylellagic acid 4-*O*-(3″-galloyl)-*β*-*D*-xylopyranoside are reported in the Burseraceae family for the first time. Crude extracts,

fractions and some isolated compounds were tested against the Chloroquine-sensitive *3D7* and the multidrug-resistant *Dd2* strains of *P. falciparum*.

The methods used for the fractionation and the isolation of the compounds were mainly liquid-liquid partition and column chromatography. Structure elucidation was achieved mainly by NMR spectroscopy including 1D (^{1}H and ^{13}C) and 2D NMR (COSY, HMQC, HSQC, HMBC and NOESY) and high-resolution mass spectrometry.

Extracts, fractions and compounds were screened for their antiplasmodial activities and the results are as followed:

Methanolic extract of the stem bark of *D. edulis* displayed good antiplasmodial activity both on *Pf3D7* and *PfDd2* with the IC_{50} values of 9.62 and 6.32 μg/mL, respectively and the hydroethanolic leaves extract from *D. edulis* exhibited pronounced antiplasmodial activity with IC_{50} values of 3.10 and 3.56 μg/mL, respectively on the same strains. The roots of *C. adolphi-friderici* showed antiplasmodial activity both on *Pf3D7* and *PfDd2* with IC_{50} values of 6.91 and 6.03 μg/mL, respectively. The EtOAc fraction of the stem bark extract exhibited the best activity (IC_{50} = 1.44 μg/mL) among other fractions from the stem bark and led to isolation of the most active compound: 3,3′,4-tri-*O*-methylellagic acid (IC_{50} = 0.63 μg/mL) on *Dd2* stain. The *n*-hexane fraction of the hydroethanolic extract of the leaves exhibited the best activity (IC_{50} = 2.70 and 2.98 μg/mL on *3D7* and *Dd2* strain, respectively) among other fractions from the leaves. The most active compound was ethylgallate with an IC_{50} = 1.15; 2.86 μg/mL on *Dd2* and *3D7* strain (EtOAc fraction). These biological results confirmed the uses of *D. edulis* in traditional medicine against malaria. *Trans-N*-feruloyltyramine isolated compounds from *C. adolphi-friderici* showed an activity with an IC_{50} value of 23.53 and 18.43 μg/mL on *Pf3D7* and *PfDd2* respectively.

Acute oral toxicity study of aqueous extract of the leaves of *D. edulis* was performed in order to verify its safety. The extract was found to display no toxicity. A preformulation of an antimalarial syrup was performed based on the above promising results. In our future studies, we will:

- Do some chemical reactions to increase the activity of most active compounds (gallic and ellagic acid derivative)
- Explore other varieties of *Dacryodes edulis* in order to confirm their activity
- Do some additional analysis on the pre-formulated phytomedicines (in vitro and in vivo studies).

CHAPTER III: GENERAL EXPERIMENT

III.1 GENERALITY

III.1.1 Chromatography techniques

The methods used for the isolation of compounds were mainly column chromatography and thin layer chromatography.

III.1.1.1 Thin layer chromatography

Analytical thin layer chromatographies were performed on 60 F254 silica gel plates (Merck, 20 cm × 20 cm) on 0.2 mm thick aluminum sheets, or SIL G / UV_{254} (POLYGRAM, 40 × 80 mm) on plastic sheets 0.2 mm thick. TLC plates were revealed, either by using ultra violet light (254 and 366 nm) or by treatment (spraying) with a developer solution, which can be either a 50% dilute sulfuric acid solution or a solution of cerium sulphate [Saturated solution of cerium sulphate (10%) in sulfuric acid (15%) and 75% (water + ice)], vanillin (1 g of powdered vanillin dissolved in 100 mL of ethanol, add 2 mL of concentrated sulfuric acid dropwise).

III-1.1.2 Column chromatography

For column chromatography, silica gel with a particle size of 70-230 μm or 230-400 μm (Merck) and Sephadex LH-20 were used as stationary phase. The diameter of the column and the height of the stationary phase were chosen according to the amount of extract or product to be treated.

III.1.2 Physico-chemical methods and apparatus

III.1.2.1 Mass spectra

The low and high resolution electron impact mass spectra (ionization energy: 70 eV) were obtained on JOEL JMS-600H-1 type spectrometers and the high resolution mass spectra were obtained with a QTOF spectrometer (Bruker, Germany) equipped with an ESI source with an HR instrument.

III.1.2.2 Nuclear Magnetic Resonance (NMR)

The ^{1}H and ^{13}C-NMR spectra were recorded on Bruker Avance- AV-400 MHz devices operating at 400 MHz (^{1}H) and 100 MHz (^{13}C), Bruker Avance AV-600 MHz operating at 600 MHz (^{1}H) and 150 MHz (^{13}C), Bruker DRX 500 MHz operating at 500 MHz (^{1}H) and 125 MHz (^{13}C) and 600 MHz operating at 600 MHz (^{1}H) and 150 MHz (^{13}C) NMR spectrometers (Bruker Corporation, Brussels, Belgium). The products were dissolved in deuterated chloroform, acetone, methanol, dimethylsulfoxide, pyridine and water. Chemical shifts (δ) were given in parts per million (ppm) with reference to the tetramethylsilane (TMS) signal as an internal standard, while coupling constants (*J*) were measured in Hertz.

III.1.2.3. Instruments

A JASCO 320-A spectrophotometer (ν_{max} in cm^{-1}) was used for scanning IR spectroscopy using KBr pellets.

Ultraviolet spectra were recorded on a Hitachi UV 3200 spectrophotometer (λmax in nm) using methanol as solvents.

Melting points were measured using the Büchi apparatus (Büchi melting point M-560).

III.1.3 Chemical characterization tests

III.1.3.1 Ferric chloride test

To a methanolic solution of the product, add a few drops of a solution of ferric chloride. The presence of phenols is manifested by the change in color to purple or blue following the formation of a complex ion $[Fe(ArO)_6]^{3-}$.

III.1.3.2 Liebermann-Burchard test

A few milligrams of product are dissolved in dichloromethane (1 ml) and to the resulting solution a few drops of acetic anhydride are added, followed by a few drops of concentrated sulfuric acid. Terpenoids appear as a purplish red color and sterols give a bluish green color.

III.1.3.3 Molish test

In a test tube, dissolve a few milligrams of the product in a solution of 1% ethanol-α-naphthol. Then let a few drops of concentrated sulfuric acid run down the sides of the tube. The presence of sugars is manifested by the appearance of a purplish red ring at the interphase.

III.1.3.4 $NaHCO_3$ (sodium bicarbonate)

The purpose of this test is to identify carboxylic acids. The reagent used is $NaHCO_3$. A small amount of the compound was dissolved in $NaHCO_3$. The presence of carboxylic acid is characterized by the complete dissolution of the product with release of CO_2. CO_2 is evidenced by cloudiness in lime water. The CO_2 discolors the filter pare soaked in an aqueous solution of purple $KMnO_4$

III.2. EXTRACTION AND ISOLATION

III.2.1. Plant material

III.2.1.1 *Celtis adolphi-friderici Engl*

The roots of *C. adolphi-friderici* were harvested in December 2013 at Mount Eloumdem (Yaoundé, Central Cameroon Region). It was identified by Mr NANA Victor, botanist at the National Herbarium of Cameroon where a reference sample was deposited under the number HNC 41571.

III.2.1.2 *Dacryodes edulis* (G.Don)

The leaves and stem bark of *D. edulis* were collected in April 2018 in Batcham village, West Region of Cameroon and identified at the National Herbarium in Yaoundé (where a voucher specimen was deposited under the reference N° 45713 HNC) by Mr. NANA Victor; botanist.

III.2.2 EXTRACTION

III.2.2.1 Preparation of extract from *C. adolphi friderici Engl*

About 1.5 kg of the air-dried and ground wood roots of *C. adolphi-friderici* were macerated with acetone (2×10 L) (72 hours, repeated three times) at room temperature. The extract was and freed from solvent under vacuum at low temperature to give 70.1 g of black-brown crude extract. The crude extract was dried in a hood.

III.2.2.2 Preparation of extracts from *D. edulis* (G.Don)

The air-dried stem bark (4.5 kg) and leaves (1.5 kg) of *D. edulis* were powdered and macerated (thrice at room temperature, within 72 hours and 15 L solvent) with MeOH and ethanol-water (70-30) respectively. The filtrate was evaporated to give 239.8 and 205.5 g of methanol and hydroethanol extract of leaves and stem bark, respectively.

III.2.3 Isolation of compounds

III.2.3.1 Isolation of compounds from *C. adolphi-friderici Engl.*

A liquid-liquid partitioning was then performed on the crude extract (which was dissolved in the mixture of MeOH-H_2O) (70.1 g) with solvents (*n*-hexane, methylene chloride, ethyl acetate and residue) to yield four different fractions (F_1-F_4). Where F1 is the *n*-hexane fraction (24.4 g), F2 stands for methylene-chloride fraction (15.0 g), F3 for ethyl acetate fraction (17.5 g) and F4 for the residue (10.3 g). F1, F2 and F3 were subjected to column chromatography over silica gel (Merck, 230-400 mesh) and no further work was done on F4. This work led to the isolation of 15 compounds.

III.2.3.1.1 Column chromatography of fraction F1 from *C. adolphi friderici Engl*

The *n*-hexane soluble fraction F1(24.4 g) was subjected to CC over silica gel (Merck, 230-400 mesh) eluting with *n*-hexane, the mixture of *n*-hexane-EtOAc (9.8:0.2-0:1, v/v), EtOAc, and EtOAc-MeOH (1:9, v/v) of increasing polarities. Fractions of 500 mL were collected to afford 4 compounds. They were grouped using TLC profiles. The table **42** below resumes these results.

Table 42: Chromatogram of fraction F1

Eluent	Fractions Nº	Observations	Compounds
n-hexane	1-17	Oily mixture of about 3 compounds	-
n-hexane- EtOAc 2-20%	18-110	Mixture of 4 compounds with one major compound	**DF8** (50.1 mg) , **CAF1** (7.5 mg) and **CAF3** (10.1 mg)
n-hexane- EtOAc 25-75%	111-220	Mixture of about 6 compounds with 2 fluorescent compounds	**CAF4** (3.3 mg), **DF1** (5.5 mg)
n-hexane- EtOAc 80%-EtOAc-MeOH 5%	221-245	Mixture of about 3 compounds	**CAF2** (40.3 mg)

III.2.3.1.2 Column chromatography of fraction F2 from *Celtis adolphi friderici Engl*

The dichloromethane soluble fraction (15.0 g) was subjected to CC over silica gel (Merck, 230-400 mesh) eluting with CH_2Cl_2, the mixture of DCM-MeOH (0.5:99.5-0:1, v/v) of increasing polarities. Fractions of 500 mL were collected and grouped using TLC profiles to give three major subfractions A1 (4.1 g), A2 (3.6 g) and A3 (2.06 g). The table 43 below summarizes these results.

Table 43: Chromatogram of fraction F2

Eluent	Fractions Nº	Observations	Compounds
100% DCM	1-77	Mixture of about 5 compounds	**CAF11** (3.2 mg)
DCM -MeOH 0.5-1.5%	78-191	Mixture of about 7 compounds visible with iodine	**CAF14** (46.1 mg), **CAF7** (18.2 mg), **CAF8** (15.4 mg), **CAF9** (40.1 mg)
DCM -MeOH 2-4%	192-259	Complex mixture with one major compound	**DF1** (10.0 mg)
DCM -MeOH 5-9 %	260-294	Mixture of about 3 compounds	**CAF2** (10.5 mg)
DCM -MeOH 12-15%	295-308	Complex mixture	-
MeOH	309	Complex mixture	-

III.2.3.1.3 Column chromatography of sub-fraction A1 from DCM fraction

The subfraction A1 (4.1 g) was subjected to CC and eluted with the mixtures of *n*-hexane/CH_2Cl_2 of increasing polarities (1:1-0:1, v/v). Fractions of 50 mL were collected to

afford 1 compound; they were and grouped using TLC profiles. The fractions obtained with *n*-hexane/ DCM 70 – 80 % was grouped, evaporated and traited with a mixture of *n*-hexane/ DCM (40/10) to afford compound CAF 10 as a white powder, soluble in DCM. The table 44 below summarizes these results.

Table 44: Chromatogram of fraction A1

Eluent	Fractions Nº	Observations	Compounds
n-hexane/ DCM 50 – 60 %	1-10	Mixture of about 3 compounds	-
n-hexane/ DCM 70 – 80 %	11-23	Mixture of about 3 compounds	**CAF10** (1.5 mg).
n-hexane/DCM 90%– DCM 100%	24-32	Complex mixture	-

III.2.3.1.4 Column chromatography of sub-fraction A2 from DCM fraction

Also, the subfraction A2 (3.6 g) was eluted using an isocratic mixture of *n*-hexane/DCM (1:1). Fractions of 50 mL were collected to afford 2 compounds. They were grouped using TLC profiles, evaporated and traited with a mixture of *n*-hexane/ DCM (40/10) to afford compound CAF 11 and 12 as a white powder and white oil respectively, soluble in chloroform. The table 45 below summarizes these results.

Table 45:Chromatogram of fraction A2

Eluent	Fractions Nº	Observations	Compounds
n-hexane/ DCM 50 %	1-16	Mixture of about 3 compounds	**CAF11** (3.5 mg) and **CAF12** (2.5 mg).

III.2.3.1.5 Column chromatography of sub-fraction A3 from DCM fraction

The subfraction A3 (2.06 g) was equally subjected to CC over silica gel 230-400 mesh (Merck), eluted with *n*-hexane/CH_2Cl_2 mixtures (4:6-0:1, v/v) and CH_2Cl_2/MeOH (9:1-95:5, v/v). Fractions of 50 mL were collected, grouped using TLC profiles. The fractions obtained with *n*-hexane/ DCM 60 – 90 % was traited to afford compounds CAF 5 and 13 as a white powder, soluble in DCM and MeOH+$CDCl_3$. The table 46 below summarizes these results.

Table 46: Chromatogram of fraction A3

Eluent	Fractions Nº	Observations	Compounds
n-hexane/ DCM 60-70 %	1-17	Mixture of about 3 compounds with one major compound	**CAF5** (1.4 mg)
n-hexane/ DCM 80-90 %	18-28	Mixture of about 3 compounds with one major compound	**CAF5** (1.0 mg)
100% DCM -DCM-MeOH 5 %	29-41	Complex mixture	**CAF13** (1.2 mg)

III.2.3.1.6 Column chromatography of fraction F3 from *Celtis adolphi-friderici Engl*

The ethyl acetate fraction F3 was subjected to CC over silica gel (Merck, 230-400 mesh) eluting with the mixtures of CH_2Cl_2/MeOH (1:0-0:1, v/v). Fractions of 500 mL were collected to afford 4 compounds; they were grouped using TLC plates. The table 47 below summarizes these results.

Table 47: Chromatogram of fraction F3

Eluent	Fractions Nº	Observations	Compounds
DCM 100%	1-22	Oily mixture	-
DCM-MeOH 2-3%	23-75	Mixture of about 4 compounds	**CAF14** (10.2 mg), **CAF7** (2.6 mg)
DCM-MeOH 4-6%	76-127	Complex mixture with two majors compounds	**CAF16** (4.1 mg), **CAF13** (1.0 mg), **CAF15** (3.1 mg)
DCM-MeOH 8-15%	128-140	Complex mixture	-
MeOH	141	Complex mixture	-

III.2.3.2 Isolation of compounds from MeOH extract of the stem bark of *D. edulis*

239.8 g of crude extract were subjected to liquid-liquid partition using *n*-hexane, dichloromethane, EtOAc and *n*-BuOH to afford 4 fractions labeled DEH (25.5 g), DEC (5.3 g), DEA (40.5 g) and DEN (110.7 g).

III.2.3.2.1 Column chromatography of hexane fraction from the stem bark of *Dacryodes edulis*

The *n*-hexane extract (25.5 g) of the stem bark was subjected to silica gel flash column chromatography and eluted with *n*-hexane-DCM gradient [100:0 to 0:100], DCM-EtOAc [100:0 to 0:100], EtOAc-MeOH [100:0 to 0:100] to give 79 fractions of 250 mL each. These

fractions were combined into four main fractions [A (1–22), B (23–39), C (40–63) and D (64-79)] based on their LC-MS profiles. Subfraction A (8.9 g) was subjected to CC over silica gel and eluted with *n*-hexane/DCM (1:0→0:1) to afford *β*-amyrin acetate (5.7 mg) and *β*-amyrin (8.4 mg). Subfraction B (7.1 g) was subjected to CC over silica gel and eluted with *n*-hexane/DCM (1:0→0:1) to yield compounds griseoxanthone C (9.4 mg) and the mixture of *α*,*β*-amyrin (50.9 mg). Subfraction C (10.4 g) was subjected to silica gel column chromatography (CC) and eluted with *n*-hexane/DCM (1:0→0:1) to give 3-oxo-lanosta-7,24-Z-dien-26-oid acid (10.5 mg) and confluentic acid (6.0 mg). The (1:1) mixture of *β*-sitosterol and stigmasterol (20.8 mg) was obtained from the subfraction D (10.4 g) which was subjected to silica gel column chromatography (CC) and eluted with *n*-hexane/DCM (1:0→0:1).

Table 48: Chromatogram of the *n*-hexane fraction from the stem bark of *D. edulis*

Eluent	Fractions Nº	Observations	Compounds
n-Hexane	A (1–22)	Oily mixture of compounds	-
n-Hex- DCM 5-50%	B (23–39)	Mixture of about 5 compounds	**DE16** (8.4 mg), **DE14** (5.7 mg), **DE8** (50.9 mg), **DF8** (15.6 mg)
n-Hex-DCM 60% - CH_2Cl_2-EtOAc 80%	C (40–63)	Mixture of about 6 compounds	**DE5** (10.5 mg), **DE10** (9.4 mg), **DE7** (6.0 mg)
EtOAc 100%-EtOAc –MeOH- MeOH 100%	D (64-79)	Complex mixture	-

III.2.3.2.2 Column chromatography of dichloromethane fraction from the stem bark of *Dacryodes edulis*

The DCM fraction (5.3 g) was subjected to CC over silica gel (Merck, 230-400 mesh) and eluted with *n*-hexane, the mixtures of *n*-hexane-EtOAc, and EtOAc-MeOH of increasing polarities to yield 3 compounds: lichexanthone (3.1 mg), 3, 3'-*O*-dimethylellagic acid (3.7 mg) and *β*-sitosterol-3-*O*-*β*-D-glucopyranoside (9.4 mg).

Table 49: Chromatogram of the DCM fraction from the stem bark of *D. edulis*

Eluent	Fractions Nº	Observations	Compounds
n-Hex 100% - *n*-Hex-EtOAc 30%	A (1–15)	Mixture of about 3 compounds	**DE2** (3.1 mg), **DF8** (13.4 mg)
n-Hex-EtOAc 40% - Hex- EtOAc 80%	B (16–22)	Mixture of about 5 compounds	**DE3** (3.7 mg)

EtOAc 100% - EtOAc-MeOH 50%	C (23-30)	Mixture of about 6 compounds	**DF1** (9.4 mg)
MeOH 100%	D (31)	Complex mixture	-

III.2.3.2.3 Column chromatography of EtOAc fraction from the stem bark of *Dacryodes edulis*

The EtOAc fraction (40.5 g) was subjected to CC over silica gel and eluted with *n*-hexane/EtOAc (1:0→0:1) and EtOAc/MeOH (1:0→0:1) to give 120 fractions of 100 mL each. These fractions were combined into four main fractions [A (1–24), B (25–63), C (64–100) and D (101-120)] based on their LCMS profiles. Subfraction B (8.5 g) was subjected to CC over silica gel and eluted with DCM-MeOH (1:0→0.8:0.2) to yield compound 3,3′,4-tri-*O*-methylellagic acid (50.0 mg). Subfraction C (5.1 g) was subjected to CC over silica gel and eluted with DCM-MeOH (1:0→1:0) to afford compounds 3,3″-di-*O*-methylellagic acid 4-*O*-(3″-galloyl)-*β*-D-xylopyranoside (6.7 mg) and 3,4-dihydroxybenzoic acid (6.5 mg).

Table 50: Chromatogram of the EtOAc fraction from the stem bark of *D. edulis*

Eluent	Fractions Nº	Observations	Compounds
n-Hex 100% - *n*-Hex-EtOAc 30%	A (1–24)	Mixture of oils	-
Hex-EtOAc 40% - Hex- EtOAc 80%	B (25–63)	Mixture of about 5 compounds	**DE4** (50.0 mg)
EtOAc 100% - EtOAc-MeOH 50%	C (64-100)	Mixture of about 6 compounds	**DE21** (6.7mg), **DE22** (6.5 mg)
MeOH 100%	D (101-120)	Complex mixture	-

III.2.3.2.4 Isolation of compounds from hydroethanolic extract of the leaves of *Dacryodes edulis*

205.5 g of hydroethanolic extract were subjected to liquid-liquid partition using *n*-hexane, dichloromethane, EtOAc and *n*-BuOH to afford 4 fractions labeled DFH (25.7 g), DFC (17.5 g), DFA (20.3 g) and DFM (102.3 g). Fractions of the hydroethanolic extract of the leaves followed the same process of purification of compounds.

III.2.3.2.4.1 Column chromatography of EtOAc fraction from the leaves of *D. edulis*

The EtOAc fraction (20.3 g) was subjected to CC over silica gel and eluted with *n*-hexane/EtOAc (1:0→0:1) and EtOAc/MeOH (1:0→0:1) to give 64 fractions of 100 mL each. These fractions were combined into four main fractions [A (1–20), B (21–43), C (44–60), and D (61-64)] based on their LC-MS profiles. Subfraction A (50 mg) was subjected to CC over

silica gel and eluted with *n*-hexane/EtOAc (1:0→0:1) to yield compound ethyl gallate (3.1 mg). Subfraction B (1.2 g) was subjected to CC over silica gel and eluted with *n*-hexane/EtOAc (1:0→1:0) to afford glyceryl-1-tetracosanoate (4.9 mg), and auranthiamide acetate (3.4 mg).

Table 51: Chromatogram of the EtOAc fraction from the leaves of *D. edulis*

Eluent	Fractions Nº	Observations	Compounds
n-Hex 100% - *n*-Hex-EtOAc 40%	A (1–20)	Mixture of 3 compounds	**DF6** (3.1 mg)
n-Hex-EtOAc 40% - Hex-EtOAc 80%	B (21–43)	Mixture of about 6 compounds	**DF5** (4.9 mg), **DF3** (3.4 mg)
EtOAc 60% - EtOAc-MeOH 50%	C (44-60)	Mixture	-
EtOAc- MeOH 50% - MeOH 100%	D (61-64)	Complex mixture	-

III.3 CHEMICAL TRANSFORMATION

1- Methanolysis of CAF2

Compound **CAF2** (10.2 mg) was refluxed with 5 mL solution of 5% HCl in MeOH at 70°C for 12 h. The reaction was monitored by TLC. On completion of the reaction, the solution was extracted with *n*-hexane. The *n*-hexane layer (5.2 mg) was separated and concentrated for further analysis using GC-MS, to yield methyl 2-hydroxytetracosanoate (*m/z* 398 $[M]^+$) (Bankeu *et al*., 2017).

III.4 EVALUATION OF BIOLOGICAL ACTIVITIES

1- P. falciparum growth inhibition assay

- ***In vitro cultivation of P. falciparum***

The chloroquine-sensitive (*Pf3D7*-(MRA-102)) and chloroquine-resistant (*PfDd2*) of *P. falciparum* strains was cultured in fresh O^+ human red blood cells at 4% haematocrit in complete RPMI 1640 medium [500 mL RPMI 1640 (Gibco, UK) supplemented with 25 *m*M HEPES (Gibco, UK), 0.50% Albumax I (Gibco, USA), 1X hypoxanthine (Gibco, USA) and 50mg/mL gentamicin (Gibco, China)] and incubated at 37°C in a humidified atmosphere with 5% CO_2. The medium was replaced with fresh complete medium daily to propagate the culture. Giemsa-stained thin blood smears were examined microscopically under immersion oil to monitor cell-cycle transition and parasitaemia evolution.

- ***Synchronization of parasite culture***

Before each experiment, synchronized ring stage parasite was obtained by 5% sorbitol (w/v) treatment in respect to Lambros and Vanderberg, 1979. It is important to note that, the use of synchronized cultures over mixed stage cultures can enable the test molecules to interact with all the three stages (ring, trophozoite and schizont) of the 48 hours long life cycle of *P. falciparum* in culture. Moreover, starting the experiment with synchronized ring stage culture provides the distinct advantage of observing growth inhibitory effects without a rise in parasitemia during the ring-trophozoite-schizont transitions.

- ***SYBR green I-based fluorescence assay***

Drug sensitivity assay was carried out in 96-well microtitration plates using SYBR green I based fluorescence assay (Smilkstein *et al*., 2004). This assay specifically based on the ability of SYBR green to give strong fluorescence only in the presence of parasite DNA during cell proliferation. The absence of nucleus in human red blood cells where the malarial parasite proliferates allows the use of SYBR green for the specific monitoring of the growth of malarial parasite.

Sorbitol-synchronized ring stage parasites (haematocrit: 1%, parasitaemia: 2%, 90 μL) under normal culture conditions were incubated in the presence of pre-diluted extracts, fractions, isolated compounds and reference drug (10 μL) following by the incubation at 37°C for 72 h. After incubation, 100 μL of SYBR Green I buffer [6 μL of 10,000 × SYBR Green I (Invitrogen) + 600 μL of Red Blood Cells lysis buffer {Tris (25 mM; pH 7.5)} + 360 μL of EDTA (7.5 mM) + 19.2 μL of parasites lysis solution {saponin (0.012%; wt/vol) } and 28.8 μL of Triton X-100 (0.08%; vol/vol)}] were added to each well, mixed twice gently with multi-channel pipette and incubated in the dark at 37°C for 1 h. Fluorescence was measured using a TECAN M 200 Microplate reader with excitation and emission at 485 and 538 nm, respectively. The fluorescence counts were plotted against the logarithme of sample concentration and the 50% inhibitory concentration (IC_{50}) was determined by the analysis of dose–response curves using GraphPad Prism 5. Experiments were done in triplicate.

- ***In vitro cytotoxicity assay***

The cytotoxicity profile of extracts, fractions and isolated compounds was assessed using the resazurin based assay (Bowling *et al*., 2012) against RAW 264.7 cells duly cultivated in complete Dulbecco's Modified Eagle's Medium (DMEM) containing 13.5 g/L of DMEM (Sigma Aldrich), 10% Fetal Bovine Serum (Sigma Aldrich), 0.2% sodium bicarbonate (w/v) (Sigma Aldrich) and 50 μg/mL of gentamicin (Sigma Aldrich). Globally, macrophages were seeded into 96-wells cell-culture flat-bottom plates at a density of 10^4 cells in 100 μL of

complete medium/well and incubated for 24 hours at 37°C, 5% CO_2 to allow cell adhesion. Following cell adhesion, ten microliter of each serially diluted test samples solution were added in assay plates and were then incubated for 48 h in the same experimental conditions. Growth control (0.1% DMSO-100% growth) and positive control wells (Podophyllotoxin at 20 μM) were included in the experiment plates. Cell proliferation was checked by adding 10 μL of a stock solution of resazurin (0.15 mg/mL in sterile PBS) to each well followed by an incubation of 4 h in the same culture condition. Fluorescence was then read on a Tecan Infinite M200 fluorescence multi-well plate reader (Tecan) at an excitation/emission of 530/590 nm. Results were expressed as 50% cytotoxic concentrations (CC_{50}) and selectivity indices (CC_{50} Mammalian cell/IC_{50} *Pf3D7*) were calculated for each test substance.

2- Acute oral toxicity study of aqueous extract of the leaves of *D. edulis*

The study was performed according to the protocol of OECD (2001), guideline 423. For this toxicity study, nine adults and non-pregnant female rats were used. These animals were randomly divided into three groups of three animals each, of which group 1, taken as a test control, was treated with distilled water at the single dose of 10 mL/kg; the other two groups (test batches) received the extract at the respective single doses of 2000 and 5000 mg/kg. The animals were fasted without water for 12 hours before the start of the experiment and 4 hours after. Oral administration of the extract and distilled water was done through a gastric tube. After administration, animals were observed individually for the first 4 hours and daily for 14 days after treatment. Special care should be taken during the first 30 minutes after administration of the substance. No signs of immediate toxicity such as aggressiveness, mobility, possible tremors, changes in coat, convulsions and other apparent signs of toxicity were noted during the experiment as well as changes in body weight. At the end of the experiment, the animals were sacrificed, their organs (liver, kidneys, spleen, lungs and heart) were removed and weighed in order to perform an autopsy on a macroscopic scale.

3- Other biological activities on *C. adolphi friderici*

- Urease inhibition

Reaction mixtures comprising 25 μL of enzyme (Jack bean Urease) solution and 55 μL of buffers containing 100 mM urea were incubated with 5 μL of test compounds (1 mM concentration) at 30℃ for 15 min in 96-well plates. Urease activity was determined by measuring ammonia production using the indophenol method as described by Weatherburn et al., 1967 with some modifications. Briefly, 45 μL each of phenol reagent (1% w/v phenol and 0.005% w/v sodium nitroprusside) and 70 μL of alkali reagent (0.5% w/v NaOH and 0.1%

active chloride NaOCl) were added to each well. The increasing absorbance at 630 nm was measured after 50 min, using a microplate reader (Molecular Device, USA). All reactions were performed in triplicate in a final volume of 200 μL. The data (change in absorbance per min) were processed using SoftMax Pro software (Molecular Device, USA). All the assays were performed at pH 8.2 (0.01 M $K_2HPO_4.3H_2O$, 1 mM EDTA and 0.01 M $LiCl_2$). Percentage inhibitions were calculated using the formula:

$$\mathbf{100} - \frac{\boldsymbol{OD_{testwell}}}{\boldsymbol{OD_{control}}} \times \mathbf{100}$$

Thiourea was used as the standard inhibitor of urease.

- **Determination of DPPH radical scavenging activity**

The free radical scavenging activity was measured by 1,1-diphenyl-2-picryl-hydrazil (DPPH) using the method described by Gulcin *et al*., 2005 with little modifications. The solution of DPPH of 0.3 mM was prepared in ethanol. Five microlitres of each sample of different concentration (62.5 μg – 500 μg) was mixed with 95 μL of DPPH solution in ethanol. The mixture was dispersed in 96 well plates and incubated at 37℃ for 30 min. The absorbance at 515 nm was measured by microtitre plate reader (spectramax plus 384 Molecular Devive, USA) and percent radical scavenging activity was determined in comparison with the methanol treated control BHA was used as standard.

$$\boldsymbol{DPPH\ scavenging\ effect}\ (\%) = \frac{\boldsymbol{Ac - As}}{\boldsymbol{Ac}} \times \mathbf{100}$$

Where Ac stands for absorbance of control (DMSO treated) and As for absorbance of sample.

- **Lipoxygenase inhibition**

The activity of compounds against lipoxygenase was determined using the method developed by Tappel et al., 1962 with slight modifications. Lipoxygenase enzyme solution was prepared so that the enzyme concentration in reaction mixture was adjusted to give rates of 0.05 absorbance/min. The reaction mixture contained 160 μL (100 mM) sodium phosphate buffer (pH 8), 10 μL of test solution and 20 μL of LOX solution, in buffer. The contents were mixed and incubated for 10 min at 25℃. The reaction was then initiated by the addition of 10 μL substrate solution (linoleic acid, 0.5 mM, 0.12% w/v tween 20 in ration of 1:2) and the change in absorbance at 234 nm was followed for 6 min. The concentration of the test compound that inhibited lipoxygenase activity by 50% (IC_{50}) was determined by monitoring the effect of increasing concentrations of these compounds in the assays on the degree of inhibition. The IC_{50} values were calculated by means of EZ-Fit, Enzyme Kinetics Program (Perrella Scientific In., amhherset, USA).

- **Butyrylcholinesterase inhibition Assay**

Butyrylcholinesterase inhibition activity was determined by the method as described by Ellman et al., 1961. Horse serum butyrylcholinesterase enzyme, EC3.1.1.8 (Sigma, USA) was prepared by dissolving the enzyme in phosphate buffer (100 mM, pH 8.0). The enzyme concentration in reaction mixture was adjusted to 0.2 U per well. Sodium phosphate buffer (180 μL, pH 8.0) and buffered Ellman's Reagent (DTNB, 5,5-dithiobis [2-nitrobenzoic acid] 0.1 M $NaHCO_3$, 17.85 mmol/L, 10 μL) was added in wells labeled as blank (B substrate and B enzyme), control and test. Test compound solution (of various concentrations of 5-500 μM, 10 μL) was added in each well labeled as test. Then, 20 μL of butyrylcholinesterase solution was added in each well including B enzyme, control and test. The contents were mixed and incubated for 15 min at 25°C. The reaction was initiated by the addition of 10 μL substrate solution butyrylcholinesterase iodide (10 mM) in each well except B enzyme. The absorbance was measured at 412 nm. The IC_{50} values were determined by monitoring the inhibition effects of various concentrations of test compounds and this was calculated by means of EZ-Fit, Enzyme Kinetics Program (Perrella Scientific In., Amhherset, USA).

III.5 PROTOCOL OF PRE-FORMULATION OF PHYTOMEDICINE FROM HYDROETHANOLIC LEAVES EXTRACT

- **Preparation of simple syrup**

Introduce the previously weighed sugar powder into a flask with sufficient volume and then add a necessary and sufficient quantity of demineralized water. Heat the mixture to 50°C while stirring for about an hour, until a clear and homogeneous solution is obtained: this is simple syrup.

- **Preparation of the phytomedicine**

Let the simple syrup cool then weigh it and deduce the mass of the active ingredient to be added into it, knowing that 1.3179% of extract corresponds to 97.782% of simple syrup. Introduce a mass of active ingredient, previously weighed, into the simple syrup contained in a flask. Let the active ingredient dissolve until a limpid and homogeneous solution is obtained. Then successively and gradually add the aroma, the stabilizer and the essence. The phytomedicine thus prepared is left to stand for 1 hour and finally bottled.

III.6 PHYSICAL AND SPECTROSCOPIC DATA FOR COMPOUNDS ISOLATED FROM *C. adolphi friderici* Engl and *D. edulis*

CAF2: Eloundemnoside, 1-(*O-β-D*-glucopyranosyl)-(2*S*,3*S*,4*R*,6*E*)-2-{[(2*R*)-2-hydroxytetracosanoyl]amino}dec-6-ene-1,3,4-triol (42)

white amorphous powder; $[\alpha]_D^{24}$ = -13.88 (*c* 0.002, MeOH);

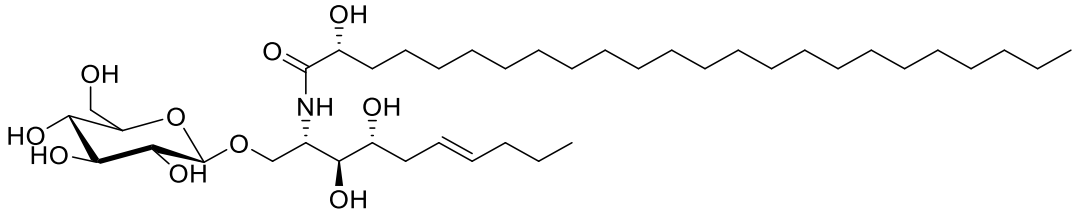

42

HR-ESI-MS (negative mode, *m/z*): 730.5460 for $[M-H]^-$, calcd for $C_{40}H_{76}NO_{10}$, 730.5475;

IR (KBr) υ_{max}: 3661 and 3421 cm^{-1} (NH and OH), 1634 cm^{-1} (NH–C=O), and 1546 cm^{-1} (olefinic group).

UV λ_{max} (MeOH): 210 and 228 nm.

^{1}H NMR (Pyridine-*d*$_5$, 400 MHz): See table 12

^{13}C NMR (Pyridine-*d*$_5$, 100 MHz): See table 12

CAF14: *Trans-N*-feruloyloctopamine (43)

yellow-orange crystals, (80.7 mg) (Ge *et al.*, 2014)

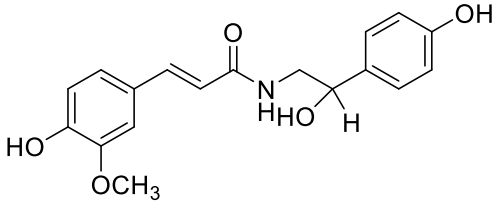

EI-MS: ***m/z*** 311.1 $[M]^+$, $C_{18}H_{19}NO_5$.

^{1}H NMR (MeOH-*d*$_4$, 400 MHz): See table 13

^{13}C NMR (MeOH-*d*$_4$, 100 MHz): **See table 13**

CAF7: *Trans-N*-feruloyltyramine (44)

yellow powder (205.3 mg), **(**Al-Taweel *et al.*, 2012).

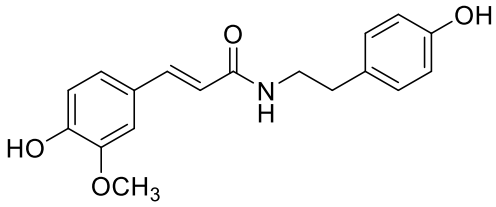

EI-MS (int. rel.): *m/z* 313 $[M]^+$ (15), 177 (100), 145 (22), 120 (18), 107 (19); $C_{18}H_{19}NO_4$.

^{1}H NMR (MeOH-*d*$_4$, 400 MHz): See table 14

^{13}C NMR (MeOH-*d*$_4$, 100 MHz): See table 14

CAF8: *Trans-N*-coumaroyltyramine (45)

White amorphous solid (150.9 mg), (Al-Taweel *et al.*, 2012).

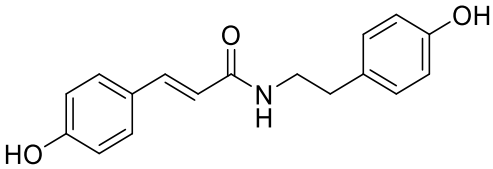

EI-MS (*m/z*): 283 [M+] (16), 176, 164, 147 (100); $C_{17}H_{17}NO_3$.

^{1}H NMR (MeOH-*d*$_4$, 400 MHz): See table 15

^{13}C NMR (MeOH-*d*$_4$, 100 MHz): See table 15

CAF9: Azelaic acid (46)

White powder (40.1 mg) (Kadhum et al., 2012).

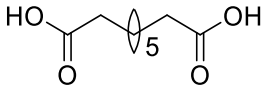

HR-ESI-MS: *m/z*: 189.1121 for $[M+H]^+$, $C_9H_{17}O_4$.

EI-MS: *m/z* 171.2 (rel int) (8.2), 152.0 (100), 124.0 (50.1), 111.0 (61.9),

^{1}H-NMR (DMSO, 400 MHz): See table 16

CAF13: **Sebacic acid (47)**

White powder (2.2 mg), (Otte *et al*., 2017).

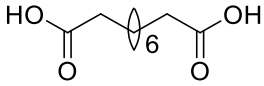

EI-MS: *m/z* 185.1 (rel int) $[M-OH]^+$ (3.5) , 138.1 (38.7), 125.1 (53.7), 98.0 (100), 84.0 (61), 60 (42.6), 55 (72.4). $C_{10}H_{18}O_4$.

^{1}H-NMR (MeOD+$CDCl_3$, 400 MHz): See table 17

CAF10: Indole 3-carboxaldehyde (48)

White powder (1.5 mg) (Evidente and Surico, 1986)

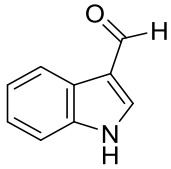

^{1}H-NMR ($CDCl_3$, 500 MHz): **See table 18**

^{13}C-NMR ($CDCl_3$, 125MHz): **See table 18**

CAF12: Laceroic acid (49)

White oil (2.5 mg), (Kalimuthu *et al*., 2011)

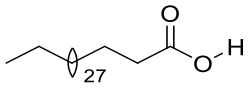

EI-MS: *m/z* 480.2 $[M]^+$, $C_{32}H_{64}O_2$

^{1}H-NMR ($CDCl_3$, 500MHz): See table 19

CAF3: Heptacosanoic acid (50)

White amorphous powder (10.1 mg), (Kovganko *et al*., 1999).

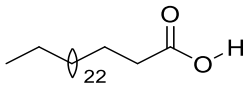

EI-MS: *m/z* 410.3 $[M]^+$, $C_{27}H_{52}O_2$

^{1}H-NMR (Pyridine-*d*$_5$, 400 MHz): See table 20

CAF15 : Allantoin (51)

White amorphous powder (3.1 mg), (Scripathi *et al*., 2011)

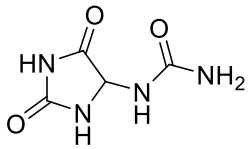

EI-MS: *m/z* 158.1 $[M]^+$, $C_4H_6N_4O_3$.

^{1}H-NMR (DMSO, 400 MHz): See table 21

CAF16: Aspartic acid (52)

Colorless crystal (4.1 mg), (Dunn and Fox, 1933)

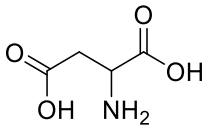

EI-MS: *m/z* 133.0 $[M]^+$, $C_4H_7NO_4$.

^{1}H-NMR (D_2O, 400 MHz): See table 22

^{13}C-NMR (D_2O, 100 MHz): See table 22

CAF5: Vanillin (53)

White amorphous powder (1.0 mg), (Costa *et al*., 2014)

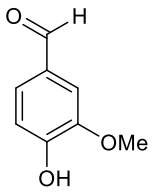

EI-MS: *m/z* 150.9 $[M-OH]^+$, $C_8H_8O_4$.

^{1}H-NMR ($CDCl_3$, 400 MHz): See table 23

^{13}C-NMR ($CDCl_3$, 100 MHz): See table 23

CAF11: Parahydroxybenzoic acid (54)

White amorphous powder (3.5 mg), (Ram *et al*., 2008/2009)

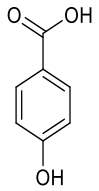

EI-MS: *m/z* 121.0 $[M-OH]^+$, $C_7H_6O_3$.

^{1}H-NMR ($CDCl_3$, 400 MHz): See table 24

^{13}C-NMR ($CDCl_3$, 100 MHz): See table 24

DE22: 3,4-dihydroxybenzoïc acid (55)

White powder (6.5 mg), (Zushang *et al*., 2017).

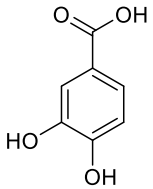

^{1}H NMR (MeOH-d_4, 600 MHz): **See table 25**

^{13}C NMR (MeOH-d_4, 150 MHz): **See table 25**

CAF4: Glycerol 1-octadecanoate (56)

White powder (3.3 mg), (Yu *et al*., 2003)

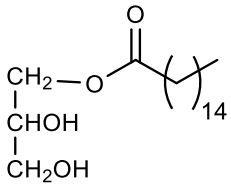

EI-MS: *m/z* 327.2 $[M-OH]^+$, $C_{20}H_{40}O_4$

^{1}H-NMR ($CDCl_3$, 400 MHz): See table 26

^{13}C-NMR ($CDCl_3$, 100 MHz): See table 26

DF5: Glyceryl-1-tetracosanoate (57)

White powder (3.1 mg), (Sultana *et al*., 1999).

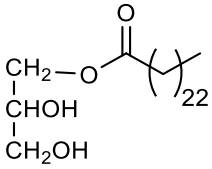

HR-ESI-MS *m/z* 465.4543 $[M+Na]^+$($C_{27}H_{54}O_4$).

^{1}H NMR ($CDCl_3$, 600 MHz): See table 27

^{13}C NMR ($CDCl_3$, 150 MHz): See table 27

DE2: Lichexanthone (58)

White powder (3.7 mg), (Buitrago *et al*., 2010).

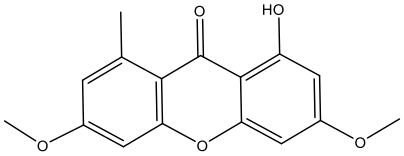

HR-ESI-MS: *m/z* 287.0935 $[M+H]^+$ (calcd for 286.084: $C_{16}H_{14}O_5$).

^{1}H-NMR (Pyridine-d_5, 600 MHz): See table 28

^{13}C-NMR (Pyridine-d_5, 150 MHz): See table 28

DE10: Griseoxanthone C (59)

White powder (9.4 mg), (Jian *et al*., 2013).

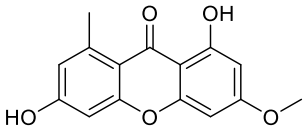

HR-ESI-MS *m/z* 274.4 $[M+2H]^+$ ($C_{15}H_{12}O_5$),

^{1}H-NMR ($CDCl_3$, 600 MHz): See table 29

^{13}C-NMR ($CDCl_3$, 150 MHz): **See table 29**

DE4: 3,3′,4-tri-*O*-methylellagic acid (60)

White powder (15.9 mg), (Khac *et al*., 2010).

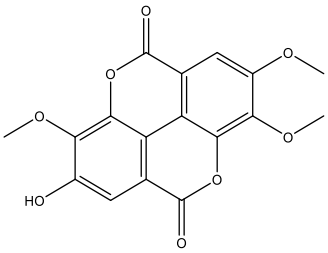

HR-ESI-MS: *m/z* 367.0458 $[M+Na]^+$ ($C_{17}H_{12}O_8$,).

^{1}H-NMR (Pyridine-d_5, 600 MHz): **See table 30**

^{13}C-NMR (Pyridine-d_5, 150 MHz): **See table 30**

DE3: 3,3′-di-*O*-methylellagic acid (61)

White powder (6.5 mg) (Khac *et al*., 2010).

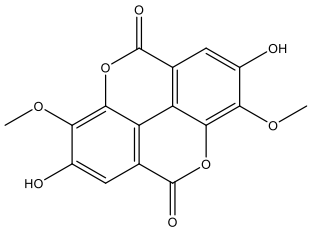

HR-ESI-MS: *m/z* 353.2329 $[M+Na]^+$ ($C_{16}H_{10}O_8$).

^{1}H-NMR (Pyridine-*d*$_5$, 600 MHz): **See table 31**

DE21: 3,3′′-di-*O*-methylellagic acid 4-*O*-(3′′-galloyl)-*β*-*D*-xylopyranoside (62)

White powder (8.1 mg), (Taylor *et al*., 1998).

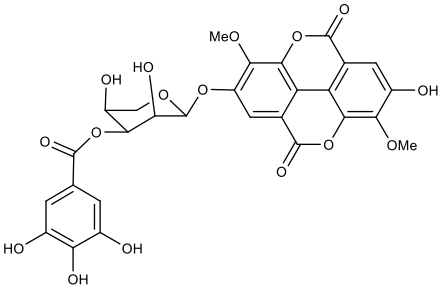

HR-ESI-MS *m/z* 637.0801 $[M+Na]^+$($C_{28}H_{22}O_{16}$).

^{1}H-NMR (MeOH-*d*$_4$, 600 MHz): See table 32

^{13}C-NMR (MeOH-*d*$_4$, 150 MHz): See table 32

DF3: Auranthiamide acetate (63)

White powder (4.9 mg), (Wahidulla *et al*., 1991).

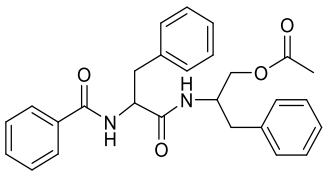

HR-ESI-MS *m/z* 455.2552 $[M+H]^+$ ($C_{27}H_{28}O_4N_2$).

^{1}H-NMR ($CDCl_3$, 600 MHz): See table 33

^{13}C-NMR ($CDCl_3$, 150 MHz): See table 33

DE7: Confluentic acid (64)

White powder (6.0 mg), (Yuichi *et al*., 1994).

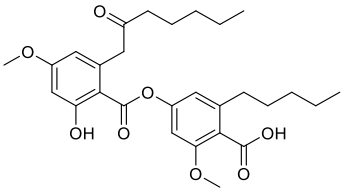

HR-ESI-MS: *m/z* 523.2429 $[M+Na]^+$ ($C_{28}H_{37}O_8$).

^{1}H NMR ($CDCl_3$, 600 MHz): See table 34

^{13}C NMR ($CDCl_3$, 150 MHz): See table 34

DF6: Ethyl gallate (65)

White powder (5.3 mg), (Atsushi *et al*., 2009).

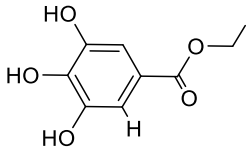

^{1}H-NMR (MeOH-d_4, 600 MHz): **See table 35**

^{13}C-NMR (MeOH-d_4, 150 MHz): **See table 35**

DE5: 3-oxo-lanosta-7,24-Z-dien-26-oid acid (66)

White powder (10.5 mg), (Barton *et al*.,1956).

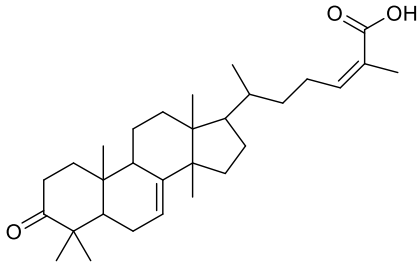

HR-ESI-MS: *m/z* 455.3526 $[M+H]^+$ ($C_{30}H_{46}O_3$).

^{1}H-NMR ($CDCl_3$, 600 MHz): **See table 36**

^{13}C-NMR ($CDCl_3$, 150 MHz): See table 36

DE14: *β*-amyrinacetate (67)

White powder (5.7 mg), (De Amorim *et al*., 2016).

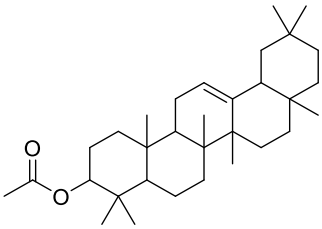

^{1}H-NMR ($CDCl_3$, 600 MHz): See table 37

^{13}C-NMR ($CDCl_3$, 150 MHz): **See table 37**

DE16: *β*-amyrin (68)

White powder (8.4 mg), (De Amorim *et al*., 2016).

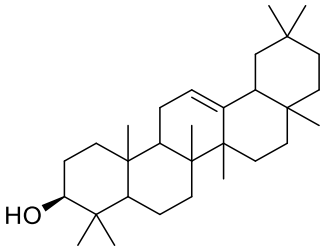

^{1}H-NMR ($CDCl_3$, 600 MHz): See table 37

^{13}C-NMR ($CDCl_3$, 150 MHz): See table 37

CAF1: Friedelin (69)

White powder (7.5 mg), (Klass *et al*., 1992)

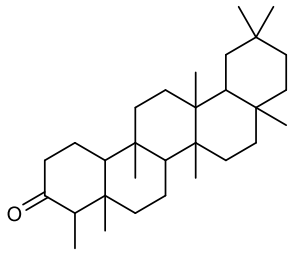

EI-MS: *m/z* 426.3 $[M]^+$, $C_{30}H_{50}O$.

^{1}H-NMR (CDCl$_3$, 500 MHz): See table 38

^{13}C-NMR (CDCl$_3$, 125 MHz): See table 38

Mixture of *β*-and *α*- amyrin (70)

White powder (50.9 mg), (De Amorim *et al*., 2016).

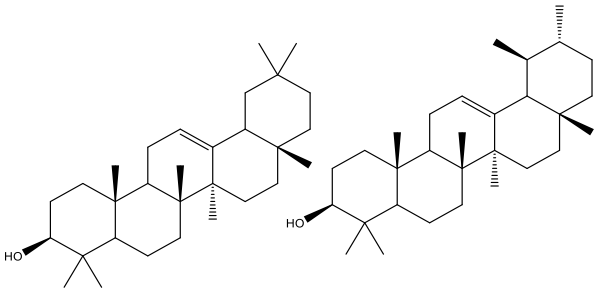

^{1}H-NMR ($CDCl_3$, 600 MHz): δ_H 5.20 (t, J = 3.7 Hz, 1H), 5.15 (t, J = 3.7 Hz, 1H), 3.25 (m, 2H).

^{13}C-NMR ($CDCl_3$, 150 MHz): δ_C 145.3 (C-13), 121.7 (C-12) for *β*- amyrin and 139.6 (C-13), 124.4 (C-12) for *α*- amyrin.

DF1: Mixture of *β*-sitosterol and stigmasterol (71):

White crystals from methanol, mp: 128-132°C (Savinova *et al*., 2012)

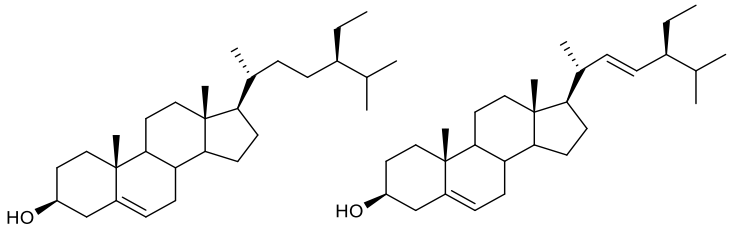

DF8: *β*-sitosterol-3-*O*-*β*-*D*-glucopyranoside (4)

White crystals from methanol, mp: 290-292°C (Wang et al., 2009).

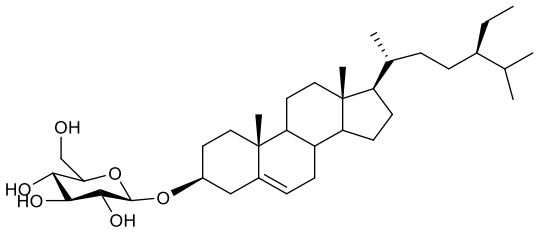
OH
O
HO
HO
O
OH

REFERENCES

Adedapo A. A., Jimoh O. F., Afolayan J. A., Masika J. P. 2009. Antioxidant properties of the methanol extracts of the leaves and stems of *Celtis africana*. *Records of Natural Products*, **3**, 23-31.

Agbo B. E., Amise A. F., Lennox A. 2017. Antimicrobial Potential of *Dacryodes edulis* against selected clinical bacteria isolates. *Microbiology Research Journal International*, **5**, 1-7.

Ahmed E., Arshad M., Bibi Y., Ahmed S. M. 2018. Phytochemical and antioxidant potential of crude methanolic extract and fractions of *Celtis eriocarpa* decne. Leaves from lesser himalaya region of pakistan. *Pakistan Journal of Botany*, **50**, 279-285.

Ajibesin K. K. 2011. *Dacryodes edulis* (G.Don) H.J. Lam: A Review on its medicinal, Phytochemical and economical Properties. *Research Journal of Medicinal plants*, **1**, 32-41.

Akhideno L. O., Rafiu B. O., Lawal I. O., Ogboru R. O. 2019. Phytochemical Screening and Mineral Potentials of the Kernel of *Dacryodes klaineana* (Pierre) H.J.Lam. *Open Science Journal of Analytical Chemistry*, **4**, 7-12.

Alioune D. F., Serigne I. M. D., Kady D., William D., Emmanuel B. 2017. Phytochemical screening, phenol content and antioxidant studies of ethanol leaf extract of *Celtis toka*. *Wood Journal of Pharmacognosy and Phytochemistry*, **6**, 488-492.

Almeida D. O. P., Boleti A P., Rüdiger L. A., Lourenço A. G., Valdir F. V. J., Lima S. E. 2015. «Anti-Inflammatory Activity of Triterpenes Isolated from *Protium paniculatum* Oil-Resins». *Evidence-Based Complementary and Alternative Medicine*, **12**, 1-10.

Alonso P., Aponte J., Aide P. 2004. Efficacy of the RTS,S/AS02A vaccine against Plasmodium falciparum infection and disease in young African children: randomized controlled trial. *The Lancet*, **364**,1411-1420.

Al-Taweel A. M., Perveen S., El-Shafaea A. M., Fawzy G., Malik A., Afza N., Iqbal L., Latif M. 2012. Bioactive Phenolic Amides from *Celtis africana*. *Molecules*, **17**: 2675–82.

Antonio-Nkondjio C., Ndo C., Njiokou F., Bigoga D. J., Awono-Ambene P., Etang J., Ekobo S. A., Wondji S. 2019. Review of malaria situation in Cameroon : technical viewpoint on challenges and prospects for disease elimination. *Parasites & vectors*, **12**, 1-23.

Anyam J. N., Tor-Anyiin T., Ogbaji I. J. 2015. Phytochemical and medicinal principles of raw seeds, *Journal of Natural Products. Plant Resource*, **2**, 13-19.

Arjen M., Dondorp L., Von S. 2017. Infectious Diseases. *Elsevier, science direct*, **2**, 1014-1025.

Atsushi O., Syuntaro H., Shinji K., Tetsuya T., Yoshiharu F., Masahiro N., Hiroshi A. 2009. Identification and activity of ethyl gallate as an antimicrobial compound produced by Geranium carolinianum. *Weed Biology and Management*, **9**, 169–172.

Badoni R., Semwal D. K., Badoni P. P., Kothiyal S. K., Rawat U. 2010. A novel bacteriohopanoid from *Celtis australis* L. bark. *Chinese Chemical Letters*, **22**, 81–84.

Bah M., Gutiérrez-Avella M. D., Mendoza S., Rodríguez-López V., Castañeda-Moreno R. 2014. Chemical constituents and antioxidant activity of extracts obtained from branch bark of *Bursera simaruba*. *Boletín Latinoamericano y del Caribe dePlantas Medicinales y Aromáticas*, **13**: 527-536.

Bankeu K. J. J., Dawe A., Mbiantcha M., Feuya T. G. R., Ali I., Tchuenmogne T. M. A., Mehreen L., Lenta N. B., Ali M. S., Ngouela S. A. 2017. Characterization of bioactive compounds from *Ficus vallis-choudae* delile (Moraceae). *Trends in Phytochemical Research*, **1**, 235‑242.

Barrett A. G. M., Beall J. C., Braddock D. C., Flack K., Gibson V. C., Salter M. M. 2000. Asymmetric allylboration and ring closing alkene metathesis: A novel strategy for the synthesis of glycosphingolipids. *Journal of Organic Chemistry*, **65**, 6508.

Bartoloni A., Zammarchi L. 2012. Clinical aspects of uncomplicated and severe malaria. *Mediterranean journal of hematology and infectious diseases*, **4**: e2012026.

Barton D. H. R., Seoane E. 1956. Triterpenoids. Part XXII. The constitution and stereochemistry of masticadienonic acid. *Journal of the Chemical Society*, **801**, 4150-4157.

Bassard J. E., Mutterer J., Duval F., Werck-Reichhart D. 2012. A novel method for monitoring the localization of cytochromes P450 and other endoplasmic reticulum membrane associated proteins: A tool for investigating the formation of metabolons. *FEBS Journal*, **279**, 1576–1583.

Bazzano L. A., He J., Ogden L. G., Loria C. M., Whelton P. K. 2003. Dietary fiber intake and reduced risk of coronary heart disease in US men and women: the National Health and Nutrition Examination Survey I Epidemiologic Follow-up Study. *Archives of Internal Medicine*, **163**, 1897-1904.

Bellakhdar J. 1997. La pharmacopée traditionnelle marocaine (Moroccan Traditional pharmacopeia). Ibis Press, Paris.

Berg C., Dahlberg S. 2001. A revision of Celtis subgroup. Mertensia (Ulmaceae). *Brittonia*, **53**, 66–81. https://doi.org/10.1007/BF028 05398.

Blume A. G., Cruz-Cañizares J. D. L., Doménech-Carbó M. T., Gimeno-Adelantado J. V., Mateo-Castro R., Bosch-Reig F. 2005. Study of Burseraceae resins used in binding media and varnishe from artworks by gas chromatography mass spectrometry and pyrolysis gas chromatography mass spectrometry. *Journal of Chromatography,* **1093**:177-194.

Bogdan M., Floare G. C., Pirnau A. 2002. ^{1}H NMR investigation of self-association of vanillin in aqueous solution. *Journal of Physics: Conference series*, **182**: 1-5.

Bouquet A. 1969. Feticheurs et médecines traditionnelles du Congo (Brazzaville). Paris: *ORSTOM*. **36,** 282.

Bousema J. T., Schneider P., Gouagna L. C., Drakeley C. J., Tostmann A., Houben R., Githure J. I., Ord R., Sutherland C. J., Omar S. A. 2006. Moderate effect of artemisinin-based combination therapy on transmission of Plasmodium falciparum. *The Journal of Infectious Diseases*; **193**, 1151-1159.

Bowling T., Mercer L., Don R., Jacobs R., Nare B., 2012. Application of a resazurin-based high-throughput screening assay for the identification and progression of new treatments for human African trypanosomiasis. *International Journal for Parasitology, Drugs Drug Resistance*, **2,** 262-270.

Brasil P., Zalis M. G., De Pina-Costa A., Siqueira A. M., Júnior C. B., Silva S. 2017. Outbreak of human malaria caused by Plasmodium simium in the Atlantic Forest in Rio de Janeiro: a molecular epidemiological investigation. *Lancet Glob Health*, **5**, 1038-46.

Brown L., Rosner B., Willett W. W., Sacks F. M. 1999. Cholesterol lowering effects of dietary fiber: a meta-analysis. *American Journal of Clinical Nutrition*, **69**, 30-42.

Bryngelsson S., Dimberg L. H., Kamal-Eldin A. 2002. Effects of commercial processing on levels of antioxidants in oats (*Avena sativa* L.). *Journal of Agricultural and Food Chemistry*, **50**, 1890-1896.

Bubb W. A. 2006. NMR Spectroscopy in the Study of Carbohydrates: Characterizing the Structural Complexity. School of Molecular and Microbial Biosciences, University of Sydney, New South Wales 2006, Australia.

Buitrago D. A., Rojas V. J., Cote V., Brunocolmenárez J., Díaz De Delgado G. 2010. NMR elucidation and crystal structure analysis of 1-hydroxy-3,6-dimethoxy-8-methyl-9hxanthen-9-one (lichexanthone) isolated from *Vismia baccifera* (Guttiferae). *Boletín Latino americano y del Caribe de Plantas Medicinales y Aromáticas*, **9**, 470-474.

Burkil H. M. 1985. The useful plants of West Africa- Whiferrers Press Limited, London. Royal Botanic Gardens, Kem Pp. 401-415.

Capanna E. 2006. Grassi versus Ross: who solved the riddle of malaria? *International Microbiology*, **9**, 69-74.

Cateni F., Zilic J., Falsone G., Scialino G., Banfi E. 2003. New Cerebrosides from *Euphorbia peplis* L.: Antimicrobial Activity Evaluation. *Bioorganic and Medicinal Chemistry Letters*, **13**, 4345-4350.

Chen B., Cai G., Yuan Y., Li T., He Q., He J. 2012. Chemical constituents in hemp pectin. *Zhongguo Shiyan Fangjixue Zazhi*, **18** : 98-100

Chen C. Y., Milbury P. E., Kwak H. K., Collins F. W., Samuel P., Blumberg J. B. 2004. Avenanthramides and phenolic acids from oats are bioavailable and act synergistically with vitamin C to enhance hamster and human LDL resistance to oxidation. *Journal of Nutrition*, **134**, 1459-1466.

Chen X., Wu Y. L., Chen D. 2002. Structure determination and synthesis of a new cerebroside isolated from the traditional Chinese medicine *Typhonium giganteum Engl*. *Tetrahedron Letters*, **43**, 3529-3532.

Chernin E. 1988. Sir Ronald Ross, malaria, and the rewards of research. *Medical History*, **32**, 119-41.

Chu Y. F, Wise M. L., Gulvady A. A., Chang T., Kendra D. F., Van Klinken B. J. W., Shi Y., O'Shea M. 2013. *In vitro* antioxidant capacity and anti-inflammatory activity of seven common oats. *Food Chemistry*, **139**, 426-431.

Collins F. W. 1989. Oat phenolics: Avenanthramides, novel substituted *N*-cinnamoylanthranilate alkaloids from oat groats and hulls. *Journal of Agricultural and Food Chemistry*, **37**, 60–66.

Collins F. W., McLachlan D. C., Blackwell B. A. 1991. Oat phenolics: avenalumic acids, a new group of bound phenolic acids from oat groats and hulls. *Cereal Chemistry*, **68,** 184-189.

Collins F. W., Mullin W. J. 1988. High-performance liquid chromatographic determination of avenanthramides, *N*-aroylanthranilic acid alkaloids from oats. *Journal of Chromatography*, **445**, 363–370.

Cook G. C. and Webb A. J. 2000. Perceptions of malaria transmission before Ross' discovery in 1897. *Postgraduate Medical Journal*, **76**, 738-740.

Cook N.C., Samman S. 1996. Flavonoids-chemistry, metabolism, cardioprotective effects, and dietary sources. *The Journal of Nutritional Biochemistry*, **7**, 66-76.

Cragg G. M., Kingston D. G., Newman D. J. 2011. Anticancer agents from natural products. *Cancer research cell press*, **2**, 784.

Cui L., Mharakurwa S., Ndiaye D., Rathod P. K., Rosenthal P. J. 2015. Antimalarial drug resistance: literature review and activities and findings of the ICEMR network. *The American journal of tropical medicine and hygiene*, **93**, 57-68.

D'Angelo G., Vicinanza M., De Matteis M. A. 2008. Lipid-transfer proteins in biosynthetic pathways. *Current Opinion in Cell Biology*, **20**, 360-370.

Demain A. L., Aiqi F. 2000. The natural functions of secondary metabolites. *History of Modern Bioltechnology*, **69**, 1-39.

Dunn M. S., Fox S. W. 1993. The synthesis of aspartic acid. *Journal of Biological Chemistry*, **101**, 493-497.

Ecology of Malaria [Online]. 2015. USA. Available: http://www.cdc.gov/malaria/about/biology/ecology.html. page consulted on the 19th April 2020.

El-Alfy S. T., El-Gohary A. M. H., Sokkar M. N., Hosny M. 2011. A new flavonoid C-Glycoside from *Celtis australis* L. and *Celtis occidentalis* L. leaves and potential antioxidant and cytotoxic activities. *Scientia Pharmaceutica*, **79**, 963-975.

Ellman G. L., Courteny D. K., Andres V. J. R., Featherstone R. M. 1961. A new and rapid colorimetric determination of acetylcholinesterase activity. *Biochemical Pharmacology*, **7**, 88.

Eudes A., Baidoo E. E. K., Tang F., Burd H., Hadi M. Z., Collins F. W., Keasling J. D., Loqué D. 2011. Production of tranilast [*N*-(3',4'-dimethoxycinnamoyl)-anthranilic acid] and its analogs in yeast *Saccharomyces cerevisiae*. *Applied Microbiology and Biotechnology*, **89**, 989-1000.

Evidente A., Surico G. 1986. Isolation of indole-3-aldehyde from *pseudomonas syringae* pv. savastanoi. *Journal of Natural Products*, **49**, 938-939.

Eyong K. O., Krohn K., Hussain H., Folefoc G. N., Nkengfack A. E., Schulz B., Hu Q. 2005. Newbouldiaquinone and newbouldiamide: a new naphthoquinone-anthraquinone coupled pigment and a new ceramide from *Newbouldia laevis*. *Chemical and Pharmaceutical Bulletin*, **53**, 616-619.

F.A.O. 1999. Données statistiques des produits forestiers non-ligneux du Cameroun. Rapport du Programme de partenariat CE-FAO (1998-2001) – GCP/INT/679/EC Collecte et analyse de données pour l'aménagement durable des forêts – joindre les efforts nationaux et internationaux. pp 12-20. published on the web site: http://www.fao.org/DOCREP/003/X6699F/X6699F03.htm.

Ferri F. F. 2009. Ferri's color atlas and text of clinical medicine, Philadelphia, PA, Saunders/Elsevier.

Filali-Ansari N., El Abbouyi A., Kijjoa A., El Maliki S., El Khyari S. 2016. Antioxidant and antimicrobial activities of chemical constituents from *Celtis australis. Der Pharma Chemica*, **8**, 338-347.

Florens L., Washburn M. P., Raine J. D., Anthony R. M., Grainger M., Haynes J. D., Moch J. K., Muster N., Sacci J. B., Tabb D. L., Witney A. A., Wolters D., Wu Y., Gardner M. J., Holder A. A., Sinden, R. E., Yates J. R., Carucci, D. J. 2002. A proteomic view of the *Plasmodium falciparum* life cycle. *Nature*, **419**, 520-6.

Francisco L., Ignacio B., Augusto R., Fernando T., Sara R., José Q., Francisco E. and Jaime B., 2006. Isolation, structure elucidation, total synthesis, and evaluation of new natural and synthetic ceramides on human SK-MEL-1 melanoma cells. *Journal of Medicinal Chemistry*, **49**, 5830-5839.

Franco-Paredes C., Santos-Preciado J. I. 2006. Problem pathogens: prevention of malaria in travellers. *The Lancet infectious diseases*, **6**, 139-149.

Fujioka T., Kashiwada Y., Kilkuskie R. E., Cosentino L. M., Balias L. M., Jiang J. B., Janzen W. P., Chen I. S., Lee K. H., 1994. Anti-AIDS agents 11. Betulinic acid and platanic acid as anti-HIV principles from *Syzigium claviflorum*, and the anti-HIV activity of structurally related triterpenoids. *Journal of Natural Products*, **57**, 243-247.

Gallup J. L. and Sachs J. D. 2001. The economic burden of malaria. *The American journal of tropical medicine and hygiene*, **64**, 85-96.

Gao Y., Li X., Hu Q. 2012. Chemical composition and antioxidant activity of essential oil from Syzygium samarangenes and perry flower-bud. *International Scientific Medical Journal*, **2**, 19-28.

Gaur R. D. 1999. Flora of district Garhwal North West Himalaya. Srinagar Trans Media House, **84**.

Ge L. L., Liao M. C., Yang F. Y., Xiong S. Y. 2014. Amide Alkaloids from *Acorus Tatarinowii* Schott**.** *Advances in Biomedical Engineering Research*, **2**, 1-4.

Greenwood B. M., Fidock D. A., Kyle D. E., Kappe S. H., Alonso P. L., Collins F. H., Duffy P. E. 2008. Malaria: progress, perils, and prospects for eradication. *The Journal of clinical investigation*, **118**, 1266-1276.

Greenwood D. 1992. The quinine connection. *The Journal of Antimicrobial Chemotherapy*, **30**, 417-427.

Gulcin I., Alici H. A., Cesur M. 2005. Determination of in vitro antioxidant and radical scavenging activites of propofol. *Chemical and Pharmaceutical Bulletin*, **53**, 281-285.

Guo W., Nie L., Wu D., Wise M. L., Collins F. W., Meydani S. N., Meydani M. 2010. Avenanthramides inhibit proliferation of human colon cancer cell lines *in vitro*. *Nutrition and Cancer*, **62**, 1007-1016.

Hakomori S., Annu. 1981. Enzymatic synthesis of oligosaccharides. *Review of Biochemistry*. **50**, 733.

Halter D., Neumann S., van Dijk S. M., Wolthoorn J., De Maziere A. M., Vieira O. V., Mattjus P., Klumperman J., van Meer G., Sprong H. 2007. Pre-and post-Golgi translocation of glucosylceramide in glycosphingolipid synthesis. *Journal of Cell Biology*, **179**, 101-115.

Hefti A.F., Weiner W. 1986. Nerve growth factor and Alzheimer's disease. *Journal Annals. Neurology*, **20**, 275.

Hefti F., Hartikka J., Knusel B. 1989. Function of neurotrophic factors in the adult and aging brain and their possible use in the treatment of neurodegenerative diseases. *Neurobiology of Aging*, **10**, 515.

https:\\www.wikiwand.com/en/Dacroydes/ page consulted on the 5th February 2020.

Hwang B. Y., Chai H. B., Kardono L. B., Riswan S., Farnsworth N. R., Cordell G. A. 2003. Cytotoxic triterpenes from the twigs of *Celtis philippinensis*. *Phytochemistry*, **62**, 197-201.

Ibrahim H. G. 2019. Antioxidant Activity and Phenolic Profile of Turkish *Celtis* tournefortii. *Chemistry of Natural Compounds*, **55**, 738–742.

Igoli J. O., Ogaji O. G., Tor-Anyiin T. A., Igoli N. P. 2005. *African Journal of Traditional Complementry and Alternative Medicine*, **2**, 134-152.

Ikhuoria E. U., Maliki M. 2007. Characterization of avocado pear (*Persea americana*) and African pear (*Dacryodes edulis*) extracts. *Africa Journal of Biotechnology*, **6**, 950-952.

Inglett G.E., Chen D. 2012. Antioxidant and pasting properties of oat *β*-glucan hydrocolloids. *Food and Nutrition Sciences*, **3**, 827-835.

Ishihara A., Kojima K., Fujita T., Yamamato Y., Nakajima H. 2014. New series of avenanthramides in oat seed. *Bioscience, Biotechnology and Biochemistry*, **78**, 1975-1983.

Jecinta N. A., Tor-Anyiin T., Ogbaji I. J. 2015. Studies on *Dacryodes edulis* 1: Phytochemical and medicinal principles of raw seeds. *Journal of Natural Product. Plant Resource*, **2**, 13-19.

Ji L. L., Lay D., Chung E., Fu Y., Peterson D. M. 2003. Effect of avenathramides on oxidant generation and antioxidant enzyme activity in exercised rats. *Nutrition Research*, **23**, 1579-1590.

Jian X. Y., Sheng X. Q., Zhigang S., Yongcheng L. 2013. A New Xanthone Derivative From The Marine Fungus Phomopsis Sp. (No. SK7RN3G1). *Chemistry of Natural Compounds*, **49**, 246-248.

Kadhum A. A. H., Wasmi B. A., Mohamad A. B., Al-amiery A. A., Takriff M. S. 2012. Preparation, characterization, and theorical studies of azelaic derived from oleic acid by use of a novel ozonolysis method. *Research on Chemical Intermediates*, **38**, 656-668.

Kagho D. U. K., Fongang Y. S. F., Awantu A. F., Bankeu J. J. K., Toghueo R. M. K., Ngouela A. S., Sewald N., Lenta B. N., Mehreen L., Ali M. S. 2020. Ceramides and other bioactive compounds from *Celtis tessmannii* Rendle. *Chemical Data Collection*, **28**, 1–10.

Kalimuthu S., Latha S., Selvamani P., Rajesh P., Balamurugan B., Chandrasekar T. M. 2011. Isolation, characterization and antibacterial evaluation on long chain fatty acids from *Limnophila polystachya* Benth. *Asian Journal of Chemistry* **23**, 791-794.

Kamkumo G. R., Ngoutane A. M., Tchokouaha L. R. Y., Fokou P. V. T., Madiesse E. A. K., Legac J. 2012. From *Sorindeia juglandifolia* (Anacardiaceae) exhibit potent antiplasmodial activities *in vitro* and *in vivo*. *Malaria Journal*, **11**, 382.

Keeler, Harriet L. 2005. Our native trees and how to identify them; a popular study of their habits and their peculiarities. Kent University Press vol 1900. Pg 582.

Khac D. D., Tran-Van S., Campos A. M., Lallemand J-Y., Freizon M. 1990. Ellagic compounds from *Diplopanax stachyanthus*. *Phytochemistry*, **29**, 251-256.

Kim D.K., Lim J. P., Kim J. W., Park H. W., Eun J. S. 2005. Antitumor and antiinflammatory constituents from *Celtis sinensis*. *Archives of Pharmacal Research*, **28**, 39-43.

Klass J., Tinto W. F., McLean S., Reynolds W. F. 1992. Friedelane Triterpennoids from *Peritassa compta*: complete ^{1}H and ^{13}C assigments by 2D NMR spectroscopy. *Journal of Natural Products*, **55**, 1626-1630.

Koduru S., Grierson D. S., Afolayan A. J. 2007. Ethnobotanical information of medicinal plants used for treatment of cancer in the Eastern Cape Province, South Africa. *Current Science*, **92**, 906.

Koella J. C., Sörensen F. L., Anderson R. 1998. The malaria parasite, *Plasmodium falciparum*, increases the frequency of multiple feeding of its mosquito vector, *Anopheles gambiae*. *Proceedings of the Royal Society of London B: Biological Sciences*, **265**, 763-768.

Koenig R. T. 2012. Avenanthramide supplementation in young and older women: Protection against eccentric exercise-induced inflammation and oxidative stress. [Ph.D. Dissertation.] Madison, University of Wisconsin.

Koenig R., Dickman J. R., Kang C., Zhang T., Chu Y-F., Ji L. L. 2014. Avenanthramide supplementation attenuates exercise-induced inflammation in postmenopausal women. *Nutrition Journal*, **13**, 21.

Koenig R., Dickman J. R., Wise M. L., Ji L. L. 2011. Avenanthramides are bioavailable and accumulate in hepatic, cardiac, and skeletal muscle tissue following oral gavage in rats. *Journal of Agricultural and Food Chemistry*, **59**, 6438-6443.

Koudou J.,Abena A. A., Ngaissona P., Bessiere J. M. 2005. Chemical composition and pharmacological activity of essential oil of *Canarium schweinfurthii*. Fitoterapia, **76**: 700-703.

Kovganko N. V., Kashkan Z. N., Borisov E. V., Batura E. V. 1999. ^{13}C-NMR spectra of *β*-sitosterol derivatives with oxidized rings A and B. *Chemistry of Natural Compounds*, **35**, 646-649.

Krief S., Hladik C. M., Haxaire C. 2005. Ethnomedicinal and bioactive properties of plants ingested by wild chimpanzees in Uganda. *Journal of Ethnopharmacology*, **101**, 1-15.

Krishna S., Pulcini S., Fatih F., Staines H: 2010. Artemisinins and the biological basis for the PfATP6/SERCA hypothesis. *Trends in Parasitology*; **26**, 517-523.

Krungkrai J., Imprasittichai W., Otjungreed S., Pongsabut S., Krungkrai S. R. 2010. Artemisinin resistance or tolerance in human malaria patients. *Asian Pacific Journal of Tropical Medicine*, **3**, 748-753.

Kuete V., Efferth T. 2010. Cameroonian medicinal plants: pharmacology and derived natural products. *Frontier in Pharmacology*, **1**, 1-20.

Lambros C., Vanderberg J. P. 1979. Synchronisation of plasmodium falciparum erythrocytic stages in culture. Journal of parasitotology, **65**, 418-420.

Lee-Manion A. M., Price R. K., Strain J. J., Dimberg L. H., Sunnerheim K., Welch R. W. 2009. *In vitro* antioxidant activity and antigenotoxic effects of avenanthramides and related compounds. *Journal of Agricultural and Food Chemistry*, **57**, 10619-10624.

Lima M. P., Braga P. A. C., Macedo M. L., Silva G. F. M. F., Ferreira A. G., Fernandes B. J., Vieira C. P. 2004. Phytochemistry of *Trattinnickia burserifolia*, *T. rhoifolia*, and

Dacryodes hopkinsii: chemosystematic implications. *Journal of the. Brazilian. Chemical society*, **15**:1-12.

Liu L., Zubik L., Collins F. W., Marko M., Meydani M. 2004. The antiatherogenic potential of oat phenolic compounds. *Atherosclerosis*, **175**, 39-49.

Mahato S. B., Kundu A. P. 1994. ^{13}C NMR spectra of pentacyclic triterpenoids, a compilation and some salient features. *Phytochemistry*, **37**, 1517-1575.

Manguro O. A. L., Ugi I., Lemmen P. 2003. Dammarane Triterpenes of *Commiphora confusa* Resin. *Chem. Pharm. Bull*, **51**: 483-486.

Martins J. L. R., Sousa F. B., Fajemiroye J. O., Ghedini P. C., Ferreira P. M., Costa E. A. 2014. Anti-Ulcerogenic and Antisecretory effects of *Celtis iguanaea* (Jacq) Sargent hexane leaf extract, *Revista Brasileira de Plantas Medicinais*, **16**, 250-255.

Mattila P., Pihlava J. M., Hellström J. 2005. Contents of phenolic acids, alkyl and alkenylresorcinols, and avenanthramides in commercial grain products. *Journal of Agricultural and Food Chemistry*, **53**, 8290-8295.

Mbiantcha M., Wembe N. A., Dawe A., Nana Y. W., Ateufack G. 2017. Antinociceptive Activities of the Methanolic Extract of the Stem Bark of *Boswellia dalzielii* Hutch. (Burseraceae) in Rats Are NO/cGMP/ATP-Sensitive-K+ Channel Activation Dependent. *Evidence-Based complementary and Alternative Medecine*, **2017**: 1-12.

Metcalfe C. R., Chalk L. 1950. Anatomy of the dicotyledons, Vol II. Oxford: The Clarendon press; 1278-1282.

Meydani M. 2009. Potential health benefits of avenanthramides of oats. *Nutrition Reviews*, **67**, 731-735.

Miguel L. M., Mokondjimobe E., Okiemy-Andissa N., Diatewa M., Moukassa D., Longo-Mbenza B., Abena A. A. 2017. Medicinal potentialities of *Dacryodes edulis* (G. don) HJ.Lam. Literature review. *International Journal of Current Research*, **9**, 63014-63018.

Minatel O. I., Borges V. C., Gomez G. A. H., Chen O. C., Lima P.P.G. 2016. Phenolic compounds: Functional properties, impact of processing and bioavailability. INTECH

Mita T., Jombart T. 2015. Patterns and dynamics of genetic diversity in *Plasmodium falciparum*: What past human migrations tell us about malaria? *Parasitology International*, **64**, 238-243.

Mondal Sumanta. 2019. Protoalkaloids (Ephedrine). *Sem_pharmacognosy&Phytochemistry-III*. DOI: 10.13140/RG.2.2.35143.44967.

Muganza D. M., Fruth B., Nzunzu J. L., Tuenter E., Foubert K., Cos P., Maes L., Cimanga K., Exarchou V., Apers S., Pieters L., 2016. "*In Vitro* antiprotozoal activity and cytotoxicity of extracts and isolated constituents from *greenwayodendron suaveolens*." *Journal of Ethnopharmacology*, **193**, 510-16.

Muralidhar P., Kumar M. M., Krishna N., Rao C. B., Rao D. V. 2005. New sphingolipids and a sterol from a *Lobophytum* species of the Indian Ocean. *Chemical and Pharmaceutical Bulletin*, **53**, 168-171.

Murray C. J., Ortblad K. F., Guinovart C., Lim S. S., Wolock T. M., Roberts D. A., Dansereau E. A., Graetz N., Barber R. M., Brown J. C. 2014. Global, regional, and national incidence and mortality for HIV, tuberculosis, and malaria during 1990-2013: a systematic analysis for the Global Burden of Disease Study 2013. *The Lancet*, **384**, 1005-1070.

Murthy K. S. R., Chandrasekhara R. M., Sandhya R. S., Pullaiah T. 2016. Bioactive principles and biological properties of essential oils of Burseraceae: *Journal of Pharmacognosy and Phytochemistry*, **2**, 247-258.

National Malaria Control Program (NMCP). 2020. Activities report 2019.

Naveen M., Kiran I., Itrat A., Abdul M. 2002. Sphingolipids from *Conyza canadensis*. *Phytochemistry*, **61**, 1005-1008.

Neeraj K., Bikram S., Ajai P. G., Vijay K. K. 2006. Lonijaposides, novel cerebrosides from *Lonicera japonica*. *Tetrahedron Letters*, **62**, 4317-4322.

Ngueyem D. T. A. 2008. Ethnobotany and traditional medicine of pygmies baka. *Scientifica Acta*, **2**, 129-133.

Nna P. J., Tor-Anyiin T. A., Igoli J. O., Khan M. E., Anyam J. V. 2017. Phytochemical and Antimicrobial Screening of Root Extracts of *Dacryodes edulis*. *British Biotechnology Journal*, **3**, 1-9.

Nosten F., White N. J. 2007. Artemisinin-based combination treatment of faalciparum malaria. American Journal of Tropical Medecine and Hygiene, **77**, 181-192.

Nwodo U. U., Nguene A. A., Iroegbu C. U., Obiiyeke G. C. 2010. Effects of fractionation on antibacterial activity of crude extracts of *Tamarindusindica*. *African journal of biotechnology*, **69**, 7108-7113.

Nwokwonkwo D.C. 2014. Phytochemical and medicinal principles of raw seeds, *American Journal of Scientic and Industrial Research*, **5**, 1-12.

Ochuko L. E., Ramgopal M., Olajumoke A. O., Neil A. k., Shahidul I. M. 2017. *Dacryodes edulis* enhances antioxidant activities, suppresses DNA fragmentation in oxidative

pancreatic and hepatic injuries; and inhibits carbohydrate digestive enzymes linked to type 2 diabetes. *Biomedicine and pharmacotherapy*, **96**, 37-47.

Odolini S., Parola P., Gkrania-Klotsas E., Caumes E., Schlagenhauf P., Lopez-Velez R., Burchard G. D., Santos-O'connor F., Weld L., Von Sonnenburg F., Field V., De Vries P., Jensenius M., Loutan L., Castelli F. 2012. Travel-related imported infections in Europe, EuroTravNet 2009. *Clinical Microbiology Infection*, **18**, 468-74.

OECD. 2001. Acute oral toxicity - method by acute toxicity class. OECD Guideline for the Testing of Chemicals, Guideline 423, 14p.

Ogboru R. O., AkidenoL. O., Rafiu B. O., Lawal I. O. 2019. phytochemical screening and mineral analysis of the pulp of *Dacryodes klaineana* (Pierre) H.J.LAM. *American Journal of Chemistry and Materials Science*, **6**, 21-24.

Okazaki Y., Iwata Y., Matsukawa T., Matsuda F., Miyagawa H., Ishihara A., Nishioka T., Iwamura H. 2004. Metabolism of avenanthramide phytoalexins in oats. *The Plant Journal*, **39**, 560-572.

Okoye N. N., Ajaghaku L. D., Okeke N. H., Ilodigwe E. E., Nworu S. C., Okoye B.C. F. 2014. Beta-Amyrin and alpha-amyrin acetate isolated from the stem bark of *Alstonia boonei* display profound anti-inflammatory activity. *Pharmaceutical Biology*, **52**, 1478–1486.

Okwu D. E., Ighodaro B. U. 2009. GC-MS evaluation of the bioactive compounds and antibacterial activity of the oil fraction from the stem barks of *Dacryodes edulis*. Don Lam. *International Journal of Drug Development and Research*, **1**,117-125.

Ominyi M.C., Agbafor K. N., Ali F. U., Ogbanshi M. E., Ebenyi L. N., Orinya O. F., 2018. Cardioprotective activity of aqueous and ethylacetate seed extracts of *Dacryodes edulis* on doxorubicin induced heartdamage in albino rats. *IJBPAS*, **6**, 1046-1064.

Orozco-Mena R., Salmerón-Ochoa I., Ortega-Rivas E., Perez-Vega S. 2014. Development of a sustainable process for the solid-liquid extraction of antioxidants from oat. *Sustainability*, **6**, 1504-1520.

Ortiz-Robledo F., Villanueva-Fierro I., Oomah B.D., Lares- Asef I., Proal-Nàjere J.B., Nàvar-Chaidez J. J. 2013. Avenanthramides and nutritional components of four Mexican oat (Avena sativa L.) varieties. *Agrociencia*, **47**, 225-232.

Orwa C., Mutua A., Kindt R., Jamnadass R., Anthony S. 2009. Agroforestree Database: a tree reference and selection guide. *World Agroforestry Centre Kenya*, **2**, 6-19.

Osta M., Gannoun-Zaki L., Bonnefoy S., Roy. C., Vial H. J. 2002. A 24 bp cis-acting element essential for the transcriptional activity of *Plasmodium falciparum* CDP diacylglycerol synthase gene promoter. *Mololecular and Biochemical Parasitology*, **121**, 87-98.

Otte K. B., Maurer E., Kirtz M., Grabs D., Althoff E., Bartsch S., Vogel A., Nestl B. M., Hauer B. 2017. Synthesis of sebacic acid using a de nove designed retro-aldolase as key catalyst. *ChemCatChem*. https://doi.org/10.1002/cctc.201601551.

Oyen L. P. A. 2012. *Celtis mildbraedii* Engl. [Internet] Record fro; PROTA4U. Lemmens, R.H.M.J., Louppe D et Oteng-Amoako, A.A. (Editors). PROTA (Plant Resources of Tropical Africa/Ressources végétales de l'Afrique tropicale), Wageningen, Netherlands. http://www.prota4u.org/search.asp. Accessed 21 November 2020.

Patra A., Chaudhuri S. K., Acharyya A. K. 1990. Applications of two-dimensional NMR in spectral assignments of some friedelanes and secofriendelanes. *Magnetic Resonance in Chemistry*, **28**, 85-89. doi:10.1002/mrc.1260280116.

Pendyala M., Muthyala M. K., Nallamothu K., Chaganty B. R., Desaraju V. R. 2005. New sphingolipids and a sterol from a *Lobophytum* species of the Indian Ocean. *Chemical and Pharmaceutical Bulletin*, **53**, 168-171.

Perveen S., Al-Taweel A. M., Fawzy G. A., El-Shafae A. M., Khan A., Proksch P. 2015. Cytotoxic glucosphingolipid from *Celtis africana*. *Pharmacognosy magasine*, **11**, 1-5.

Pittaya T., Yupa P., Photchana P., Walter C. T. 2004. Cerebrosides and monoacyl monogalactosyl glycerol from *Clinacanthus nutans*. *Chemical and Pharmaceutical Bulletin*, **52**, 27-32.

Poorter L., Bongers F., Kouamé F. N., Hawthorne W. D. 2004. Biodiversity of West African forests: an ecological atlas of woody plant species. *Global Ecology and Biogeography*, **26**, 1423-1434.

Ram C. D., Meena R., Surya K. K., Suresh A., Mohan. B. G. 2009. Phytochemical Constituents of the Bark of *Vitex negundo* L. *Journal of Nepal Chemical Society*, **23**, 89-92.

Reiter P. 2000. From Shakespeare to Defoe: malaria in England in the Little Ice Age. *Emerging Infectious Diseases*, **6**, 1-11.

Rodriguez-Morales A. J., Orrego-Acevedo C. A., Zambrano-Munoz Y., Garcia-Folleco F. J., Herrera-Giraldo A. C., Lozada-Riascos C. O. 2015. Mapping malaria in municipalities of the Coffee Triangle region of Colombia using Geographic Information Systems (GIS). *Journal of Infection and Public* Health, **8**, 603-611.

Romero-Estrada A., Maldonado-Magaña A., González-Christen J., Bahena S. M., Garduño-Ramírez M. L., Rodríguez-López V., Alvarez L. 2016. Anti-inflammatory and antioxidative effects of six pentacyclic triterpenes isolated from the Mexican copal resin of *Bursera copallifera*. *BMC Complementary and Alternative Medicine*, **16**: 1-10.

Sachs J., Malaney P. 2002. The economic and social burden of malaria. *Nature*, **415**, 680-685.

Sattarian A. 2006. Contribution to the biosystematics of *Celtis* L. (Celtidaceae) with special emphasis on the African Species. Dissertation, Wageningen University, Wageningen, Guéldria.

Savinova T. S., Diet N. T., Voishvillo N. E., Andryushina V. A., Karpova N. V., Beletskaya I. P., Huy L D. 2012. Extraction of a mixture of phytosterols from soybean processing by-product and its used in the manufacture of 9α-hydroxyandrost-4-en-3,17-dione. *Pharmaceutical Chemistry Journal*, **46**, 183-186.

Schmidt R. R. 1989. Recent developments in the synthesis of glycoconjugates. *Pure and Applied Chemistry*, **61**, 1257.

Schoch G., Goepfert S., Morant M., Hehn A., Meyer D., Ullmann P., Werck-Reichhart D. 2001. CYP98A3 from *Arabidopsis thaliana* is a 30-hydroxylase of phenolic esters, a missing link in the phenylpropanoid pathway. *Journal of Biological Chemistry*, **276**, 36566-36574.

Schwikkard S., VavHeerden F. R. 2006. Antimalarial activities of plant metabolites. *Natural Product Reports*, **19**, 675-692.

Scripathi K. S., Gopal P., Lalitha P. 2011. Allantoin from the Leaves of *Pisonia grandis* R.Br. *International journal of Pharmacy and Life Sciences*. University of Women- India. Pp 815-817.

Seethapathy S. G., Wold W. C., Ravikumar K., Hugo J. B., Wangensteen H. 2021. Ethnopharmacology, biological activities and chemical compounds of *Canarium strictum*: An important resin-yielding medicinal tree in India. *Fitoterapia*, **152**, doi : 10.1016/j.fitote.2021.104920.

Serafini S., Regard S., Mahounde B. I., Massenet D. 2011. Presumptive clinical diagnosis of malaria in children in a hospital in the north region (Cameroon). *Bulletin de la Societe de Pathologie Exotique*, **104**, 271–373.

Shashi B. M., Ashoke K. N. G. 1991. Triterpenoids, reviews article number 67. *Phytochemistry*, **31**, 2199-2248.

Shigemori H., Toshinori K., Haruaki I., Morah F., Ayumi O., Jun'ichi K. 2003. Naucleamides A-E, new monoterpene indole alkaloids from *Nauclea latifolia*. *Journal of Chemical and Pharmaceutical Bulletin* **51**, 58-61.

Showkat A., Rajendra S., Surabhi M., Ankur G. 2012. *International Journal of Pharmacy and Pharmaceutical Sciences*, **4**, 629-631.

Siddiqui, S., Hafeez, F., Begum, S., Siddiqui, B. S., 1988. *Nerium oleander* L. *Journal of Natural Products*, **51**, 229.

Singh R., De S., Belkheir A. 2013. *Avena sativa* (oat), a potential neutraceutical and therapeutic agent: an overview. *Critical Reviews in Food Science and Nutrition*, **53**, 26-144.

Singh S. 2011. Current scenario of control of malaria. *Tropical Parasitology*, **1**, 52-3.

Skoglund M., Peterson D. M., Andersson R., Nilsson J., Dimberg L. H. 2008. Avenanthramide content and related enzyme activities in oats as affected by steeping and germination. *Journal of Cereal Science*, **48**, 294-303.

Smilkstein M., Sriwilaijaroen N., Kelly J. X., Wilairat P., Riscoe M. 2004. Simple and inexpensive fluorescence-based technique for high-throughput antimalarial drug screening. *Antimicrobial Agents and Chemotherapy*, **48**, 1803-1806.

Sokoudjou J. B., Atolani O., Njateng S. S. G., Khan A., Tagousop N. C., Bitombo N. A., Kodjio N. Gatsing D. 2020. Isolation, characterization and in-vitro anti-salmonellal activity of compounds from stem bark extract of *Canarium schweinfurthii*. *BMC Complementary Medicine and Therapies*, **20**, 1-10.

Soulard V., Bosson-Vanga H., Lorthiois A., Roucher C., Franetich J. F., Zanghi G., Bordessoulles M., Tefit M., Thellier M., Morosan S., Le Naour G., Capron F., Suemizu H., Snounou G., Moreno-Sabater A., Mazier D. 2015. *Plasmodium falciparum* full life cycle and *Plasmodium ovale* liver stages in humanized mice. *Nature Communications*, **6**, 7690.

Sousa G., Duarte L., Alcântara A., Silva G., Vieira-Filho S., Silva R., Oliveira D., Takahashi J., 2012. New triterpenes from *Maytenus robusta*: structural elucidation based on nmr experimental data and theoretical calculations. *Molecules*, **17**, 13439-13456.

Sultana N., Armstrong A. J., Watermana G. P. 1999. Benzopyran derivatives from the aerial parts of *Eriostemon rhomboideus*. *Phytochemistry*, **52**, 895-900.

Sur R., Nigam A., Grote D., Liebel F., Southall M.D. 2008. Avenanthramides, polyphenols from oats, exhibit anti-inflammatory and anti-itch activity. *Archives of Derma- tological Research*, **300**, 569-574.

Tafesse F. G., Ternes P., Holthuis J. C. 2006. The multigenic sphingomyelin synthase family. *Journal of Biological Chemistry*, **281**, 29421-29425.

Takahiro I., Tatsufumi O., Yosuke M. 2006. A ceramide and cerebroside from the starfish *Asterias amurensis* L. and their plant-growth promotion activities. *Journal of Natural Products*, **69**, 1080-1082.

Tan R. X., Chen J. H. 2003. The cerebrosides. *Natural Product Reports*, **20**, 509-534.

Taylor H. W., Sinha A., Khan A. I., McDaniel T. S., Esko D. J. 1998. Primers of glycosaminoglycan biosynthesis from peruvian rain forest plants. *The Journal of Biological Chemistry*, **273**, 22260-22266.

Tee L. H., Yang B., Prasad N., Ramanan N., Sun J., Seng C. E., Ti T. B., Azlan A., Ismail A., Lau C. Y., Jiang Y. 2014. Nutritional compositions and bioactivities of *Dacryodes* species. *Journal of Food* Chemistry, **6**, 3-27.

Teixeira de Silva. 2004. Mining the essentiel oil of the anthemidene. *African Jounal of Biotechnology*, **3**, 706-720.

Todou G., Doumenge T. 2008. *Dacryodes buettneri* (Engl.) HJ Lam. *Plant Resources of Tropical Africa*, **7**, 203-207.

Uhunmwangho S. E., Omoregie S. E. 2018. Isolation, Identification and Antioxidant Properties of Anthocyanins Rich Fractions of *Dacryodes edulis* (African pear) Fruit peels. *Saudi Journal of Biomedical* Research, **1**, 1-5.

Veiga J. V. F., Rüdiger A. L., Siani A. C. 2007. The Chemistry and Pharmacology of the South America genus *Protium* Burm (Burseraceae). *Journal of Pharmacognosy and Phytochemistry*, **6**, 3-17.

Viquar U. A., Javid H., Hidayat H., Umar F., Erum A., Sarfraz A. N., Muhammad I. C., 2004. Two ceramides from *Tanacetum artemesioides*. *Zeitschrift für Naturforschung*, **59**, 329-333.

Wahidulla S., D'souza L., Kamat Y. S. 1991. Dipeptides From The Red Alga *Acantophora Spicifera*. *Phytochemistry*, **30**, 3323-3325.

Wang H. X., Tian Y., Guo J. Z., Fan P. Z., Qui K. D., Zeng D. M. 2009. Cholesterol metabolism and expression of its relevant genes in cultured steatotic hepatocytes. *Journal of digestive diseases*, **10**, 310-314.

WHO. 2000. General methodical principles for traditional medicine research and evaluation 2015: Summary. WHO / EDT / TRMP. World Health Organization, Geneva, Switzerland, 87p.

Witchi M., Anton R. 2003. Plantes therapeutiques- Tradition, pratique officinale, science et thérapeutique, 2ème edition, Ed. TEC, DOC.

World Health Organization. 2016. Fact Sheet on the World Malaria Report 2015

World Health Organization. 2020. Fact Sheet on the World Malaria Report 2019.

Yang M. Q, Velzen R. V., Bakker F.T. 2013. Molecular phylogenetics and character evolution of Cannabaceae. *Taxon*, **62**, 473-485.

Yasunori Y., Rie K., Rie K., Koichi M., Masao K. 2001. Ceramide constituents from five mushrooms. *Chemical and Pharmaceutical Bulletin*, **50**, 681-684.

Yu C. C., Lee Y. S., Cheon B. S., Lee S. H. 2003. Synthesis of glycerol monostearate with high purity. *Bulletin of the Korean Chemical Society*, **24**, 1229-1231.

Yuichi E., Hiroko H., Toshisugu S., Masao M., Tomihisa O., Shigeo N. 1994. Confluentic acid and 2′-*O*-methylpertolic acid, monoamine oxidase B inhitors in a Brazilian plant, *Himatanthus sucuuba*. *Chemical and Pharmaceutical Bulletin*, **42**, 1198-1201.

Zavada M. 1983. Pollen morphology of Ulmaceae. *Grana*, **22**, 23-30.

Zhiyong H., Wenshui X., Jie C. 2008. Isolation and structure elucidation of phenolic compounds in Chinese olive (*Canarium album* L.) fruit. *European Food Research and Technology* **, 226**: 1191–1196.

Zhou Z., Bruce B. 2003. CANNABACEAE. *Flora of China*, **5**, 74-75.

Zofou D., Tematio E. L., Ntie-Kang F., Tene M., Ngemenya M. N., Tane P., Titanji V. P. K., 2013. New Antimalarial Hits from *Dacryodes edulis* (Burseraceae) - Part I: Isolation, *In Vitro* Activity, In Silico “drug-likeness” and Pharmacokinetic Profiles. *PLoS ONE*, **8**, e79544.

Zoller T., Naucke T. J., May J., Hoffmeister B., Flick H., Williams C. J., Frank C., Bergmann F., Suttorp N., Mockenhaupt F. P. 2009. Malaria transmission in non-endemic areas: case report, review of the literature and implications for public health management. *Malaria Journal*, **8**, 71.

Zushang S., Ping W., Wei Y., Greg G., Shiyou L. 2017. Phenolics from the Fruits of *Maclura pomifera*. *Natural Product Communications*, **12**, 1743-1745.

ANNEXE

PUBLICATION RESULTING FROM THIS WORK

1- **Jumeta D. J. K.**, Kagho K. D. U., Ateba T. E. J., Fotsing F. Y. S., Bankeu K. J. J., Sewald N., Lenta N. B., Mehreen L., Ali S. M., Ngouela S. A. 2021. A new cerebroside and bioactive compounds from *Celtis adolphi-friderici* Engl. (Cannabaceae) *Biochemical Systematic and Ecology* **94**, 104201; DOI: https://doi.org/10.1016/j.bse.2020.104201.